STATUS OF THESIS

Title of thesis

| HOMOGENEOUS CHARGE COMPRESSION IGNITION COMBUSTION CONTROL BY CNG DIRECT INJECTION |

I _____ NAVEENCHANDRAN PANCHATCHARAM _____

(CAPITAL LETTERS)

hereby allow my thesis to be placed at the Information Resource Centre (IRC) of Universiti Teknologi PETRONAS (UTP) with the following conditions:

1. The thesis becomes the property of UTP

2. The IRC of UTP may make copies of the thesis for academic purposes only.

3. This thesis is classified as

☐ Confidential

√ Non-confidential

If this thesis is confidential, please state the reason:

The contents of the thesis will remain confidential for _____ years.

Remarks on disclosure:
_____
_____
_____

Endorsed by

_____   _____
Signature of Author   Signature of Supervisor

Permanent address:_____   Name of Supervisor
S/o A. Panchatcharam,   Assoc. Prof. Dr. A. Rashid bin A. Aziz
391, Sourna Nagar, Lalpuram - 608602,
Cuddalore Dt, Tamil nadu, India.

Date : _____   Date : _____

ii

UNIVERSITI TEKNOLOGI PETRONAS

HOMOGENEOUS CHARGE COMPRESSION IGNITION COMBUSTION

CONTROL BY CNG DIRECT INJECTION

by

NAVEENCHANDRAN PANCHATCHARAM

The undersigned certify that they have read, and recommend to the Postgraduate Studies Programme for acceptance of this thesis for the fulfilment of the requirements for the degree stated.

Signature: _____

Main Supervisor: _Assoc. Prof. Dr. A. Rashid bin A. Aziz_____

Signature: _____

Co-Supervisor: _____

Signature: _____

Head of Department: _Assoc. Prof. Dr. Ahmad Maidi Bin Abdul Rani_

Date: _____

HOMOGENEOUS CHARGE COMPRESSION IGNITION
COMBUSTION CONTROL BY CNG DIRECT INJECTION

by

NAVEENCHANDRAN PANCHATCHARAM

A Thesis

Submitted to the Postgraduate Studies Programme

as a Requirement for the Degree of

DOCTOR OF PHILOSOPHY

MECHANICAL ENGINEERING DEPARTMENT

UNIVERSITI TEKNOLOGI PETRONAS

BANDAR SERI ISKANDAR,

PERAK.

MARCH 2011

DECLARATION OF THESIS

| Title of thesis | HOMOGENEOUS CHARGE COMPRESSION IGNITION COMBUSTION CONTROL BY CNG DIRECT INJECTION |

I, _____NAVEENCHANDRAN PANCHATCHARAM_____
(CAPITAL LETTERS)

hereby declare that this thesis is based on my original work except for quotations and citations which have been duly acknowledged. I also declare that it has not been previously or concurrently submitted for any other degree at Universiti Teknologi PETRONAS or other institutions.

Witnessed by

_____   _____
Signature of Author   Signature of Supervisor

Permanent address:_____   Name of Supervisor
 S/o A. Panchatcharam,_____   Assoc. Prof. Dr. A. Rashid bin A. Aziz
 391, Sourna Nagar, Lalapuram -608602,
 Cuddalore Dt., Tamilnadu, India_____

Date:_____   Date:_____

v

ACKNOWLEDGEMENTS

ABSTRACT

Homogenous Charge Compression Ignition (HCCI) is a combustion process that emits very low nitrogen oxides and has high thermal efficiency. It is one of the few solutions on hand that looks very promising to address the issues on the atmospheric air pollution and depleting fossil fuel resources exacerbated by increasing energy consumption of the world. However, currently there is no established means for HCCI combustion control and it has high HC and CO emissions. In this project, CNG direct injection was proposed as a tool for HCCI combustion control. Proportion of gasoline and CNG flow rates and degree of stratification of CNG were identified as potential parameters for HCCI combustion control. Role of CNG direct injection on HCCI combustion control and corresponding effects on performance and emission characteristics were experimentally investigated.

The studies were carried out on a single cylinder, CNG direct injection (CNG DI) research engine. A gasoline fuel injection system and an intake air heater were fitted to the engine to operate the engine with dual fuels and in HCCI mode. Compression ignition combustion of homogeneously premixed charge of gasoline was achieved by heating the intake air and CNG was directly injected. CNG stratification was achieved by direct injection on a specially designed piston with a groove on its crown. The degree of stratification was varied by changing the start of CNG injection. Early injection (300° BTDC) created homogeneous mixtures and stratified mixtures were obtained by retarding the injection timing. High degrees of stratification were obtained by injecting at 80° and 120° BTDC, that is, after the closure of intake valves (132° BTDC). To study the effect of fuel proportions, CNG injection rate was varied at constant equivalence ratio of gasoline (ϕ_g) at 0.20 to 0.26. The effects of CNG stratification were studied by changing the injection timing form 300° to 80° BTDC and all experiments were repeated at different engine speeds ranging from 1200 to 2100 rpm.

It was observed that heat released by gasoline HCCI combustion resulted in the subsequent combustion of CNG and the engine load could be increased by varying the CNG injection rate. Proportions of gasoline and CNG and degree of stratification of CNG were found to be effective means of combustion control within certain limits of engine load and HC and CO emissions could be significantly reduced.

ABSTRAK

Homogen Charge Compression Ignition (HCCI) adalah proses pembakaran yang menghasilkan oksida nitrogen yang sangat rendah dan mempunyai kecekapan terma yang tinggi. Ini adalah salah satu cara penyelesaian yang berpotensi untuk mengatasi isu-isu tentang pencemaran udara dan pengurangan sumber bahan bakar fosil diburukkan lagi dengan peningkatan penggunaan tenaga dunia. Namun, pada masa initiada cara yang diketahui untuk kawalan pembakaran HCCI dan ia menghasilkan pembebasan HC dan CO yang tinggi. Dalam projek ini, suntikan langsung CNG dicadangkan sebagai alat kawalan pembakaran HCCI. Kadar aliran antara petrol dan CNG dan tahap stratifikasi CNG dikenalpasti sebagai parameter yang berpotensi untuk kawalan pembakaran HCCI. Peranan suntikan langsung CNG terhadap kawalan pembakaran HCCI dan kesan langsung kepada prestasi dan cirri-ciri pembebasan diselidik secara eksperimen dan pembebasan yang eksperimental diselidiki.

Penyelidikan dilakukan pada enjin silinder tunggal, CNG suntikan langsung (CNG DI). Sebuah sistem pancitan bahan bakar petrol dan pemanas udara masuk yang dipasang pada enjin untuk mengendalikan enjin dengan dua bahan bakar dan dalam mod HCCI. Mampatan pembakaran kos homogen premixed petrol dicapai dengan memanaskan udara masuk dan suntikan langcung CNG. CNG stratifikasi diperoleh dengan suntikan langsung pada omboh yang direka khas dengan alur pada mahkota ombohnya. Darjah stratifikasi berubah-ubah dengan menukar permulaan suntikan CNG. Suntikan awal (300° BTDC) menghasilkan campuran homogen dan campuran bertingkat tersebut diperoleh dengan melambatkan waktu suntikan. Darjah tinggi stratifikasi diperolehi dengan menyuntikkan pada 80° dan 120° BTDC, iaitu, selepas penutupan injap masukan (132° BTDC). Untuk mengetahui kesan perkadaran minyak, kadar suntikan CNG dipelbagaikan kepada nisbah kesetaraan malar petrol (φg) pada 0.20 hingga 0.26. Kesan stratifikasi CNG dipelajari dengan menukar waktu suntikan daripada 300° sampai 80° BTDC dan semua eksperimen diulangi pada kelajuan enjin yang berbeza bermula dari 1200 hingga 2100 rpm.

Didapati bahawa haba yang dilepaskan oleh pembakaran petrol HCCI hasil daripada pembakaram pembakaran lanjutan CNG dan beban enjin dapat dipertingkatkan dengan mempelbagaikan kadar suntikan BBG. Perkadaran petrol dan CNG serta darjah stratifikasi CNG didapati boleh menjadi cara yang berkesan untuk mengawal pembakaran dalam batas tertentu dari beban enjin dan pembebasan HC dan CO dapat dikurangkan secara signifikan.

TABLE OF CONTENTS

LIST OF TABLES

LIST OF FIGURES

xvii

xxiii

NOMENCLATURE

General Abbreviations

AFR	-	Air to Fuel Ratio
ATAC	-	Active Thermo Atmosphere Combustion
ATDC	-	After Top Dead Centre
AVT	-	Active Valve Train
BDC	-	Bottom Dead Centre
BMEP	-	Brake Mean Effective Pressure
BTDC	-	Before Top Dead Centre
BSFC	-	Brake Specific Fuel Consumption
CAD	-	Crank Angle Degrees
CNG	-	Compressed Natural Gas
COV	-	Coefficient of Variation
CO	-	Carbon Monoxide
CO_2	-	Carbon Dioxide
CH_4	-	Methane
CR	-	Compression Ratio
CI	-	Compression Ignition
CV	-	Calorific Value
DAQ	-	Data Acquisition
Deg	-	Degrees
DICI	-	Direct Injection Compression Ignition
DI	-	Direct Injection
DME	-	Di-methyl Ether
DEE	-	Di-ethyl Ether
ECU	-	Electronic Control Unit
EGR	-	Exhaust Gas Recirculation
EVC	-	Exhaust Valve Closure
EVO	-	Exhaust Valve Opening

FTIR	-	Fourier Transform Infrared
FID	-	Flame Ionization Detector
GDI	-	Gasoline Direct Injection
H_2O	-	Water
HC	-	Hydrocarbons
HCCI	-	Homogeneous Charge Compression Ignition
HRR	-	Heat Release Rate
IMEP	-	Indicated Mean Effective Pressure
ISCO	-	Indicated Specific Carbon Monoxide
ISEC	-	Indicated Specific Energy Consumption
ISHC	-	Indicated Specific Hydrocarbons
IP	-	Indicated Power
$ISNO_x$	-	Indicated Specific Nitrogen Oxides
IVC	-	Intake Valve Closure
IVO	-	Intake Valve Opening
LPG	-	Liquefied Petroleum Gas
LTR	-	Low Temperature Reactions
LHV	-	Lower Heating Value
MEP	-	Mean Effective Pressure
MFB	-	Mass Fraction Burned
MTBE	-	Methyl Tetra Butyl Ether
NO	-	Nitric Oxide
NO_2	-	Nitrogen Oxide
NO_x	-	Nitrogen Oxides
NVO	-	Negative Valve Overlap
O_2	-	Oxygen
PFI	-	Port Fuel Injection
PM	-	Particulate Matter
ppm	-	Parts Per Million
PRF	-	Primary Reference Fuel
RON	-	Research Octane Number
RPM	-	Revolutions per Minute
SCCI	-	Stratified Charge Compression Ignition

SEFC	-	Specific Equivalent Fuel Consumption
SI	-	Spark Ignition
SOI	-	Start of Injection
TDC	-	Top Dead Centre
THC	-	Total Hydrocarbon
TSDI	-	Two Stage Direct Injection
WOT	-	Wide Open Throttle

General Notations

σ	-	Standard Deviation
AF_{St}	-	Stochiometric Air to Fuel Ratio
$AF_{St\text{-}g}$	-	Stochiometric Air to Fuel Ratio of Gasoline
$AF_{St\text{-}CNG}$	-	Stochiometric Air to Fuel Ratio of CNG
C	-	Celsius
c	-	Specific Heat Capacity
h	-	Enthalpy
h_c	-	Convective Heat Transfer Coefficient
m_a	-	Mass Flow Rate of Air
m_g	-	Mass Flow Rate of Gasoline
m_{CNG}	-	Mass Flow Rate of CNG
m_{CH4}	-	Mass flow Rate of Methane
K	-	Kelvin
M	-	Molecular weight
N	-	Engine Speed
n	-	Number of Revolutions
P	-	Power
p	-	Incylinder Pressure
Q	-	Heat
R	-	Gas Constant
T	-	Temperature
U	-	Internal Energy
V	-	Volume of Gases

V_s	-	Swept Volume
W	-	Work Done
x_b	-	Mass Fraction Burned
ϕ_g	-	Individual Equivalence Ratio of Gasoline
ϕ_{CNG}	-	Individual Equivalence Ratio of CNG
ϕ_{Total}	-	Total Equivalence Ratio
ω	-	Angular Velocity
γ	-	Ratio of Specific Heats
τ	-	Torque
η_C	-	Combustion Efficiency
$\eta_{Thermal}$	-	Thermal Efficiency

CHAPTER 1

INTRODUCTION

1.1   The Engine, Energy and Emission

The invention of engine is a major milestone in the transportation of man and materials and it led to a grand leap in the economic development of the people of this planet. However, at the time when it was introduced the main technical considerations for the design of the engines were to serve the purpose of transportation with high load carrying capacities at higher speeds. The efficiency of energy conversion and the emission characteristics of an engine were of least significance for the society of automotive engineers and designers.
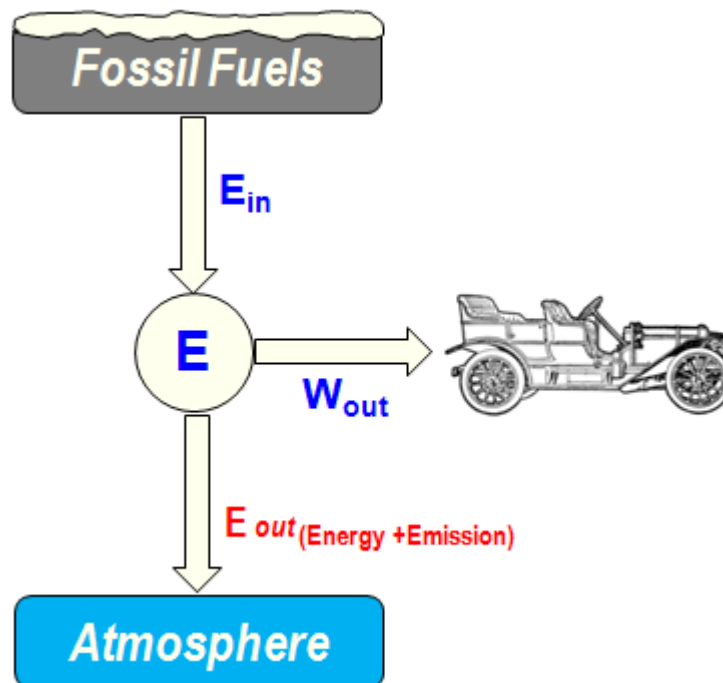
Figure 1.1 First and second laws of thermodynamics applied to the engines.

Obeying the first law of thermodynamics, the engine converts heat energy into mechanical energy. However, as explained by the second law of thermodynamics,

1

the complete conversion of heat into work is limited and some energy is always rejected. Figure 1.1 shows the first and second laws of thermodynamics applied to engines in the closed system of earth and its atmosphere. Energy is rejected from the engines in the form of heat carried away by the cooling medium, hot exhaust gases and by friction caused by the moving components. Thanks to decades of research, the energy conversion efficiency of the engines has greatly increased. However, rapidly depleting sources of fossil fuels and ever increasing energy requirements leave a lot to be desired. It is likely that research on the engines will be dominated by the emission control requirements, use of new fuels and energy saving in future decades and it is predicted that there would be 6 to 15% increase in efficiencies of the engines with some degree of trade off of emission characteristics [1].

1.2   Current and Future Energy Scenario of the World

Although the world energy consumption derived from the fossil fuels dropped significantly in 2009 for the first time after 1981 due to the economic crisis, it is reported that it would reach much higher levels in 2035 due to the rapid economic developments in certain regions of the world.
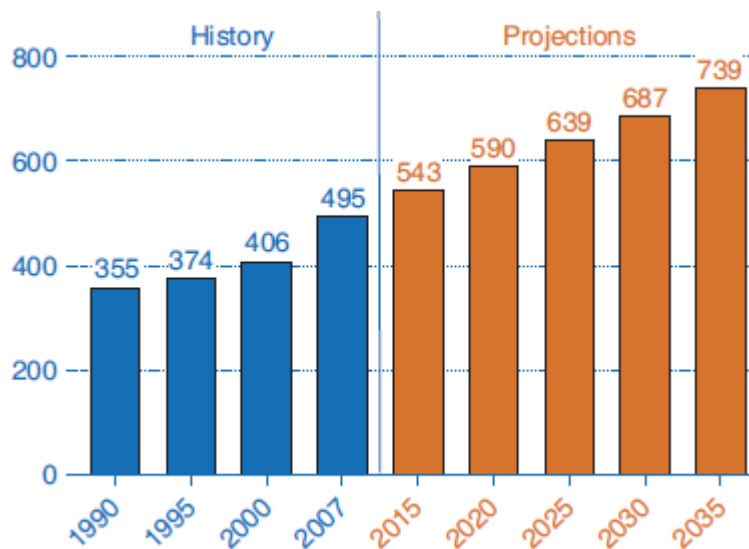
Figure 1.2 World marketed energy consumption (Quadrillion Btu)[2].

About 20% of the world's delivered energy and more than 50% of the energy from liquid fuels is spent for the transportation of passengers and freight. As liquid

2

fuels dominate the transportation sector, it is estimated to increase to about 81% of the total liquid fuel consumption of the world in 2035 [2].

Figure 1.2 shows the current and projected energy consumption of the world that indicates an increasing trend in the energy consumption. The energy consumption of a particular country and the world is sometimes seen as an economic indicator of growth of that country or the world. Therefore, it should not be deduced that the energy consumption should be reduced but it should be met with higher productivity, effective utilisation and development of alternative energy sources and new energy conversion techniques.

Therefore, it is time to direct the research on the automotive power plants to focus on the development of new technologies that have higher efficiencies and can use alternative energy sources.

1.3   Environmental Issues Associated with the Engines

Utilization of energy using the currently available technologies results in emission of harmful pollutants and greenhouse gases that result in global warming and deteriorated quality of atmospheric air. The internal combustion engine, the most widely used type of engine for automotive applications, uses air as the working medium and as a source of oxygen for the combustion of fuel. The mechanism of conversion of heat into work starts with the liberation of heat energy contained in the fuel by the combustion process. The process of combustion is complex with many intermediate chemical reactions involving several components of the fuel. Combustion produces harmful gases as by-products which are often formed especially due to incomplete chemical reactions. Some of the major pollutants emitted by the engines are oxides of carbon, oxides of nitrogen, sulphur oxides and hydrocarbons in the fuel itself. This is another major issue that appears to restrict the application of IC engines in the future.

Automotive engines also distribute the pollutants especially in densely populated urban areas deteriorating the quality of atmospheric air. In 2008, about 22% of the total CO_2 was emitted by the transport industry and the total number of transport

3

vehicles would be 45% higher by 2030 [3]. It may be noted that higher thermal efficiency of an engine indirectly means reduced formation and emission of pollutants.

Concisely speaking, given the rate of depleting fuel resources and the increasing awareness and effects of atmospheric pollution, research on the engines with a view to developing a combustion technology that has high fuel conversion efficiencies and emits virtually no harmful pollutants has become timely and significant.

1.4   Types and Future Requirements of Engines

Engines are of two main types, namely, the spark ignition (SI) or gasoline engines and compression ignition (CI) or diesel engines. In case of SI engines, the premixed fuel is ignited by a spark at one point of the cylinder and the rest of the fuel is burnt by flame propagation. As flame propagation with high compression ratios result in knocking, SI engines operate with limited compression ratios in the range of 8 to 12 and have low thermal efficiencies. Also, as the charge is premixed and typically stochiometric to match the requirements of the catalytic converters, very low amounts of soot are emitted compared to CI engines. However, operating the engine with fixed air to fuel ratio means that the engine load must be controlled by regulating the amount of mixture flowing into the cylinder. A throttle valve is used for this purpose and this leads to pumping losses, which are especially significant at part loads. Therefore, the low efficiency at part loads is the major disadvantage of SI engines.

CI engines, on the other hand, can operate at higher compression ratios with higher efficiencies enhanced by the absence of throttling. In CI engines, the fuel is delivered to the cylinder by fuel injectors and the ignition is caused by the compression process. The method and point of fuel delivery creates a heterogeneous mixture and leads to the formation of zones of high fuel concentration and high flame temperature. A part of the fuel that is well mixed will burn fast and the larger fraction of the fuel has less access to oxygen resulting in high levels of soot formation. When the combustion temperature is increased in order to reduce the soot,

a trade-off of NO_x emissions is observed. Currently, after-treatment to reduce NO_x emissions is expensive.

Obviously, a new combustion technology that combines the high efficiency and low emissions would be the choice for the future automobiles. One such method that looks very promising is Homogeneous Charge Compression Ignition (HCCI) combustion. In HCCI engines, the fuel is premixed and is ignited by compression. As HCCI combustion takes place at low temperatures with no flame propagation, high thermal efficiencies with very low NO_x emissions are obtained. However, there are certain technical barriers such as uncontrollable combustion, narrow load range, high CO and HC emissions and lack of cold start strategy that prevent HCCI engines from practical application. Several researchers all over the world have been working on HCCI combustion for the past three decades.

1.5   Problem Statement

One of the most researched features of HCCI combustion is the difficult control of combustion. As described in Section 1.4, combustion is initiated at multiple points in the cylinder resulting in high rates of heat release and pressure rise. Therefore, HCCI engine needs to be operated with ultra lean mixtures. Since enriching the fuel in the intake air is the method for increasing the engine load, this phenomenon restricts the load to a very narrow range. In addition, to realise the benefit of higher thermal efficiency and avoid negative work on the piston during the compression stroke, the timing of autoignition needs to take place around TDC for all engine operating conditions. Therefore, finding a strategy of controlling autoignition timing and combustion phasing is one of the important objectives of researchers at present.

In this project, a new approach is proposed for controlling dual fuel HCCI combustion. The approach is the combination of varying the proportions of gasoline and CNG and varying the degree of CNG stratification in the gasoline air mixture. Apart from combustion control, the combined benefits of dual fuel operation and stratification can be obtained using the proposed strategy.

1.6   Objectives

The major objectives of this project are:

a. To experimentally investigate the characteristics of combustion of homogeneously mixed dual fuels of gasoline and CNG by compression ignition.

b. To study the effect of proportion of gasoline and CNG on the combustion phasing and the effectiveness of the proportions of the fuels as a tool for control of HCCI combustion.

c. To study the effect of proportion of gasoline and CNG on the performance and emission characteristics of the engine.

d. To study the effects of varying CNG stratification on the combustion characteristics of the dual fuel HCCI combustion.

e. To propose control of the degree and amount of stratified distribution of CNG by direct injection in the homogeneous charge of gasoline as a method of combustion control and experimentally study its effectiveness.

f. To study the effects of CNG stratification on the performance and emission characteristics of the dual fuel HCCI engine.

1.7   Outline of the Thesis

Chapter 1 briefly discusses the current trends in research in combustion technologies. The research problem considered for this work is introduced and a brief description of the problem studied and its significance to the automotive industry is highlighted.

In Chapter 2, a brief history and evolution of HCCI combustion systems are presented. The basic characteristics of HCCI combustion and its limitations are also discussed and methods of combustion control reported by several researchers in the past are reviewed.

A basic description of the engine test facility and the appropriate modifications carried out to meet the objective of this work is given in Chapter 3. The various

instruments used for measurement of engine parameters are described and the experimental methodology is explained.

The results are presented and discussed in Chapter 4. The effects of CNG injection and its degree of stratification on the characteristics of the HCCI combustion are analysed in detail.

Finally, the conclusions and recommendations are given in Chapter 5.

CHAPTER 2

LITERATURE REVIEW

2.1 Introduction

One of the advanced methods of combustion that has a rare combination of high thermal efficiencies and ultralow NO_x emissions is Homogeneous Charge Compression Ignition or HCCI combustion. The HCCI combustion features diesel like thermal efficiencies and emits virtually no harmful pollutants produced from nitrogen. Apart from the issues of cold start-ability, high CO and HC emissions, the technical barriers limiting HCCI combustion from practical use is the difficulty of controlling the point of autoignition and subsequent burning rate. There are researches going on in several aspects in view to find a practical means of combustion control so as to achieve full load operation on par with present day SI and CI engines. This chapter provides a review of trends and developments of research on HCCI combustion in the past with particular focus on the recent developments in HCCI combustion control.

2.1.1 Historical Background

The HCCI combustion can be compared to the hot bulb engines [4] developed in the early stages of evolution of internal combustion engine. The hot bulb engines used an auxiliary chamber that could be externally heated for start up. The fuel was injected into the passage that connected the heated chamber and the main combustion chamber. As the fuel was injected during the early part of the compression stroke, it had ample time to get mixed with the air after being vaporised by the surfaces of the hot bulb. This resulted in the formation of homogeneous

charge in the cylinder and the engine was operating on the combustion with homogeneous charge and autoignition.

However, the first pioneering work carried out by Onishi et al. [5] and Noguchi et al. [6] on the concept of autoignition of homogeneous charges in view of controlling the irregular lean burn combustion in two stroke engines had opened new doors in understanding and applying the HCCI combustion for internal combustion engines. Another milestone was reached in 1983 by Najt and Foster [7], when they showed that the HCCI combustion was applicable to four stroke engines by heating the intake charge. However, extremely lean mixtures needed to be used to control heat release rates and this led to a very narrow range of operable engine loads.

Later in 1989, Thring [8] showed that the energy required for intake charge heating could be reduced by using high EGR rates from 13 to 33% and achieved HCCI combustion in an engine of compression ratio of 8:1. He had also shown that heat release rates could be controlled by varying the rate of exhaust gas recirculation (EGR) but limited to low engine speed and load. The engine had low indicated specific fuel consumption in the range of 180 to 200g/kWhr at part loads.

Stockinger et al. [9], in 1992, showed that a four cylinder engine could be operated in HCCI mode within a narrow range of speed and load using intake air heating and high compression ratio. In a more recent study on a multi cylinder engine, Zhao et al. [10] showed that a reduction of about 93% of NO_x emissions could be achieved over a range of speed from 1000 to 3500 rpm and loads from 0.5 to 4 bar BMEP.

Perhaps the most significant progress towards a practical application of HCCI concept was the use of internal recirculation of exhaust gases by revised valve timings that formed a Negative Valve Overlap or NVO. When the exhaust valves were closed early, some of the burnt gases got trapped in the cylinder which promoted the auto ignition of the charge inducted in the following cycle [11, 12].

While the feasibility and potential of HCCI combustion are well demonstrated as discussed above, its practical application is still hindered due to lack of means of combustion control that limits the engine operation to narrow range of load and

speed. In the recent decades, a number of research works had been carried out all over the world in view of understanding the fundamentals of HCCI combustion and to establish a practical method of combustion control to obtain loads comparable to SI and CI engines.

2.2   Characteristics of HCCI Combustion

In HCCI combustion systems, as the name that was first introduced by Thring [8] suggests, the fuel is premixed with air to form a homogeneous intake charge like in SI engines and is ignited by compression like in diesel engines. The premixed fuel gets combusted by auto ignition at several points in the cylinder. Figure 2.1 shows the basic differences in the combustion phenomenon of SI, CI and HCCI combustions.
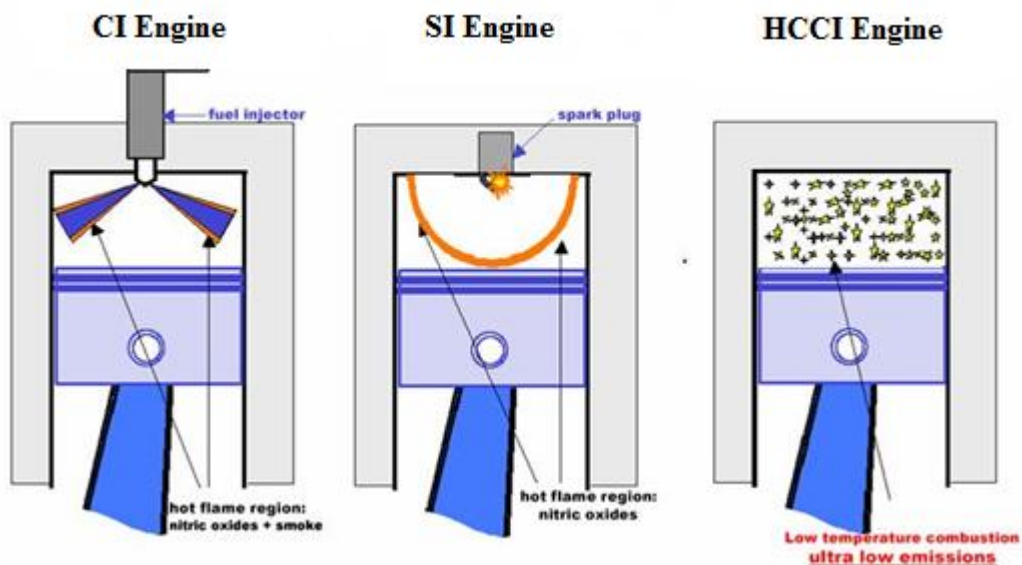
Figure 2.1 Comparison of CI, SI and HCCI combustions.

However, in order to achieve HCCI combustion of fuels that have high autoignition temperature, additional energy is needed to bring the premixed charge in the cylinder to the thermodynamic state that promotes auto ignition. One of the basic approaches to achieve HCCI combustion is to use high compression ratio that suits the auto ignition temperature of the fuel used. However, for fuels having high auto ignition temperature such as gasoline, very high compression ratio would be required

which is not desirable from the practical operation point of view. Several methods have been reported to achieve HCCI combustion with moderate compression ratios for a range of fuels by carrying out minor modifications or adding suitable subsystems to the engine. Some of the widely applied methods of HCCI operation include intake air heating, use of excessive exhaust gas recirculation, use of additives as ignition promoters and blending a fuel of low autoignition temperature with the main fuel.

However, for any combustion method applied for engines, it is highly desirable to have an externally controllable tool to place the ignition and the combustion process according to the operating conditions such as engine speed and load. In the case of SI engines, the timing of the ignition or start of combustion is controlled by altering the timing of the spark generation and in case of CI engines, the timing of diesel injection takes over the role of combustion control. But in HCCI engines since the charge is premixed it can combust at any instance at which physical and thermal conditions inside the cylinder favour autoignition. Several studies based on experiments and numerical computations have shown that the auto ignition and subsequent combustion are governed by the chemical kinetics. Also, the fuel chemistry, temperature and pressure history and other engine operating parameters significantly affect the ignition timing and subsequent burning process [13].

While the issue of control over the point of autoignition remains yet to be addressed, the rapid combustion results in high heat release rates with corresponding pressure rise rates. There is no flame development and the whole process of combustion takes place in very short duration at low temperatures compared to SI or CI engines. By this rapid combustion the most part of the heat is liberated and added to the working medium almost at a constant volume process. This makes the thermal efficiency of the HCCI engines reach close to the efficiencies of theoretical *Otto cycle*. Absence of flame fronts as found in SI combustion and diffused burning of heterogeneous mixture as observed in CI combustion make the combustion take place at low temperatures all over the cylinder and results in near zero NO_x emissions [14].

11
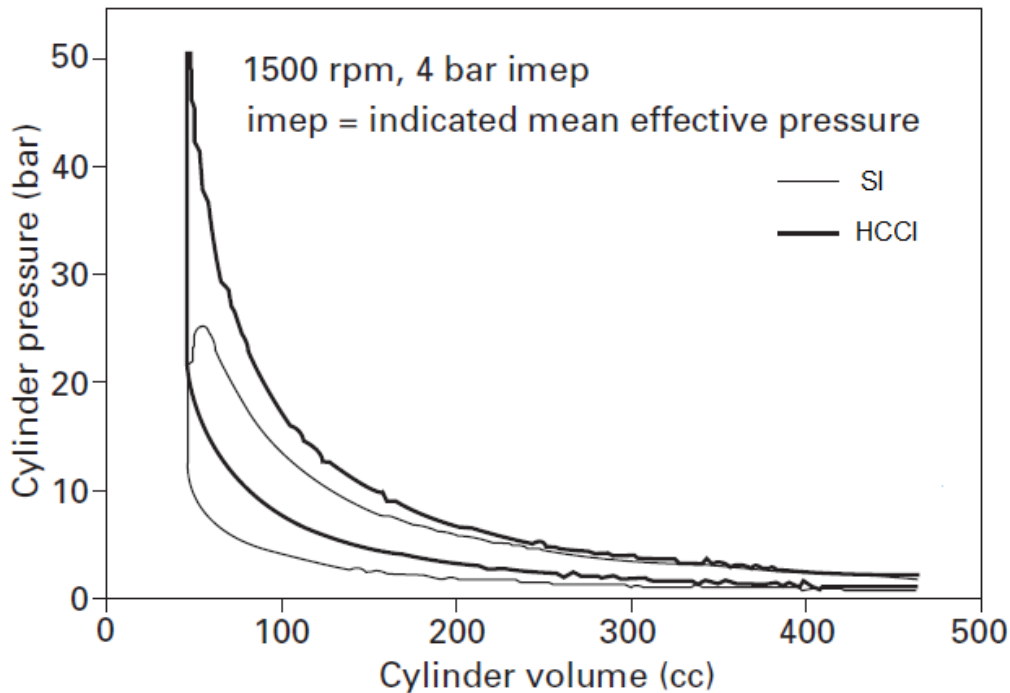
Figure 2.2 Pressure traces of SI and HCCI combustion at same operating conditions[14].

Figure 2.2 shows the differences in pressure rise rates of SI and HCCI combustion at same engine speed and load [14]. The pressure rise rate due to any method of combustion is limited to 10bar/CAD by the materials currently used for building the engines [15]. In order to limit the high heat release rate and avoid autoignition at an early instance during compression stroke, the engine has to be operated with extremely lean mixtures. Like diesel engines, HCCI engine is operated at wide open throttle (WOT) and the load on a HCCI engine is met by increasing the fuel concentration in the air. Since the HCCI engine has to be operated at far leaner than the stochiometric condition to manage high heat release rates, the load range that can be handled is very limited when compared to engines of same size operating on SI or CI combustion. In other words, the maximum load operable with HCCI combustion is very low, often falling within 30% of the peak torque or IMEP that is attained with SI or CI combustion [16].

2.2.1 Emission Formation in HCCI Combustion

NO_x represents the combined emission of nitrogen oxide (NO_2) and nitric oxide (NO). In HCCI combustion, due to extreme dilution of the mixture and the nature of

low temperature combustion, NO_x emissions are reduced by 90 to 98% compared to SI and CI combustion. A SI engine emits about 6 g/kWhr of nitrogen oxides at 2-3 bars of IMEP and 1500rpm and at comparable conditions HCCI emits much lower than 0.35 g/kWhr [14]. The high temperature flame front in SI engines and fierce burning at fuel rich zones in CI engines contribute to high levels of NO formation. It is worthy to mention here that NO is a major component of NO_x in conventional engines.

NO emissions are highly dependent on the temperature as high activation energy is needed for Zeldovich and Lavoie reactions that explain the mechanism of formation of NO emissions [17]. The governing equations of NO formation are:

$$O + N_2 \quad = \quad NO + N \tag{2.1}$$

$$N + O_2 \quad = \quad NO + O \tag{2.2}$$

$$N + OH \quad = \quad NO + H \tag{2.3}$$

Other factors affecting the formation of NO_x are equivalence ratio and residual time available for the reactions. The other component of NO_x, the nitrogen oxide (NO_2) is formed by rapid conversion of NO via reaction such as:

$$NO + HO_2 \quad = \quad NO_2 + OH$$
(2.4)
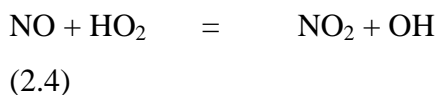
Subsequently, conversion of this NO_2 to NO occurs as:

$$NO_2 + O \quad = \quad NO + O_2$$
(2.5)
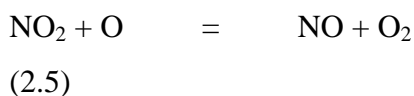
However, the conversion of NO_2 to NO may be quenched during the reduction in temperature due to mixing with a cooler fluid. For this reason, ratio of NO_2/NO_x is higher in diesel engines in the range of 10 to 12% compared to that of SI engines which is below 5% [18].

HCCI combustion results in significantly high levels of HC and CO emissions. It is well known that in any engine a significant portion of fuel is stored in crevices

during the compression stroke and they are emitted unburned or partially combusted. As the engine has to be operated at very lean conditions HCCI combustion often results in incomplete combustion and misfire which lead to high HC emissions. In addition to that, as combustion temperatures are too low, in the range lower than 1400K or 1500K, the complete oxidization process of CO is hindered and results in high CO emissions, especially at low fuelling rates [19]. Other factors that govern the formation of CO are fluid-wall interactions, the wall temperature and spatial and temporal inhomogeneity inside the cylinder [20]. CO emissions increase with an increase in engine speed due to reduced time available for chemical reactions. HCCI combustion results in low exhaust gas temperatures due to its fundamental characteristics of low temperature combustion. As conversion efficiency of exhaust gas after-treatment systems highly dependent on the temperature of exhaust gases, the high HC and CO emissions of HCCI combustion attract higher significance.

2.2.2 Effects of Fuel Characteristics

One of the main appealing features of HCCI combustion is its intrinsic fuel flexibility. A wide range of fuels has been shown operable with little difference in characteristic advantages of high thermal efficiency and low NO_x emissions [21]. However, the method of charge preparation and strategy of achieving HCCI combustion largely depends on fuel properties such as autoignition temperature and volatility. High volatile fuels like gasoline are suitable for HCCI combustion as it is easy to prepare homogeneous mixtures of air and fuel. However, fuels having high autoignition temperature need higher thermal energy to initiate combustion by compression [16]. Several methods have been shown to achieve HCCI combustion with a wide range of fuels with moderate compression ratios.

With experimental investigation on a variable compression ratio engine, Christensen et al. [21] studied the effects of octane number by varying the proportion of n-heptane and iso-octane between 0 and 100 and demonstrated that almost any liquid fuel can be used for HCCI combustion.
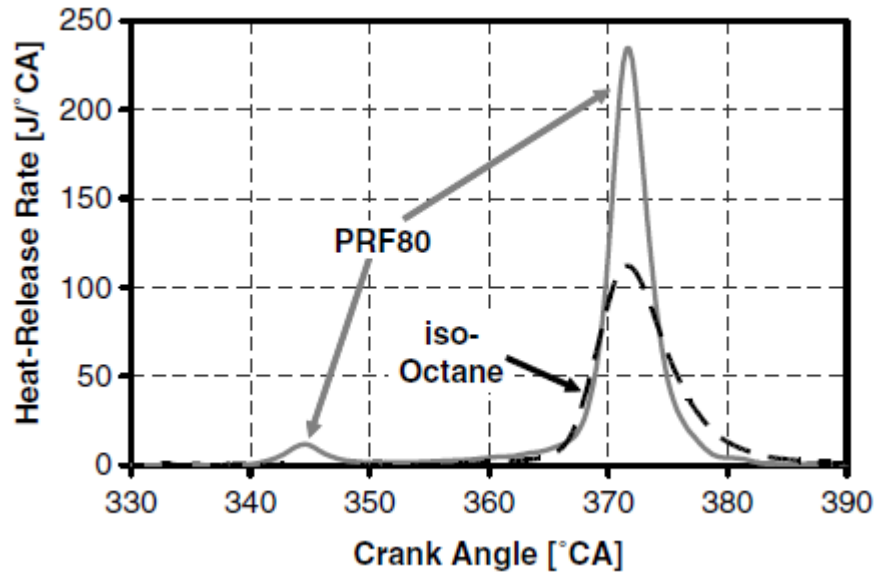
Figure 2.3 Heat release traces for iso-octane and PRF 80 [22].

However, when fuels having low octane number are used for HCCI combustion, a portion of heat is released before the main combustion due to the low temperature reactions or LTR that take place well below the autoignition temperature of the fuel [23]. By a study on the chemical kinetics of combustion, Westbrook [24] had shown that the heat and intermediate radicals produced by LTR significantly affected the timing of the main combustion. The heat released in an HCCI engine due to LTR for a primary reference fuel (PRF 80) and single stage combustion of iso-octane is shown in Figure 2.3. However, fuels having high octane ratings exhibited less tendency for LTR [25, 26]. Xing-Cai et al. [27] studied the effects of octane number of a fuel by an experimental investigation using blends of n-heptane and iso-octane. The study confirmed that heat release due to low temperature reactions reduced with an increase in fuel octane number.

2.2.3   Effects of Exhaust Gas Recirculation

Exhaust gas recirculation (EGR) has significant effects on the HCCI combustion. Using high rates of EGR is one of the most practical methods to achieve autoignition of fuels that have high auto ignition temperature. Conventionally, the exhaust gases can be recirculated by using a passage connecting exhaust and intake manifolds and the rate of recirculation can be varied by a control valve. Or by using modified valve

timing events that leads to early closure of exhaust valves, part of the burnt gases can be retained in the cylinder. The trapped gases can be used to heat the intake charge and cause auto ignition of the fuel. This method is called internal EGR. The high load limit of HCCI combustion can be extended as EGR significantly reduces heat release rate and high cylinder pressure. Zhao et al. [28] analytically studied the various effects of EGR and grouped them as follows:

a. Charge Heating Effect

When burnt gases are mixed with cooler inlet mixture of fuel and air, the charge gets heated. This leads to a higher temperature during the compression stroke and promotes autoignition. The temperature of the charge significantly affects the timing of autoignition. In other words, by varying the rate of exhaust gas recirculation ignition timing can be controlled.

b. Dilution and Chemical Effect

When the exhaust gases are mixed with the fresh charge, a chemical dilution is introduced. Oakley et al. [29] confirmed that the recirculated chemical compounds replace some of O_2 and decreases its distribution in the mixture. This causes a reduction in the rate of combustion reactions and leads to a longer combustion duration and reduced NO_x emissions. However, ignition timing was more dependent on charge heating or intake temperature and there was no significant delay in ignition timing observed due to charge dilution effect.

c. Heat Capacity Effect

The heat capacity of the burnt gases is higher than that of the fresh charge due to higher specific heat values of carbon dioxide and water vapour in the exhaust gases. This increase in heat capacity results in prolonged combustion and retarded auto ignition. Replacement of some O_2 by CO_2 and H_2O reduces the ratio of specific heats (γ value) of the cylinder charge. This results in a lower temperature at the end of compression stroke and autoignition of the fuel is delayed. Combustion duration increases and heat release rate reduces due to the thermal cushioning caused by higher energy absorption.

d. Stratification Effect

When internal EGR is used, mixture homogeneity of the charge is greatly affected by exhaust gas recirculation. As incomplete mixing of EGR and charge in the cylinder results in thermal and mixture stratification, ignition timing and combustion duration are significantly affected.

As discussed above, since EGR has significant effects on combustion, it has been proven by several researchers that rate of EGR is one of the effective parameters for combustion control [30, 31]. With the advent of active valve trains (AVT), the amount of residual gases trapped inside the cylinder and the effective compression ratio can electronically be varied by changing the valve timing events [32]. Therefore, the use of internal EGR is one of the most practical methods for achieving and controlling HCCI combustion.

2.2.4   Compression Ratio, Intake Temperature and Charge Inhomogeneity

Compression ratio has significant effects on HCCI combustion and affects the maximum load limits operable. Olsson et al. [33] studied the influence of compression ratio on HCCI combustion and reported that increasing compression ratio resulted in advanced ignition timing at high loads and reduced the required intake temperature for autoignition. However, it had least significance on combustion at light loads. It is worth remembering here that varying compression ratio during operation is less practical. However, by using electronic valve control systems, the effective compression ratio can be varied by changing the valve timing events of intake and exhaust valves and this method has been used in combination with internal EGR.

By heating the intake air, autoignition of fuels having high autoignition temperature could be achieved at a moderate compression ratio [7]. The intake temperature had significant effects on combustion and emission characteristics. Flowers et al. [34], by an experimental study, revealed that increase in intake temperature reduced HC and CO emissions but resulted in shorter combustion duration. Sjoberg and Dec [35] carried out a computational study in view of defining

17

the optimum intake and combustion temperature for HCCI combustion and found that higher intake temperatures are required as the engine speed increased, as the time available for chemical reactions were reduced at higher engine speeds. However, given the thermal inertia and high flow rates of intake air, it is practically difficult to control the intake temperature in order to control HCCI combustion.

Mixture and temperature distribution in the cylinder have significant effects on HCCI combustion. In practice, a significant degree of mixture and thermal stratification exists in any method of charge preparation. In addition, in-cylinder turbulence results in charge stratification and was found to have significant effects on the combustion [36-38]. A visualization study by Richter et al. [39] showed that temperature stratification had more significant effects on the combustion duration than mixture stratification. To realise the benefits of thermal stratification in combustion control, as suggested by Noda and Foster [40], the ideal HCCI combustion system should comprise of a small hot region to initiate combustion and a greater amount of relatively colder region to prolong it. As there is no practical means established yet to control the degree of thermal stratification, application of thermal stratification for HCCI combustion control needs further research. However, with the advent of direct injection systems, creating and controlling mixture stratification have become feasible and are discussed in more detail in Section 2.3.1.

2.3   Control of HCCI Combustion

Thanks to decades of research, a range of potential parameters have been identified for HCCI combustion control. It includes compression ratio, intake pressure and temperature, fuel properties, mixture homogeneity, rate of exhaust gas recirculation, coolant temperature and many others. Several strategies for HCCI combustion control have been framed around the above parameters. In this section, the approaches of dual fuel operation and mixture stratification, which are applied in this project, are discussed in detail with a review on past research and recent developments.

2.3.1 Evolution of HCCI Combustion – Mixture Stratification

It has been reported by several researchers that a slight deviation in homogeneity in terms of mixture concentration and temperature has significant effects on the HCCI combustion process. In practice, preparation of charge that is absolutely homogeneous is in fact impossible. There exists a small degree of inhomogeneity in all methods of charge preparation. As this inhomogeneity has important effects on autoignition and combustion, one of the ways of finding a solution for combustion control is to have a variable degree of mixture and/or thermal stratification thereby adopting a change in the basic concept of HCCI itself.

Christensen and Johansson [41] carried out an experimental investigation to find out the role of mixture inhomogeneity caused by recirculated exhaust gases. The study revealed that mixture conditions had significant effects on the combustion. Mixture stratification significantly retarded ignition timing and reduced heat release rates. As the amount of fresh charge residing in the quenching zones was reduced due to stratification, reduced HC emissions were obtained. Richter and co-workers [39], used fuels with a blend of n-heptane (65%) and iso-octane (35%), compared the effects of mixture created by port injection and a more homogeneous mixture prepared using a separate mixing chamber on HCCI combustion. An optical study of combustion in an engine with these two mixtures showed that mixture in-homogeneity had significant effects on the onset of combustion. By a numerical study with seven different kinds of imposed theoretical stratification, Zheng and Yao [42] confirmed that mixture stratification resulted in reduced HC emissions. In addition, it was found that mixture stratification also resulted in some degree of temperature stratification.

In a recent study, by Jung et al. [43], using a rapid compression machine with DME (Dimethyl Ether) as a fuel, it was found that stratified charge would result in longer combustion duration and lower peak pressures compared to those resulted in by the combustion of homogeneous mixture. With charge stratification, the maximum load limit could be extended and higher IMEP were obtained, however, NO_x emissions increased at high loads. CO emissions were high at low loads while HC emissions were significantly reduced with charge stratification. Reduction in HC

emissions is an important advantage of mixture stratification as high unburned hydrocarbon emission is one of the main disadvantages of HCCI combustion and with homogeneous charges about 10% of the fuel can be emitted unburned [44].

Therefore, it is obvious that charge stratification is an important path to find a means of HCCI combustion control. One of the most practical ways of achieving and controlling the scale and level of charge stratification is direct injection of the fuel with or without other combustion control strategies such as EGR, dual fuel operation etcetera.

2.3.1.1 *Mixture Stratification by Direct injection*

Direct injection of the fuel into the cylinder is a feasible method of preparing stratified mixtures in the cylinder. In addition to that the scale and level of stratification can easily be controlled by varying the injection timing on cycle to cycle basis. It has been shown by several researchers that direct injection of the fuel during the intake stroke resulted in a homogeneous mixture and stratified charge could be created by injecting the fuel during the compression stroke. In addition, by using piston with a special bowl or groove on its crown, enhanced control of degree of stratification of the mixture can be implemented [45-50] as will be discussed in Section 2.3.1.2.

With a detailed spectral analysis of the HCCI combustion of gasoline, Kim et al. [48] studied the effects of stratification on the combustion characteristics by varying the injection timing from 300° to 60° BTDC. It was found that stratified charge suppressed low temperature reactions and resulted in advanced ignition. With stratified charge, like diesel engines, fast burning was observed at the initial stages of combustion and slower rate of combustion was observed at the latter stages. With homogeneous mixture, the rate of combustion was slow at the beginning of combustion and was faster at the end. By a study on rapid compression machine with CNG as the fuel, Huang et al. [51] reported similar results that charge stratification resulted in faster burning at early stages of combustion. By an experimental study on a direct injection engine with n-heptane as fuel, Ma et al. [52] confirmed that late injection timings resulted in stratified charge in the cylinder and reported that

stratified charge compression ignition (SCCI) resulted in reduced combustion durations and increased HC emissions. However, HC emissions were lower than conventional direct injection compression ignition (DICI) combustion.

2.3.1.2 *Mixture Stratification by Direct Injection and Piston Geometry*

The effect of injection timing on the degree of stratification can be enhanced by using specially designed piston with a groove on its crown. It provides a better control and increased degree of stratification due to fuel jet impinging is deflected by the piston groove. Marriott and Reitz [47] used a piston with a groove shaped like Mexican hat with a sharp edged crater on its crown in a gasoline direct injection HCCI engine. In that study, HC emissions were measured by fast response flame ionization detector (FID). The experimental study showed that higher combustion efficiency was obtained at light loads with stratification. Due to increased combustion efficiency and as less fuel was trapped in the quench zones thanks to charge stratification, retarded injection timings resulted in a significant reduction in HC emissions. Sjoberg et al. [46] studied the effects of inhomogeneity in a gasoline engine with a similar piston with a groove on its crown. By spray visualisation, they showed that stratified mixtures could be created by retarding injection timing of the fuel.

While HC emissions were reduced with retarded injection timings, it was found that NO_x and CO emissions increased at high engine loads. Ishiyama et al. [53] studied the effects of mixture homogeneity in an engine with a dog dish shaped groove on the piston and natural gas as fuel and found that thermal efficiency increased at moderate degrees of stratification. The study reported similar trends in emission with the earlier works on gasoline engines that stratification of natural gas resulted in reduced HC emissions and high CO and NO_x emissions. By an experimental study of compression ignition combustion of diesel, Kim et al. [50] confirmed that thermal efficiency increased with late injection timings, however, with an increase in smoke and NO_x emissions.

2.3.1.3 *Partial Mixture Stratification by Direct Injection*

In another approach by Canakci and Reitz [54], to obtain the combined benefits of homogeneous and stratified charges, the fuel was injected in parts at different timings and this method was called split injection strategy. The percent mass of gasoline supplied in each injection and dwell between the pulses were found to be effective parameters of combustion control and significant reduction in the emissions of HC and particulate matter were obtained. This strategy was also referred to as partially stratified charge compression ignition combustion.

With a similar approach by Wang et al. [55], gasoline was injected in two stages, first during the intake stroke and the second during the compression stroke and this strategy created partial stratification. By varying the split injection ratio, the amount of gasoline in stratified condition was varied. Increasing the duration of second injection resulted in longer combustion durations. However, NO_x emissions were higher due to fierce burning in the fuel rich zones created by late injection timings. In another study, in view of achieving high load limits and better ignition control, Wang et al. [56] investigated the effects of charge and temperature stratification using the combination of split injection and internal EGR. In a similar approach of Two Stage Direct Injection called TSDI, gasoline was injected in early and later during compression and exhaust gases were recirculated using negative valve overlap (NVO). Due to thermal stratification created by injecting the fuel during NVO, enhanced ignition was observed and COV of IMEP reduced. It was shown that both timing of the first stage injection and ratio of quantities of fuel injected in first and second stages were effective parameters for combustion control.

With an objective of extending the high load limits of gasoline HCCI, Yoshizawa et al. [57] studied an approach of engine operation with a fuel rich zone at the centre created by late direct injection and early injection at port which created a homogeneous charge. Combustion was achieved in two steps by igniting the rich fuel in the centre by a spark plug which led to the combustion of the rest of the fuel by autoignition. It was shown that this method reduced heat releases rates without sacrificing the benefits of high thermal efficiency. However, at a relatively high air-

fuel ratio of 26:1, NO_x emissions were higher (350 ppm) than that emitted by typical HCCI combustion (below 100 ppm).

2.3.1.4 *Factors Influencing the Effects of Stratification*

The influence of compression ratio and intake temperature on the effects of charge stratification was studied by using a gasoline direct injection engine by K. Lee and C. Lee [58, 59]. It was found that increase in compression ratio and intake temperature improved combustion stability of stratified charge combustion. With a high compression ratio and stratified charge, higher load ranges and high IMEP could be obtained.

Chang et al. [60] studied the effect of swirl and mixture preparation on gasoline HCCI combustion by measuring wall heat flux using heat flux probes. While external EGR was used to promote autoignition, part of the fuel was premixed by port injection and the rest was injected directly into the cylinder. It was found that retarding the direct injection resulted in larger spatial variations in heat flux. Increase in NO_x emissions due to high degrees of stratification was observed, however, significant reduction in NO_x resulted at conditions which resulted in delayed ignition.

The influence of boost pressure on the effects of injection timing of gasoline was studied by Canakci [61]. By increasing the boost pressure and retarding injection timing, increase in torque and combustion efficiency was obtained. However, at a given injection timing, HC emissions increased with an increase in boost pressure. NO_x emissions increased at late injection timings but reduced with an increase in boost pressure. That is, emission characteristics could be effectively controlled by injection timing at high torques obtained by increasing the intake boost pressure.

Therefore, it can be concluded that direct injection is a practical method to create mixture stratification and to control the degree of stratification in order to control HCCI combustion.

2.3.2   Dual Fuel HCCI Combustion

Given the state of the art electronic fuel injection systems that can precisely meter and deliver the fuels to the engines, used of two fuels of different properties has become one of the practically feasible methods of controlling the combustion. By dual fuel operation, preferential combustion of fuels of low and high autoignition temperatures [62] can be obtained. While the presence of low autoignition temperature fuel causes ignition and thereby indirectly controls ignition timing, the other fuel will help extend the combustion duration as it will burn later resulting in longer duration of overall combustion [26]. In other words, the ignition timing can be controlled by increasing the ratio of ignition promoter and combustion duration can be prolonged by increasing the ratio of the fuel having high octane rating. Apart from combustion control, dual fuel operation results in extended load limits, improved thermal efficiency and facilitates the use of alternative fuels.

The dual fuel HCCI combustion can be divided into two groups as those in which a low autoignition fuel is added to promote ignition and as those in which a high octane rated fuel is added to prolong combustion and suppress heat release rates. Tanapiyawanit and Huai [63] studied dual fuel HCCI combustion of n-heptane and iso-octane mixtures and found that higher loads could be operated by increasing the amount of iso-octane at a fixed flow rate of n-heptane. While HC emissions could be contained within 530 ppm for a range of loads, NO_x emissions were higher than single fuel n-heptane HCCI combustion at high loads, however, were still less than 500 ppm. Indicated thermal efficiency was higher at high loads than single fuel operation.

Hou et al. [64] studied the effect of blends of low octane and high octane fuels. The fuels of n-heptane and blends of n-heptane and MTBE (RON 108), ethanol (RON 111) and methanol (RON 114) were used. The combustion characteristics of each combination and pure n-heptane at same operating conditions were studied. It was found that increasing the proportion of the blended fuel suppressed low temperature reactions of n-heptane and altered ignition timing and location of peak pressure of the main combustion. Due to difference in fuel properties, the effects of MTBE, ethanol and methanol blends on the combustion were little different,

24

however, the trends were similar. Methanol blending had the most significant effect on combustion phasing and the highest load range could be obtained.

Lu et al. [65] used blend of n-heptane and ethanol and extended attainable IMEP to 5.1 bars as against 3.38 bars of IMEP operable with pure n-heptane with a significant increase in indicated thermal efficiency to about 50%. From the experimental study, it was found that increasing the ethanol content in the blend significantly delayed low temperature reactions and ignition timing. However, HC emissions increased significantly when the amount of ethanol was increased while CO emissions were stronger function of total equivalence ratio than the proportion of fuels.

As DME has high potential as an alternative fuel for compression ignition engines [66], several researchers have used DME as a fuel and ignition promoter for dual fuel HCCI combustion. Yao et al. [67] studied the characteristics of dual fuel HCCI combustion with port injection of DME and natural gas as fuels. As DME has a high cetane number (55 to 60), it was used to promote autoignition of natural gas. It was observed that varying the mass ratio of DME and natural gas was an effective parameter of combustion control. Ignition timing was found to be dependent on the percent of DME. Increase in DME resulted in increased cylinder pressures and NO_x emissions; however, HC and CO emissions were reduced. By a numerical simulation of DME and CNG dual fuel HCCI combustion, Kong [68] and Gusakov et al. [69] confirmed that increasing DME would result in advanced ignition timing and HC and CO emissions would increase when percent of CNG was higher than an optimum level.

Tsutsumi et al. [70] carried out an experimental study to find out the potential of ratio of DME and methane as a tool for combustion control. They confirmed that ignition timing was a function of the amount of DME. While the engine load could be increased by increasing methane at a given DME flow rate, the ratio of DME and methane had no significant effect on the rapidity of combustion. However, retarded ignition timing and lower heat release rates resulted when DME content was reduced. They also found that low temperature reactions were dependent on the amount of DME and not on methane.

In another experimental study, with DME and methanol as fuels, Yao et al. [71] studied the use of EGR to further extend the load limits of dual fuel HCCI combustion and found that use of EGR could not increase the load range. However, higher ratio of DME could be used without excessive pressure rise. Due to higher amounts of DME and EGR, peak pressures and HC emissions could be reduced significantly.

Jothi et al. [72] carried out similar experiments with Diethyl ether (DEE) and Liquefied Petroleum Gas (LPG) as fuels and studied the effects of EGR on the dual fuel HCCI combustion. It was found that varying the mass proportion of the fuels and rate of EGR had significant effects on the combustion. While DEE ignited first and LPG combusted subsequently, it was observed that EGR increased the thermal efficiency by about 2.5%. Increasing EGR rate reduced heat release rates, NO concentration and HC in the exhaust gases.

Therefore, from the above discussion, it is obvious that dual fuel operation extends the high load limits of HCCI combustion and ignition timing can be controlled by varying the ratio of the low octane and high octane fuels. However, increasing the ratio of high octane fuel may result in higher HC emissions.

2.3.2.1 *Premixed/Directly-Injected Dual Fuel Engines*

In order to have a direct control of ignition timing of a dual fuel HCCI engine, one of the fuels that has low autoignition temperature can be directly injected into premixed charge of air and higher number fuel. An array of combination of fuels has been studied by several researchers with homogeneous mixture of one fuel and direct injection of the other.

Yeom et al. [73] used LPG, a low carbon high octane fuel, and DME as fuels and compared the results obtained with the characteristics of single fuel gasoline HCCI combustion. While LPG was injected at the port, DME was directly injected to have a control over ignition timing in addition to variable valve timing (VVT). It was found that HC and CO emissions were higher than gasoline HCCI combustion, however, heat release rates were lower. Another study by Yeom and Bae [74],

reported that similar results of higher HC and CO emissions were obtained with gasoline as the premixed fuel and DME as the direct injected. Carlucci et al. [75] used CNG as the premixed fuel with direct injection of diesel and obtained reduction in particulate matter but NO_x emissions increased due to stratification of diesel.

In a more recent study with port injected diethyl ether (DEE) and diesel direct injection (fixed at 24°BTDC) as fuels, Cinar et al. [76] studied the dual fuel HCCI combustion. It was found that combustion of premixed DEE occurred earlier than diesel. Increasing the premixed ratio of DEE was limited to 40% due to increased knock tendency and higher emissions of NO_x, HC and CO than single fuel HCCI combustion were observed.

Ghazikhani et al. [77] carried out an experimental study on a dual fuel engine with port injected gasoline and directly injected diesel as fuels with high EGR to promote auto ignition of gasoline. It was found that injection timing of diesel had significant effects on mixture stratification. HC and CO emissions increased when EGR rate and engine speed were increased. However, using gasoline as the premixed fuel and direct injection of diesel, Kim et al. [78] had reported that HC and CO emissions could be significantly reduced by heating intake air.

In another recent approach on dual fuel operation, the fuel having low autoignition temperature can be homogeneously premixed and the other fuel having higher autoignition temperature can be directly injected. The directly injected fuel gets ignited by active thermo atmosphere created by the heat released by the prior combustion of the premixed fuel. However, the proportion of fuels still has significant effects on combustion along with mixture stratification.

Ma et al. [79] studied characteristics of a dual fuel engine with premixed n-heptane and directly injected diesel as fuels. The effects of premixed ratio and injection timing of diesel on the combustion were investigated. It was found that the combustion occurred in three stages: low temperature reactions of n-heptane, HCCI combustion of n-heptane and diffusion burning of diesel. Significant effects on combustion were observed when the injection timing of diesel was varied from 5°, 7° to 9° BTDC and led to a conclusion that changing premixed ratio of n-heptane

and injection timing were effective parameters of combustion control. Similar pattern of three stage combustion was confirmed by Kim and Lee [80] by their experiments with port injected n-heptane and directly injected diesel as fuels. It was also found that, with a fixed injection timing of diesel at 158° BTDC, increasing the premixed ratio significantly advanced the HCCI combustion of n-heptane, it resulted in drastic increase in NO_x emissions. However, it may be noted that as diesel has low volatility, classical homogeneous mixture conditions and combustion characteristics cannot be created by direct injection of diesel.

In a recent experimental study, the effects of mixture stratification on a dual fuel HCCI engine with a bowl on the piston crown were studied by Chen et al. [81]. The port injection of DME resulted in homogeneous mixtures of DME and methanol was directly injected at different timings ranging from 66° BTDC to 6° BTDC. It was found that methanol concentration and its injection timing had significant effects on the combustion. In addition, a numerical part of the study revealed that direct injection of methanol and its timing resulted in thermal and mixture stratification. At retarded injection timings of methanol, heat release was smoother and high loads could be operated with a significant reduction in HC emissions. However, at low flow rates of DME, early injection of methanol developed higher IMEP than with late injection.

Ji et al. [82] carried out a similar experimental study with port injected n-heptane and directly injected iso-octane. The effects of premixed ratio of n-heptane and that of injection timing of iso-octane were studied. At a total equivalence ratio of 0.37 and at different premixed ratios ranging from 0.30 to 0.70, the injection timing of iso-octane was varied from 15° to 35° BTDC. It was found that iso-octane was ignited due to the heat released by the prior HCCI combustion of n-heptane. When the premixed ratio of n-heptane was increased and injection timing of iso-octane was advanced, the effect of thermo atmosphere on the ignition of iso-octane enhanced. However, NO_x emissions increased and HC and CO emissions reduced at a moderate retardation in injection timing.

From the above discussion, it can be concluded that proportion of fuels and mixture stratification have significant effects on combustion and by using a direct

injection system, a practical HCCI combustion control system may be implemented. Therefore, by combining the methods of dual fuel operation and varying stratification by direct injection, HCCI combustion can be controlled. In this project, it is proposed to use gasoline and CNG dual fuel combustion system with a variable degree of CNG stratification in the premixed charge of gasoline and air. By using the proposed strategy, high HC emissions resulting from the presence of high octane fuel in the mixture can be reduced by stratifying its distribution in the cylinder.

2.4 Summary

The fundamentals and basic characteristics of HCCI combustion have been discussed in this chapter. The importance of HCCI combustion control and different methods studied by researchers in the past have been reviewed and presented. The potential of the combination of dual fuel operation and mixture stratification for HCCI combustion control has been highlighted.

CHAPTER 3

METHODOLOGY

3.1 Introduction

This chapter describes the engine test facility used for this study. The CNG direct injection engine available in the university has been suitably modified to facilitate dual fuel operation by adding a liquid fuel injection system. This engine has various features suitable for research such as measurement of engine operating parameters, control of injection parameters of CNG direct injection, control of exhaust gas recirculation and optical access to the combustion chamber. The important systems that were used for this study include the computer software interfaced to the engine control unit (ECU) for controlling and measuring the engine operating parameters by using various sensors and the pressure measurement system. The engine is equipped with a pressure transducer to measure instantaneous pressure inside the cylinder and a LABVIEW program is used to log the pressure data with respect to crank angle.

This chapter also describes the data analysis and experimental procedures. The equations and models used for the analysis of combustion and performance characteristics of the engine are listed in this section. Techniques applied to operate the engine in HCCI mode and at given conditions are also presented along with experimental procedures followed.

3.2 Description of the Engine Test Facility

The engine used for this experimental study houses the fuel system of direct injection of compressed natural gas (CNG) or a gaseous fuel and has high compression ratio suitable for operation with CNG as a fuel with spark ignition. This engine, briefly mentioned as CNG DI Engine in this thesis hereafter, is a single

cylinder water cooled engine coupled to an electric dynamometer that can be used for starting the engine and measuring the brake torque produced by the engine. Figure 3.1 shows a schematic drawing of the CNG DI engine.
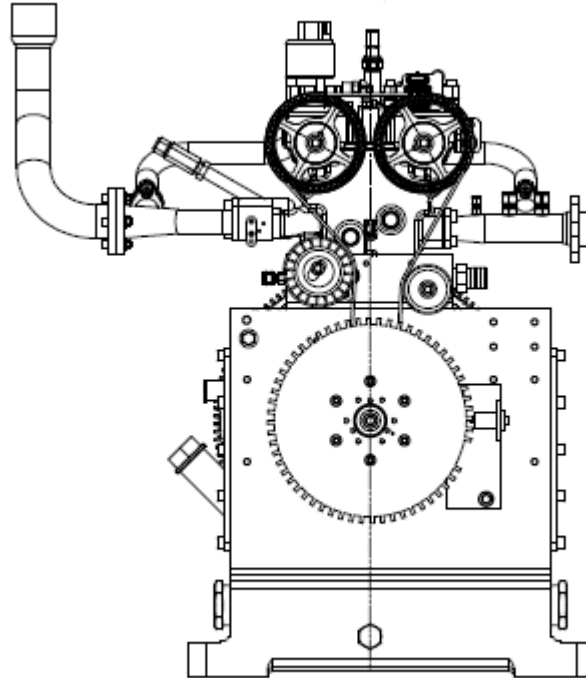
Figure 3.1 The single cylinder CNG DI research engine [83]

An electric heater is provided to heat the lubricant oil to help warm up the engine faster. A separate control unit controls the operation of the pumps and the temperature of the oil and water by temperature controllers. The control unit also controls the operation of the dynamometer which also serves as the starter motor and the engine can be motored at a wide range of speeds. There are standard features of safety included in the control unit such as emergency switch, automatic shut down upon the excessive rise in the oil and/or coolant temperatures or any abnormal conditions of electrical power supply.

3.2.1 Features of the CNG DI Engine

The CNG DI engine is basically designed for operation with gaseous fuels with particular attention to operation with CNG. As The CNG has higher octane rating which means better knock resistance when combusted with spark ignition, the engine

has been designed to have a high compression ratio of 14:1 so as to assist spark ignition and to realise the benefits of higher thermal efficiency.

Another notable feature of this engine is that it has a direct injection system with optimised valve timing events for gaseous fuels. The direct injection of CNG minimizes the displacement of air that would be caused by low density CNG if it is injected at the intake port. This leads to higher volumetric efficiency which is otherwise significantly lower with port fuel injection or carburetion. The specifications of the engine are listed in Table 3.1.

Table 3.1 Summary of specifications of the CNG DI engine.

Fuel Type	Gaseous Fuel (CNG)
Fuel Supply System	Direct Injection (DI)
	a. High Pressure Direct injection (12 to 18 bars) b. Air assisted low pressure injection (4 to 6 bars).
No. of Cylinders	Single cylinder (399.25 cc)
Bore	88 mm
Stroke	132 mm
Compression Ratio	14:1 (Geometric)
No. of Valves	4
Valve Timing Events	
Intake Valve Open (IVO)	372° BTDC
Intake Valve Closure (IVC)	132° BTDC
Exhaust Valve Open (EVO)	225° ATDC
Exhaust Valve Closing (EVC)	350° BTDC

3.2.2 Homogeneous and Stratified Operation Pistons

In addition to the special features of high compression ratio and direct fuel injection, the CNG DI engine has the provision to operate with homogeneous or stratified CNG distribution inside the cylinder. There are two different types of pistons with

two different shapes of bowls on the face as shown in Figure 3.2 and Figure 3.3. The homogeneous piston has a small bowl and the stratified piston has bigger bowl with its centre aligned to the axis of fuel injection.
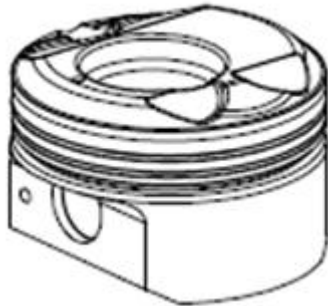
Figure 3.2 Piston with larger bowl to create CNG stratification [83]
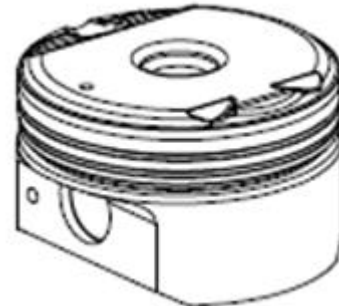
Figure 3.3 Piston with smaller bowl creates homogeneous mixtures [83]

When the homogeneous piston is used a relatively more homogeneous mixture of CNG and air is created in the cylinder regardless of the timing of injection. The stratified piston creates a stratified charge of CNG in the cylinder especially when the fuel injection is retarded close to the TDC.

Figure 3.4 shows the arrangement of piston and injector for homogeneous and stratified conditions. The axis of the injector is aligned to the centre of the bowl of the stratified piston. When the CNG is injected, it impinges on the bowl and is guided by the bowl to create a stratified mixture in the cylinder. The injector and the spark plug are located in such a way that rich mixtures are formed near the spark plug tip. The homogeneous piston has a smaller bowl just to accommodate the spark plug end.

It has been shown experimentally [84, 85] that the use of a larger bowl creates stratified mixtures when the CNG is directly injected. In this method, the degree of stratification is largely dependent on the distance between the injector tip and the bowl. At a given engine speed, the degree of stratification can be varied by changing the distance between the piston and the injector at the start of injection. In other words, the degree of stratification can be altered by varying the injection timing of the CNG.
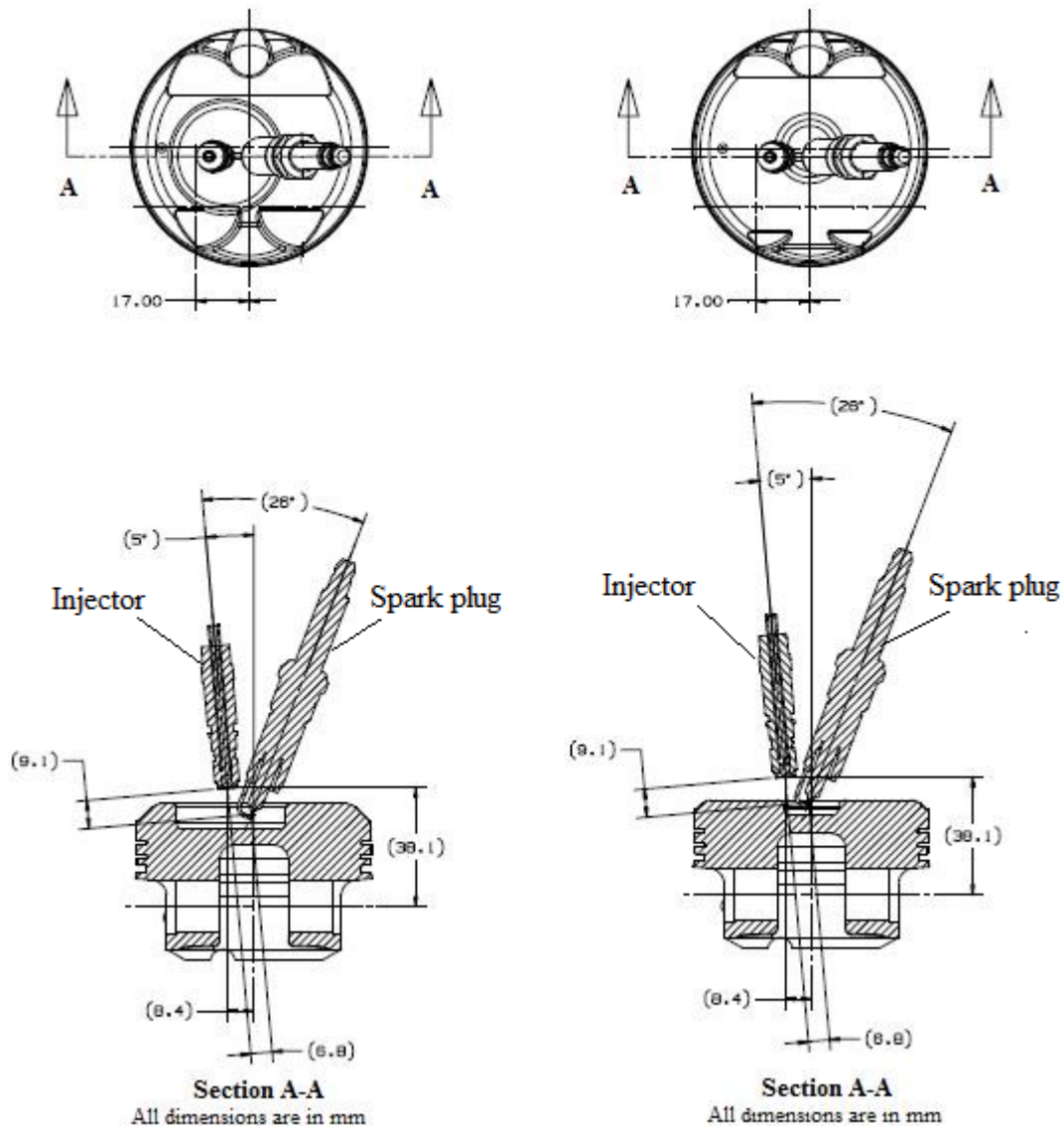
Figure 3.4 The arrangement of piston, injector and spark plug for stratified and homogeneous mixture formation [83].

However, injection during the intake stroke at early injection timings of 300° BTDC has least influence on the mixture formation and results in homogeneous mixtures. Similarly, the degree of stratification is particularly effective when the CNG is injected after the intake valve is closed (132° BTDC). For this project, the stratified piston was used so as to create stratified mixing of CNG in the premixed gasoline charge.

3.3 Modifications of the Engine for Dual Fuel Operation

3.3.1 CNG Direct Injection System

The direct injection system of the CNG DI engine as supplied by the manufacturer was used unaltered. The direct injection system consists of a fuel injector that has a large orifice diameter to match the low density of gaseous fuels and is fitted to the fuel rail connected to the CNG supply line. The fuel, CNG, is supplied from the storage tanks to the fuel rail through pressure regulators to reduce and maintain the pressure in the fuel rail and thereby the injection pressure. The CNG DI system, which is operated by the engine ECU, can be controlled by the interface software. The injection parameters such as injection timing with respect to the crank angle and the injection duration can be controlled by this software. A CNG mass flow meter is used to measure the mass flow rate of CNG as shown in Figure 3.5. A more detailed discussion on the method of measurements of CNG flow rate can be found in Section 3.5.2.

3.3.2 Gasoline Fuel Injection System

An additional gasoline supply system was fitted to the CNG DI engine to operate with CNG and gasoline simultaneously so that the engine could meet the requirement of dual fuel capability for this study. The gasoline was injected into the manifold at a location about 44cm from the intake valve. The distance between the point of gasoline injection and the intake valve was kept long to ensure homogeneous mixing of gasoline and air [86, 87]. The gasoline manifold injection comprises of two systems; the basic fuel supply system and an electronic control system that is synchronized with the CNG DI engine.

The main components of the gasoline fuel injection system are a fuel tank, fuel pump, fuel rail, pressure regulator and an injector. An in-tank submersible electrical fuel pump was employed to pump the gasoline from the tank into the fuel rail that houses the fuel injector. Since the manifold pressure varies with engine speed, it is necessary to use a fuel pressure regulator to maintain the pressure difference between

the manifold pressure at the tip of the injector nozzle and the fuel rail. This pressure difference is referred to as fuel injection pressure and it was kept at 3 bars to match the specifications of the injector throughout the experiments.

The fuel rail and the injector boss were designed and fabricated to match the specifications of the gasoline injector. A detailed drawing of the fuel rail assembly can be found in Appendix A. The fuel injector boss was fabricated and positioned with high precision to inject the fuel along the axis of the manifold so as to minimize wall wetting. With an elevated inlet air temperature of 320°C and given the moderately high volatility of gasoline the effect of wall wetting was assumed to be negligible. Figure 3.5 is the schematic representation of the gasoline fuel supply system.
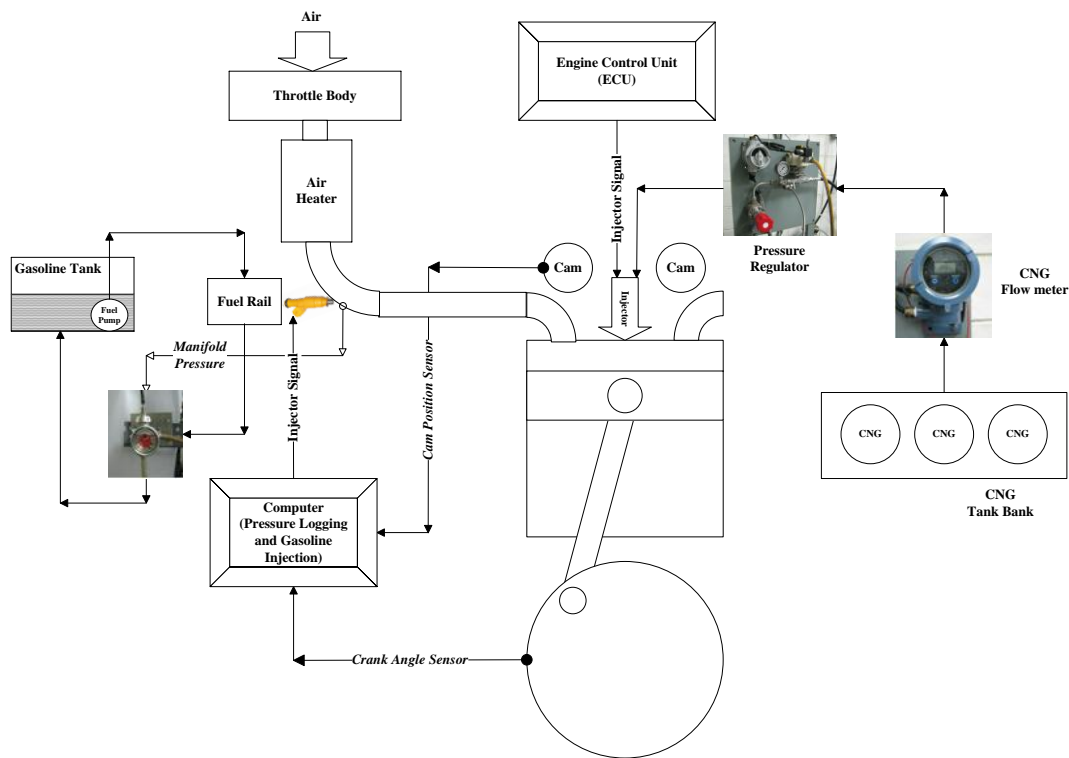
Figure 3.5 Gasoline and CNG fuel supply systems.

A commercially available gasoline port fuel injector was used and its specifications can be found in Table 3.2. This injector has low flow rates and was selected to match the requirement of injecting very low quantities of gasoline to operate in HCCI mode with ultra lean mixtures. The injector comes calibrated in the

36

factory to inject and precisely meter the volume against the specified injection duration.

Table 3.2 Specifications of the gasoline injector.

Make/Part Number	Bosch/ 0 280 155 710	
Type	High Impedance	
Fuel injection Pressure	3 bar	
Fuel flow rate	191.8 cc/min	
Power Supply	12V DC	

3.3.2.1 *Control of the Gasoline Fuel Injection using LabVIEW*

The essential technical requirement of any fuel injection system is to precisely meter the quantity of the fuel and to inject it at the required timing synchronized with the engine speed and piston position during the required stroke. In the modern day vehicles, this task is carried out by electronic control units with associated sensors and actuators in the fuel injection system. For this study, a separate control system that comprises of a LabVIEW program and an injector driver circuit was designed and used for gasoline fuel injection. As mentioned earlier, the CNG DI engine is equipped with an electronic control unit (ECU) and sensors for controlling the CNG direct injection and engine operational parameters. The original cam position sensor used by the ECU of the CNG DI engine and the crank angle sensor that was connected to the pressure data acquisition program were used for the control system.

Figure 3.6 shows the schematic representation of the control system of gasoline injection. The task of controlling the injection process can be divided into: identification of TDC, identification of the power stroke and measurement of crank angle.

The crank angle sensor produces 720 pulses for every rotation of the crank. That is, for every 0.5° of rotation of the crank a tick is produced. This is referred to as the resolution of the crank angle sensor and is termed as 'N' signal. An additional pulse is produced by the crank angle encoder for every revolution that is called TDC

trigger. However, when the engine is assembled it is difficult to match the TDC trigger exactly to the TDC position. Instead the offset from the position of the TDC is measured after assembling the engine and its value is used for the calculations of the real position of TDC. It should be noted that this TDC signal is produced for every revolution and not every thermodynamic cycle which would complete in two revolutions of the crank for a 4 stroke engine. In order to find the TDC at which the compression stroke ends, a sensor is fitted to the cam shaft.
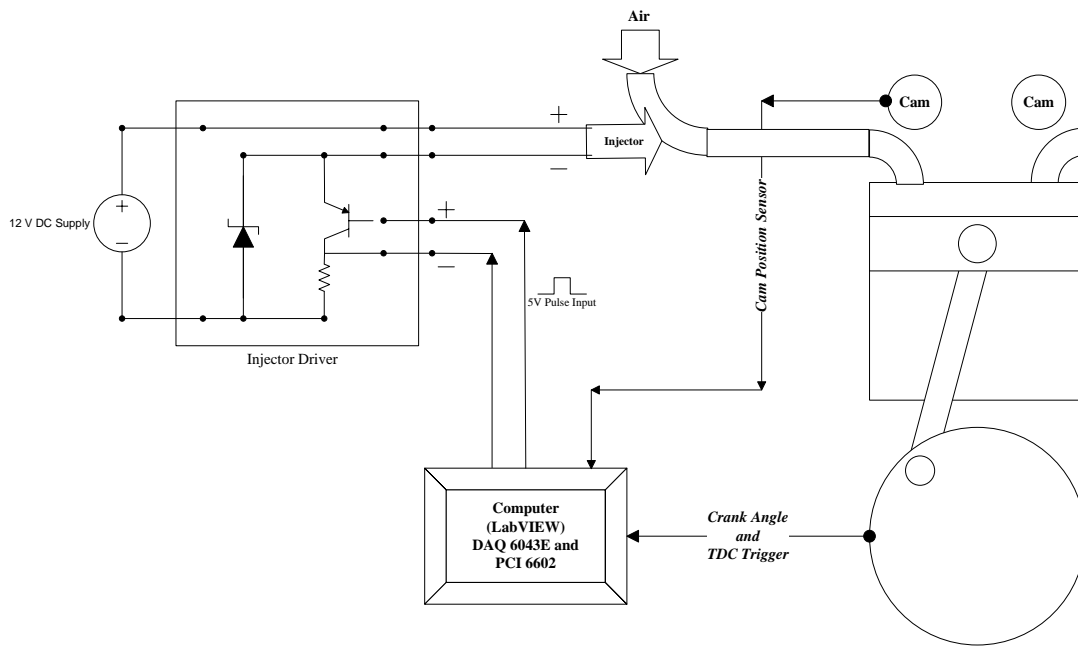
Figure 3.6 LabVIEW based control system of gasoline injection.

The cam shaft produces a pulse at every revolution of the cam which is referred to as "Ge" signal. As the cam shaft rotates at half the speed of the crank for a 4 stroke engine, the Ge signal is produced only once for every two revolutions of the crank or for every thermodynamic cycle. By using both N and Ge signals, the TDC at which compression stroke ends can be identified and by using the crank angle sensor the start of injection and its duration in terms of crank angle degrees can be defined.

An oscilloscope was connected to a CAM sensor, Crank Angle Sensor, TDC trigger, 5V pulse train output and across the terminals of the gasoline injector. The oscilloscope was used to monitor the proper functioning of the gasoline injection

process and to measure the injection duration. The actual injection duration was the time duration measured across the terminals of the gasoline injector.

Figure 3.7 shows the various sensors signals and their phasing with respect to the crank position. Although the control system is capable of changing the timing of the gasoline injection, the start of the gasoline injection was fixed at 350° BTDC, that is, at the timing of exhaust valve closure so as to eliminate the loss of fresh charge through the exhaust valves.
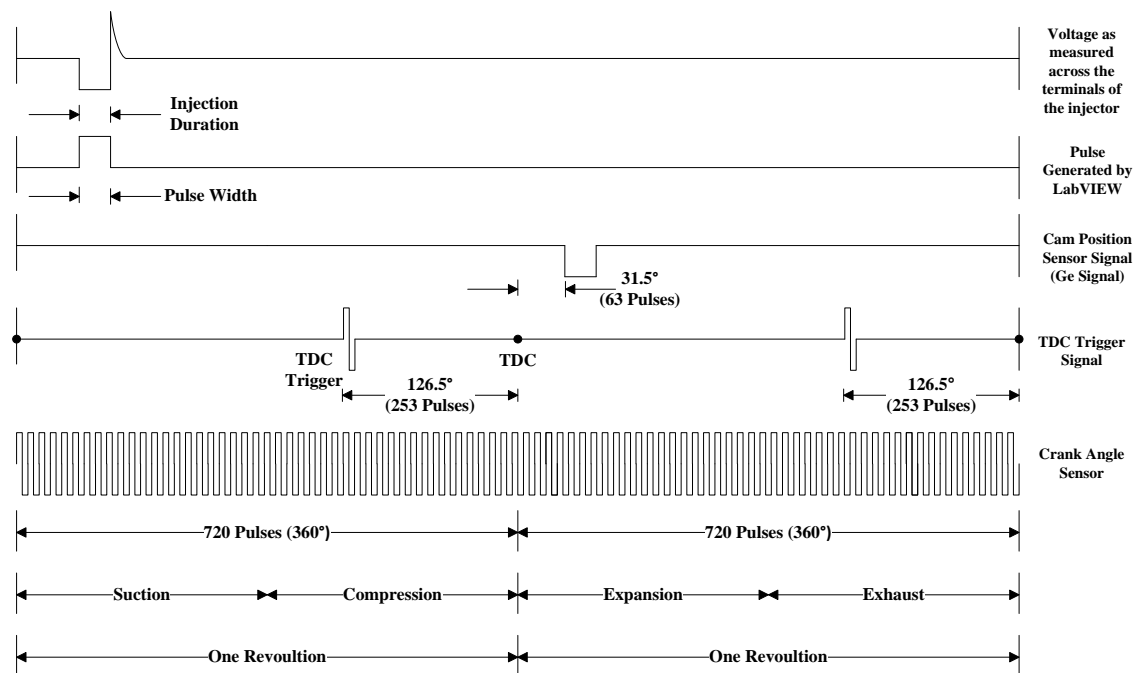
Figure 3.7 Phasing of different sensor signals with respect to crank angle.

3.4   Modifications of the Engine for HCCI Operation

As discussed in Chapter 2, there are several methods used by researchers to achieve the HCCI combustion of gasoline at moderate compression ratios. They include the use of heated intake air by separate electric heaters or by external or internal exhaust gas recirculation, use of additives or fuels of low autoignition temperatures as ignition promoters, spark assistance etcetera. The recirculation of exhaust helps achieve HCCI combustion but has significant effects on the combustion characteristics making it difficult to isolate the effects of CNG direct injection. Therefore for this study, the method of intake air heating using an electric heater has

been chosen over exhaust gas recirculation in order to study the sole effect of CNG direct injection on the combustion. The use of ignition promoters also was ruled out for the same reason.

3.4.1 Intake Air Heater

Application of the method of heating intake air to achieve HCCI combustion has practical limitations given the high flow rates and low heat transfer coefficients of air. The open coil heaters are used for heating fluids that have low heat transfer coefficient such as air. The selection of the air heater is also dependent upon the flow rate of air and the temperature required. For the purpose of this study, an open coil air heater was fabricated in house and attached to the intake manifold. The schematic of the intake system is shown in Figure 3.8. The air heater is attached to the intake manifold downstream to the throttle body and air flow sensors and upstream to the intake valves.
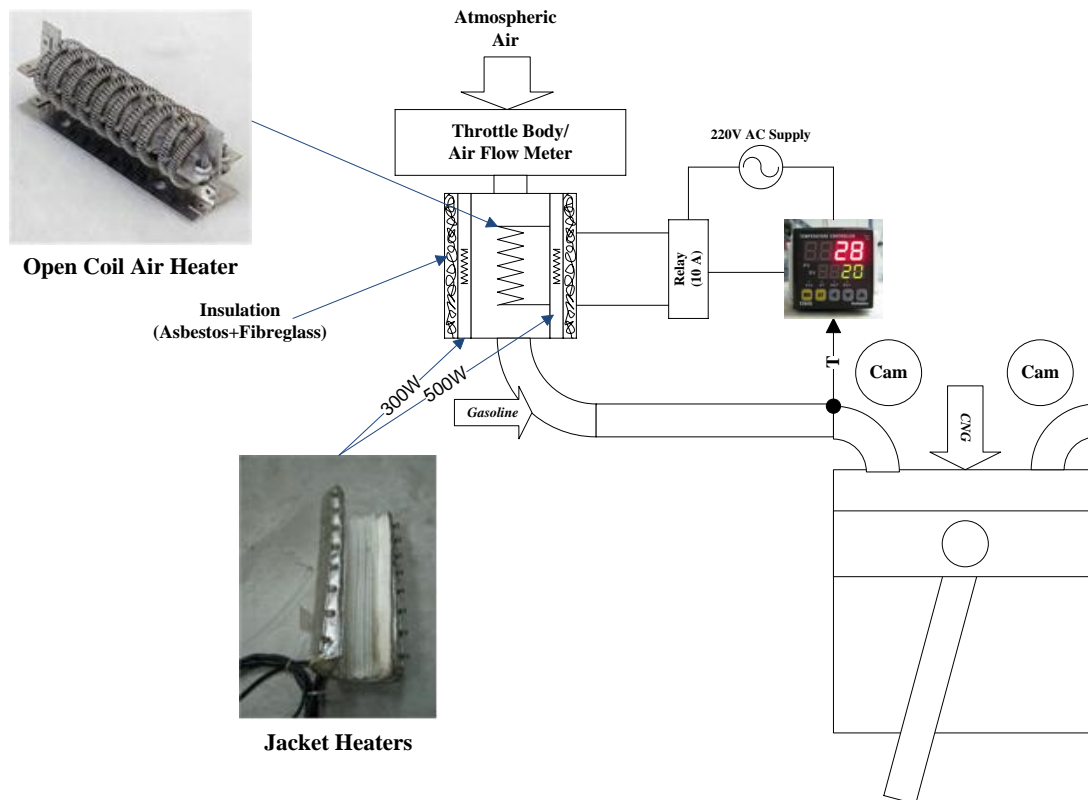
Figure 3.8 The modified intake system added with intake air heater

The intake air stream was heated by direct contact with the electrified high resistance coil made of Nickel(Ni) and Chromium(Cr) alloy commercially known as Nichrome. The high corrosion resistance even at elevated temperatures makes Nichrome one of the most widely used materials for the manufacture of heating element. It also has high electrical resistance with good thermal and mechanical properties. Nichrome wire of 1mm diameter was coiled and the coils were wound around a mica structure. The specifications and drawing of the intake heater are listed in the following Table 3.3.

Table 3.3 Specifications of the open coil air heater.

Type	Coil Type
Specifications	Nichrome (1mm wire) coiled
Power Rating	1.6 kW
Maximum Wire Temperature	780°C
Maximum Air Outlet Temperature	550°C
Maximum Current	6.5 A
Voltage	220-230V

In addition to the open coil heater, two jacket heaters of 300W and 500W were wrapped around the heater pipe to achieve uniform heating and reduce temperature difference within the hot air stream. The jacket heaters also served as the insulators and reduced the power required by reducing the heat transferred to the inner walls of the pipe thereby effectively restricting *thermal bridging*. A thick layer of insulation of fibre glass was provided on the heater pipe. The whole path of the intake air stream from the inlet of the air heater to the point of entry to the engine was insulated with a sufficiently thick layer of fibre glass. Aluminium foil was wrapped around the fibre glass insulation so as to prevent the fibre glass from absorbing moisture from the atmospheric air which in turn would increase the thermal conductivity of the insulation with the course of time.

A PDI temperature controller was used to control the intake charge temperature. Two K type thermocouples were used to measure the intake air (T_{air}) and charge temperatures (T_{in}). The thermocouples were mounted at the centre of the intake manifold to measure the temperature of the air stream. Sufficient care was taken to

ensure that the thermocouples were not in contact with the walls of the manifold. The output signal from the thermocouple installed after the gasoline injector (T_{in}) was fed to the closed loop temperature controller and the intake charge temperature was kept constant at 300±1°C. This temperature is referred to as the intake temperature in this study and it was kept constant throughout all the experiments. A schematic drawing of the experimental facility of the dual fuel HCCI engine is shown in the Figure 3.9.
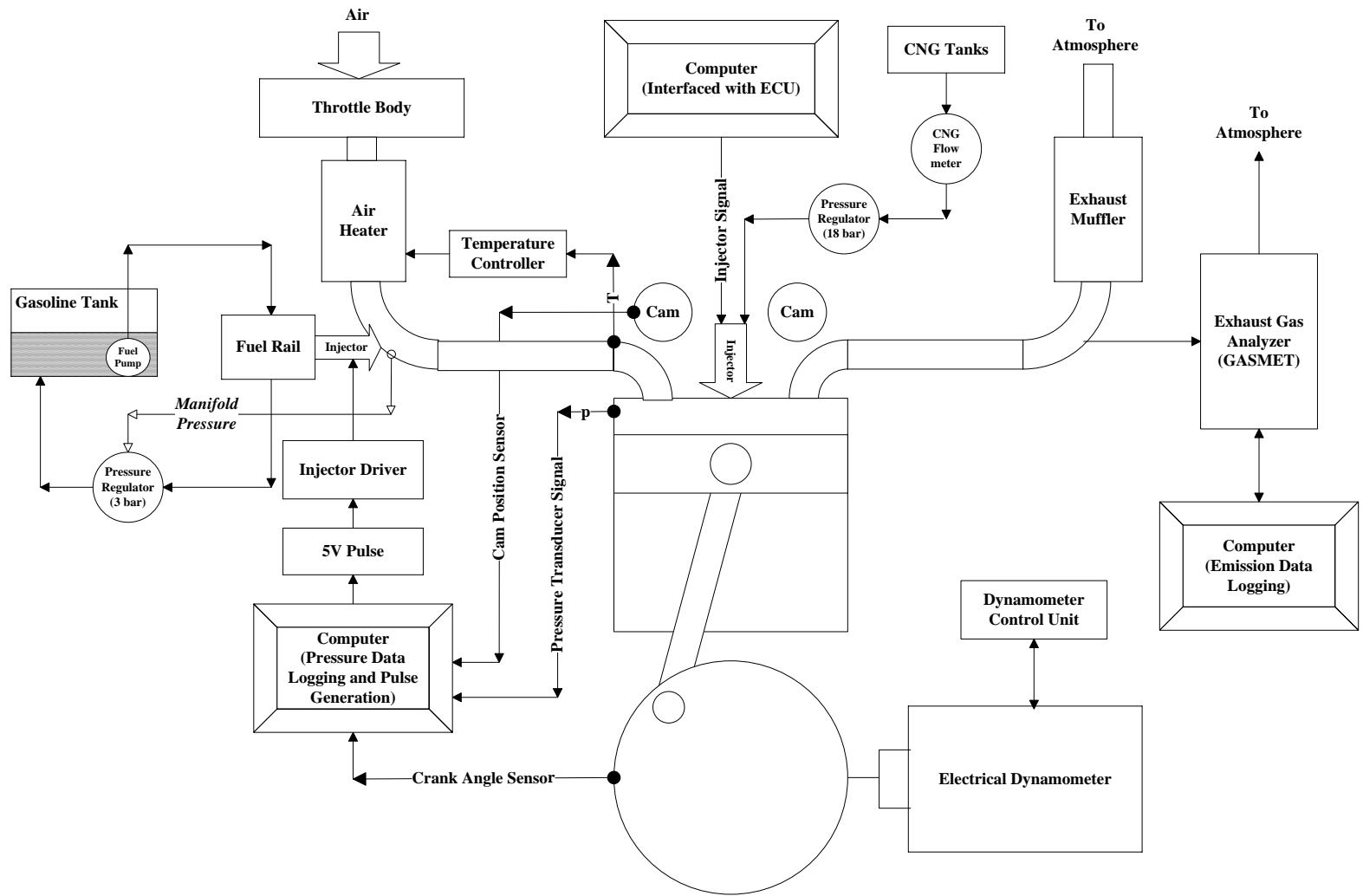
Figure 3.9 Experimental setup

43

3.5   Measurement Equipment and Data Acquisition

3.5.1   Parameters Measured by Engine Sensors and ECU Interface Software

The electronic control unit is programmed to manage the engine operation with pre-loaded engine maps of parameters. With the usage of interface software, it is possible to manually alter the engine operating conditions. The interface software can also be used to measure the engine operating parameters by using the various sensors connected to the ECU.

Figure 3.10 shows the output screen of the ECU interface as shown in the computer screen listing the engine operating parameters.
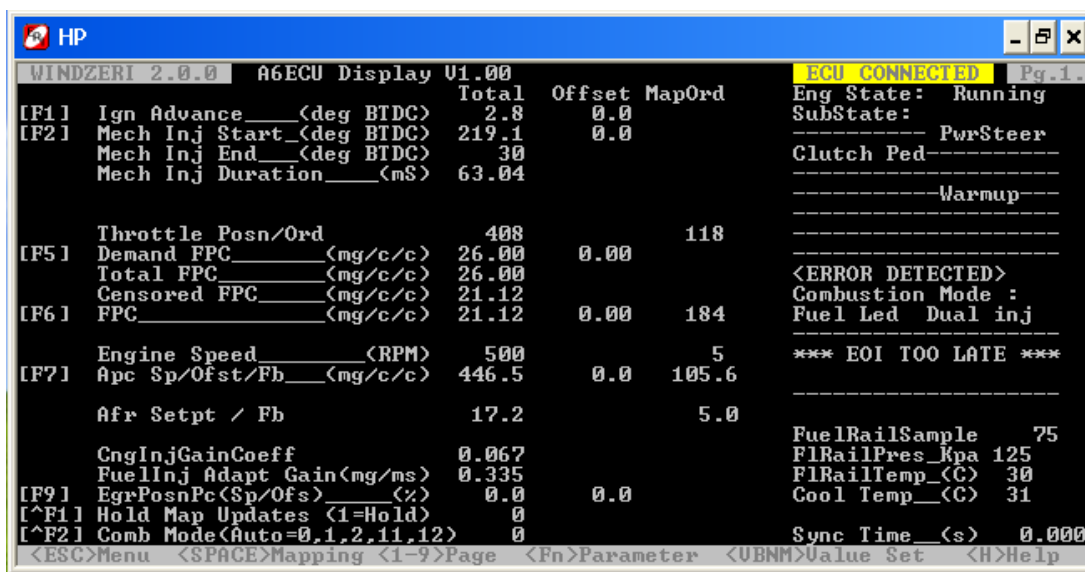
Figure 3.10 Sample interacting screen of the ECU interface as shown to the user

Apart from the measurements of the engine operating conditions such as the engine coolant and oil temperatures, intake air temperature and its flow rate and fuel injection pressure, the ECU interface can be used to control the injection timing and duration. The ECU and the interface software are the main controlling tools of the event of CNG direct injection. The quantity of CNG injected can be metered by varying the duration of injection at a given fuel pressure that is maintained constant in the CNG fuel rail.

44

3.5.2 Measurement of Mass Flow Rates of Air, Gasoline and CNG

The flow rate of air was measured by the mass flow sensor (MAF) fitted to the engine. The value of mass flow rate was measured and logged by the ECU interface. The engine was operated with wide open throttle throughout the experiments. The CNG flow rate was measured by using a micro motion mass flow meter. The flow meter is also known as inertial or Cariolis flow meter and it measures the mass flow rate of a fluid that flows through it. The specifications of the CNG mass flow meter are given in Table 3.4.

Table 3.4 Specifications of the CNG flow meter.

Flow accuracy	±0.05% of flow rate
Gas accuracy	±0.35% of flow rate
Density Accuracy	±0.0002 g/cc
Wetted Materials	304L, 316L Stainless steel or Nickel Alloy
Temperature Rating	-400 to 800°F (-240 to 427°C)
Pressure Rating	1450 to 6000psi (100 to 413 bar)

The quantity of gasoline injected can be calculated from the injection duration. The injection duration of gasoline was measured using an oscilloscope connected across the injector terminals as discussed in Section 3.3. From the measurements of air, gasoline and CNG flow rates, the equivalence ratios can be calculated as follows:

Individual equivalence ratio of gasoline is given by,

$$\varphi_g = \frac{\dot{m}_g \times AF_{St-g}}{\dot{m}_a} \tag{3.1}$$

Individual Equivalence ratio of CNG is given by,

$$\varphi_{CNG} = \frac{\dot{m}_{CNG} \times AF_{St-CNG}}{\dot{m}_a} \tag{3.2}$$

The total equivalence ration is defined as and calculated by:

$$\varphi_{Total} = \frac{\{\dot{m}_g \times AF_{St-g}\} + \{\dot{m}_{CNG} \times AF_{St-CNG}\}}{\dot{m}_a} \tag{3.3}$$

Where, φ_g - Individual equivalence ratio of gasoline.

φ_{CNG} - Individual equivalence ratio of CNG.

φ_{Total} - Total equivalence ratio.

$\dot{m}_a$ - Mass flow rate of air in g/s.

$\dot{m}_g$ - Mass flow rate of gasoline in g/s.

$\dot{m}_{CNG}$ - Mass flow rate of CNG in g/s.

AF_{St-g} - Stochiometric air fuel ratio of gasoline = 14.7.

AF_{St-CNG} - Stochiometric air fuel ratio of CNG   = 17.2.

3.5.3 Engine Brake Torque Measurement

The engine is coupled to an electric dynamometer which can be used to measure the brake torque produced and to motor the engine. The dynamometer is of the eddy current type and has a maximum rating of 50Nm of torque at a maximum speed of 100 revolutions per second. The dynamometer was calibrated by applying a load using known dead weights before conducting the experiments. From the measurements of the torque produced by the engine, the brake power can be calculated as follows:

Brake power (BP) $=$ $\tau\omega$ (3.4)

Where, τ - Brake Torque measured by the dynamometer in Nm.

ω - Angular velocity and is given by, $\omega = 2\pi N$ in rad/s.

N   - Speed of the engine in rev/s.

From the equation 3.4, it can be observed that the power delivered by an engine is the product of torque and speed of the engine. Depending on the application of the engine, the range of torque is specified at a given engine speed. For most of the automotive applications, it is preferable to have a flat torque curve for the entire engine speed range.

3.5.4 In-cylinder Pressure Measurement

A water cooled piezoelectric pressure transducer was used to measure the instantaneous pressures inside the cylinder. This transducer works on the principle of the piezoelectric effect. The application of pressure on certain materials results in the production of a small electrical charge. This effect is called piezoelectric effect and is widely applied to build devices for measuring pressure.
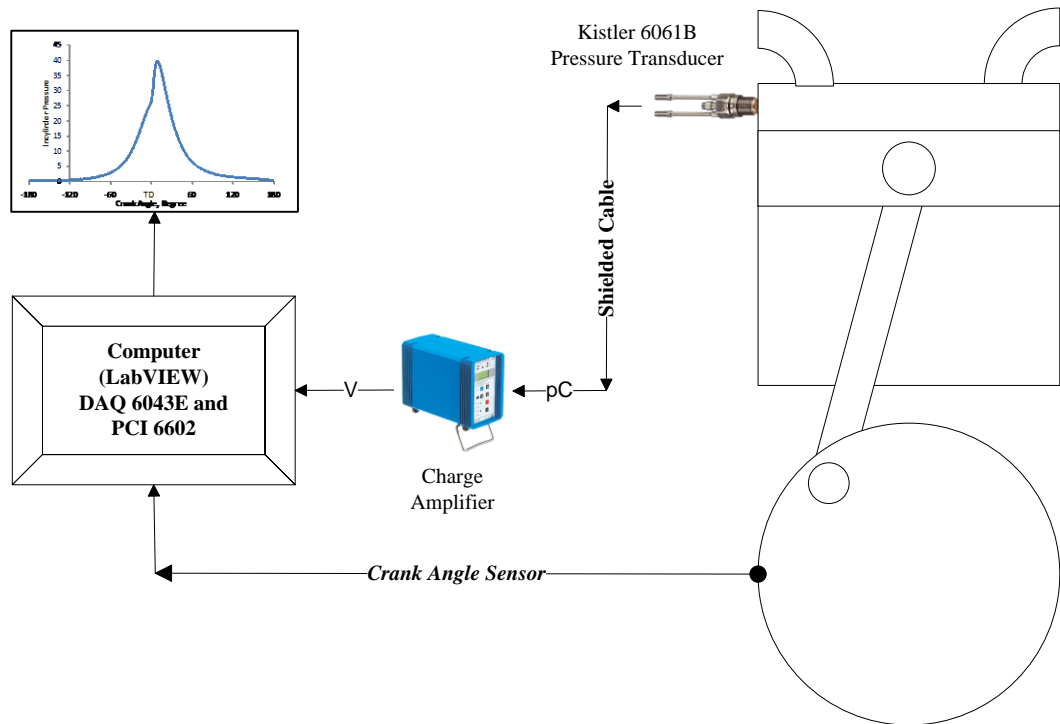
Figure 3.11 Incylinder pressure measurement system

A pressure transducer (Kistler 6061B) is fitted to the engine at top of the combustion chamber. The pressure transducer generated a small charge in proportion to the pressure inside the cylinder. This charge output from the pressure transducer was fed to the charge amplifier. A high impedance shield cable was used to feed the charge output to the amplifier to avoid any signal loss as the charge output was very small. The charge amplifier converted the charge from the transducer into voltage and then amplified the voltage as per the amplification factor preset by the user. The amplified voltage was fed to the computer that housed the data acquisition system (DAQ 6043E) loaded with a LabVIEW program that was developed for the purpose of engine pressure measurement and data analysis. The DAQ system was also connected to the crank angle encoder and the LabVIEW program was designed to

47

show the instantaneous pressures plotted against the crank angle as shown in Figure 3.11. The LabVIEW program displayed the pressure against the crank angle or cylinder volume and stored the data to a computer disk.

3.5.5   Emission Measurement

An exhaust gas analyser operating on the principles of Fourier Transform Infrared (FTIR) manufactured by GASMET was used to measure the engine emissions.

Table 3.5 Specifications of GASMET exhaust gas analyzer

General parameters	
Measuring Principle:	Fourier Transform Infrared, FTIR
Performance:	simultaneous analysis of up to 50 gas compounds
Response time:	typically <<25s, depending on the gas flow and measurement
Operating temperature:	15-25°C non condensing
Storage temperature:	-20 - 60°C non condensing
Power supply	100-115 or 230V / 50-60 Hz
Power consumption:	300 W
Measuring parameters	
Zero point calibration:	24 hours, calibration with nitrogen
Zero point drift:	<2 % of measuring range per zero point calibration interval
Sensitivity drift:	none
Linearity deviation:	<2 % of measuring range
Temperature drifts:	<2 % of measuring range per 10 K temperature change
Pressure Influence:	1 % change of measuring value for 1 % sample pressure change. Ambient pressure changes measured and compensated

The specifications of the exhaust gas analyzer can be found in Table 3.5. The measurements were in parts per million and were logged to a computer directly. The gas analyser was capable of measuring up to 50 species of gases. This facilitated the measurement of NO_2 and CH_4 emissions and more detailed emission analysis was possible. To ensure accuracy of measurements, the exhaust gas analyser was calibrated using the calibration procedures as prescribed the manufacturer.

3.6   Data Processing and Analysis

3.6.1   Indicated Mean Effective Pressure (IMEP)

Indicated mean effective pressure is an excellent indicator of the engine load. IMEP is the pressure inside the cylinder averaged over its volume. It is defined as the positive part of the area that represents the mean work done by the engine in one thermodynamic cycle as plotted in the PV diagram. Although the brake torque indicates the ability of a particular engine to do work, it is applicable only to that particular engine and its size. Therefore it is more useful to calculate the mean effective pressure when analyzing the engine performance as it is a measure of the work done per cycle averaged over the volume of the cylinder.

IMEP is represented by the following relationship:

$$IMEP = \frac{1}{V_d} \oint P dV \qquad (3.5)$$

And Mean effective pressure can be calculated from the following equation [17]:

$$MEP = \frac{Pn}{V_s N}$$

$$(3.6)$$

Where,

$\quad\quad P$ – Power developed by the engine in Watts.

$\quad\quad n$ – Number of revolutions to complete one thermodynamic cycle.

N – Speed of the engine in rev/s.

V_s – Swept volume of the cylinder in m^3 and

MEP – Mean Effective Pressure in N/m^2;

If the power (P) substituted in the equation of MEP is the brake power, the result is called brake mean effective pressure (BMEP) and if indicated power is used the indicated mean effective pressure (IMEP) is calculated. Similarly, IMEP can be calculated considering all the four strokes thereby including the engine pumping work and it is called gross IMEP or it can be calculated only considering the compression and expansion strokes and is called Net IMEP.

For this study, the average value of gross IMEP of 80 consecutive cycles was calculated and used for the performance analysis.

3.6.2 Coefficient of Variation of IMEP

The value of coefficient of variation often termed as COV of IMEP is important for defining the suitability of the engine for automotive applications. It is widely accepted and established [17] that the valued of COV of IMEP of an automotive engine should not exceed 10% for acceptable driveability, while below 5% COV is more desirable. COV of IMEP can be calculated by the following equation.

$$COV_{IMEP} = \frac{\sigma_{IMEP}}{IMEP} \times 100(\%) \tag{3.7}$$

Where, IMEP is the value calculated as discussed in Section 3.6.1, σ_{IMEP} is the standard deviation of IMEP.

3.6.3 Identification of Knocking Combustion

It is well established and has been reported by several researchers that the knocking combustion limits the maximum load or fuelling rate obtainable from a HCCI engine. The characteristically high heat release rates of HCCI results in a rapid pressure rise that creates high levels of noise and vibration and eventually leads to physical damage to the engine components.
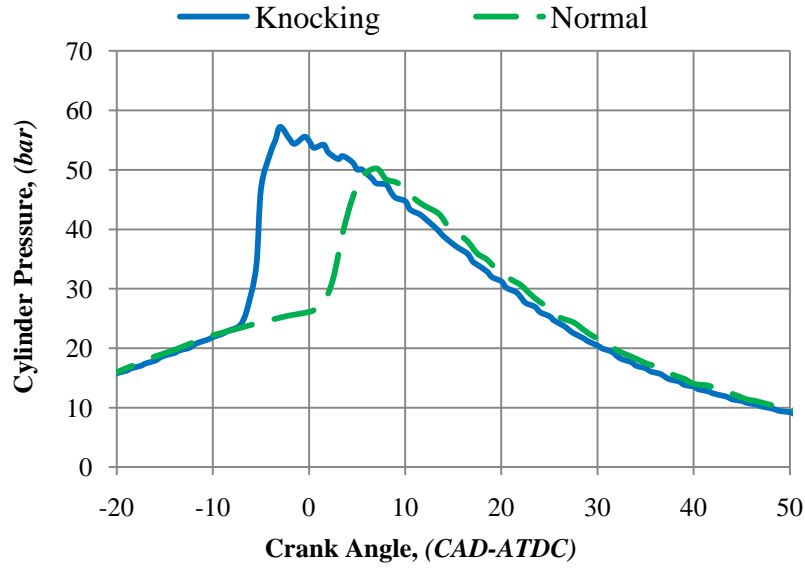
Figure 3.12 Pressure traces of normal and knocking combustions.

The occurrence of knocking combustion can be identified by the pressure rise rates. When the pressure rise rate exceeds the limit of 10bar/CAD, combustion has widely been considered to be of knocking nature by several researchers. Figure 3.12 shows the pressure traces observed with normal and typical knocking combustion with pressure waves. During the study was carried out, when the CNG injection rate was increased beyond certain limits knocking conditions did occur and were audible. Data acquired in such operating conditions and that showed a pressure rise rate more than 10bar/CAD were precluded for the analysis.

3.6.4 Combustion Efficiency

Typical HCCI combustion results in high CO and HC emissions due to lead operation that sometimes results in misfire or partial combustion. Therefore, it is useful to calculate the combustion efficiency and include in the analysis of combustion characteristics. The combustion efficiency was calculated by using the following relation for this study.

$$\eta_c = \left[1 - \frac{(\dot{m}_{CO} \times LHV_{CO}) + (\dot{m}_{HC} \times LHV_{HC}) + (\dot{m}_{CH_4} \times L\dot{H}V_{CH_4})}{(\dot{m}_g \times LHV_g) + (\dot{m}_{CH_4} \times LHV_{CH_4})}\right] \tag{3.8}$$

Where, $\dot{m}_{CO}$ - mass flow rate of CO in emissions g/hr.

51

LHV_g - lower heating value of gasoline = 44000 kJ/kg

$\dot{m}_{HC}$ - mass flow rate of unburned hydrocarbons that were constituents of the gasoline g/hr.

$\dot{m}_{CH_4}$ - mass flow rate of unburned methane

$L\dot{H}V_{CH_4}$ - lower heating value of CH₄, assumed to be equal to that of CNG = 45000kJ/kg.

The measured concentrations of species of incomplete combustion and their respective heating values can be used to calculate the combustion efficiency as shown in the above equation. The heating value of CO was known as 10.1MJ/kg and that of CH₄ was taken as 45MJ/kg and the remaining unburned hydrocarbons were considered as 41MJ/kg.

3.6.5 Fuel Conversion Efficiency

It is the amount of the chemical energy contained in the fuel that is converted into pressure energy in the cylinder. It can be noted that combustion efficiency is another parameter that defines how much energy in the fuel is liberated into heat by combustion. Fuel conversion efficiency is also referred to as thermal efficiency and can be calculated by using the following equation:

$$\eta_{Thermal} = \frac{P}{(\dot{m}_g \times LHV_g) + (\dot{m}_{CNG} \times LHV_{CNG})} \times 100 \qquad (3.9)$$

Where,

P - Indicated or Brake Power in kW

$\dot{m}_g$ and $\dot{m}_{CNG}$ - Mass flow rates of gasoline and CNG respectively in kg/s

LHV_g and LHV_{CNG} - Lower heating value of the respective fuel kJ/kg

The fuel conversion efficiency may be calculated against the brake power available at the drive shaft of the engine or the indicated power generated in the cylinder and these are called brake and indicated thermal efficiency respectively.

3.6.6 Specific Energy Consumption

For the purpose of comparison, it is useful to normalize the fuel consumption with respect to either brake power or indicated power. While the brake specific fuel consumption (BSFC) is useful to quantify the amount of energy consumed taking frictional and other losses in the engine into account, indicated specific fuel consumption(ISFC) is a measure of fuel spent for power generation inside the cylinder measured from the pressure history. However, for dual fuel engines, as two fuels are used and each has different physical and energy density, the term indicated specific energy consumption can be used to represent the fuel consumption in terms of units of fuel energy supplied.

$$ISEC = \frac{[m_g \times LHV_g] + [m_{CNG} \times LHV_{CNG}]}{IP \times 10^3} \tag{3.10}$$

Where,

ISEC – Indicated Specific Energy Consumption in kJ/kWhr.

m_g and m_{CNG} – Mass flow rates of gasoline and CNG respectively in g/hr.

LHV_g and LHV_{CNG} – Lower heating value of gasoline and CNG respectively in kJ/kg.

The brake specific energy consumption can be calculated by replacing the term indicated power by brake power in the above equation. In view of comparing the fuel consumption with the conventional single fuel gasoline or single CNG engines, the specific equivalent fuel consumption (SEFC$_g$) in terms of mass flow rate of gasoline can be calculated as:

$$SEFC_g = \frac{ISEC}{LHV_g} \tag{3.11}$$

Where, ISEC - the specific energy consumption in kJ/kWhr

LHV$_g$ - Lower heating value of gasoline in kJ/g.

Similarly, the specific equivalent fuel consumption in terms of CNG (SEFC$_{CNG}$) can be calculated by replacing LHV$_g$ by LHV$_{CNG}$ in the above equation. Figure 3.13 shows the relationship between the various quantities described above.
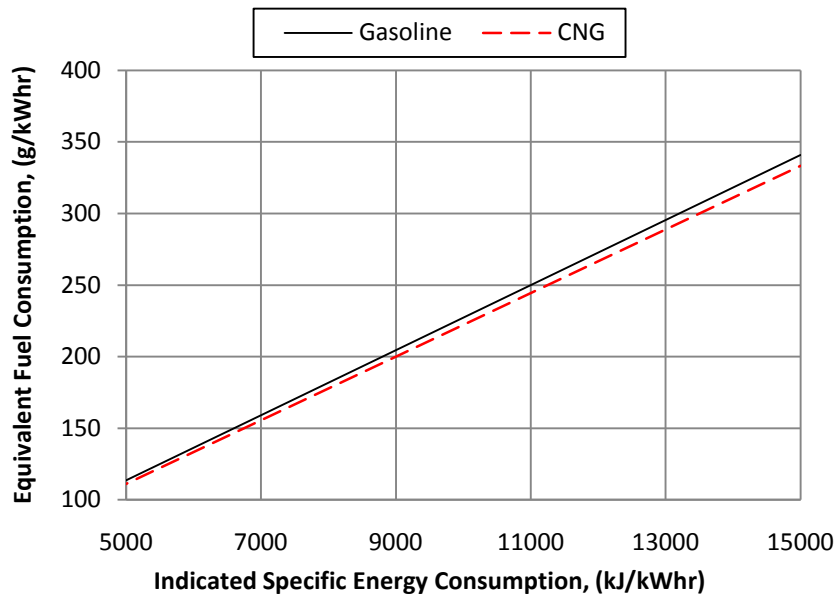
Figure 3.13 Energy consumption and equivalent fuel consumption rates

3.6.7   Estimation of Heat Release Rates

The amount of heat released by the combustion in the engines can be estimated from the history of instantaneous cylinder pressure with respect to the cylinder volume or indirectly with the crank angle. The method of estimation of heat releases can be extended to calculate the mass fraction burned and its start, end and duration of burning.

There are several methods used for the estimation of heat release rates and mass fraction burned. Application of the first law of thermodynamics to the thermodynamic processes is the basic governing law for calculating heat release rates. The model used to estimated heat release rates can be classified as single zone and multi zone models. In the single zone models, the thermodynamic properties and composition of the working substance in the cylinder are considered to be uniform throughout the cylinder. In case of multi zone models, the cylinder volume is divided into multiple or at least two zones of different properties and composition. Obviously, multi zone models are more accurate at the expense of computational simplicity and processing time. However, single zone models are sufficiently accurate and are the most widely used for online estimation of heat release rates. In

54

this project, Rassweiler Withrow model [88], a single zone model has been used for the combustion analysis.

3.6.7.1 *Definition of Ignition Timing and Combustion Duration*

There is no external controlling tool for ignition control in HCCI combustion. However, the ignition timing can be found from the heat release analysis. Traditionally, about 5 to 10% of the total heat released is considered as the point of ignition for SI engines. Considering the speed of combustion and characteristic high rate of heat release, the point at which about 10% of the total heat is released is considered the ignition timing for HCCI combustion [51]. Similarly, the combustion duration is defined as the duration in which 10% to 90% of the total heat is released [82].

3.7   Experimental Procedure and Test Methodology

The experimental procedure comprises of operating the engine with HCCI combustion of gasoline and increasing the engine load by CNG direct injection. The effects of the CNG direct injection at various injection timings on the engine characteristics were studied at different speeds. The following sections discuss the experimental procedure and the range of various parameters.

3.7.1   Start up Procedure of the Engine and Safety Measures

With preliminary checks of equipments and following standard safety procedures of operating an engine, the engine was motored at a constant speed (initially, 1200rpm). The coolant and oil heaters were switched on so as to help warm up the engine to the operating temperatures. The gasoline pump was switched on before the air heater was switched on so as to keep the injectors cooled by gasoline circulation and to prevent any possible damage of the injector nozzles due to exposure to air at elevated temperatures.

The intake air heater was switched on and the intake air was heated to 320°C. The separate temperature controller was employed to keep the intake air temperature constant within ±1°C. The coolant and oil temperatures were maintained at 75°C and 90°C respectively by the temperature controllers connected to the dynamometer control unit and the engine was motored with constant intake air temperature for about 15 minutes so as to reduce any thermal gradients inside the engine cylinder and other contact surfaces. During this time, all the other measuring instruments such as exhaust gas analyser were switched on and prepared for operation.

3.7.2 Achieving HCCI Combustion of Gasoline

Once the engine has reached a steady state with constant intake air, coolant and lubricant temperatures under motoring, the gasoline injector circuit was switched on, gasoline was injected and the duration of injection was gradually increased until HCCI combustion occurred. If HCCI combustion could not be achieved by gasoline fuelling, then the intake air temperature was set to a higher value and the above trial was repeated. From various trial runs, it was found that HCCI combustion of gasoline could be achieved at an intake air temperature of 320°C after sufficient warming up operation of the engine. The intake air temperature was reduced to 300°C upon the injection of gasoline as measured at the intake manifold. This temperature was maintained constant at 300°C for all the experiments and was used as the intake charge temperature in this thesis. The engine was run at slightly richer than required for about 30 minutes so that the engine operation in HCCI mode was stable. Then the amount of gasoline injected was reduced to find out the leanest possible equivalence ratio of gasoline with stable engine operation.

3.7.3 CNG Direct Injection

The engine was run at the leanest equivalence ratio of gasoline for about 30 minutes so as to establish the steady state operating conditions. The observations were made at this lean limit of gasoline first and then the CNG injection system was activated. The CNG injection pressure was kept constant at 18 bars using a pressure regulator and for all the experiments. The CNG was injected at specified injection timing

(initially at 300° BTDC) with the lowest injection duration (0.41ms) possible. The amount of CNG injected was increased in steps to the highest possible quantity limited either by knocking or instability. The CNG direct injection increased the total fuelling rate or the combined total equivalence ratio of gasoline and CNG or, in simple terms, the engine load. The above procedure was repeated for various injection timings of CNG namely 240°, 180°, 120° and 80° BTDC. Thus, the readings were recorded for each quantity of CNG injection with constant gasoline flow rate and different injection timings. This completed one set of readings at the leanest operable gasoline flow rate and at different timings and quantities of CNG injection.

As the objective of this study was to suggest a strategy for controlling HCCI combustion, the range of individual equivalence ratio of gasoline to be studied was from the lean limit to the value at which there is no effect on combustion by the CNG injection. It was found experimentally that the CNG direct injection had significant effects on the combustion with individual gasoline equivalence ratios ranging from 0.20 to 0.26. Therefore, the above procedure was repeated at $\phi_g = 0.20$; 0.22; 0.24 and 0.26.

The above procedure was repeated at various speeds ranging from 1200 rpm to 2100 rpm in steps of 300 rpm. The change in air flow rate and volumetric efficiency at different engine speeds were taken into account and the gasoline injection durations were adjusted so as to operate with constant equivalence ratios of gasoline from 0.20 to 0.26. Table 3.6 shows the matrix of experiments and lists the variable parameters of the experiments conducted for this study.

Table 3.6 Matrix of experiments

Engine Speed (N)	Equivalence Ratio of Gasoline (φ_g)	Timing of CNG Injection (SOI)	CNG Quantity (m_{CNG})
RPM	*Ratio*	*CAD-BTDC*	*mg/cycle*
1200	0.20	300	Up to the knocking limit or unstable engine operation
1500	0.22	240	
1800	0.24	180	
2100	0.26	120	
		80	

Thus the readings were obtained at different speeds, different gasoline flow rates, and different injection timings with various quantities of CNG injected. The data obtained were analysed as described in Section 3.6 and are discussed in the following chapters.

3.8   Summary

In this chapter, the features and specifications of the engine used for this study was presented. The modifications on the engine and subsystems added so as to operate it with dual fuel HCCI combustion were discussed and the various equipment and instruments used for measurements and data acquisition were also listed. The methods of data analysis and important calculations and assumptions were described and the experimental procedures and the matrix of operating conditions maintained and varied for each experiment were also explained.

CHAPTER 4

RESULTS AND DISCUSSION

4.1   Introduction

The main objective of this project is to study CNG direct injection as a tool for controlling HCCI combustion. Combustion control by CNG direct injection can be achieved using two different strategies;

a.   Homogeneous mixing:

As CNG has a higher octane number than gasoline, its addition to a mixture of a primary fuel (gasoline) and air will result in a delay in the ignition timing and an increase in the combustion duration. Therefore, combustion phasing can be controlled by varying the proportion of the CNG into the mixture. This can be achieved by controlling the injection duration of the CNG and gasoline.

b.   Variable stratification:

It is generally accepted that fuel stratification has a significant effect on the HCCI combustion. Stratification of CNG and a homogeneously premixed gasoline-air charge in the cylinder can be achieved through a combination of CNG direct injection and a specially machined groove on the piston crown. The degree of stratification can be varied by changing the CNG injection timing.

Both strategies were used in this study and their effects on the performance of compression ignition of CNG and gasoline-air mixture are discussed in this chapter.

4.2 Range of Operable Loads at Different Engine Speeds

The maximum load operable was found to be dependent on the equivalence ratio of gasoline and the injection timing or degree of CNG stratification. The minimum and maximum loads operable without knocking or misfire at all gasoline equivalence ratios and CNG injection timings are shown in Figure 4.1.
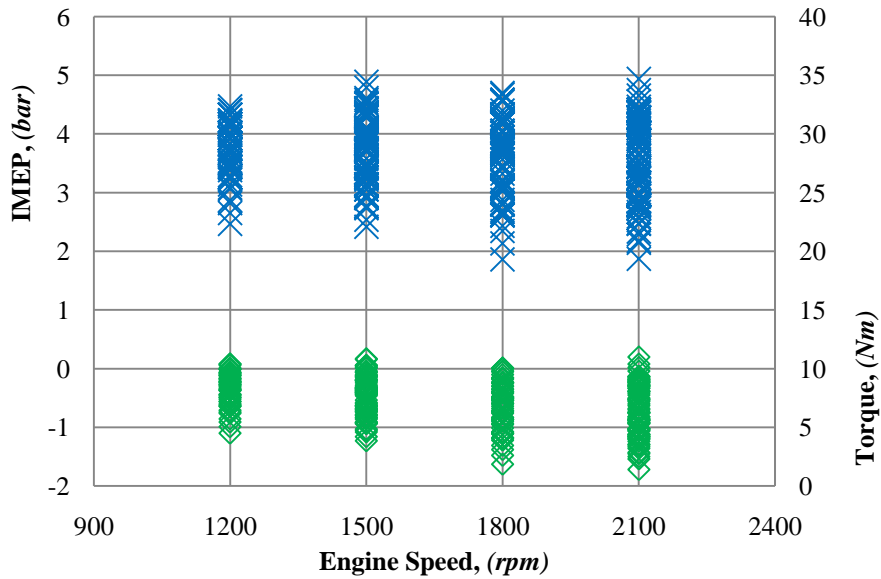

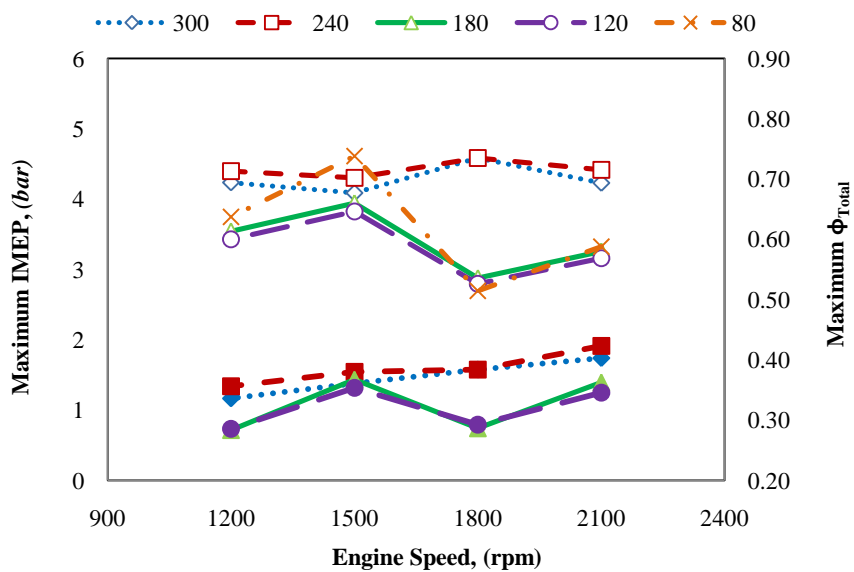*Figure 4.1 Load range operable with dual fuel HCCI combustion*

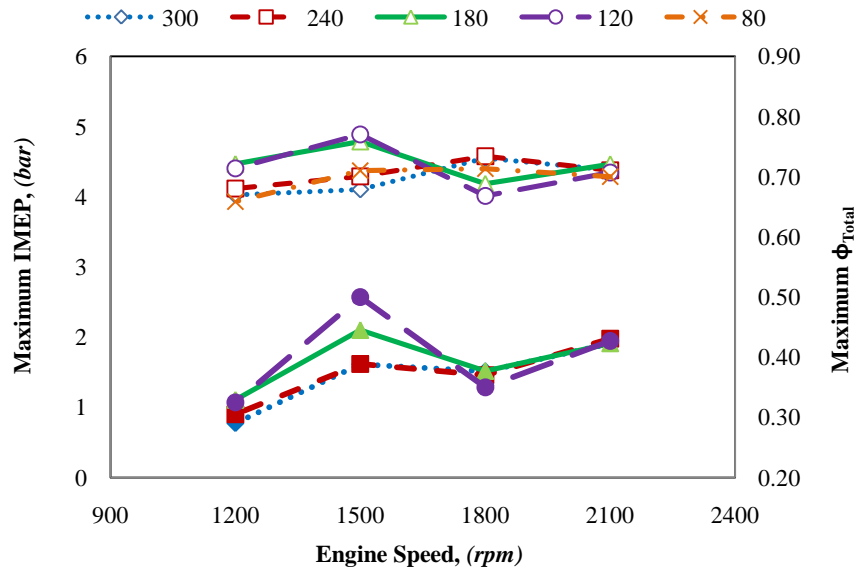*Figure 4.2 Maximum load range obtained at $\phi_g=0.20$.*

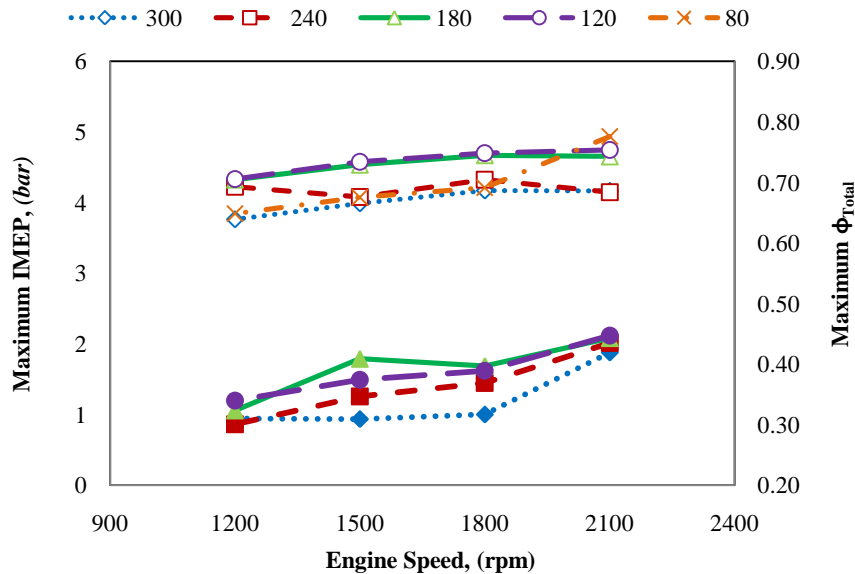*Figure 4.3 Maximum load range obtained at ϕ_g=0.22.*

Figure 4.4 Maximum load range obtained at ϕ_g=0.24.

As can be seen from Figure 4.2 to Figure 4.5, at $\phi_g = 0.20$ and at 1800rpm, the highest maximum load could be achieved with CNG injection at 240° BTDC which was marginally higher than that obtained with CNG injection at 300° BTDC. Increasing degree of stratification at $\phi_g = 0.20$, resulted in misfire or no fire. That is, higher gasoline equivalence ratio was required to ignite CNG when it was stratified. At higher gasoline equivalence ratios of 0.22 and 0.24, the maximum IMEP was obtained with CNG injection at 180° BTDC with a little difference in the maximum

IMEP obtained at 120° BTDC. With $\phi_g = 0.26$, the highest IMEP was obtained with CNG injection at 120° BTDC.
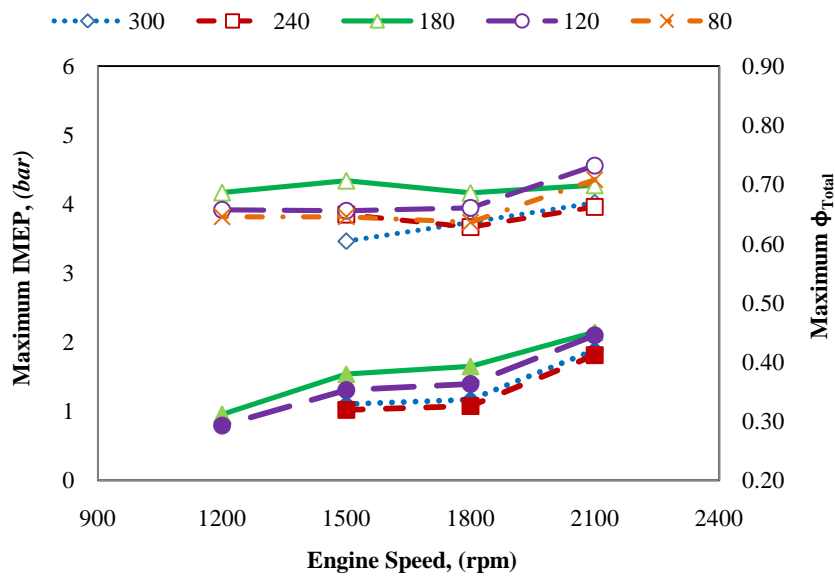

Figure 4.5 Maximum load range obtained at $\phi_g=0.26$.

Similarly, the maximum and minimum loads attained were dependent on the engine speed. The maximum range of loads could be achieved at 2100 rpm and at 1200 rpm the operable load range was limited.

4.3   Homogeneous CNG and Gasoline-air Mixing

As explained in Chapter 3, gasoline was injected into the intake manifold and the CNG was directly injected into the cylinder. It has been observed by earlier workers on the CNG DI engine that direct injection, at the early intake stroke, results in homogeneous mixture of CNG and air [84, 85]. Therefore, start of CNG injection (SOI) was fixed at 300° BTDC for homogeneous mixing of CNG with the intake charge of gasoline and air and the corresponding effects on the combustion were studied at different speeds. The scope of this section is to discuss the characteristics of compression ignition combustion of dual fuels with both fuels homogeneously mixed.

4.3.1 Overview of Engine Load Range and Operation

Gasoline plays a significant role in the initiation and characteristics of HCCI combustion of a dual fuel mixture of gasoline and CNG. As mentioned earlier, there exists a minimum equivalence ratio of gasoline only above which HCCI combustion could be achieved at intake charge temperature of 300°C in the engine of geometrical compression ratio of 14:1. It was observed that in the dual fuel operation, the heat liberated by the combustion of gasoline was essential for the combustion of CNG. This is a closely matching condition and example of Active Thermo Atmosphere Combustion as the thermodynamic atmosphere resulted from the HCCI combustion of gasoline promotes the ignition of CNG and confirmed to literature [76, 82]. Therefore, it is important to study the effects of individual gasoline equivalence ratio on the characteristics of the dual fuel HCCI combustion.
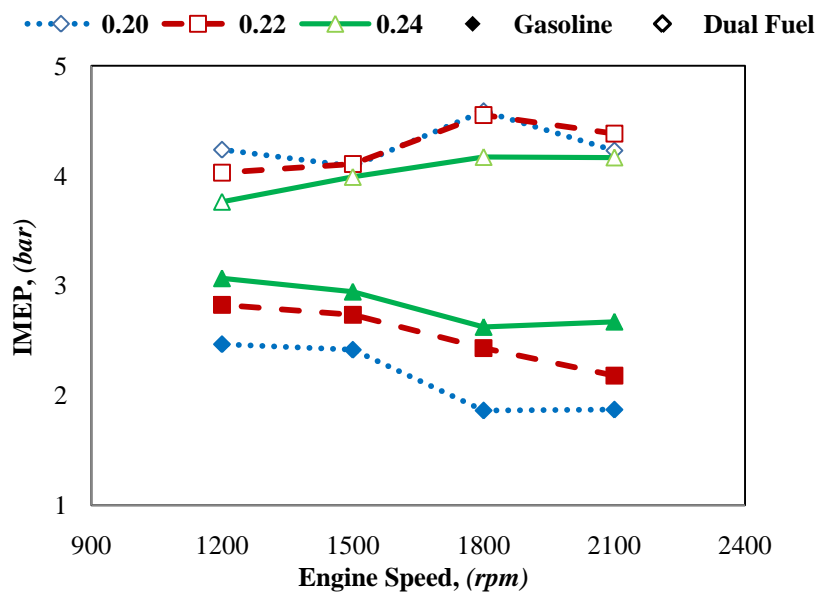

Figure 4.6 Maximum operable load range at different ϕ_g and engine speed at 300° BTDC.

The maximum load range operable was dependent upon the individual equivalence ratio of gasoline at a given engine speed. Figure 4.6 shows the maximum loads that could be operated without knocking, misfire, or partial burning at various gasoline equivalence ratios of $\phi_g = 0.20$; 0.22 and 0.24. When CNG was injected it increased the total equivalence ratio at a constant gasoline equivalence ratio (ϕ_g). And the ϕ_g was found to be a significant factor in defining the upper limit

of the IMEP obtainable. From Figure 4.6, it can be seen that the highest IMEP was obtained at 1800 rpm and was almost same for $\phi_g = 0.20$ and 0.22 at all the speeds.
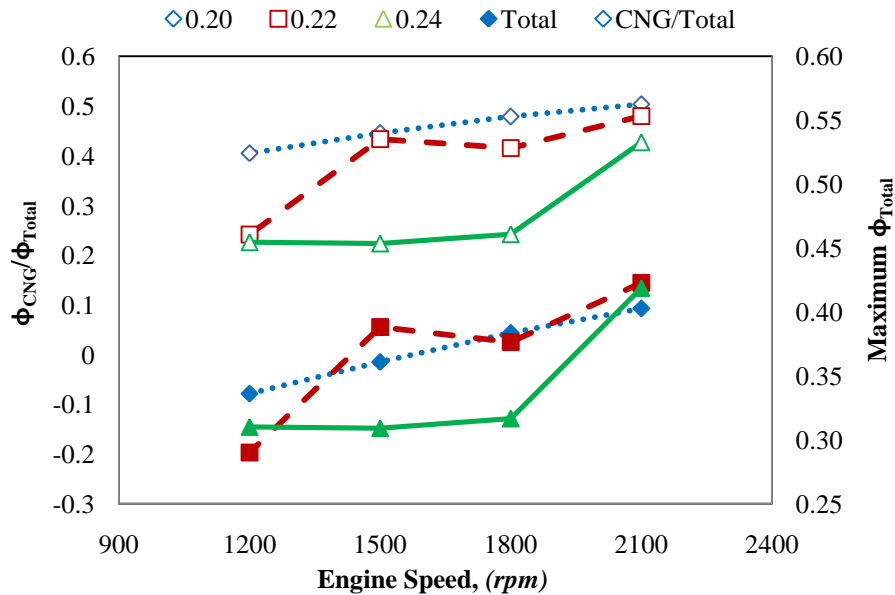

Figure 4.7 Maximum limits of ϕ_{CNG}/ϕ_{Total} and ϕ_{Total} at different ϕ_g and engine speed at 300° BTDC.

From Figure 4.7, the maximum amount of CNG (ϕ_{CNG}/ϕ_{Total}) that could be injected was at $\phi_g = 0.20$ and 2100 rpm. At 2100 rpm, the effect of ϕ_g on the maximum total equivalence ratio operable was less noticeable.

It is worth remembering here that as the engine speed increased the time duration for rotation of one degree of crank angle (1° CAD) decreased. As knock limit was sensitive to the heat release and pressure rise rates per CAD, operation at higher speeds are favourable for rapid combustion such as in HCCI combustion.

4.3.2 Effects of Gasoline Equivalence Ratio (ϕ_g) with Homogeneous Mixture of Gasoline and CNG

As mentioned earlier in Section 4.3.1, the combustion of CNG is initiated by the heat released by the combustion of gasoline. Therefore, the amount of gasoline present in the overall mixture significantly affects the characteristics of the combustion. This section discusses the effects of gasoline flow rates that are represented in terms of

equivalence ratio of gasoline. As the highest total equivalence ratios could be operated at the engine speed of 2100 rpm, the results at this speed were considered for the analysis.
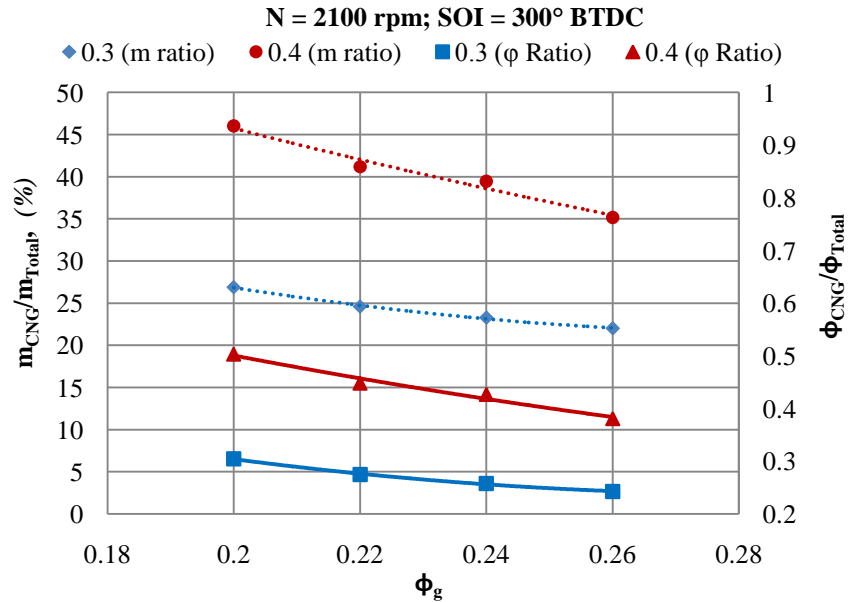
N = 2100 rpm; SOI = 300° BTDC

Figure 4.8 The range of ϕ_{CNG}/ϕ_{Total} and m_{CNG}/m_{Total} at ϕ_{Total} = 0.3 and 0.4.

In order to study the effects of equivalence ratio of gasoline in the total fuel supplied, two total equivalence ratios, 0.30 ± 0.02 with low ranges of ϕ_{CNG}/ϕ_{Total} and m_{CNG}/m_{Total} and 0.40 ± 0.02 with higher values of ϕ_{CNG}/ϕ_{Total} and m_{CNG}/m_{Total} at 2100 rpm were selected for the analysis. The ϕ_{Total} = 0.30 represented a moderate load and was operable over a wide range of injection timings of CNG and engine speeds and 0.40 produced higher engine loads.

It is worthy to note that at ϕ_{Total} = 0.30, the mass ratio of CNG in the total fuel was less than that at ϕ_{Total} = 0.40 as shown in Figure 4.8. The scope of this section is to analyse the role of gasoline flow rates in the dual fuel HCCI combustion at two different loads and not to analyse the effect of mass ratio of gasoline or CNG in the total fuel.

Figure 4.9 shows the IMEP of the engine, as the engine was loaded by increasing the amount of CNG injection at various gasoline flow rates (ϕ_g = 0.2; 0.22; 0.24 and 0.26). It can be observed from Figure 4.9 that at a given gasoline flow rate (ie. at constant ϕ_g), the IMEP increased as the total fuel flow rate was increased by

injecting CNG. This showed that CNG addition was an effective tool for controlling the engine load.
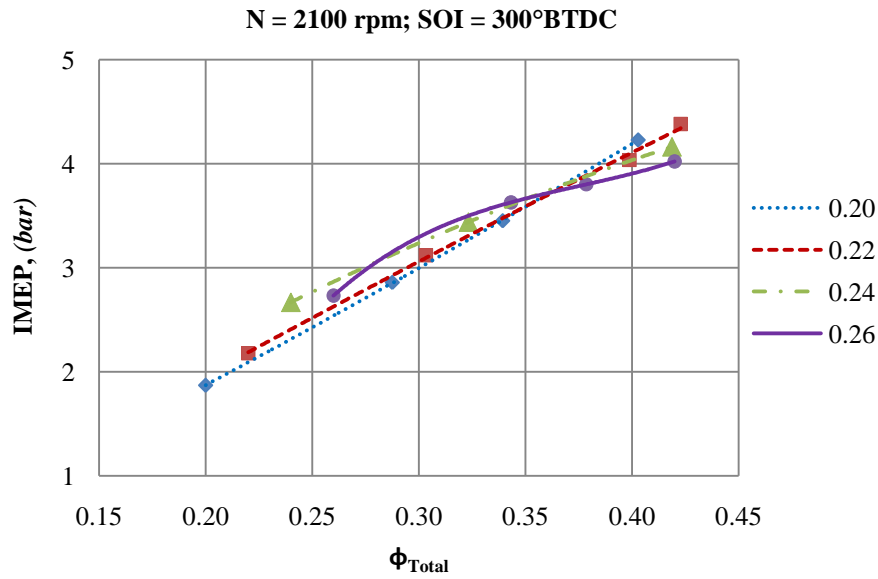
N = 2100 rpm; SOI = 300°BTDC

Figure 4.9 Effect of ϕ_g on the IMEP obtained at various total equivalence ratios

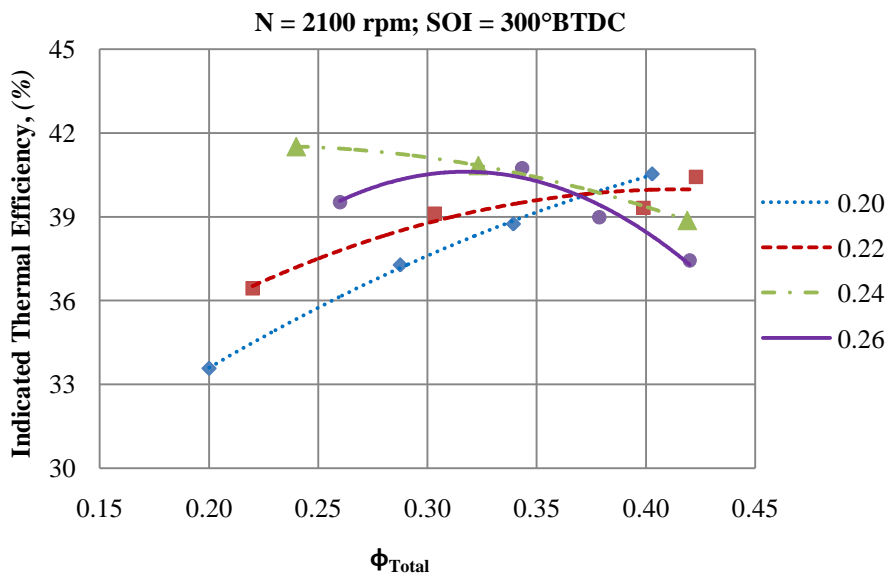**N = 2100 rpm; SOI = 300°BTDC**

Figure 4.10 Indicated thermal efficiency at different ϕ_g

The corresponding values of indicated thermal efficiency follow the trend of IMEP as shown in Figure 4.10. At $\phi_g = 0.20$ and 0.22, the indicated thermal efficiency increased with an increase in CNG injection rate. At $\phi_g = 0.24$, thermal efficiency decreased with an increase in CNG injection rate. At $\phi_g = 0.26$, thermal

efficiency increased initially but again decreased at around $\phi_{Total} = 0.32$ due to advanced ignition as shown Figure 4.11.
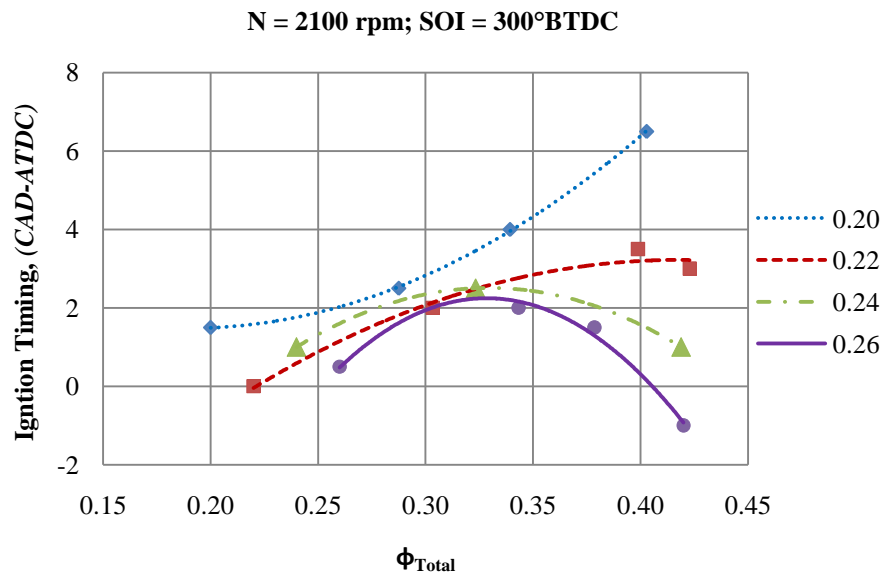
N = 2100 rpm; SOI = 300°BTDC

Figure 4.11 Effect of ϕ_{Total} on ignition timing at various ϕ_g

There were significant effects of ϕ_g found on the combustion characteristics of dual fuel HCCI combustion. Figure 4.11 shows the ignition timing of the combustion at various ϕ_g. The direct injection of CNG delayed the autoignition for all values of ϕ_g up to the total equivalence ratio of around 0.32 to 0.33. That is, ignition timing could be altered by changing the ratio of ϕ_g and ϕ_{CNG} in the total mixture up to this point for all values of ϕ_g and confirmed with the findings of Tsutsumi [70]. However, with $\phi_g = 0.20$, the CNG injection delayed autoignition for the entire range of ϕ_{Total}. With $\phi_g = 0.20$, the ignition timing was fully dependent on the CNG injection and with higher ϕ_g, the ignition timing was affected by both CNG injection and the total equivalence ratio of the mixture. But when ϕ_g was increased, the effect of CNG injection on the timing of the autoignition tended to reverse after certain values of ϕ_{Total}.

Higher concentration of gasoline ($\phi_g = 0.24$ and 0.26) in the overall mixture may initiate combustion at more locations than with lower gasoline concentration ($\phi_g = 0.20$ and 0.22) resulting in early auto ignition. At $\phi_g = 0.24$ and 0.26, CNG

injection did not delay the timing of autoignition and the ignition timing was again more dependent on ϕ_g and ϕ_{Total}.
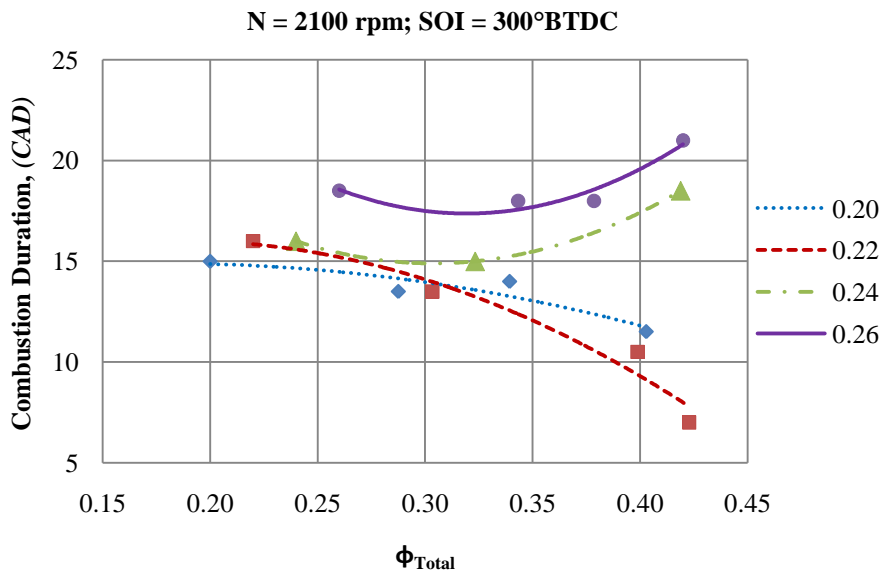

Figure 4.12 Effect of ϕ_g and the total equivalence ratio on the combustion duration

Although, at $\phi_g = 0.20$, while CNG injection delayed the auto ignition, it reduced the combustion duration as shown in the Figure 4.12. However, up to around $\phi_{Total} = 0.32$ or 0.33, the combustion duration reduced for all values of ϕ_g and after this point, CNG injection at higher ϕ_g increased the combustion duration and CNG injection with lower ϕ_g reduced the duration of combustion.

Figure 4.13 to Figure 4.16 show the pressure history and heat release rates of combustion for different values of ϕ_g. When the engine load was increased by CNG injection with $\phi_g = 0.20$, the ignition was delayed and the peak pressure increased marginally as shown in Figure 4.13. However, due to the delayed ignition as the major part of heat release occurred after TDC, the increase in the volume of the gases during the expansion stroke resulted in less increase in pressure rise rates for a given increase in heat release rates. The late ignition timings might result in higher HC and CO emissions and the corresponding effects on the HC emissions are shown in Figure 4.30 and Figure 4.32 and will be discussed at a later point in this section. However, the heat release rates significantly increased at $\phi_g > 0.20$ as shown in Figure 4.14, Figure 4.15 and Figure 4.16. Increasing CNG injection rate at $\phi_g = 0.22$, less significantly delayed ignition compared to delay resulted at $\phi_g = 0.20$.
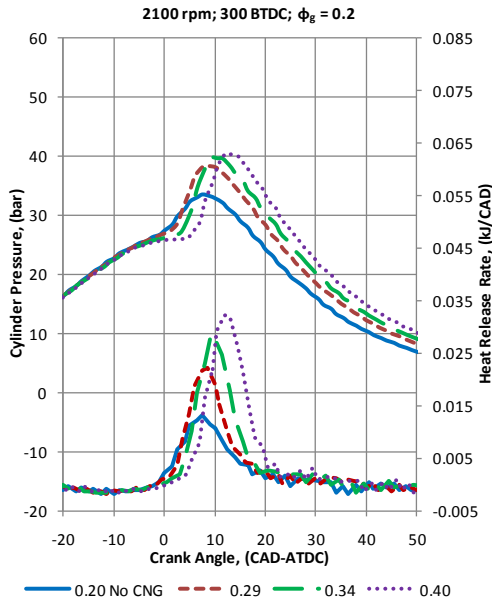
68

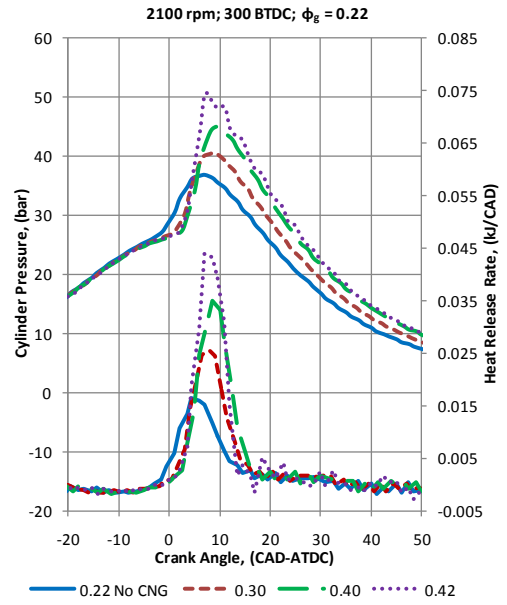*Figure 4.13 Pressure history and heat release rates with $\phi_g = 0.20$.*

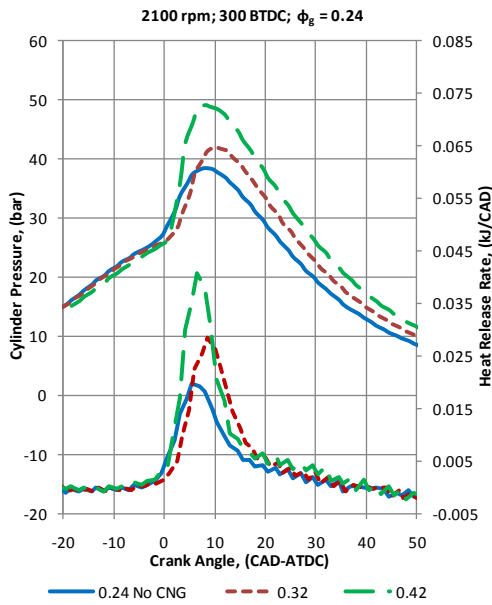*Figure 4.15 Pressure history and heat release rates with $\phi_g = 0.22$.*

Figure 4.14 Pressure history and heat release rates with $\phi_g = 0.24$.
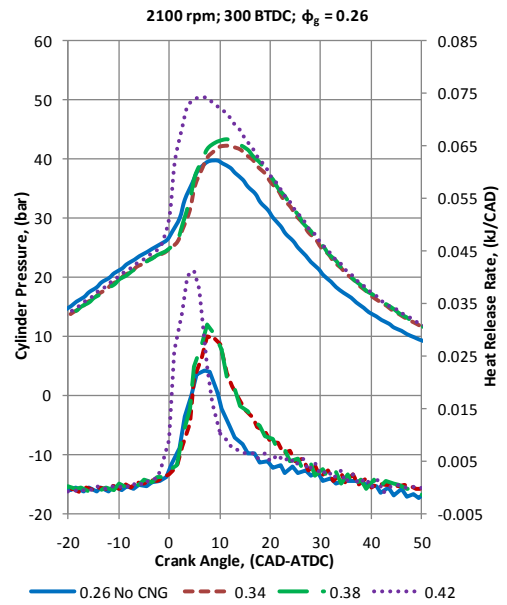
Figure 4.16 Pressure history and heat release rates with $\phi_g = 0.26$.

As shown in Figure 4.15, at $\phi_g = 0.22$, higher heat release rates and peak pressures than those observed at $\phi_g = 0.20$. At $\phi_g = 0.24$ and 0.26, although ignition timing advanced with an increase in CNG injection rate, rate of pressure rise and heat release were less affected due to prolonged combustion duration. However, at $\phi_g = 0.26$, increase in CNG injection rate led to a reduction in thermal efficiency due to high heat release rates because of advanced ignition timing.

69

At $\phi_{Total} = 0.40$, the highest thermal efficiency was obtained with $\phi_g = 0.2$, due to the increase in pressure and at $\phi_{Total} = 0.30$, the highest thermal efficiency was obtained at $\phi_g = 0.26$ as shown in Figure 4.17. The thermal efficiencies are lower at higher loads when ϕ_g is more than 0.20 as the higher heat release rates break the thermal boundary layer and increase wall heat loss.
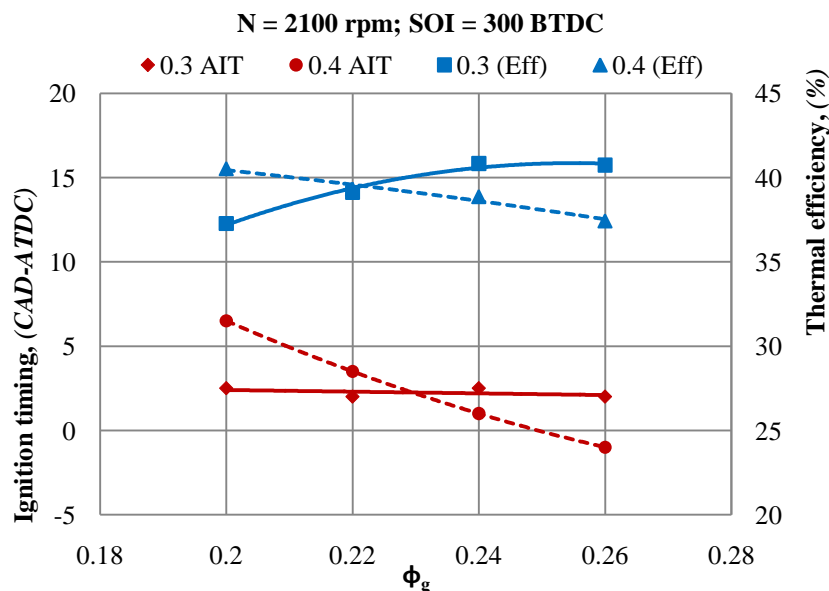

Figure 4.17 Effect of ϕ_g and ignition timing at $\phi_{Total} = 0.30$ and $\phi_{Total} = 0.40$.

Figure 4.18 to Figure 4.21 show the mass fraction burned and heat released due to low temperature reactions. From Figure 4.18, for pure gasoline combustion with $\phi_g = 0.20$ and 0.24, about 10% of the mass of the fuel burned before TDC. And for pure gasoline combustion with $\phi_g = 0.24$ and 0.26, the low temperature mass fraction burned reduced to about 5% as shown in Figure 4.19 and Figure 4.21.

That is, with pure gasoline operation, low temperature heat releases were higher with lower values of ϕ_g. This may be due to the extremely lean mixtures with very low concentration of gasoline that contains lower quantities of additives or chemical compounds that are added to the commercially available gasoline to increase its octane number.
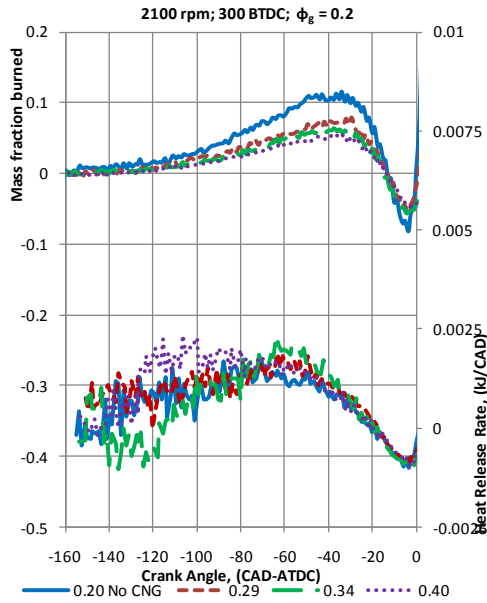
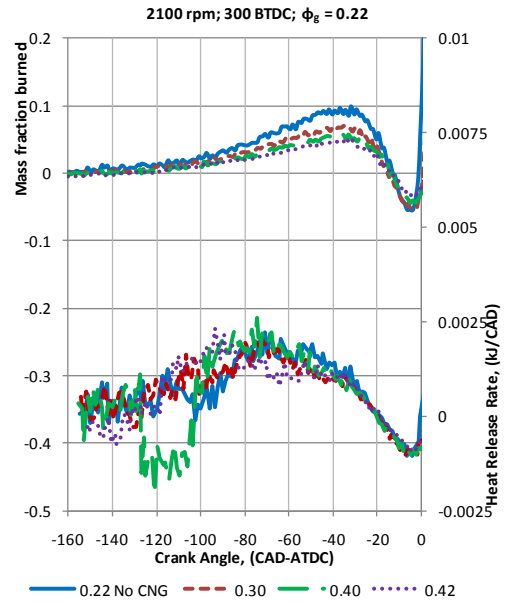*Figure 4.18 Heat release and mass fraction burned due to LTR at* $\phi_g = 0.20$.

Figure 4.20 Heat release and mass fraction burned due to LTR at $\phi_g = 0.22$.
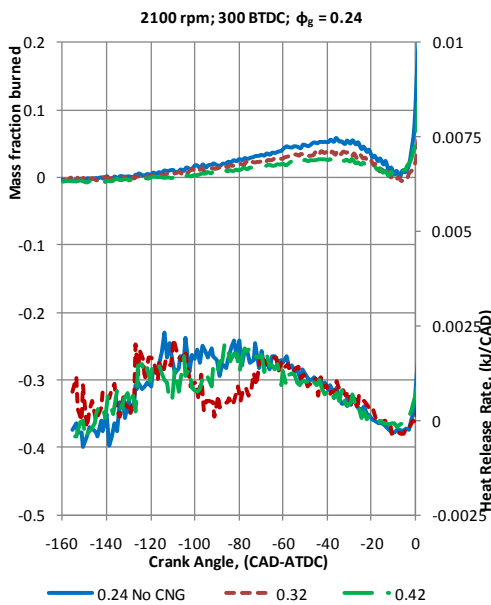

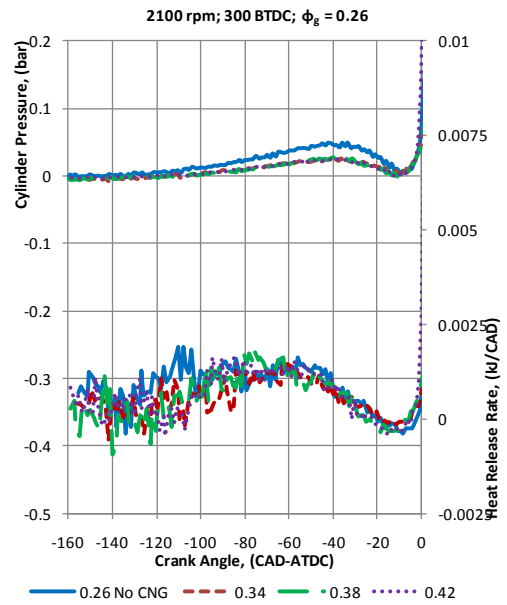*Figure 4.19 Heat release and mass fraction burned due to LTR at* $\phi_g = 0.24$.

Figure 4.21 Heat release and mass fraction burned due to LTR at $\phi_g = 0.26$.

It is believed that increasing the total equivalence ratio by increasing the CNG concentration suppressed the low temperature reactions for all values of ϕ_g. However, this reduction was relative to the levels of mass fraction burned for pure gasoline and therefore the heat release due to low temperature reactions was mainly governed by the ϕ_g.
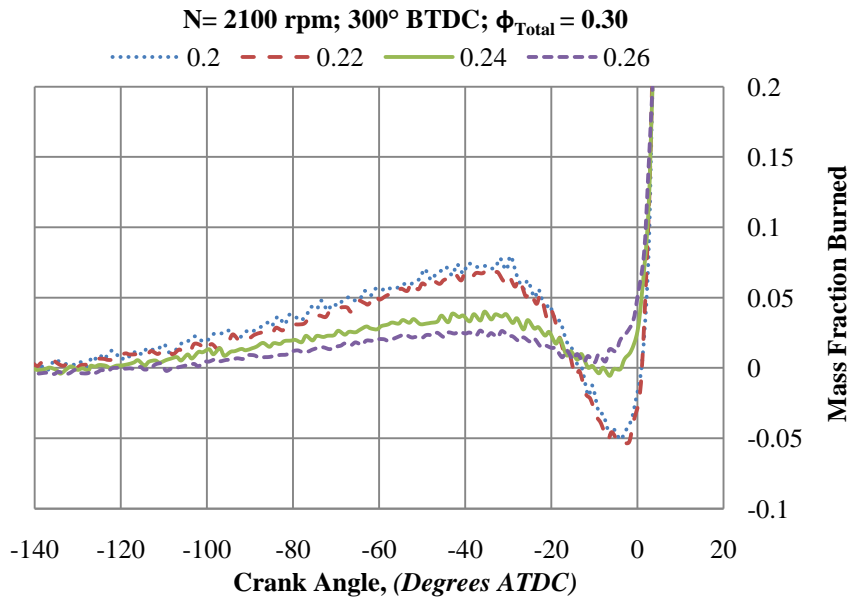
.... 0.2   – – – 0.22   ——— 0.24   – – – – 0.26

Figure 4.22 Mass fraction burned due to LTR at ϕ_{Total}=0.30.

Figure 4.22 shows the significance of ϕ_g at the total equivalence ratio of 0.30. It can be noted that at ϕ_g = 0.24 to 0.26 there was a drastic reduction in mass fraction burned. This may be partially the reason for the longer combustion durations that were observed with lower rates of ϕ_g as shown in Figure 4.12.

At ϕ_g = 0.20, as the CNG injection rate was increased, ignition was delayed. However, as shown in Figure 4.23, at ϕ_{Total} = 0.29, ignition was delayed but rate of burning was faster than pure gasoline combustion. When CNG injection rate was increased to ϕ_{Total} = 0.34 and to ϕ_{Total} = 0.40, ignition retarded further and the fuels burned in a similar fashion as at ϕ_{Total} = 0.29. At ϕ_g = 0.22, when CNG rate was increased to ϕ_{Total} = 0.30, ignition was delayed significantly and the rate of mass fraction burned increased as shown in Figure 4.24. When CNG injection rate was further increased, there was marginal difference in mass fraction burned at ϕ_{Total} = 0.40 and ϕ_{Total} = 0.42.

As shown in Figure 4.25 and Figure 4.26 , at ϕ_g = 0.24 and 0.26, rate of mass fraction burned was reduced compared to those at ϕ_g = 0.20 and 0.22. At ϕ_g = 0.24, when CNG injection rate was increased to ϕ_{Total} = 0.32, ignition was delayed, however, rate of burning was similar to ϕ_g = 0.22 in the initial stages but it was slightly higher at the last stages of combustion as shown in Figure 4.25. At ϕ_{Total} =

0.42, ignition advanced again but, at the last stage of combustion, rate of burning was higher than that at $\phi_g = 0.22$. At $\phi_g = 0.26$, when total equivalence ratio was increased to $\phi_{Total} = 0.34$ and 0.38, there was no significant difference in mass fraction burned resulted as shown in Figure 4.26. At $\phi_{Total} = 0.42$, due to high concentration of fuels, there was significant advance in ignition timing and increase in the rate of burning, however, combustion slowed down at the last stages.
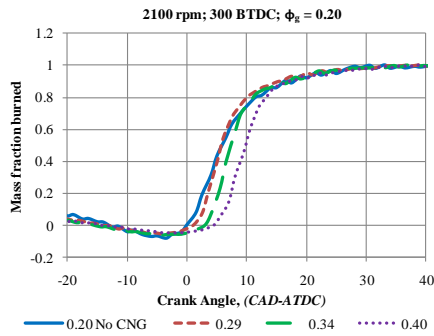

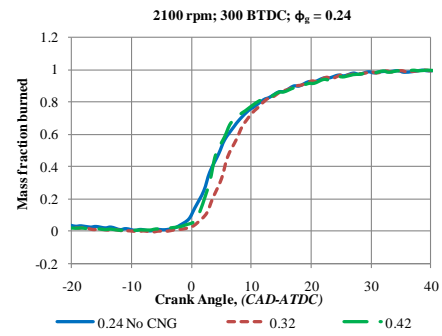*Figure 4.23 Mass fraction burned at $\phi_g= 0.20$*

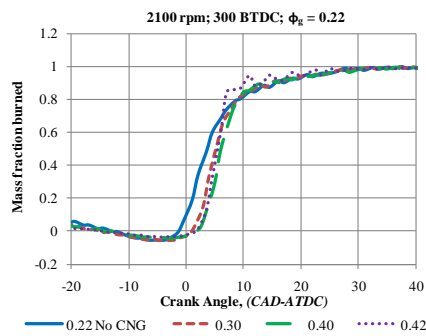*Figure 4.25 Mass fraction burned at $\phi_g= 0.24$*

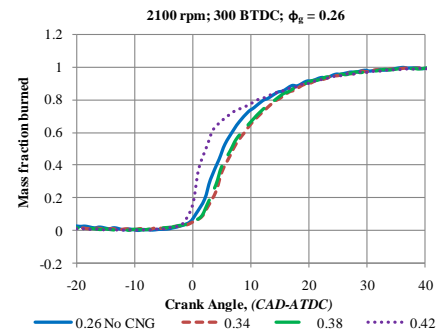*Figure 4.24 Mass fraction burned at $\phi_g= 0.22$*

Figure 4.26 Mass fraction burned at $\phi_g= 0.20$

Figure 4.27 shows the significance of gasoline equivalence ratio on combustion efficiency against total equivalence ratio. With an increase in ϕ_g, combustion efficiency increased and the lowest combustion efficiency was obtained at $\phi_g = 0.20$ due to low gasoline concentration. At $\phi_g > 0.22$, there was a marginal increase in combustion efficiency with an increase in ϕ_g. Similarly, the effect of gasoline equivalence ratio became less significant at high values of ϕ_{Total} and combustion efficiency was more dependent on ϕ_{Total} than ϕ_g at high loads and confirmed the findings of Cinar et al. [76], Mack et al. [89] and Yao et al. [71] that the increase in the proportion of the low autoignition temperature fuel improves the combustion efficiency of the high autoignition temperature fuel.
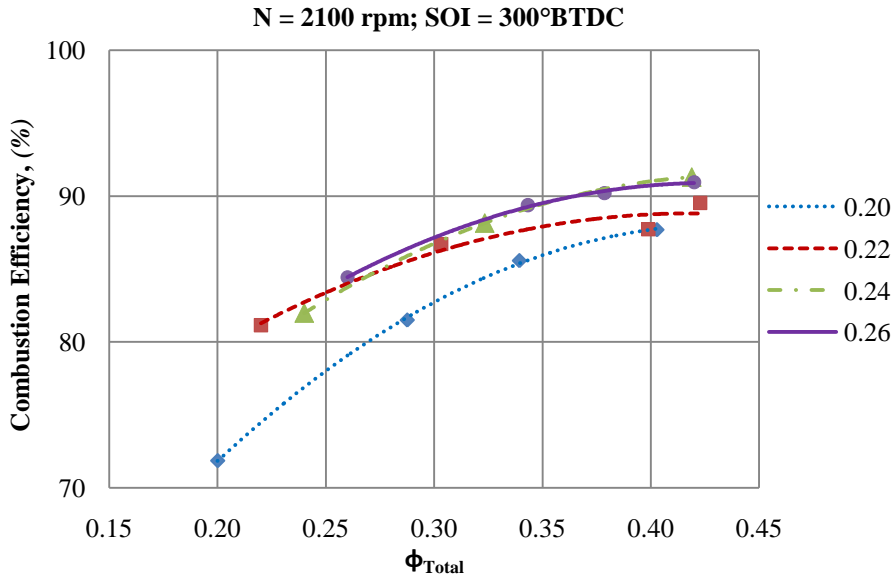
Figure 4.27 Effect of CNG injection rate and ϕ_g on combustion efficiency.

Figure 4.28 shows the NO_x emissions with increasing CNG injection rate at various gasoline equivalence ratios. At $\phi_g = 0.20$, the highest NO_x was observed, however, the differences were marginal. Above $\phi_{Total} = 0.40$, NO_x emissions tended to increase exponentially, following the typical trend of HCCI [14, 16]. However, the NO_x emissions were less than 300 ppm/kW for all cases.
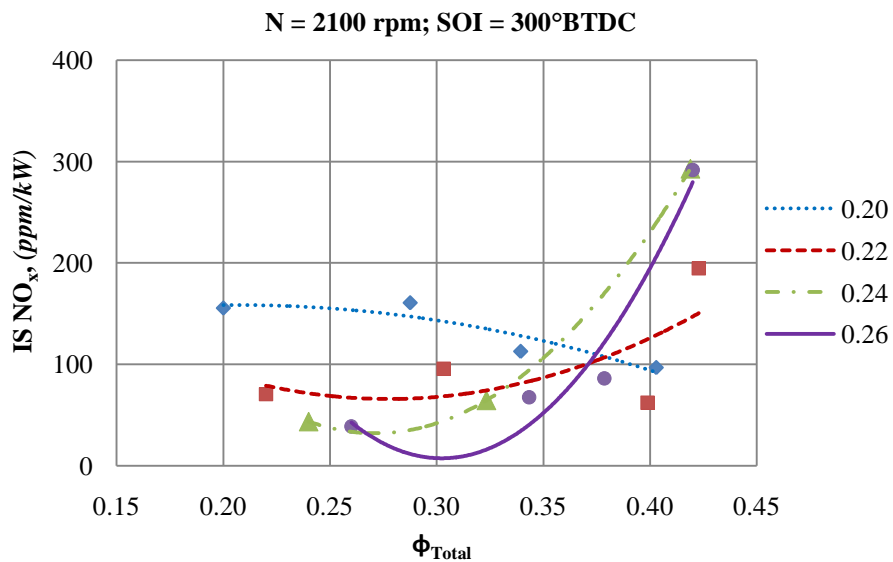

Figure 4.28 Effect of CNG injection rate and ϕ_g on the NOx emissions.

As discussed earlier, the formation of nitrogen compounds during the combustion process is sensitive to the temperature of combustion. From Figure 4.29,

it can be seen that NO_2/NO_x ratio increased up to $\phi_{Total} = 0.33$, for all the cases of ϕ_g, and then it declined. The reduction in NO_2/NO_x was the lowest above $\phi_{Total} = 0.33$ for the value of $\phi_g = 0.20$ and NO_2/NO_x was the highest at all loads or ϕ_{Total}. This suggests that the presence of CNG in the mixture reduced the combustion temperature leading to the formation of more NO_2.
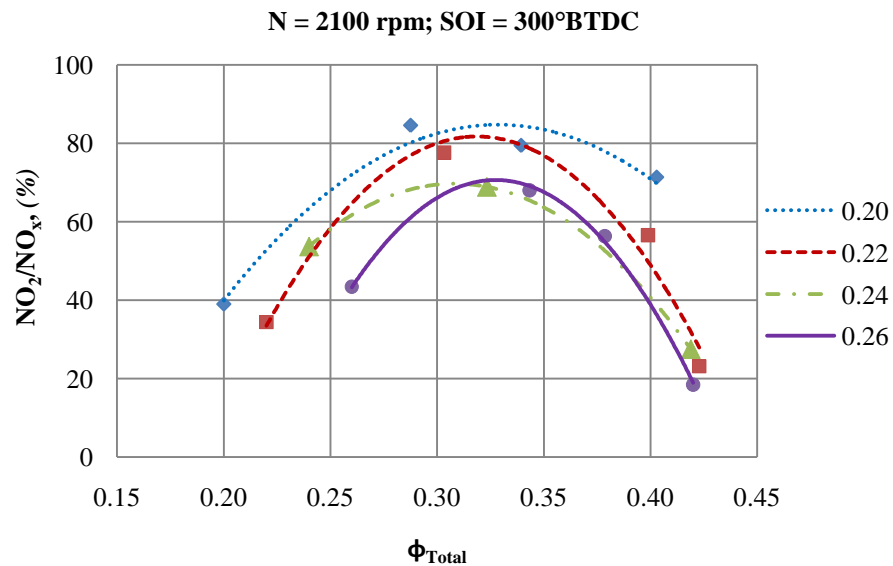
N = 2100 rpm; SOI = 300°BTDC

Figure 4.29 The ratio of NO_2 to NO_x at various ϕ_g against the engine load.

Form Figure 4.29, it can also be noted that, for pure gasoline operation, NO_2/NO_x ranges from 35% to 54% which was higher than typical values in SI and CI engines. As the NO_2/NO_x ratio for SI engine was less than 5% and for diesel engines it was about 10 to 12% [18] and many exhaust gas analysers convert NO_2 to NO prior to measuring NO_x, the molecular weight of NO is usually assumed as that of NO_x. Therefore, it is conventional to calculate the NO_x emissions in mass units (g/kWhr) usually assuming the molecular weight of NO ($M_{NO} = 30.0064$ g/mole) for the total NO_x emissions. However, from the above findings, it appears that it is better to consider NO_2 emissions ($M_{NO2} = 44.06$ g/mole) for the estimation of NOx emissions for HCCI combustion.
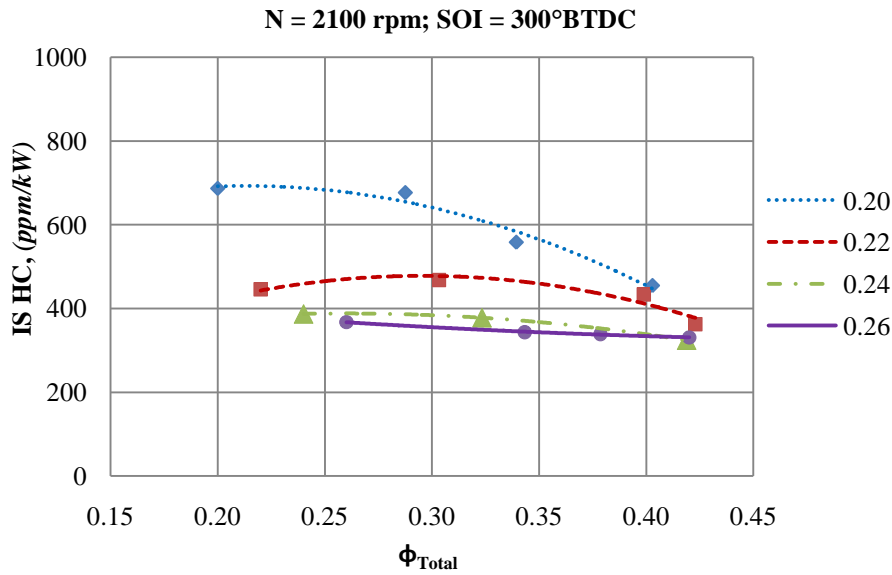
N = 2100 rpm; SOI = 300°BTDC

Figure 4.30 Effect of CNG injection rate on HC emissions

The increase in ϕ_{Total} reduced the HC and CO emissions as shown in Figure 4.30 and Figure 4.32. The highest reduction was observed with $\phi_g = 0.20$ and with other ϕ_g values HC emissions reduced marginally. However, higher values of ϕ_g resulted in low HC emission at all ϕ_{Total} and this confirmed the findings of Yao et al. [67]. The effect of ϕ_g was more significant at lower loads than at higher ones. The effect of ignition timing as discussed earlier was less significant and the HC emissions were dependent on ϕ_{Total} and ϕ_g.
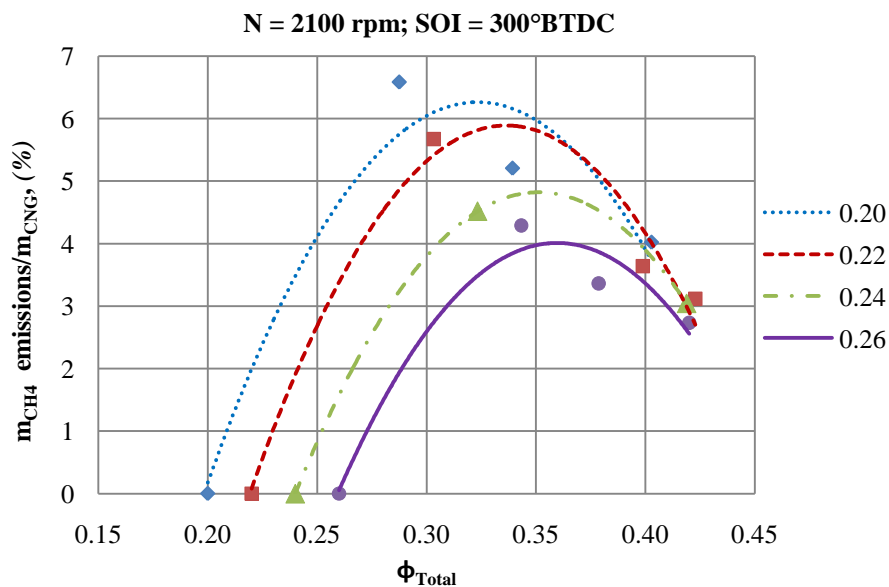

N = 2100 rpm; SOI = 300°BTDC

Figure 4.31 Effect of CNG injection rate and ϕ_g on CH$_4$ emissions

76

The measurement of CH_4 emissions was useful in finding the approximate efficiency of CNG combustion in the overall mixture and its trends as the main component of CNG is CH_4 (83 to 94 %) [90, 91]. As shown in Figure 4.31, increase in gasoline equivalence ratio significantly reduced the CH_4 emissions and this confirmed the findings of Mack et al. [89]. However, at $\phi_{Total} > 0.40$, ϕ_g became less significant and CH_4 emissions were more dependent on ϕ_{Total} and reduced to around 3% for all values of ϕ_g.
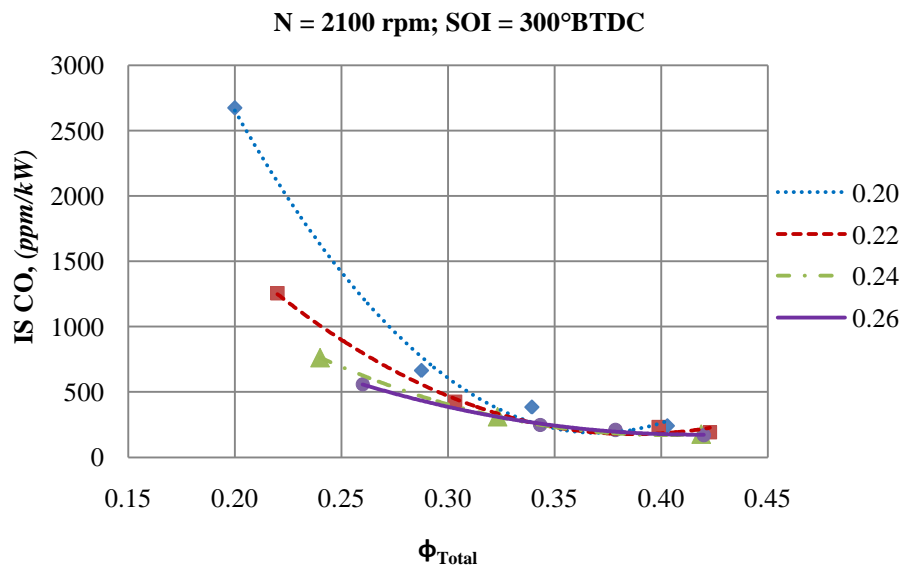
N = 2100 rpm; SOI = 300°BTDC

Figure 4.32 Effect of ϕ_g and CNG injection rate on CO emissions

As was found from Figure 4.32, CO emissions were dependent only on the ϕ_{Total} at higher loads and at lower loads both ϕ_g and ϕ_{Total} were significant and this confirmed the findings of Lu et al. [92]. There were drastic reductions achieved in CO emissions with CNG injection at lower loads also and at lower loads ϕ_g played a significant role in CO emissions, especially with pure gasoline combustion.

Above the point of $\phi_{Total} = 0.33$, the CO emissions were reduced almost to the same value for all cases of ϕ_g. The highest reduction was observed with $\phi_g = 0.2$ at which CO emissions wee very high especially when compared to CO emissions with pure gasoline operation.

4.4   Combustion with Stratified Distribution of CNG in the Homogeneous Mixture of Gasoline and Air

4.4.1   Effects of Degree of CNG Stratification

The degree of stratification of CNG in the total mixture was found to have significant effects on the maximum load in terms of the IMEP attainable and ϕ_{Total}. From Figure 4.33, it can be seen that at 300° and 240° BTDC injection higher total equivalence ratios could be operated. But with 180° and 120° BTDC, the maximum operable ϕ_{Total} was limited with reduced IMEP at a given ϕ_{Total} when compared to the 300° and 240° BTDC cases.
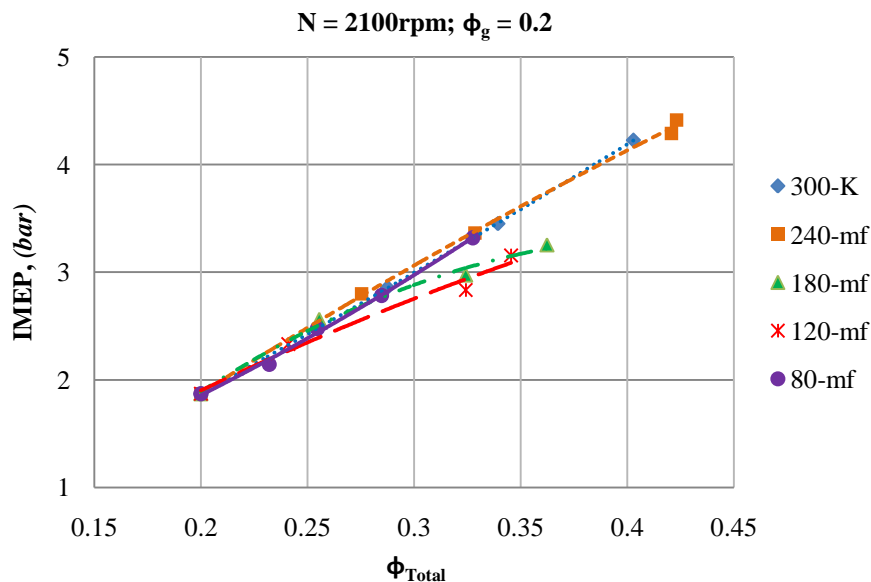

Figure 4.33 Effect of degree of stratification of CNG on IMEP.
(K –Limited by Knocking; mf-Limited by misfire).

With the highest degree of stratification, although the maximum load was limited there was no significant drop in the IMEP and the trend was similar to 300° and 240° BTDC conditions. The corresponding values of indicated thermal efficiencies are shown in Figure 4.34. The maximum load was observed to be limited by knocking when CNG was injected at 300° BTDC and for the other cases, increasing CNG injection rate led to unstable operation or misfire.
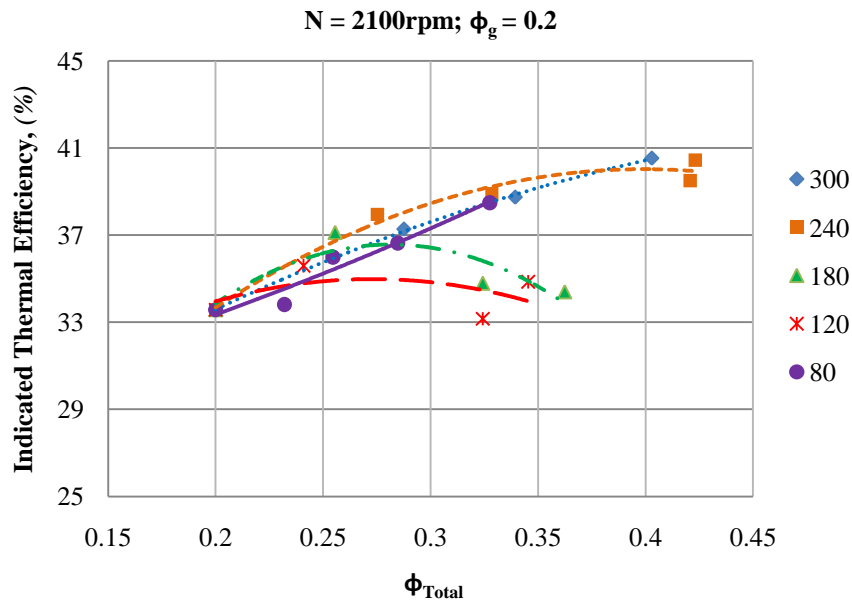
Figure 4.34 Effect degree of CNG stratification on the indicated thermal efficiency
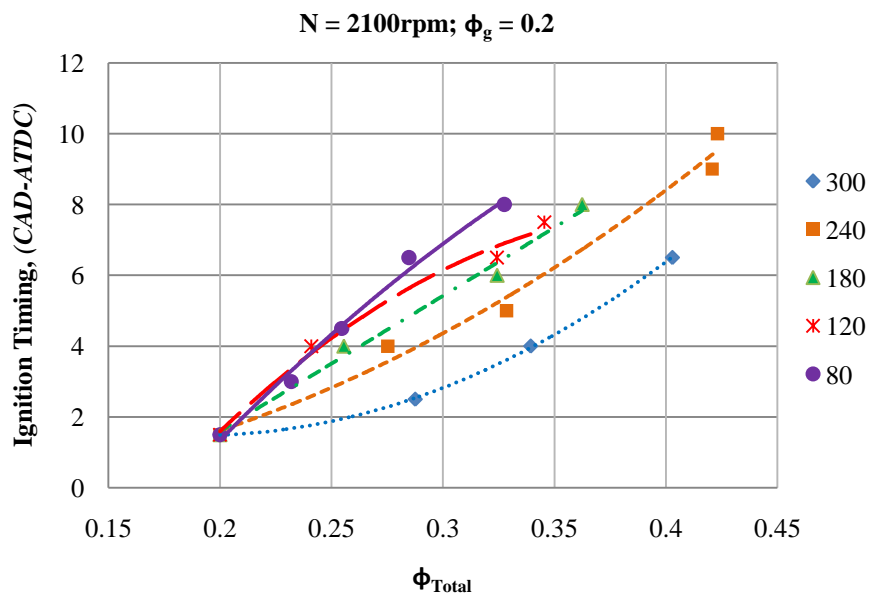

Figure 4.35 Effect of degree of CNG stratification on ignition timing.

From Figure 4.35, it can be seen that the ignition timing could be altered by changing the timing of injection of CNG at a given load. When the rate of CNG injection was increased the ignition timing was delayed due to the higher octane number of CNG. Also higher degrees of stratification resulted in higher increments in the delay of ignition timing as the CNG injection rate was increased. The slope of the curves was steeper when the injection timing was delayed. For a given increase in the CNG injection rate, the increase in delay in ignition timing was higher when the degree of stratification was increased as reported by Richter et al. [39]. That is,

both the injection rate and the degree of stratification of CNG had significant effects on the ignition timing when operated with $\phi_g = 0.20$. However, the maximum total equivalence ratio was less than that obtained with CNG injection at 300° BTDC and 240° BTDC.

It was found that the combustion duration was reduced when CNG injection rate was increased at 300°, 240° and 80° BTDC. When CNG was injected at 180° and 120° BTDC, the combustion duration was marginally affected and it initially decreased up to certain values of CNG injection rate and then it increased again.
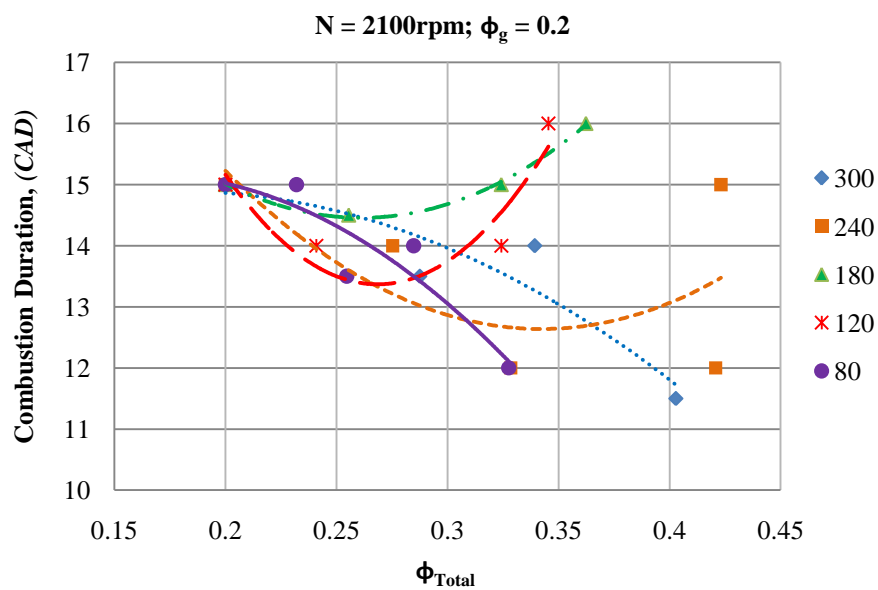

Figure 4.36 Effect of degree of CNG stratification of CNG on the combustion duration

Figure 4.13 and Figure 4.37 to Figure 4.40 show the rate of heat release and pressure rise at various injection timings. Increasing the rate of CNG injection at 300° BTDC was limited by knocking as shown in Figure 4.13. But with later injection timings, with $\phi_g = 0.20$, any increase in CNG injection rate resulted in a delayed autoignition and reduced peak pressure. Therefore, increasing CNG injection rate beyond certain levels led to misfire or no fire, thereby defining the maximum load limit.

As shown in Figure 4.37, when CNG injection rate was increased, it resulted in delayed ignition timing. Up to $\phi_{Total} = 0.33$, the resultant peak pressure increased and with a further increase in CNG injection rate it decreased. Also above $\phi_{Total} = 0.33$,

the delay in ignition timing was more significant and resulted in decreased peak pressures. As will be discussed later in this section, combustion efficiency of both the fuels increased and CH_4 emissions decreased with an increase in ϕ_{Total} above 0.33 as shown in Figure 4.45 and Figure 4.51.

Figure 4.37 Pressure history and heat release rates with CNG injection at 240° BTDC.

Figure 4.39 Pressure history and heat release rates with CNG injection at 120° BTDC.
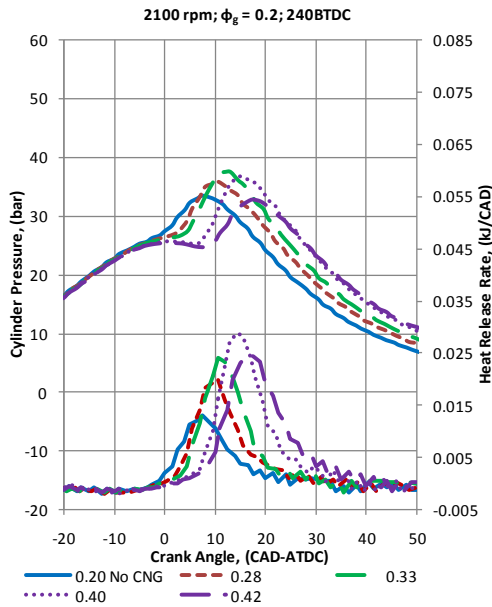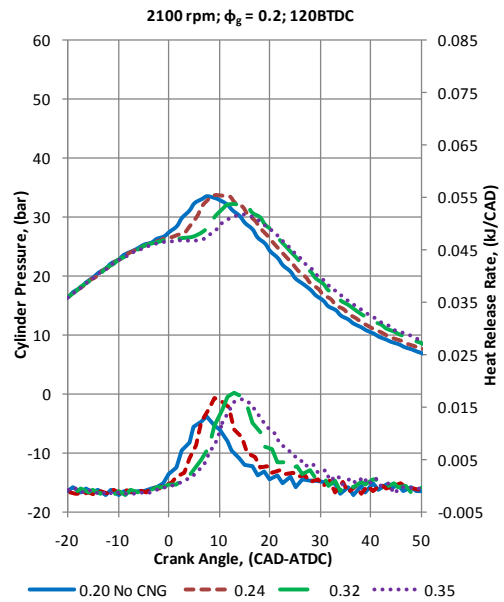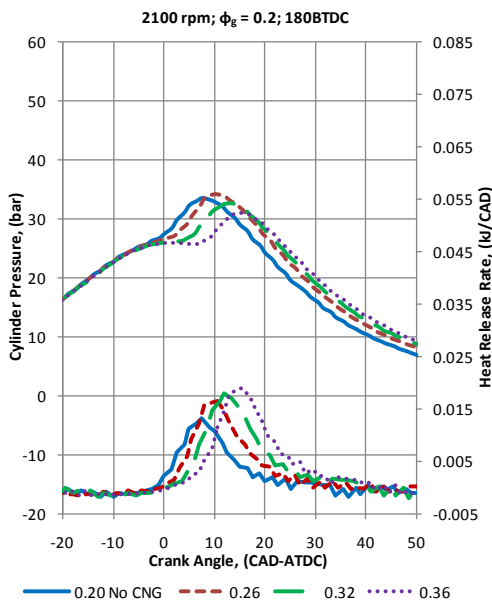

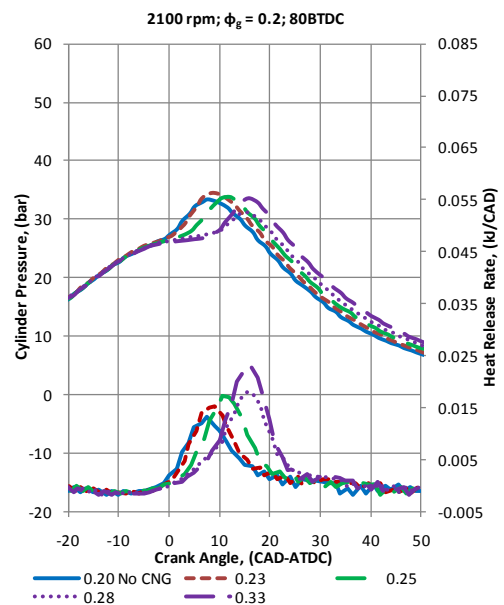*Figure 4.38 Pressure history and heat release rates with CNG injection at 180° BTDC.*

Figure 4.40 Pressure history and heat release rates with CNG injection at 80° BTDC.

Therefore, it can be concluded that, above $\phi_{Total} = 0.33$, the peak pressure was reduced due to delayed in ignition and the combustion was more complete with

81

increase in injection rate at 240° BTDC. That is, increasing ϕ_g above 0.33, resulted in reduced peak pressures without a decrease in thermal efficiency as shown in Figure 4.34. Heat release rates increased with an increase CNG injection rate up to $\phi_{Total} = 0.40$ above which it reduced again. Above $\phi_{Total} = 0.42$, increasing CNG injection rate resulted in misfire or no fire and both gasoline and CNG combustion was quenched.

With CNG injection at 180° BTDC, increase in CNG injection rate resulted in a more significant delay in ignition timing. There was a marginal increase in peak pressure when ϕ_{Total} was increased to 0.26 above which it reduced again. Heat release rate increased with an increase in CNG injection rate as shown in Figure 4.38. However, increasing CNG injection rate above $\phi_{Total} = 0.26$ resulted in decreased overall combustion efficiency and high CH_4 emissions as shown in Figure 4.45 and Figure 4.51. This suggests that the degree of stratification created at 180° BTDC injection results in deterioration in combustion and leads to decreased in thermal efficiency as shown in Figure 4.34. Similar, trends were observed with CNG injection at 120° BTDC when ϕ_{Total} was increased above 0.24 as shown in Figure 4.39.

When CNG injection was retarded to 80° BTDC, increase in injection rate resulted in significant delay in ignition, however, there was less noticeable effect on peak pressures up to $\phi_{Total} = 0.28$. Increasing ϕ_{Total} above resulted in a more significant delay in ignition and peak pressure and heat release rates increased. Thermal efficiency and combustion efficiency increased primarily due to remarkable increase in completeness of CNG combustion as suggested by CH_4 emissions as shown in Figure 4.51.

As shown in Figure 4.41, increasing CNG injection rate at 240° BTDC resulted in delayed ignition. At $\phi_{Total} = 0.28$ and 0.33, there was a slight increase in burning rate at the last stage of combustion compared to combustion with pure gasoline. At 180° and 120° BTDC, there was no significant effect on the burning rate of the fuels due to increase in CNG injection rate but it caused a significant delay in ignition as shown in Figure 4.42 and Figure 4.43. Similar results were obtained with CNG

injection at 80° BTDC, however, at ϕ_{Total} = 0.28 and 0.33, the combustion was slower at the initial stages and was faster at latter stages as shown in Figure 4.44.
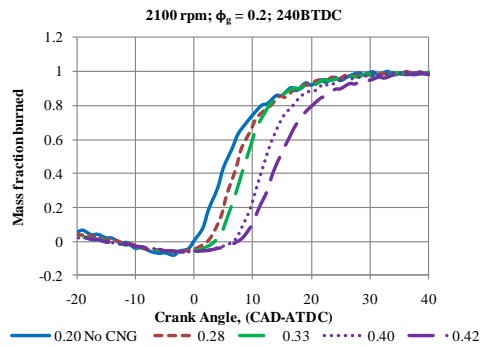

Figure 4.41 Mass fractions burned with CNG injection at 240° BTDC.
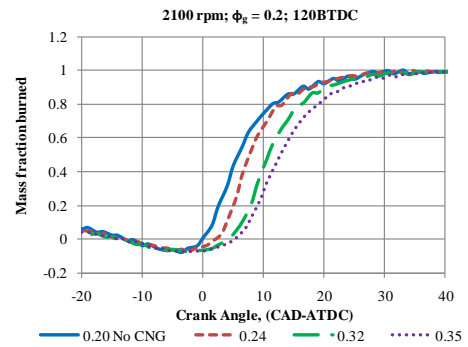
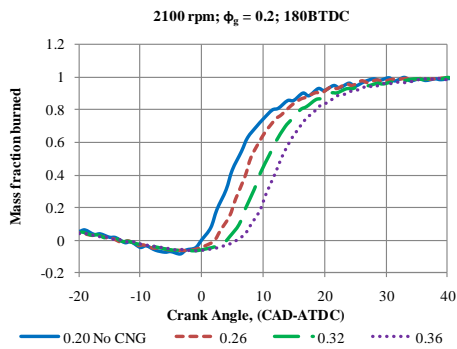Figure 4.43 Mass fractions burned with CNG injection at 180° BTDC.

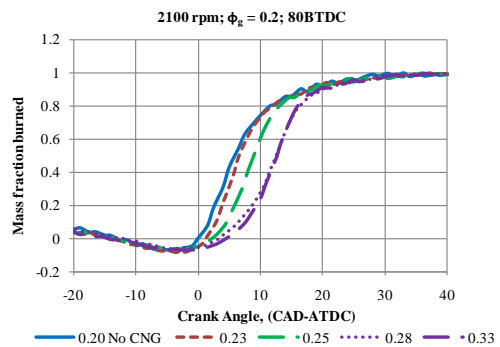Figure 4.42 Mass fractions burned with CNG injection at 120° BTDC.

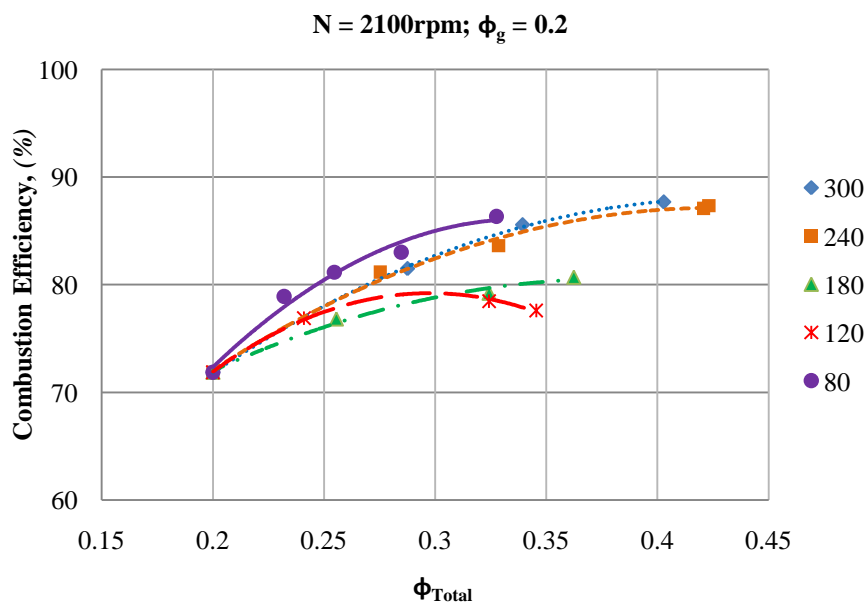Figure 4.44 Mass fractions burned with CNG injection at 80° BTDC.

Figure 4.45 Effect of degree of stratification on combustion efficiency

As shown in Figure 4.45, with an increase in ϕ_{Total} by CNG injection at 300°, 240° and 80° BTDC, combustion efficiency increased and confirmed with Marriot and Reitz [47]. The highest increment was obtained with CNG injection at 80° BTDC for a given increase in ϕ_{Total} due to mixture stratification. However, CNG injection at 180° and 120° BTDC, combustion efficiency increased initially but decreased again and was below 80% for all ϕ_{Total}.

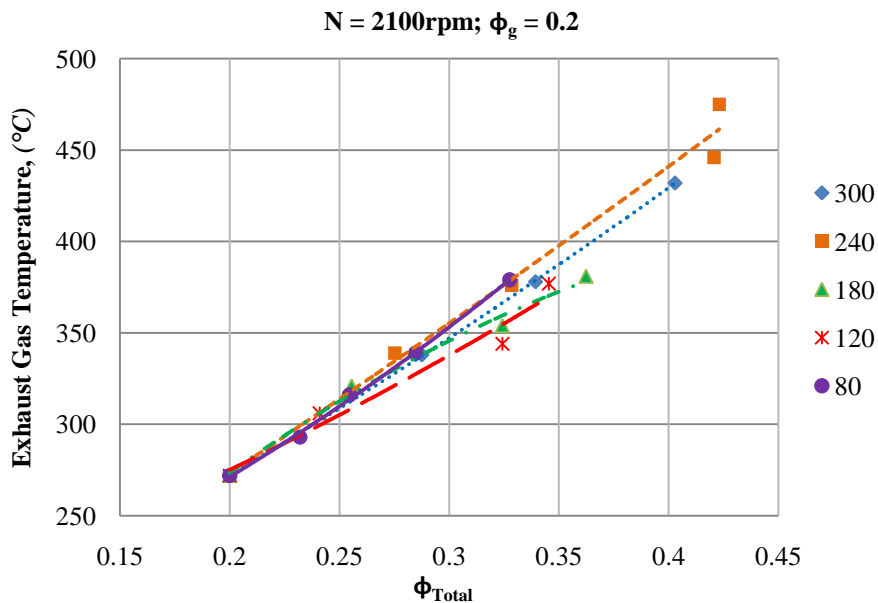**N = 2100rpm; $\phi_g = 0.2$**

Figure 4.46 Effect of CNG injection on the exhaust gas temperature

The exhaust gas temperature was observed to increase as the CNG injection rate was increased as shown in Figure 4.46. The increase in exhaust gas temperature with increasing CNG injection rates at 180° BTDC and 120° BTDC was less than that observed with increasing CNG injection rates at 300°, 240° and 80° BTDC. When the fuels were homogeneously mixed it resulted in higher exhaust gas temperatures due to rapid burning. Similarly, when CNG was highly stratified, it also led to higher exhaust gas temperatures.

Figure 4.47 shows the total NO_x emissions. The NO_x emissions were marginally affected and were around the same levels for all test conditions. However, different trends were observed at different injection timings and CNG injection rates.

Increasing the CNG injection rate resulted in a drastic increase in the NO_2/NO_x ratio up to a certain point and then it decreased. As shown in Figure 4.48, the ratio of NO_2/NO_x almost doubled when the CNG injection rate was increased to around

$\phi_{Total} = 0.33$ before decreasing again. That is, up to a certain value of CNG injection rate, CNG reduced the combustion temperature and led to formation of higher amounts of NO_2.

N = 2100rpm; ϕ_g = 0.2

Figure 4.47 Effect of degree of CNG stratification on NO_x emission.

N = 2100rpm; ϕ_g = 0.2

Figure 4.48 Effect of degree of CNG stratification on NO_2 formation

The CO emissions were reduced significantly as the mixture was enriched with CNG by direct injection at all injection timings as shown in Figure 4.49. However, the reduction obtained was the highest when CNG was injected at 300° and 240° BTDC. Any increase in CNG injection rate at later injection timings resulted in

85

less reductions in CO emissions and this confirmed with the findings of Sjoberg et al. [46]. The lowest reduction was obtained at the injection timing of 80° BTDC, as the high degree of stratification of CNG limited the availability and distribution of oxygen and temperature differences in the CNG and air particles [20].
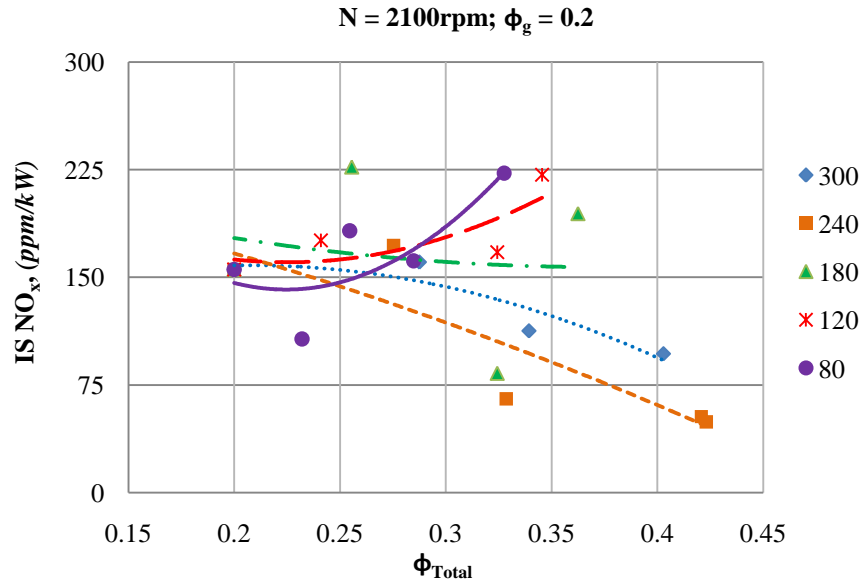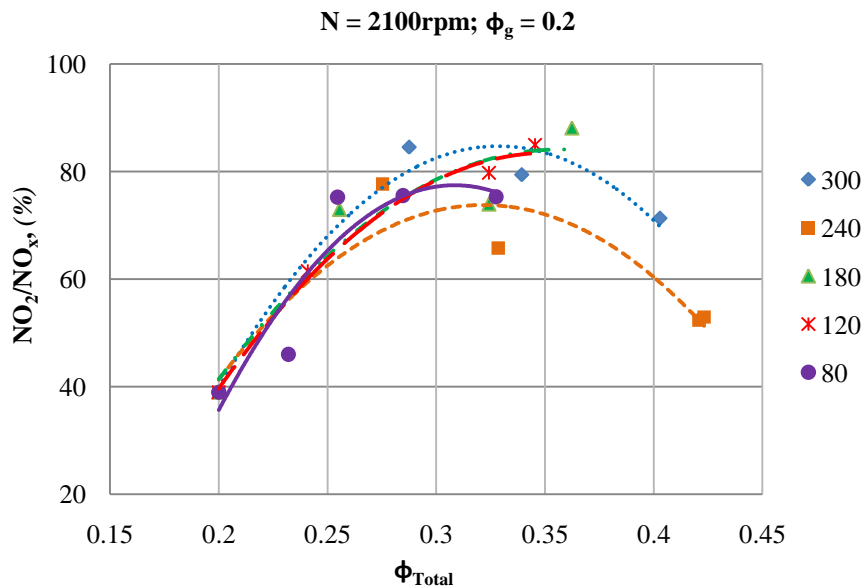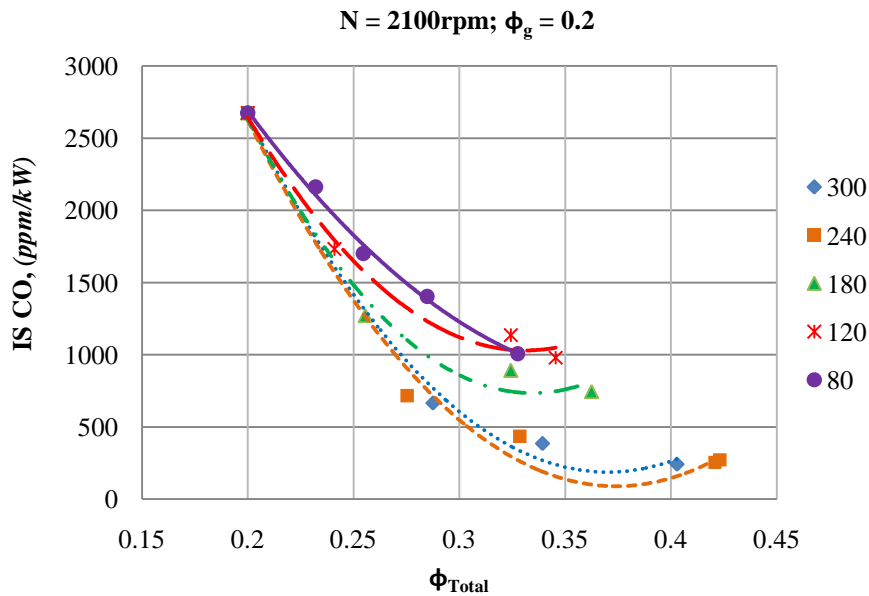

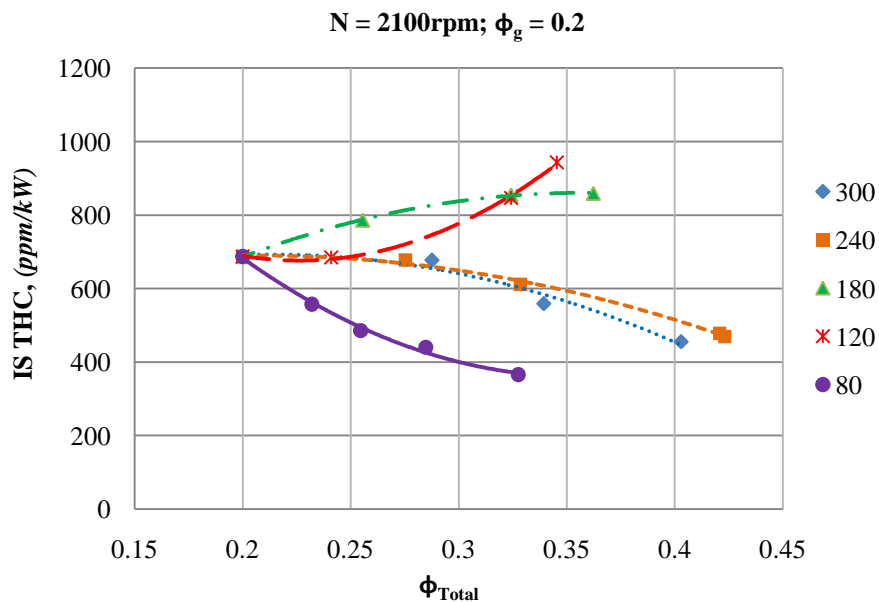*Figure 4.49 Effect of degree of CNG stratification on CO emissions*

Figure 4.50 Effect of degree of CNG stratification on HC emissions

The HC emissions were found to be significantly affected by the degree of stratification of CNG as shown in Figure 4.50. The highest reduction in HC emissions was obtained with CNG injection at 80° BTDC. Higher degrees of

stratification of CNG resulted in more complete combustion as reported by Sjoberg et al. [46].
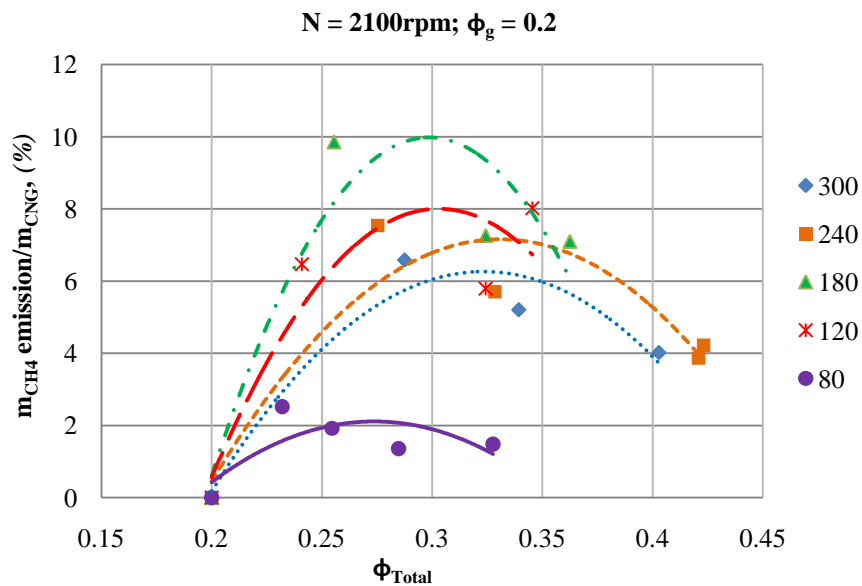

N = 2100rpm; ϕ_g = 0.2

Figure 4.51 Effect of injection timing on the emission of CH_4 with φ_g = 0.20.

Figure 4.51 shows the mass ratio of flow rates of CH_4 in the exhaust emissions and mass flow rate of CNG injected into the cylinder. At a given constant gasoline equivalence ratio of ϕ_g = 0.20, CNG direct injection at 80° BTDC resulted in the least emission of CH_4. Therefore, the combustion of CNG was more complete when it was stratified. CNG injection at 300° and 240° BTDC resulted in moderate levels of CH_4 emissions and highest values were obtained with CNG injection at 180° BTDC. This was due to the turbulence created and mixing conditions in the cylinder when the piston changed its direction at 180° BTDC.

4.4.2   Influence of Gasoline Equivalence Ratio on the Effects of Degree of CNG Stratification

The effect of CNG injection rate and timing was significantly influenced by the gasoline equivalence ratio. At ϕ_{Total} = 0.30, increasing the gasoline equivalence resulted in increased IMEP at a given degree of stratification. The highest IMEP was obtained with CNG injection at 300° BTDC and ϕ_g = 0.26 as shown in Figure 4.52.

At a higher load ($\phi_{Total} = 0.40$), the effect of CNG injection timing was marginal with the highest IMEP was obtained with CNG injection at 80° BTDC and with $\phi_g = 0.26$ as shown in Figure 4.53. When the gasoline equivalence ratio was increased to 0.26 with CNG injection at 300° BTDC, it resulted in reduced IMEP due to more complete combustion resulted when the gasoline equivalence ratio was higher.
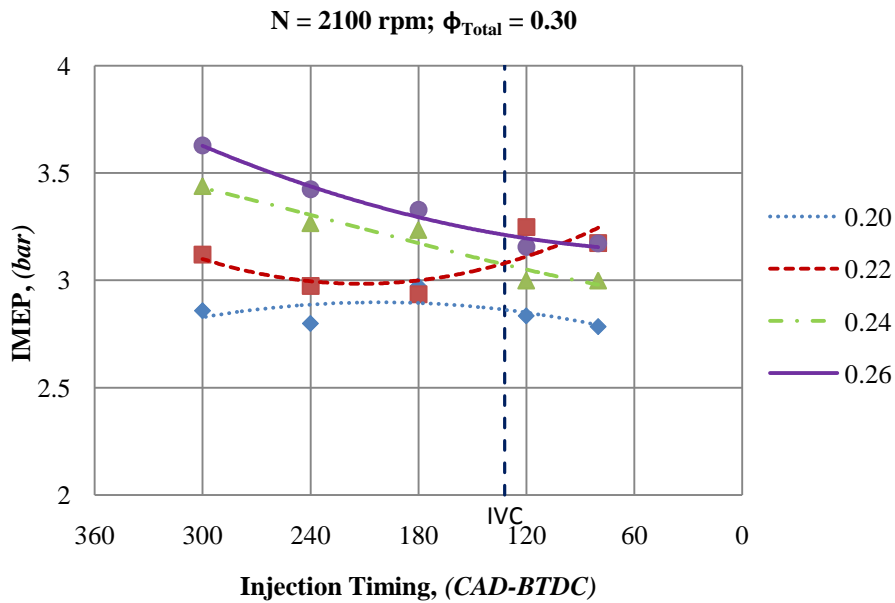

Figure 4.52 Effect of degree of stratification on the IMEP at a low CNG injection rate.
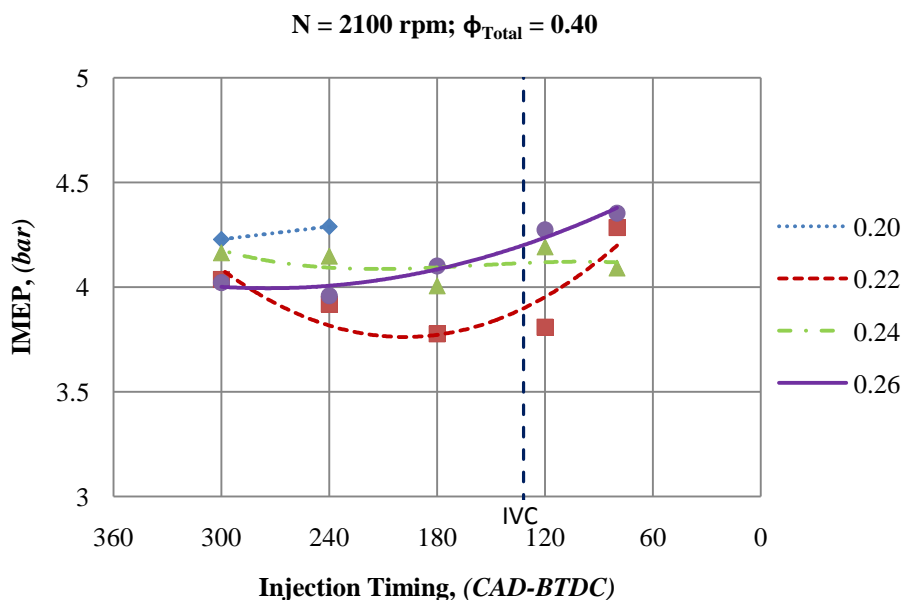

Figure 4.53 Effect of degree of stratification on the IMEP at higher CNG injection rate

However, as the injection timing was retarded it resulted in an increase in IMEP and the highest IMEP was achieved with CNG injection at 80° BTDC. Therefore, at $\phi_{Total} = 0.30$, low degrees of stratification resulted in higher IMEP and at $\phi_{Total} = 0.40$, increasing the degree of stratification increased the IMEP. Increasing the degree of stratification resulted in misfire and led to quench of combustion when CNG injection rate was increased at $\phi_g = 0.20$. That is, higher equivalence ratio of gasoline needed to achieve combustion when CNG injection rate was high and it was stratified as CNG rich zones required more energy to get ignited.

At $\phi_{Total} = 0.30$, the most significant effect of the degree of stratification of CNG was observed with gasoline equivalence ratios of $\phi_g = 0.20$ and 0.22. At $\phi_g = 0.24$ and 0.26, ignition timing was a function of ϕ_g and the effect of stratification of CNG was marginal. At $\phi_g = 0.24$, the ignition delay was marginally affected by both the gasoline equivalence ratio and degree of stratification.

With CNG injection at 300° BTDC, there was no significant effect on the ignition timing by the gasoline equivalence ratio. But at 80° BTDC, increasing the gasoline equivalence ratio significantly advanced the ignition delay. At $\phi_{Total} = 0.3$, with homogeneous mixtures created by injecting CNG at 300° BTDC, both gasoline equivalence ratio and the presence of CNG had a marginal effect on ignition timing as shown in Figure 4.11 and Figure 4.54. However, when CNG was stratified by retarding the injection timing, both the degree of stratification and gasoline equivalence ratio became significant. Therefore, at the low load of $\phi_{Total} = 0.30$ at which CNG injection rate was low ($m_{CNG}/m_{Total} < 30\%$ as shown in Figure 4.8), the ignition timing could be controlled by varying the gasoline equivalence ratio only when the CNG was stratified.

This suggests that the limit of the minimum required amount of CNG to control the ignition timing could be extended by stratifying the CNG at low gasoline equivalence ratios of $\phi_g = 0.20$ and 0.22. This led to a trade off between controllability and performance as IMEPs obtained at $\phi_g = 0.20$ and 0.22 are lower than those obtained with higher gasoline equivalence ratios as shown in Figure 4.52.
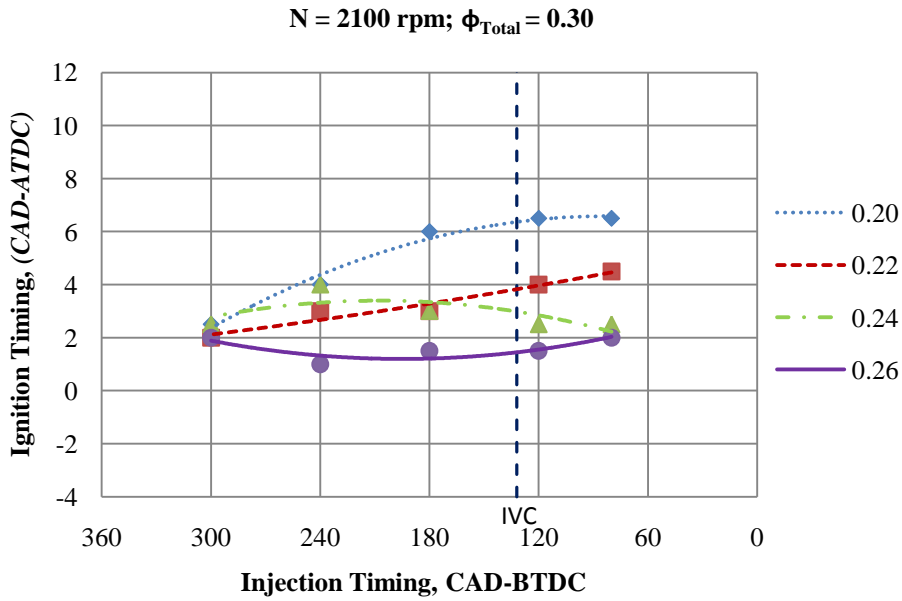
$$N = 2100 \text{ rpm}; \; \phi_{Total} = 0.30$$

Figure 4.54 Effect of CNG stratification and ϕ_g on ignition timing at a low CNG injection rate
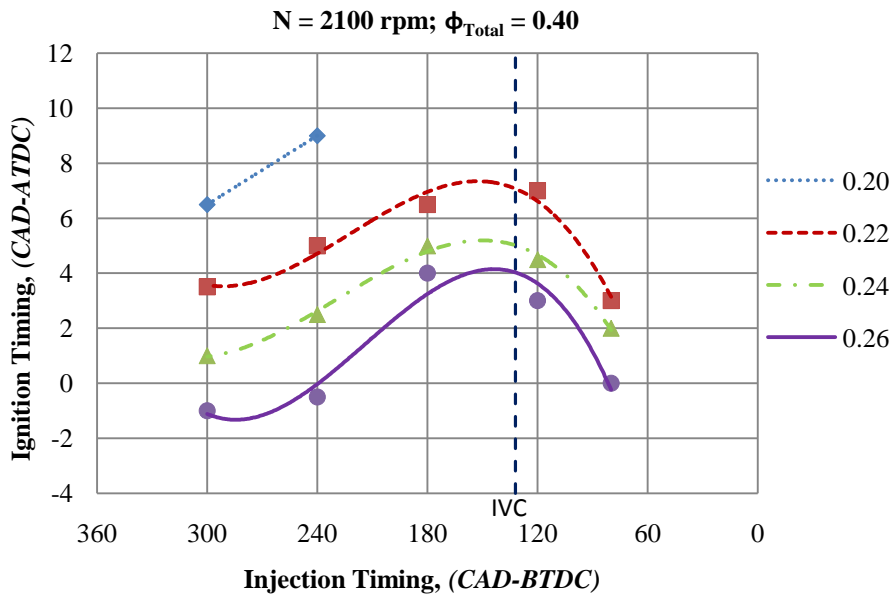

$$N = 2100 \text{ rpm}; \; \phi_{Total} = 0.40$$

Figure 4.55 Effect of CNG stratification and ϕ_g on ignition timing at a higher CNG injection rate

At a high load ($\phi_{Total}= 0.40$), the CNG injection rate had a significant effective on the ignition timing at all injection timings and for all cases of ϕ_g as shown in Figure 4.55. When the injection timing was retarded at a given ϕ_g, it caused a delay in ignition timing. The ignition was initially delayed when the injection timing was retarded from 300° to a point between 180° and 132° BTDC and then it advanced again. Injection of CNG after inlet valve closure (IVC), results in a sharp advance of ignition timing. This was due to the fact that the injection after the intake valve closed resulted in a higher degree of stratification.

90

The highest delay was obtained when CNG was injected between 180° BTDC (or BDC) and 132° BTDC. It may be noted that the piston comes to zero velocity at 180° BTDC and reverses its direction of motion and at 132° BTDC the intake valves are closed. This caused a significant turbulence in the cylinder. When CNG was injected at this instance, the turbulence generated in the cylinder greatly affects the spatial and temporal distribution of CNG in the premixed gasoline charge [37, 93].

In addition to that, the engine intake charge temperature was kept at 300°C. During the intake stroke, the charge got cooled by the cylinder wall which was at a lower temperature. However, during the compression stroke the temperature of the charge again increased due to compression. That is, the intake charge reaches the lowest value of temperature at 180° BTDC.

Therefore, when CNG was injected at 180° BTDC, it was exposed to turbulent conditions and low charge temperature. Also, CNG injection at 180° BTDC offered less time for CNG to get mixed than 300° BTDC injection. Therefore, with CNG injection at 180° BTDC, a mixture with spatial and temporal stratification of CNG was formed.
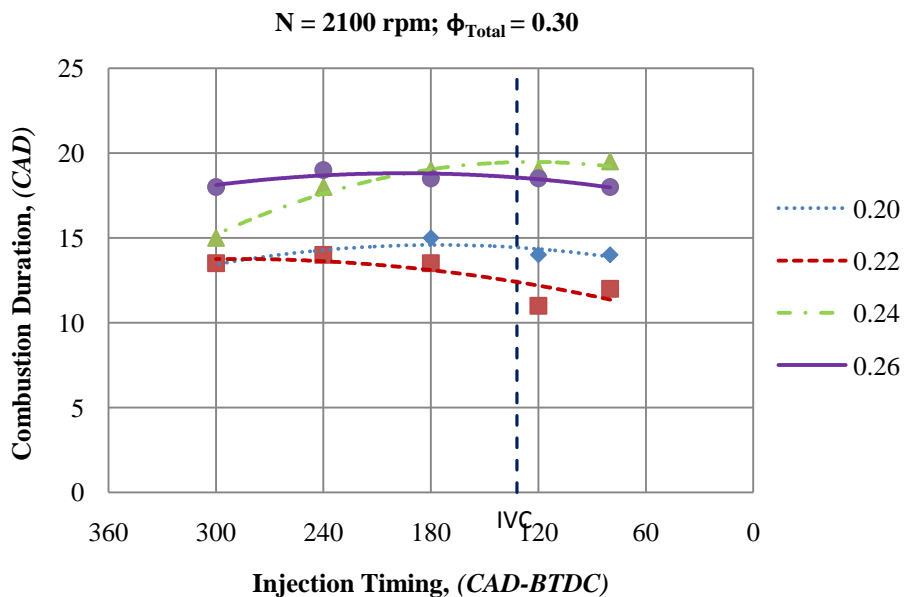

Figure 4.56 Effect of CNG stratification and ϕ_g on combustion duration at a low CNG injection rate
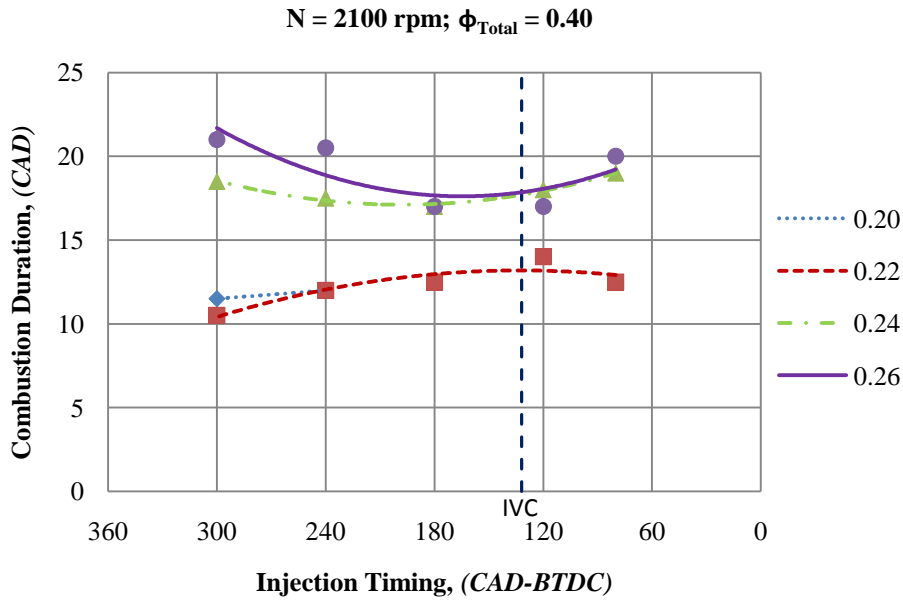
N = 2100 rpm; ϕ_{Total} = 0.40

Figure 4.57 Effect of CNG stratification and φ_g on combustion duration at higher CNG injection rate

However, any effects of thermal stratification were overcome by the high degree of mixture stratification resulted with CNG injection after intake valve closure, especially at 80° BTDC. Similarly, when CNG was injected early at 300° BTDC, it had ample time to mix and get heated by the gasoline charge. This led to the formation of homogeneous mixture of CNG, gasoline and air in terms of both mixture concentration and temperature distribution.

At both low and high loads (ϕ_{Total}= 0.30 and 0.40), combustion duration was marginally affected by the injection timing as shown in Figure 4.56 and Figure 4.57. It was a strong function of ϕ_g with higher gasoline equivalence ratios resulting in longer combustion durations. The increase in combustion duration was highest when the gasoline equivalence ratio was increased from 0.22 to 0.24. At ϕ_{Total} = 0.40, a smaller increases and decreases in combustion duration was observed with ϕ_g = 0.22 and ϕ_g = 0.26 respectively. Overall, the higher gasoline equivalence ratios advanced the autoignition and prolonged the combustion duration.

The pressure history and heat release rates at various injection timings are shown in Figure 4.58 to Figure 4.61. The most significant effects on the pressure rise rates were observed with ϕ_g = 0.20. The resulting peak pressures were reduced when the degree of stratification was increased except when the ϕ_g = 0.26.
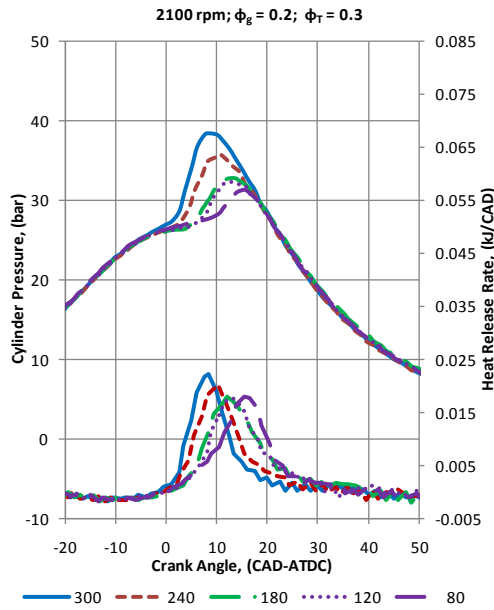
92

2100 rpm; ϕ_g = 0.2; ϕ_T = 0.3

Figure 4.58 Pressure and heat release rate at $\phi_g = 0.20$ and $\phi_{Total} = 0.30$.

2100 rpm; ϕ_g = 0.24; ϕ_T = 0.3
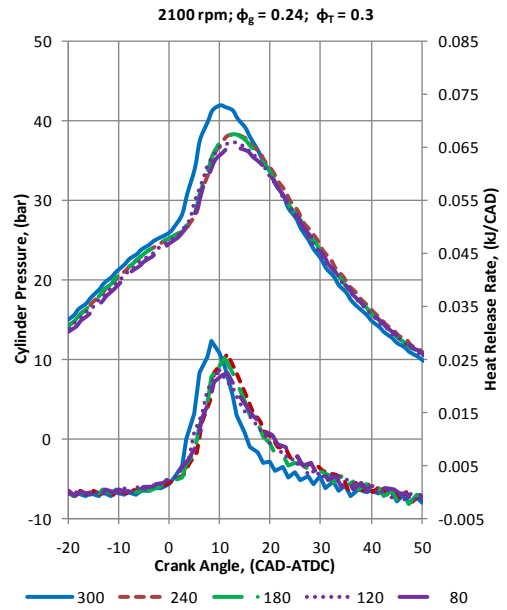
Figure 4.60 Pressure and heat release rate at $\phi_g = 0.24$ and $\phi_{Total} = 0.30$.

2100 rpm; ϕ_g = 0.22; ϕ_T = 0.3
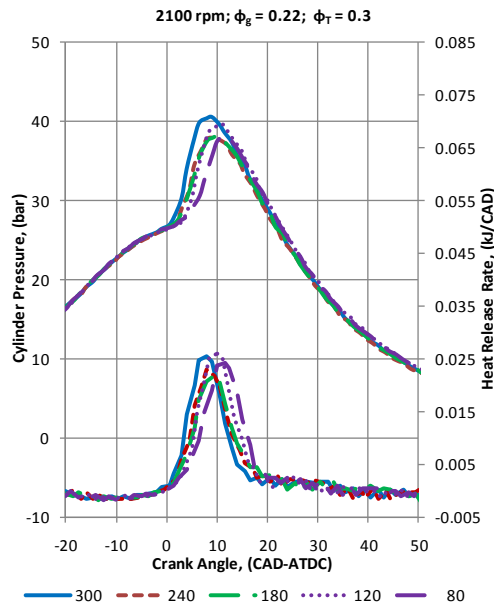
Figure 4.59 Pressure and heat release rate at $\phi_g = 0.22$ and $\phi_{Total} = 0.30$.

2100 rpm; ϕ_g = 0.26; ϕ_T = 0.3
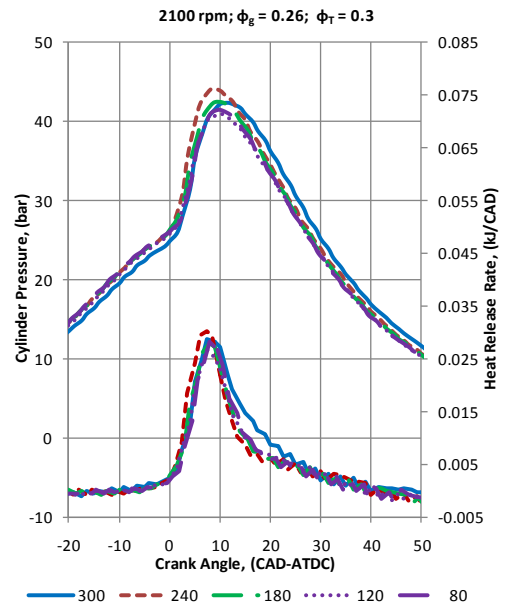
Figure 4.61 Pressure and heat release rate at $\phi_g = 0.26$ and $\phi_{Total} = 0.30$.

As shown in Figure 4.58, at $\phi_{Total} = 0.30$ and $\phi_g = 0.20$, when the degree of CNG stratification was increased by retarding injection timing, a significant delay in ignition timing and reduction in peak pressure were observed. However, pressure rise and heat release rate was marginally affected when injection was retarded from 180° to 120° BTDC at $\phi_g = 0.20$.

93

2100 rpm; ϕ_g = 0.2; ϕ_T = 0.40

Figure 4.62 Pressure and heat release rate at $\phi_g = 0.20$ and $\phi_{Total} = 0.40$.

2100 rpm; ϕ_g = 0.22; ϕ_T = 0.40
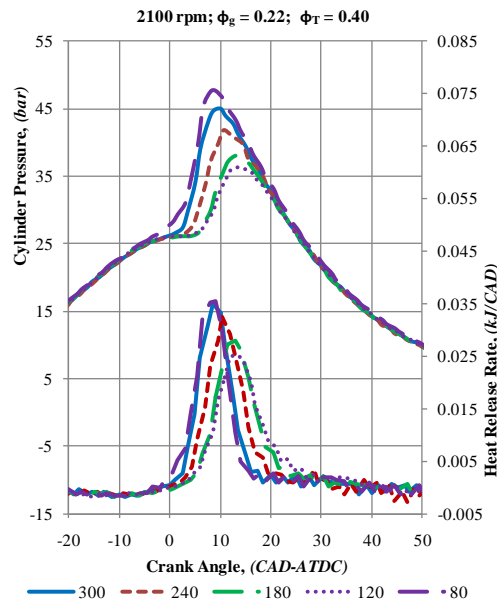
Figure 4.64 Pressure and heat release rate at $\phi_g = 0.20$ and $\phi_{Total} = 0.40$.

2100 rpm; ϕ_g = 0.24; ϕ_T = 0.40
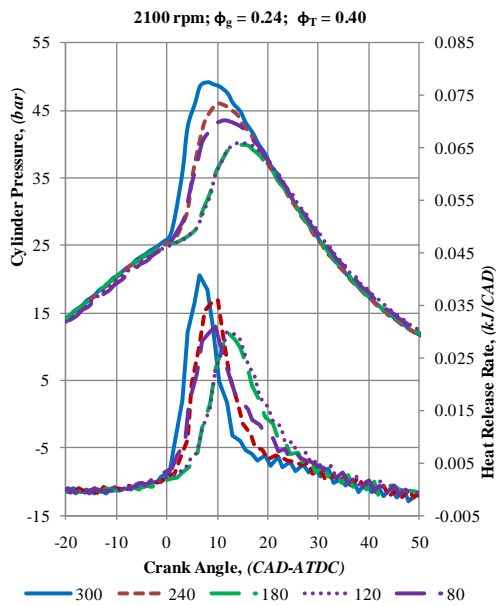
Figure 4.63 Pressure and heat release rate at $\phi_g = 0.20$ and $\phi_{Total} = 0.40$.

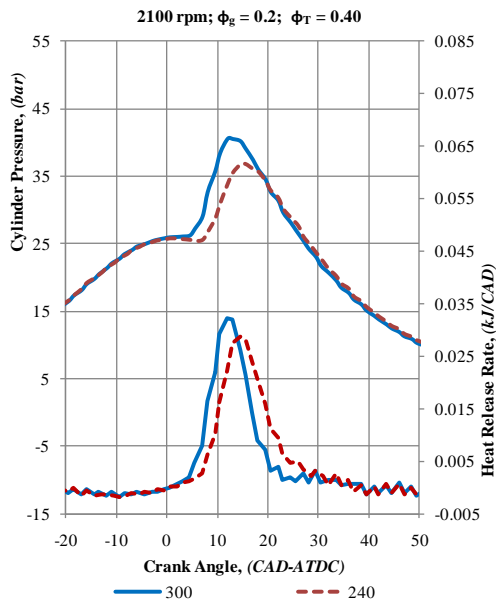**2100 rpm; ϕ_g = 0.26; ϕ_T = 0.40**

Figure 4.65 Pressure and heat release rate at $\phi_g = 0.20$ and $\phi_{Total} = 0.40$.

When ϕ_g was increased to 0.22, at ϕ_{Total} = 0.30, it resulted in higher peak pressure and heat release rate at all injection timings as shown in Figure 4.59. However, when injection timing was retarded, there was less reduction in pressure rise, heat release rate and ignition timing than that obtained with $\phi_g = 0.20$.

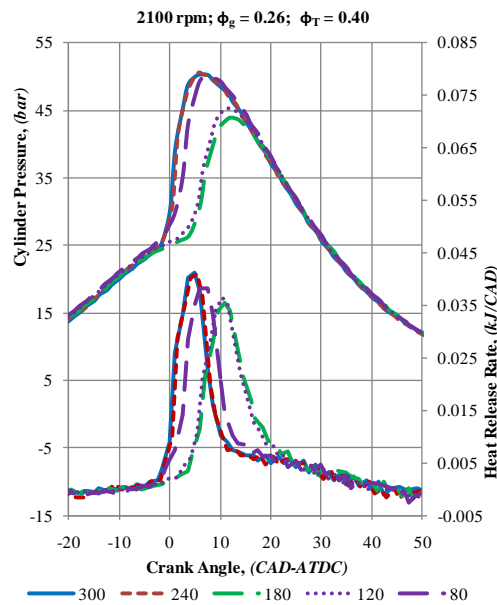At ϕ_{Total} = 0.30 and ϕ_g = 0.24, there was a marginal increase in peak pressures except at 300° BTDC as shown in Figure 4.60. At 300° BTDC peak pressure was significantly higher than that resulted at other injection timings and that resulted at ϕ_g = 0.22. At ϕ_g = 0.26, the effect of injection timing was less significant and ignition timing and heat release rate were marginally different from one another as shown in Figure 4.61. At ϕ_{Total} = 0.40 and at ϕ_g = 0.20, similar to the case of ϕ_{Total} = 0.30 and ϕ_g = 0.20, peak pressures and heat release rate reduced and ignition was delayed as shown in Figure 4.62. However, at ϕ_{Total} = 0.40 and ϕ_g = 0.22, a different trend was observed.

When injection timing was retarded from 300° BTDC to 120° BTDC, peak pressure and heat release rates reduced. However, at 80° BTDC it again increased and closely matched the pressure traces obtained with injection at 300° BTDC as shown in Figure 4.62. Similar trend was observed when ϕ_g was increased to 0.24, however, peak pressure and heat release rate obtained were less than those resulted at 300° BTDC as shown in Figure 4.64. At ϕ_g = 0.26, high heat release and peak pressure were observed at 300°, 240° and 80° BTDC. However, CNG injection at 180° and 120° BTDC resulted in reduced peak pressure and heat release rate due to mixture and thermal stratification as shown in Figure 4.65.
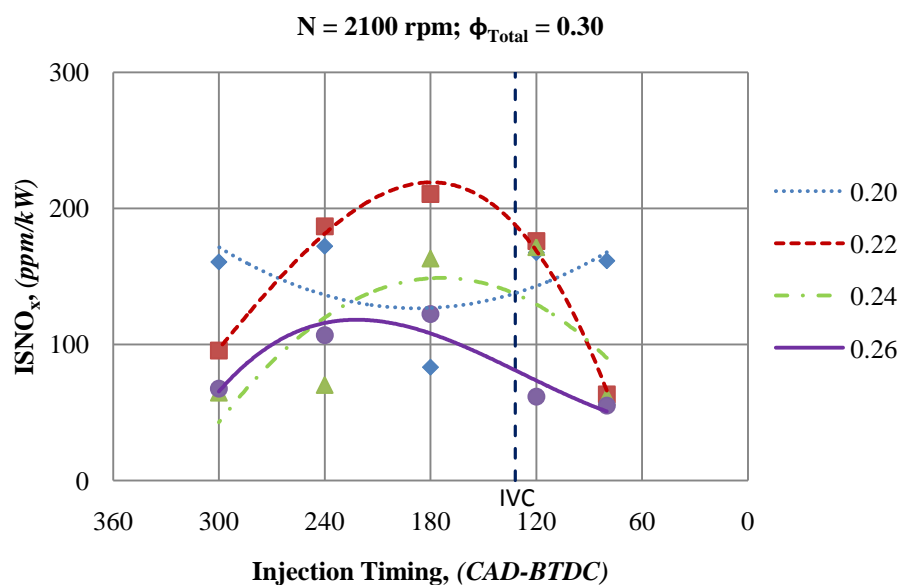

Figure 4.66 Effect of CNG stratification and ϕ_g on NO_x emissions at a low CNG injection rate

N = 2100 rpm; ϕ_Total = 0.40
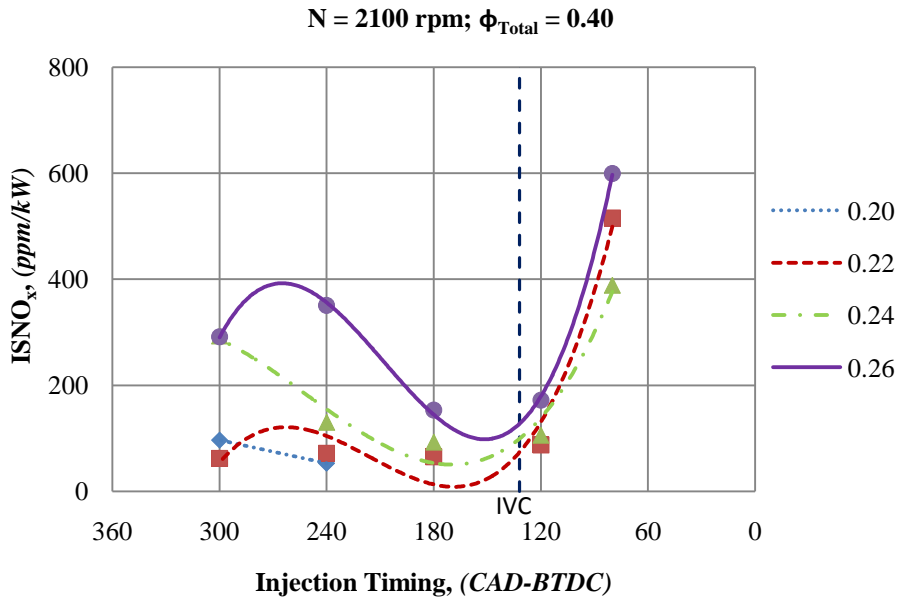
Figure 4.67 Effect of CNG stratification and ϕ_g on NO_x emissions at higher CNG injection rate

Figure 4.66 and Figure 4.67 show the NO_x emissions at ϕ_g = 0.30 and 0.40 respectively. NO_x emissions were lower than 250 ppm/kW for all cases at ϕ_{Total} = 0.30. At ϕ_{Total} = 0.40, the highest NO_x emissions were obtained with CNG injection at 80° BTDC. The high degree of stratification of CNG and high ϕ_{Total} resulted in high temperature combustion leading to more NO_x emissions.

N = 2100 rpm; ϕ_Total = 0.30

Figure 4.68 Effect of CNG stratification and ϕ_g on the formation of NO_2 at a low CNG injection rate

96

N = 2100 rpm; ϕ_{Total} = 0.40
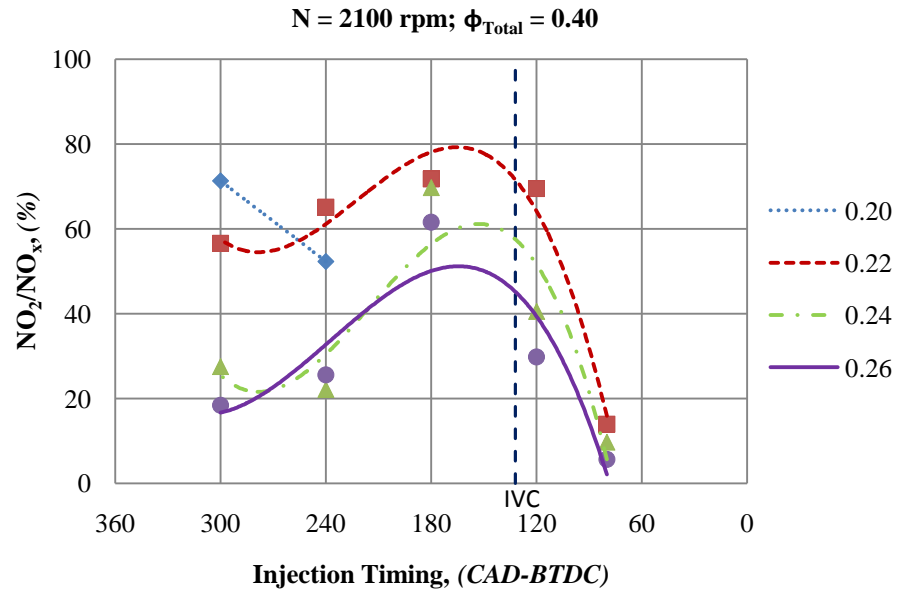
Figure 4.69 Effect of CNG stratification and ϕ_g on the formation of NO_2 at higher CNG injection rate

However, significant effects were observed on the ratio of NO_2 to NO_x. At ϕ_{Total} = 0.30, NO_2/NO_x ratio was higher than 50% for all cases as shown in Figure 4.68. When the degree of stratification of CNG was increased, the formation of NO_2 was reduced at both loads. However, the reduction was more significant at ϕ_{Total} = 0.40 due to the higher degree of stratification and higher amounts of CNG. NO_2 formation was also reduced when ϕ_g increased at both the loads.

N = 2100 rpm; ϕ_{Total} = 0.30

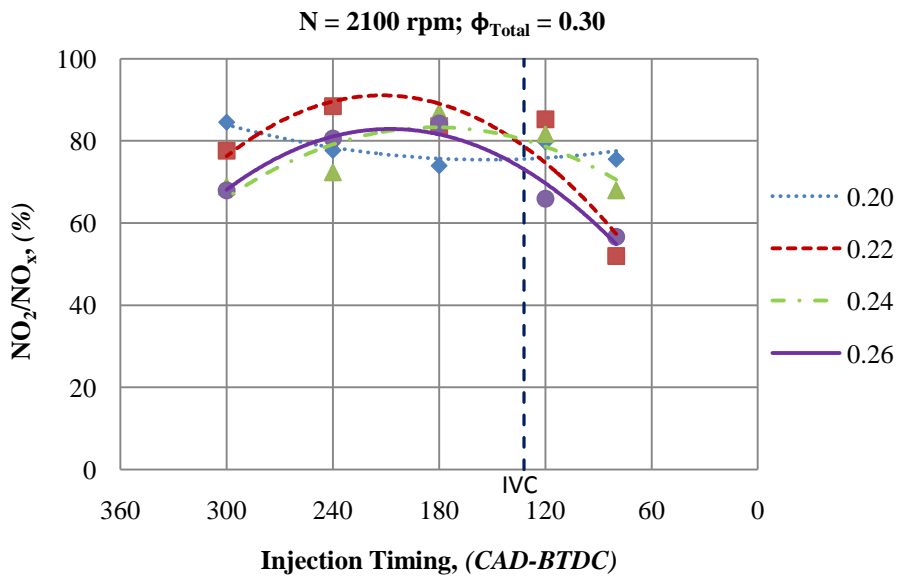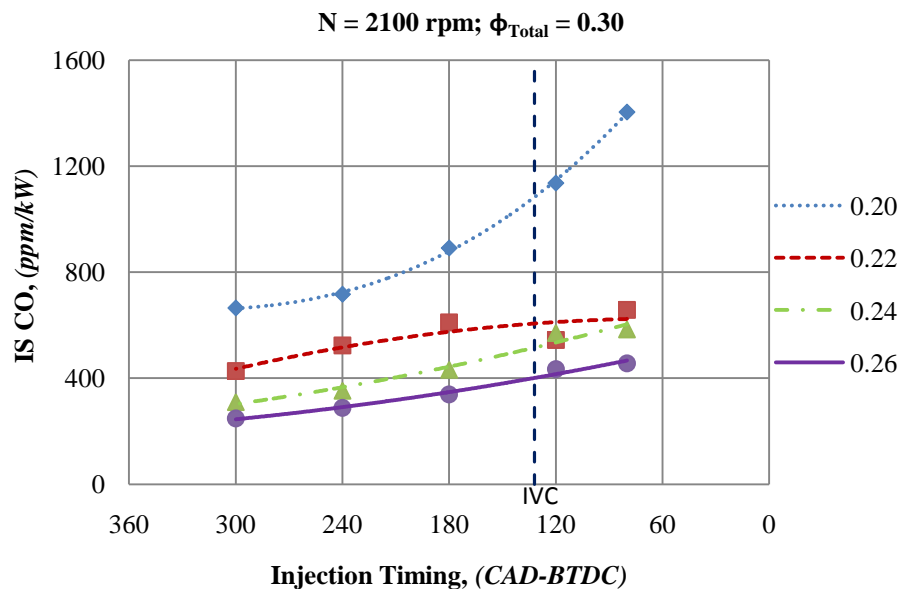*Figure 4.70 Effect of CNG stratification and ϕ_g on CO emissions at a low CNG injection rate*

Figure 4.71 Effect of CNG stratification and ϕ_g on CO emissions at higher CNG injection rate

As shown in Figure 4.70, CO emissions at $\phi_{Total} = 0.30$ were marginally affected by injection timing except for the case of $\phi_g = 0.20$. As the degree of CNG stratification was increased, CNG rich zones may result in less complete combustion as the heat liberated from gasoline combustion was low at $\phi_g = 0.20$ leading to overall increase in CO emissions. The CO emission was reduced for all the cases with an increase in gasoline strength in the mixture.

At $\phi_{Total} = 0.40$, peak values of CO emissions were obtained with injection at around 180°BTDC and further retardation in injection timing resulted in a reduction in CO emission as shown in Figure 4.71. However, CO emissions at $\phi_{Total} = 0.40$ were less than that obtained at $\phi_{Total} = 0.30$ for all cases.

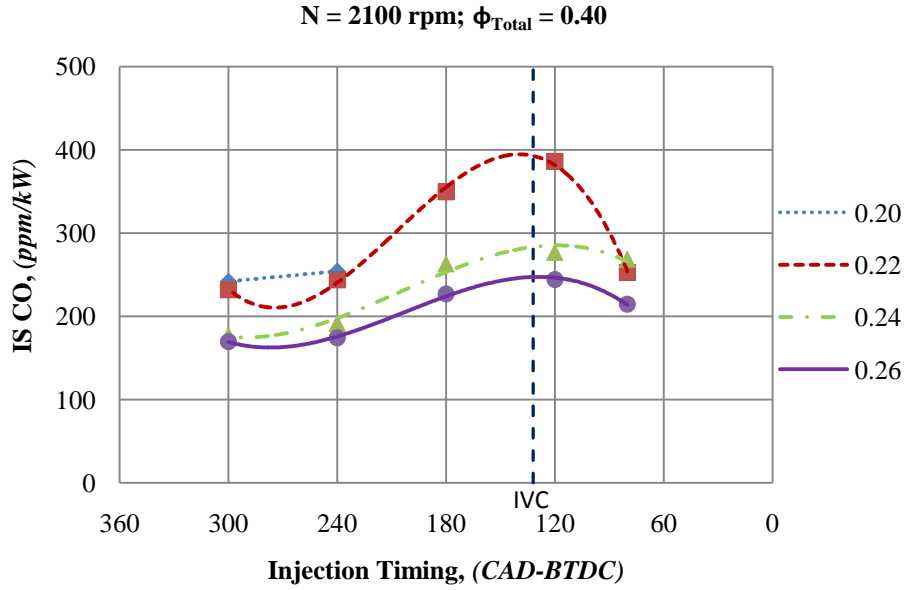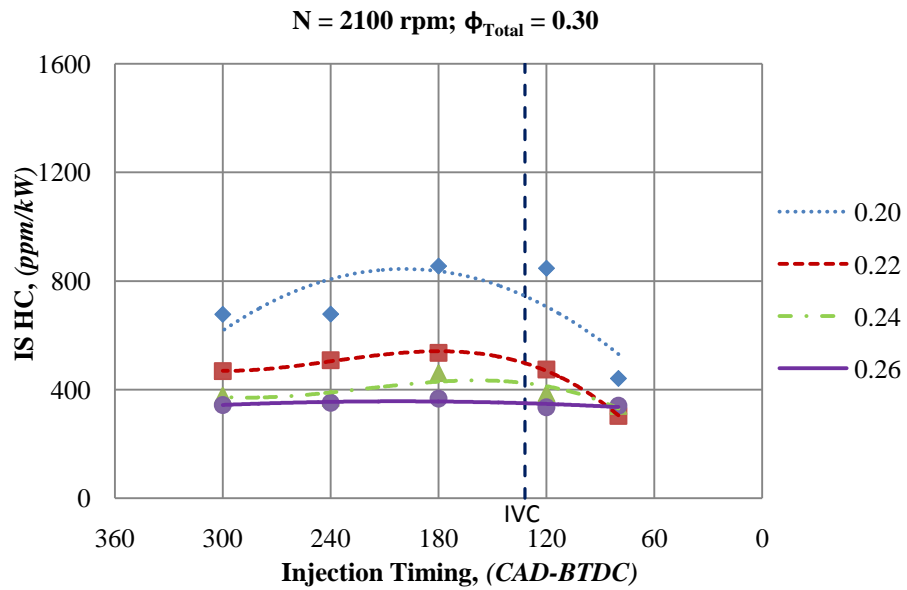*Figure 4.72 Effect of CNG stratification and ϕ_g on HC emissions at a low CNG injection rate*
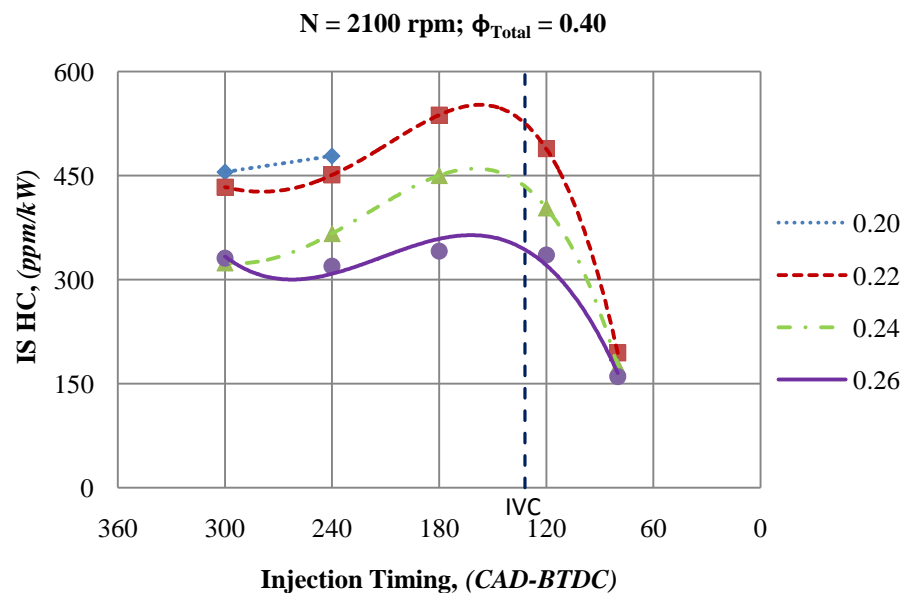
Figure 4.73 Effect of CNG stratification and ϕ_g on HC emissions at higher CNG injection rate

As shown in Figure 4.72, HC emissions were more significantly affected by the gasoline equivalence ratio than the degree of CNG stratification at $\phi_{Total} = 0.30$. But at $\phi_{Total} = 0.40$, there was a significant reduction in HC emissions at 80° BTDC as shown in Figure 4.73.

From Figure 4.74, it can be seen that more complete combustion of CNG resulted when it was stratified. However, for the all cases, the ratio was less than 8% which was further reduced with injection at 80° BTDC.

N = 2100 rpm; ϕ_{Total} = 0.30
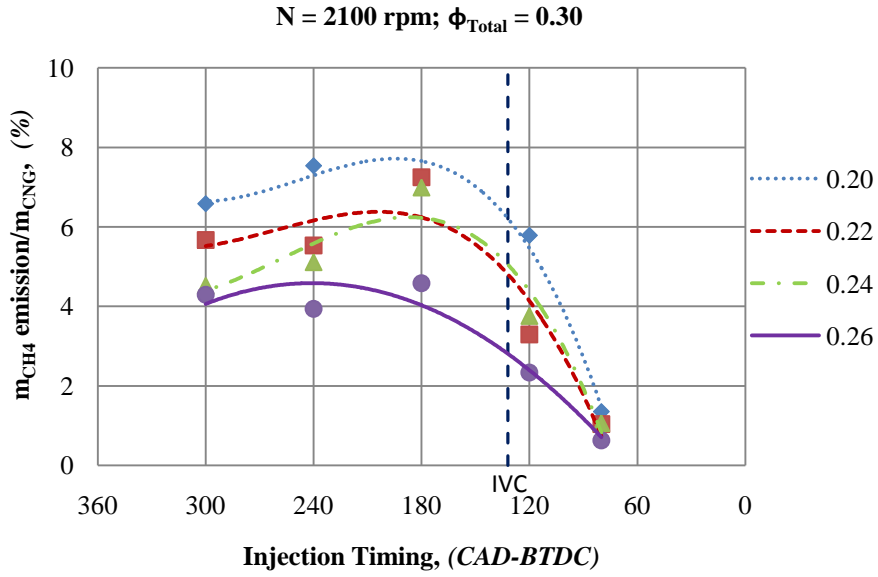
Figure 4.74 Effect of CNG stratification and ϕ_g on the CH_4 emissions at a low CNG injection rate

N = 2100 rpm; ϕ_{Total} = 0.40

Figure 4.75 Effect of CNG stratification and ϕ_g on the CH_4 emissions at higher CNG injection rate

Similar trends were observed at ϕ_{Total} = 0.4 and the ratio was less than 6% for all the cases as shown in Figure 4.75. Higher gasoline equivalence ratios resulted in more complete combustion of CNG at both high and low loads and at all injection timings.

4.4.3 Influence of Engine Speed on the Effects of Degree of CNG Stratification

The scope of this section is to discuss the effects of degree of stratification of CNG and that of engine speeds on the combustion. As at $\phi_g = 0.22$, the engine could be operated for a wide range of engine speeds at all injection timings of CNG. Therefore, the effects of degree of stratification at $\phi_g = 0.22$ and at two total equivalence ratios, $\phi_{Total} = 0.30$ that produced a moderate load and $\phi_{Total} = 0.35$ that produced a higher engine load, are discussed in this section.

At 1200 rpm, engine operation at $\phi_{Total} = 0.35$ was limited due to knocking; therefore, discussion at this load is limited to engine speeds from 1800 to 2100 rpm. As the engine speed was increased, IMEP generated decreased as shown in Figure 4.76. IMEP was a stronger function of engine speed and there was a marginal effect on IMEP by degree of CNG stratification as shown in Figure 4.76. However, at $\phi_{Total} = 0.35$, there were significant effects on the IMEP generated when the degree of stratification was varied as shown in Figure 4.77.
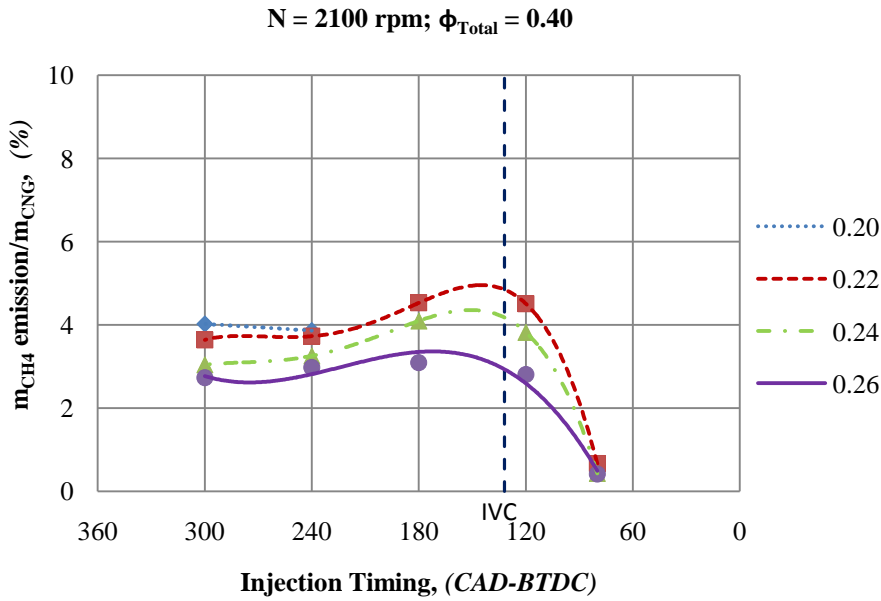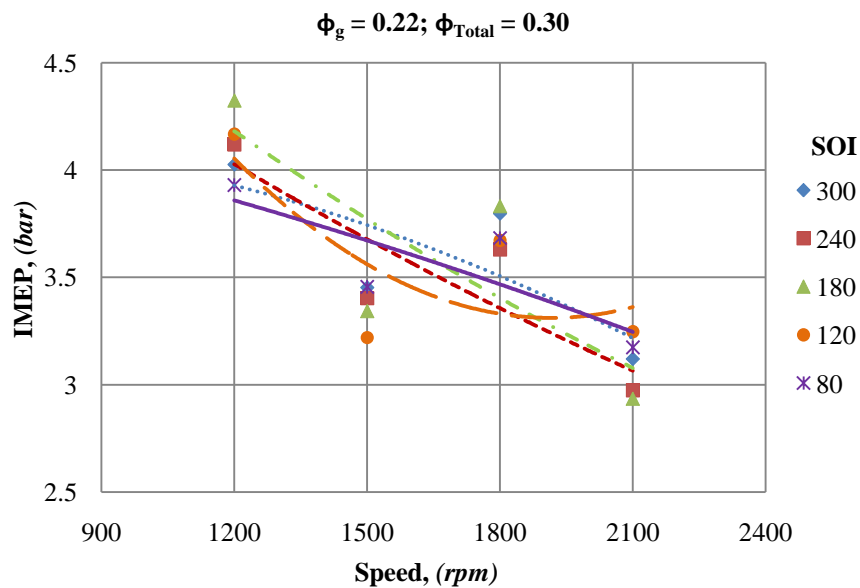

Figure 4.76 Effect of CNG stratification on IMEP generated at a low CNG injection rate
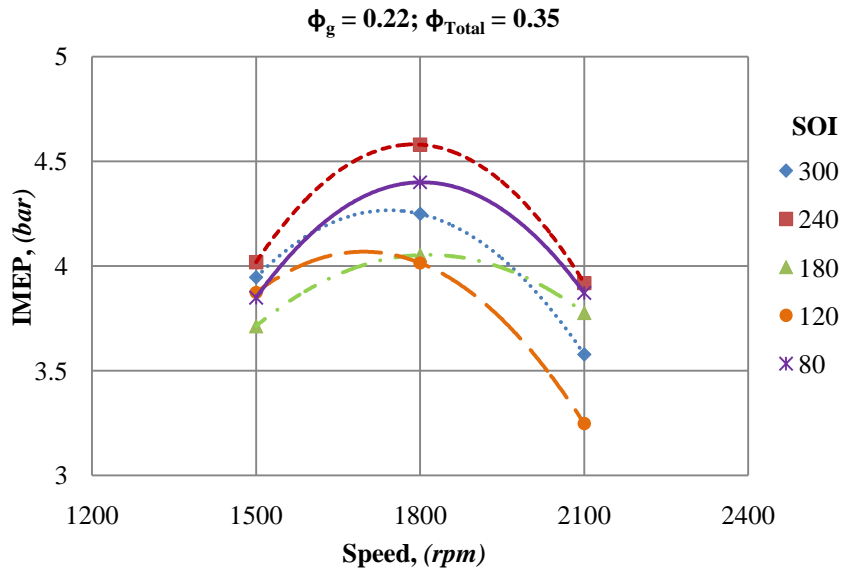
Figure 4.77 Effect of CNG stratification on IMEP at a higher CNG injection rate

At $\phi_{Total} = 0.35$, CNG injection at 300°, 240°BTDC resulted in higher IMEP due to homogeneous mixing which resulted in more complete combustion. CNG injection at 180° and 120° BTDC generated lower IMEP due the presence of zones of lower temperature and mixture concentration which led to incomplete combustion. At 1800 rpm higher IMEPs were obtained for all injection timings than other engine speeds and the highest IMEP was generated at 240° BTDC and 1800 rpm.

Figure 4.78 Effect of CNG stratification on indicated thermal efficiency at a low CNG injection rate

102

$\phi_g = 0.22; \phi_{Total} = 0.35$
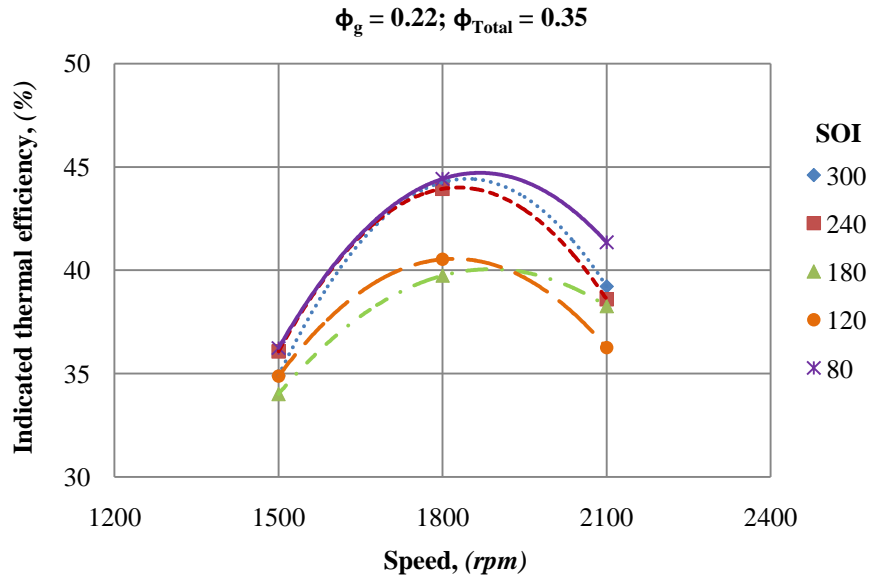
Figure 4.79 Effect of CNG stratification on thermal efficiency at a higher CNG injection rate

Figure 4.78 and Figure 4.79 show the indicated thermal efficiencies obtained at $\phi_{Total} = 0.30$ and $\phi_{Total} = 0.35$ respectively. The highest thermal efficiency was achieved at 1800 rpm at both loads. Higher thermal efficiencies were obtained at 300° and 240° BTDC due to homogeneous mixing which resulted in better combustion. Similarly, CNG injection at 80° BTDC created highly stratified mixture which resulted in more complete combustion of CNG and high thermal efficiency was obtained.

$\phi_g = 0.22; \phi_{Total} = 0.30$

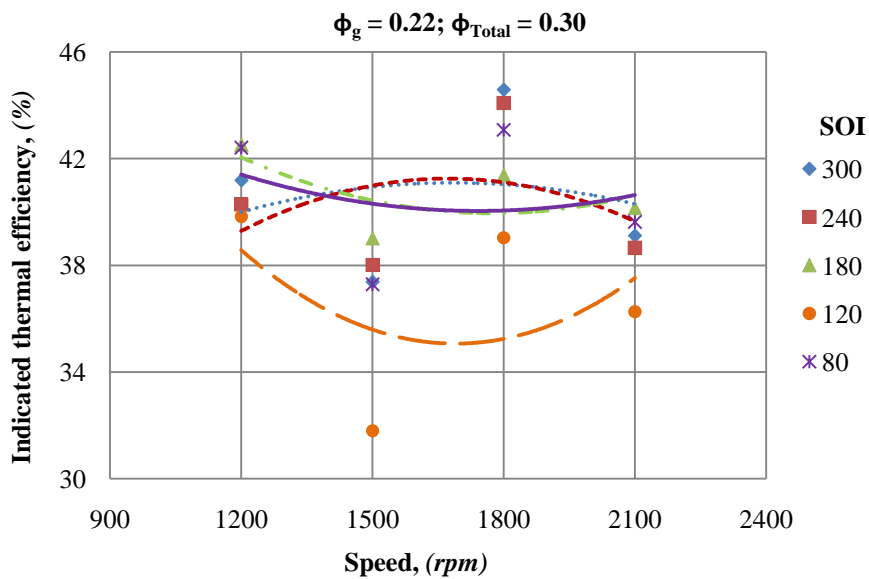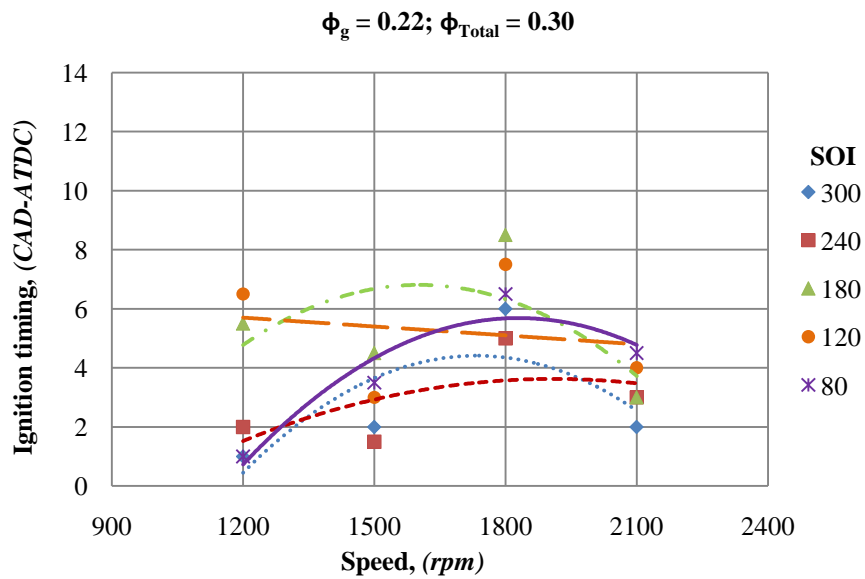*Figure 4.80 Effect of CNG stratification on ignition timing at a low CNG injection rate*
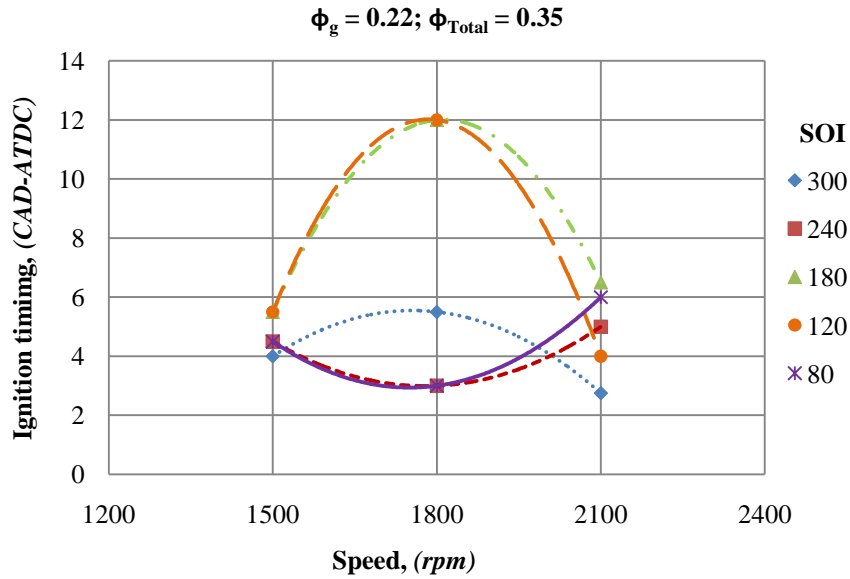
103

Figure 4.81 Effect of CNG stratification on ignition timing at higher CNG injection rate

As shown in Figure 4.80, engine speed and degree of stratification had significant effects on the ignition timing at $\phi_{Total} = 0.30$. The highest delay in ignition timing was observed at 180° and 120° BTDC due to combined mixture and thermal stratification. CNG injection at 300° and 240° BTDC resulted in advanced ignition timings and that at 80° BTDC resulted slightly delayed ignition timing compared to the cases of 300° and 240° BTDC. Similar trends were obtained at $\phi_{Total} = 0.35$ as shown in Figure 4.81. However, CNG injection at 180° and 120° BTDC resulted in more significant delay in ignition timing at 1800rpm.

CNG injection at 180° and 120° BTDC resulted in prolonged combustion duration at both $\phi_{Total} = 0.30$ and $\phi_{Total} = 0.35$ as shown in Figure 4.82 and Figure 4.83. Increase in engine speed resulted in an increase in combustion duration and at $\phi_{Total} = 0.30$ up to 1800 rpm and then decreased marginally. The longest combustion duration was obtained at 1800 rpm and at 180° BTDC at both loads. At $\phi_{Total} = 0.30$, the shortest combustion duration was obtained with CNG injection at 80° BTDC due to high degree of CNG stratification.

CNG injection at 300° and 240° BTDC had marginal differences in the resultant combustion duration, however the combustion duration increased with an increase in engine speed at these injection timings at $\phi_{Total} = 0.30$.
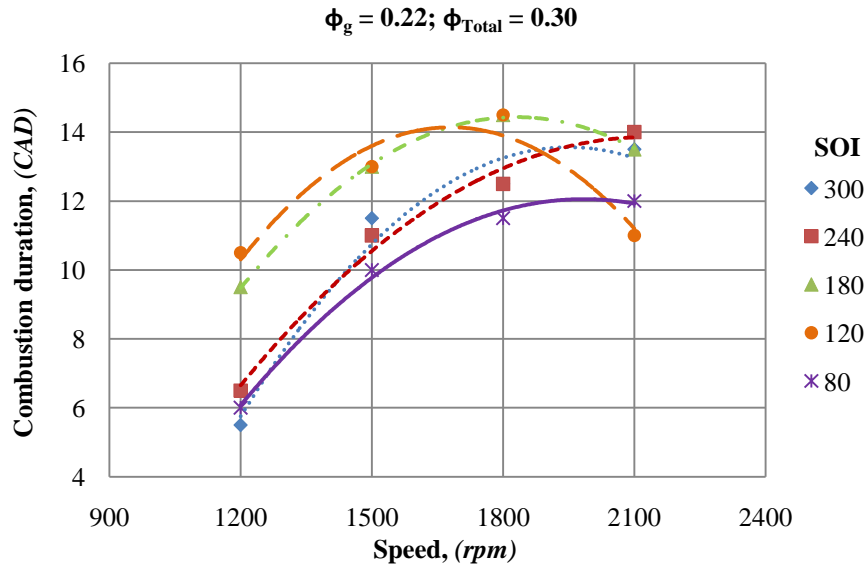
Figure 4.82 Effect of CNG stratification on combustion duration at a low CNG injection rate
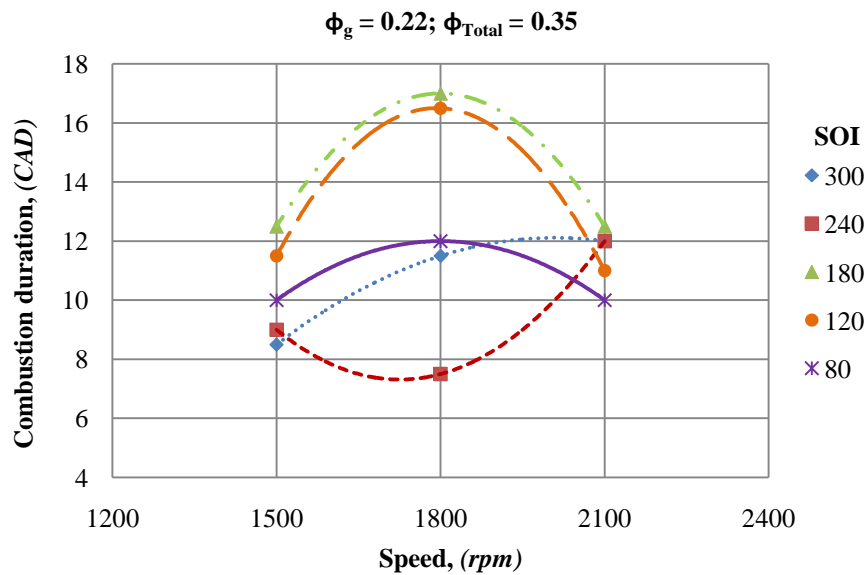
Figure 4.83 Effect of CNG stratification on combustion duration at a higher CNG injection rate

At $\phi_{Total} = 0.35$, more significant increase in combustion duration was observed at 180° BTDC and 120° BTDC due to higher amounts of CNG in the mixture as shown in Figure 4.83. There was a marginal effect on combustion duration due to change in engine speed at 80° BTDC. The difference in combustion duration obtained at 300°BTDC and 80° BTDC was less noticeable. However, the highest combustion duration was obtained at 1800 rpm at all injection timings except 240° BTDC.
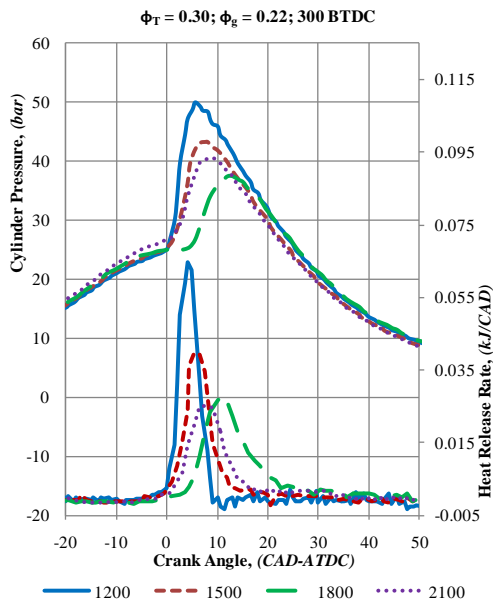
Figure 4.84 Pressure history and heat release rates at different engine speeds with homogeneous mixing.
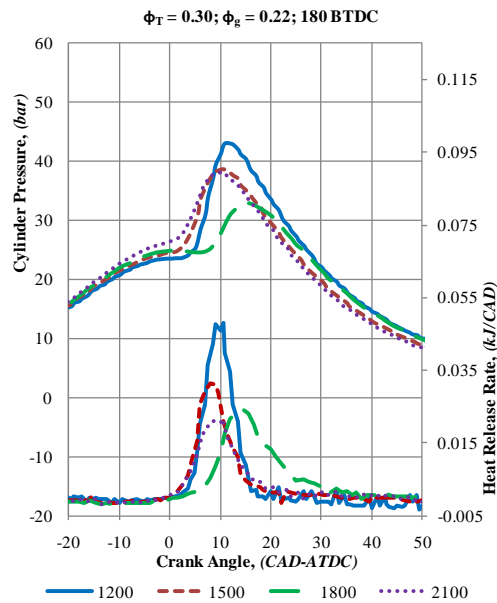
Figure 4.86 Pressurre history and heat release rates at different engine speeds with thermal and mixture stratification.
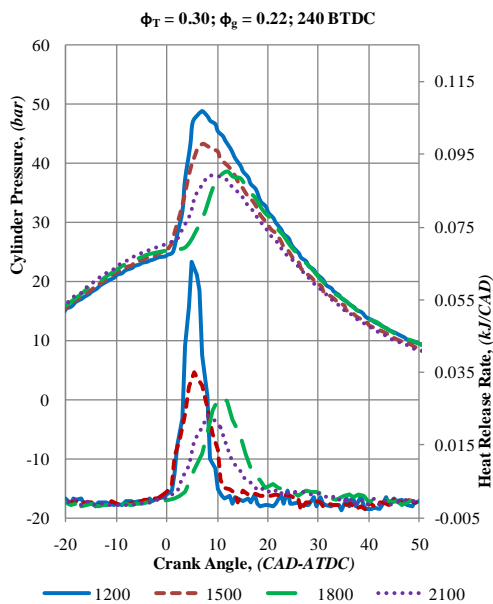
Figure 4.85 Pressure history and heat release rates at different engine speeds with slight stratification.

Figure 4.87 Pressure history and heat release rates at different engine speeds with CNG injection at 120 °BTDC.

As shown in Figure 4.84, with CNG injection at 300° BTDC, with an increase in engine speed the peak pressure and heat release rates reduced up to 1800 rpm and they increased again at 2100 rpm. The highest peak pressure (49.9 bars) was obtained at 1200 rpm.
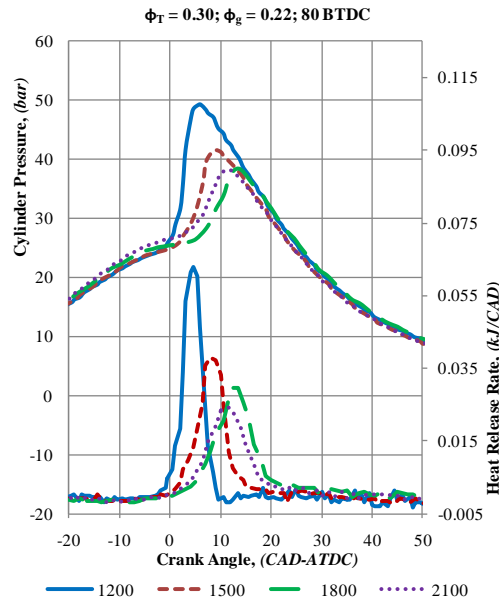
Figure 4.88 Pressure history and heat release rates at different engine speeds with high degree of CNG stratification.

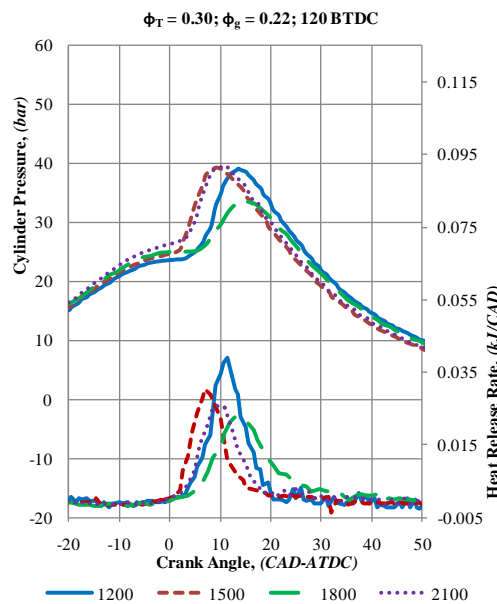At 1200 rpm, as the injection timing was retarded from 300° to 120° BTDC, peak pressure and heat release rate reduced. However, peak pressure again increased (to 49.2 bars) at 80° BTDC due to high CNG stratification that promoted rapid burning as shown in Figure 4.88. That is, at 1200 rpm CNG injection at 300° BTDC and 80° BTDC resulted in the highest heat release rates and peak pressures.

As shown in Figure 4.85, with slight stratification of CNG created by injection at 240° BTDC, a small decrement in peak pressures was observed at all speeds compared to injection those obtained at 300° BTDC. However, there was no significant difference in the trends in peak pressure and heat release rates between injection at 240° BTDC and 300° BTDC.

At 1800rpm, significant delay in ignition timing was observed at all cases. As the combustion was phased after TDC, it resulted in a reduction of peak pressures and heat release rates due to simultaneous expansion of the gases as the piston moves down to BDC. This resulted in higher IMEP and 1800 rpm was observed to be optimum for performance and was operable at both $\phi_{Total} = 0.30$ and 0.35 at all engine speeds. With CNG injection at 180° BTDC that resulted in thermal stratification, the peak pressure and heat release rate were significantly lower than those obtained with homogeneous mixture created by injection at 300° BTDC as shown in Figure 4.86. As shown in Figure 4.87, similar trends were observed with

107

CNG injection at 120° BTDC and the difference in pressure history observed at 1500 rpm and 1800 rpm was less noticeable at 180° BTDC and 120° BTDC. With high degree of CNG stratification created by injection at 80° BTDC, there was a slight reduction in peak pressure and heat release rate at all speeds except at 1200 rpm as shown in Figure 4.88. At $\phi_{Total} = 0.35$ and 300° BTDC, there was a marginal difference in pressure rise rate between 1500 and 2100 rpm as shown in Figure 4.89.

Figure 4.89 Pressure and heat release rates at 300° BTDC at $\phi_T = 0.35$.
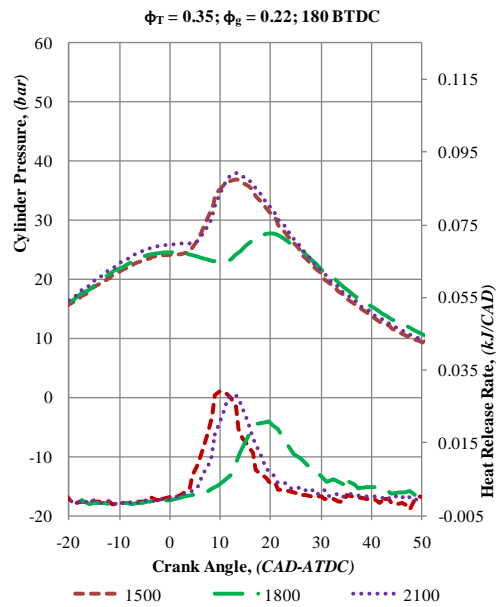
Figure 4.91 Pressure and heat release rates at 180° BTDC at $\phi_T = 0.35$.

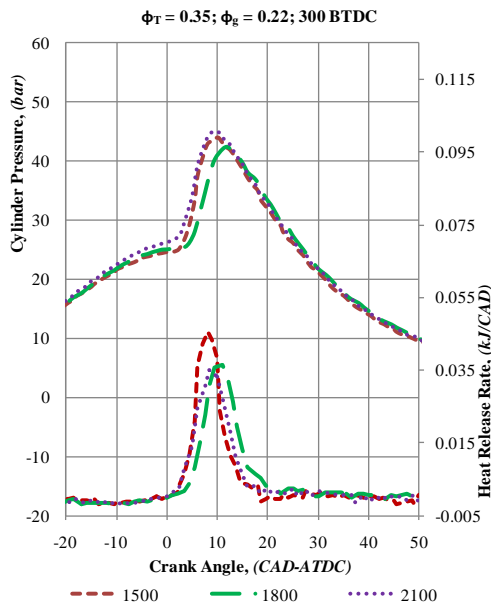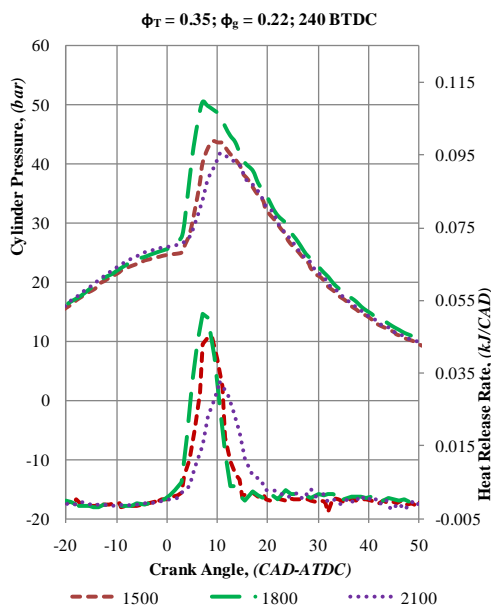*Figure 4.90 Pressure and heat release rates at 240° BTDC at $\phi_T = 0.35$.*
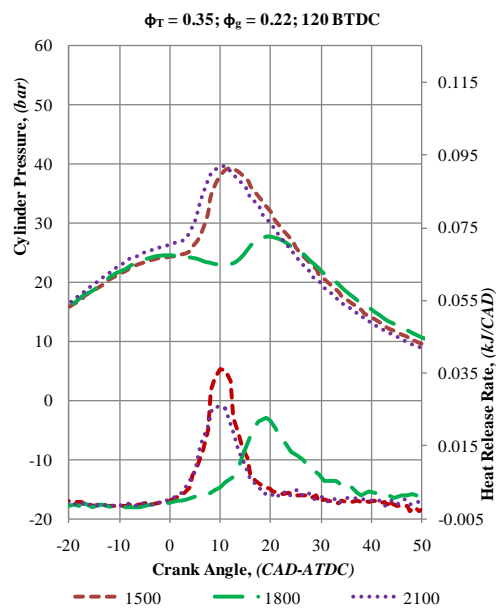
Figure 4.92 Pressure and heat release rates at 120° BTDC at $\phi_T = 0.35$.
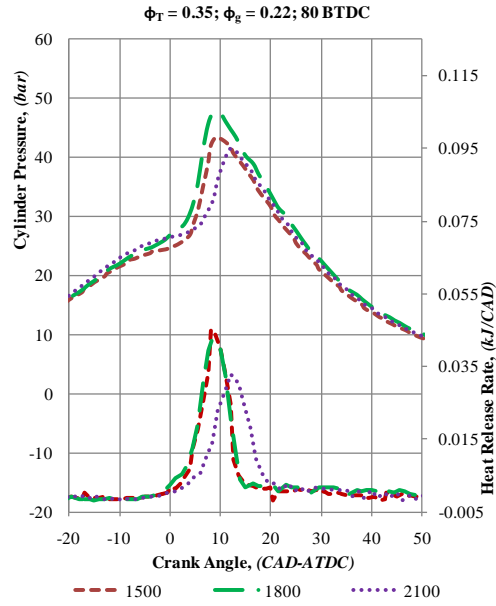
Figure 4.93 Pressure and heat release rates at 80° BTDC at $\phi_T = 0.35$.

The peak pressure and heat release rates reduced as the injection timing was retarded to 240° and 180° BTDC as shown in Figure 4.90 and Figure 4.91. At 120° BTDC and $\phi_{Total} = 0.35$, ignition was more advanced at 2100 rpm than 1500 rpm, however, heat release rates were lower as shown in Figure 4.92. However, at 80° BTDC, at 2100 rpm, ignition was later than that occurred at 1500 rpm as shown in Figure 4.93.

At 1800 rpm, there was a reduction in peak pressure and heat release rates due to delayed ignition. When CNG injection was retarded to 240° BTDC, at 1800 rpm, ignition advanced significantly and resulted in high peak pressure and heat release rates. With a further retardation in injection timing to 180° and 120° BTDC, ignition was delayed again and pressure rise and heat release rates reduced as shown in Figure 4.90 and Figure 4.91. However, CNG injection at 80° BTDC again resulted in high peak pressure due to advanced ignition timing as shown in Figure 4.93.

As shown in Figure 4.94, at 300° BTDC and $\phi_{Total} = 0.30$, rapid burning of the fuels was observed at 1200 rpm due to more homogeneous mixing and longer duration available for mixing and reactions. When the engine speed was increased, rate of burning slowed down at the last stage of combustion. At 1800 rpm, there was a significant difference in burning rate due to more significant delay in ignition. At

109

$\phi_{\text{Total}} = 0.35$ and 300° BTDC, at 1500 rpm and 2100 rpm there was a reduction in rate of burning compared to that at $\phi_{\text{Total}} = 0.30$. However, at 1800 rpm, the reduction in burning rate was less compared to that observed at 1500 rpm and 2100 rpm.

Figure 4.94 Mass fraction of fuels burned at 300° BTDC at $\phi_T = 0.35$.
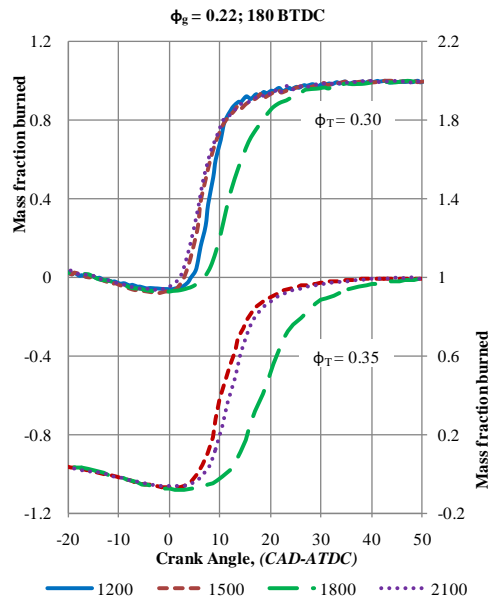
Figure 4.96 Mass fraction of fuels burned at 180° BTDC and $\phi_T = 0.35$.
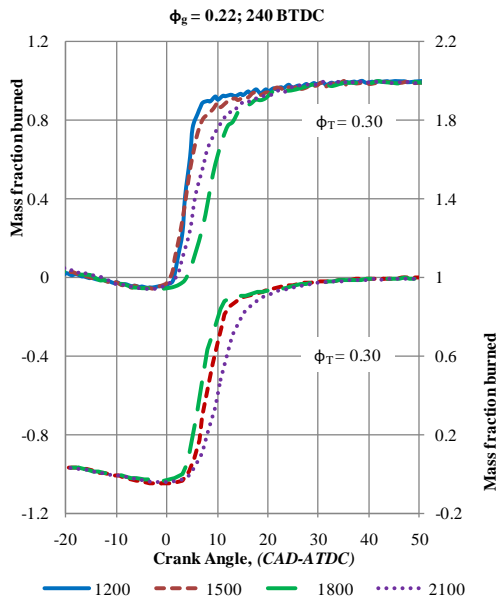
Figure 4.95 Mass fraction of fuels burned at 240° BTDC at $\phi_T = 0.35$.

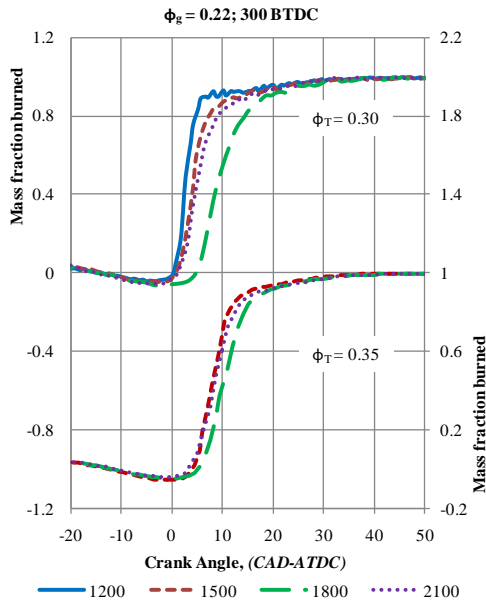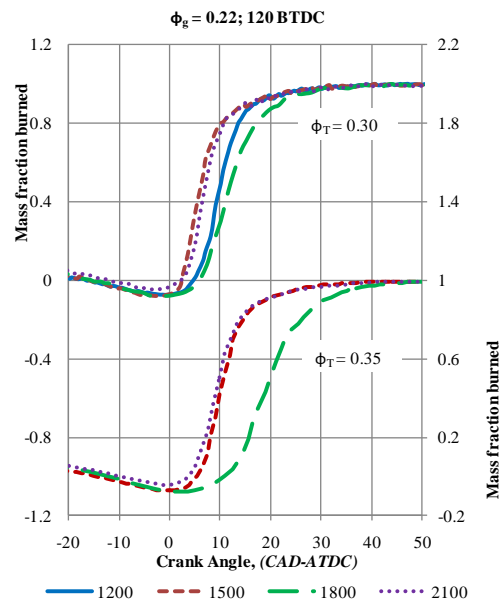*Figure 4.97 Mass fraction of fuels burned at 120° BTDC and $\phi_T = 0.35$.*

At $\phi_{\text{Total}} = 0.30$, when CNG injection was retarded to 240° BTDC, a slight reduction in rate of burning resulted at 1200, 1500 and 2100 rpm as shown in Figure

4.95. However, at 1800 rpm, a significant increase in burning rate at the last stage of combustion was observed. At $\phi_{Total} = 0.35$ and 240° BTDC, at 2100 rpm, the ignition was delayed and there was a significant reduction in burning rate at the last stages of combustion due to increased amounts of CNG and reduced time available. At $\phi_{Total} = 0.30$, with CNG injection at 180° BTDC, burning rate were significantly more gradual at all speeds as shown in Figure 4.96 and similar trends were observed with CNG injection at 120° BTDC as shown in Figure 4.97. There was a further reduction in burning rate in all the cases as the CNG injection rate was increased to $\phi_{Total} = 0.35$ and a larger portion of burning occurred between 10 to 20 CAD-ATDC.
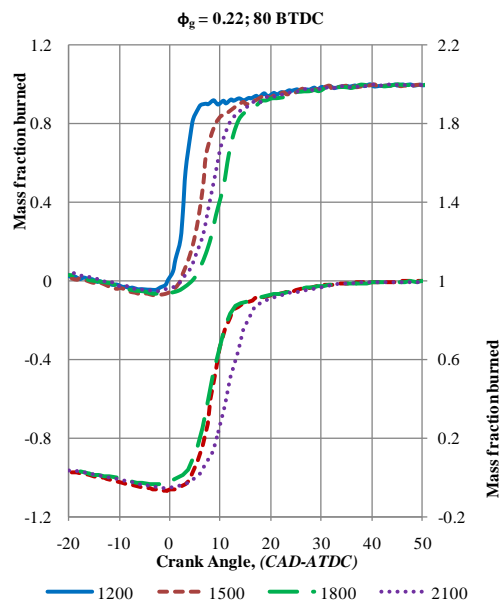
Figure 4.98 Mass fraction of fuels burned at 80° BTDC and $\phi_T = 0.35$.

However, at $\phi_{Total} = 0.30$, when CNG injection was further retarded to 80° BTDC, the burning rate again increased due to more rapid burning at the last stage of combustion as shown in Figure 4.98. The most significant increase in burning rate was observed at 1200 rpm. However, increasing CNG injection rate to $\phi_{Total} = 0.35$, resulted in a reduction in burning rate at the last stages of combustion at all speeds and the most significant reduction was observed at 2100 rpm.

As shown in Figure 4.99, combustion efficiency was significantly affected by the degree of CNG stratification. However, at 1200 rpm, degree of stratification was less significant than at other speeds. The highest combustion efficiency was obtained with CNG injection at 80° BTDC at both $\phi_{Total} = 0.30$ and 0.35 as shown in Figure

4.100. At $\phi_{Total} = 0.30$, combustion efficiency was lowest at 180° BTDC and at $\phi_{Total} = 0.35$, lowest combustion efficiency was obtained at 120° BTDC due to mixture conditions.

$\phi_g = 0.22$; $\phi_{Total} = 0.30$
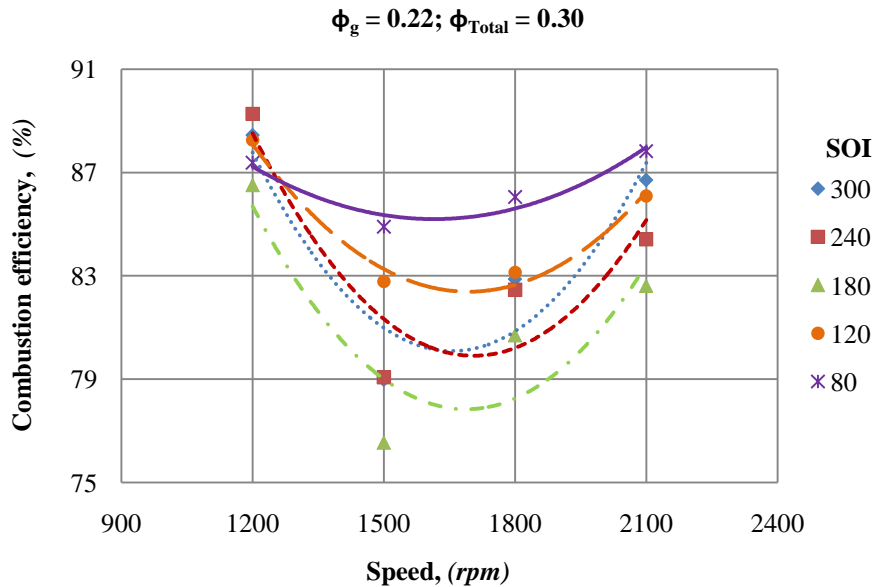
Figure 4.99 Effect of CNG stratification on combustion efficiency at a low CNG injection rate

$\phi_g = 0.22$; $\phi_{Total} = 0.35$
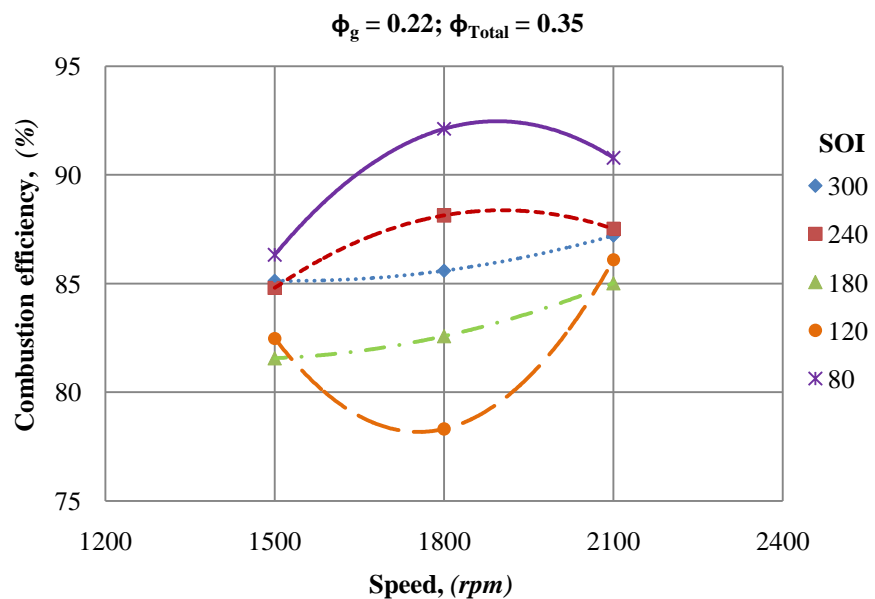
Figure 4.100 Effect of CNG stratification on combustion efficiency at higher CNG injection rate

At 1200 rpm, NO_x emissions were higher than that emitted at other speeds at all injection timings as shown in Figure 4.101. At 1200 rpm, the highest NO_x emissions were observed with CNG injection at 80° BTDC followed by injection at 240° and 300°BTDC. As the engine speed increased NO_x emissions were reduced at

112

$\phi_{Total} = 0.30$ and degree of stratification of CNG had less significant effect on NO_x emissions. At $\phi_{Total} = 0.35$, high NO_x emissions were observed with CNG injection at 80° BTDC and at 1800 rpm. However, NO_x emissions were below 500 ppm/kW at all speeds and degrees of stratification as shown in Figure 4.102.

$\phi_g = 0.22; \phi_{Total} = 0.30$
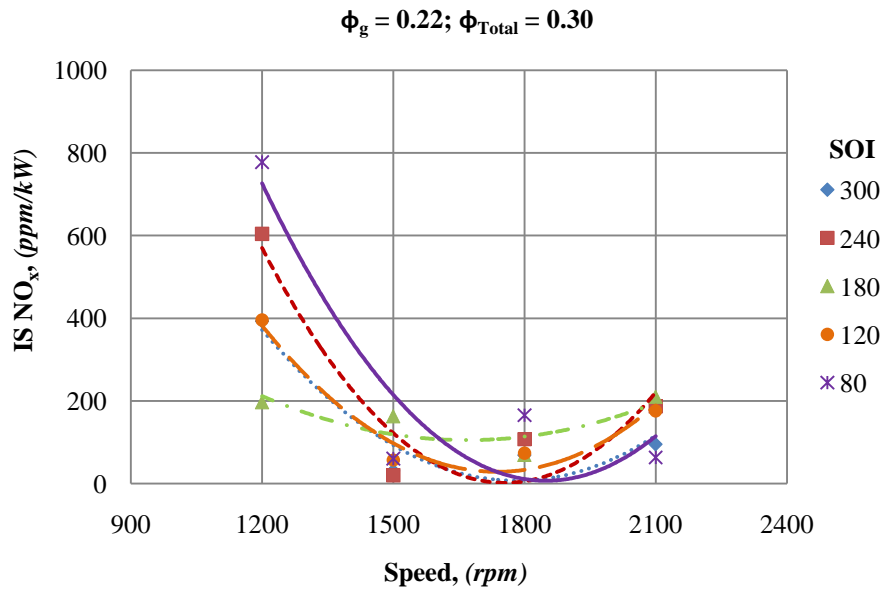
Figure 4.101 Effect of CNG stratification on NO_x emissions at a low CNG injection rate

$\phi_g = 0.22; \phi_{Total} = 0.35$
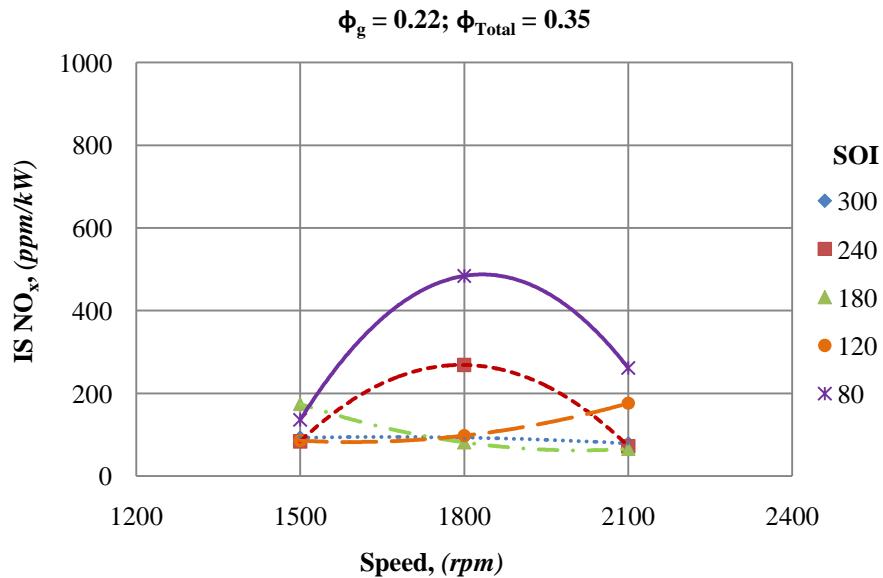
Figure 4.102 Effect of CNG stratification on NO_x emissions at higher CNG injection rate

Formation of NO_2 was found to be a strong function of engine speed. NO_2/NO_x ratio drastically increased with an increase in engine speed for all injection timings except 80° BTDC at both loads as shown in Figure 4.103 and Figure 4.104. At 2100

rpm, NO_2 was the major component of total NO_x emissions. NO_2/NO_x ratio was significantly low with CNG injection at 80° BTDC due to high degree of stratification that results in high combustion temperature. However, at 1200 rpm and at $\phi_{Total} = 0.30$, NO_2/NO_x ratio was higher for CNG injection at 80° BTDC.
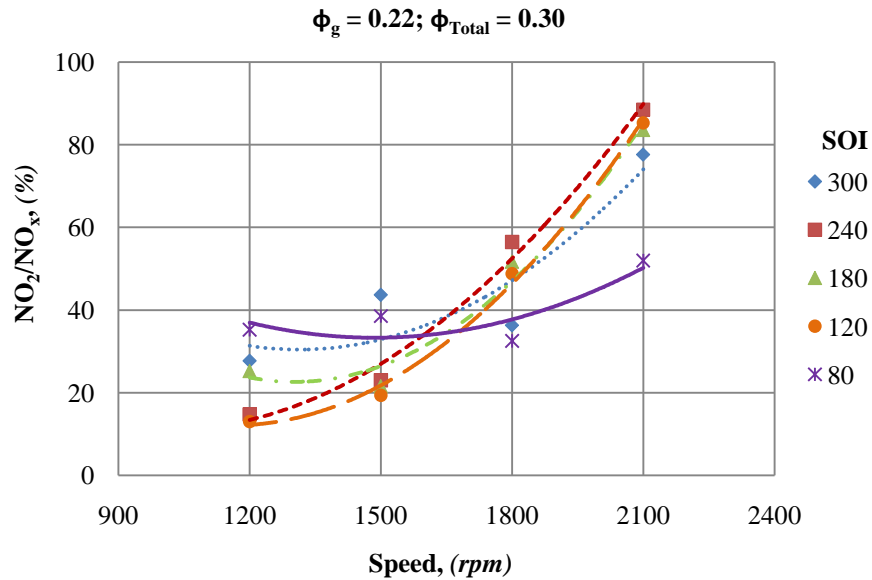
Figure 4.103 Formation of NO_2 at different engine speeds at a low CNG injection rate
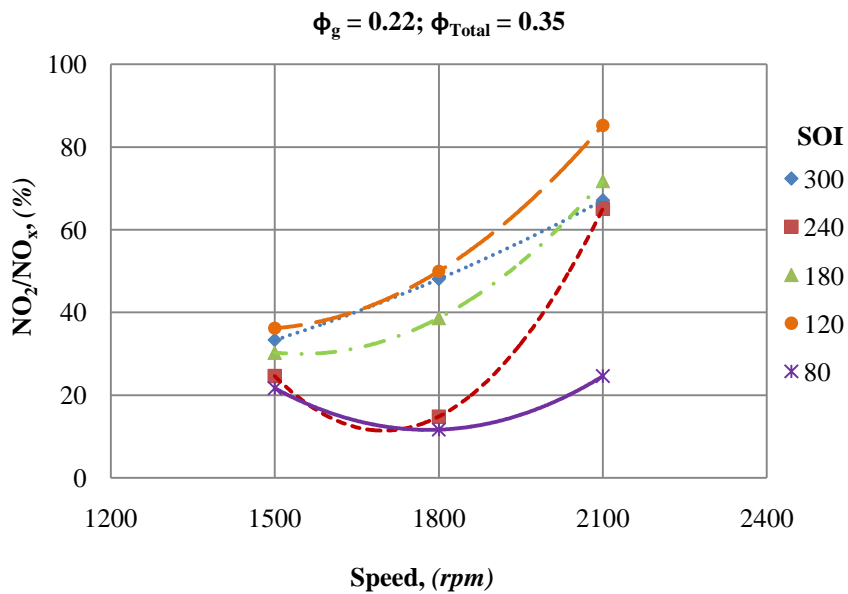
Figure 4.104 Formation of NO_2 at different engine speeds at higher CNG injection rate

Similar trends in NO_2/NO_x were observed at $\phi_{Total} = 0.35$ as shown in Figure 4.104. However, degree of stratification had a significant effect on NO_2/NO_x due to higher amount of CNG. At 120° BTDC, NO_2/NO_x ratio was the highest followed by

injection at 180° BTDC due to thermal stratification and presence of low temperature regions. Injection at 240° BTDC and 80° BTDC resulted in low NO_2 formation. At $\phi_{Total} = 0.35$, CNG injection at 80° BTDC resulted in almost half of that observed at $\phi_{Total} = 0.30$, due to higher combustion temperature because of higher amounts of stratified CNG in the mixture.

CO emissions increased with an increase in degree of stratification at $\phi_{Total} = 0.30$ as shown in Figure 4.105. At 80° BTDC, the highest amount of CO was emitted at all speeds due to reduced oxygen availability at CNG rich zones in the mixture. CO emissions were low with CNG injection at 300°, 240° BTDC and at 1200 rpm due to homogeneous mixing the fuels with air. CO emissions were higher also at 2100 rpm due to reduction in time available for the oxidation.

$\phi_g = 0.22; \phi_{Total} = 0.30$
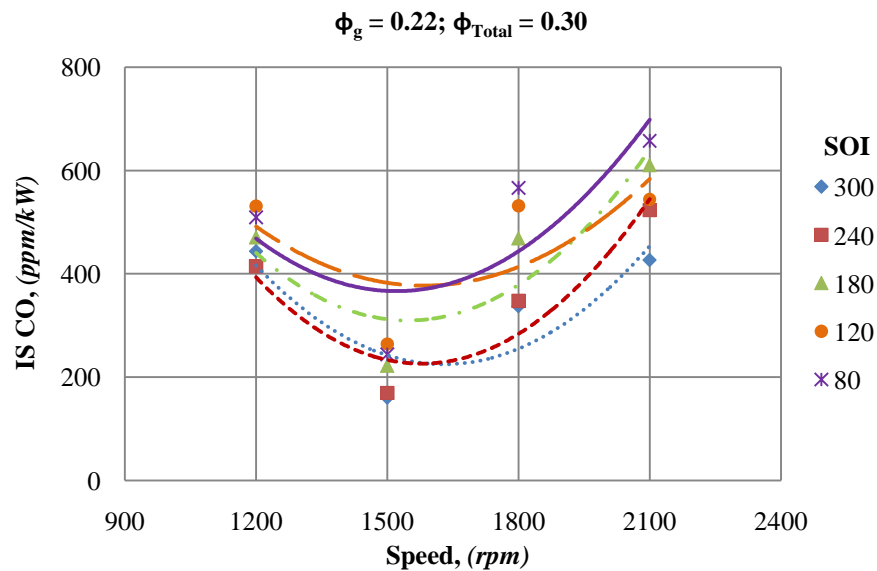
Figure 4.105 CO emissions at various degrees of stratification at a low CNG injection rate

However, at $\phi_{Total} = 0.35$, CO emissions were lower at 300°, 240° and 80° BTDC with marginal increase with an increase in engine speed as shown in Figure 4.106. Due to high concentration of fuels CO emissions were reduced at $\phi_{Total} = 0.35$. Both thorough mixing obtained with early injection timings (300° and 240° BTDC) and high degree of stratification resulted with injection at 80° BTDC resulted in a reduction CO emissions. High CO emissions resulted with injection at 180° and 120° BTDC due to thermal stratification that led to reduced combustion temperatures.
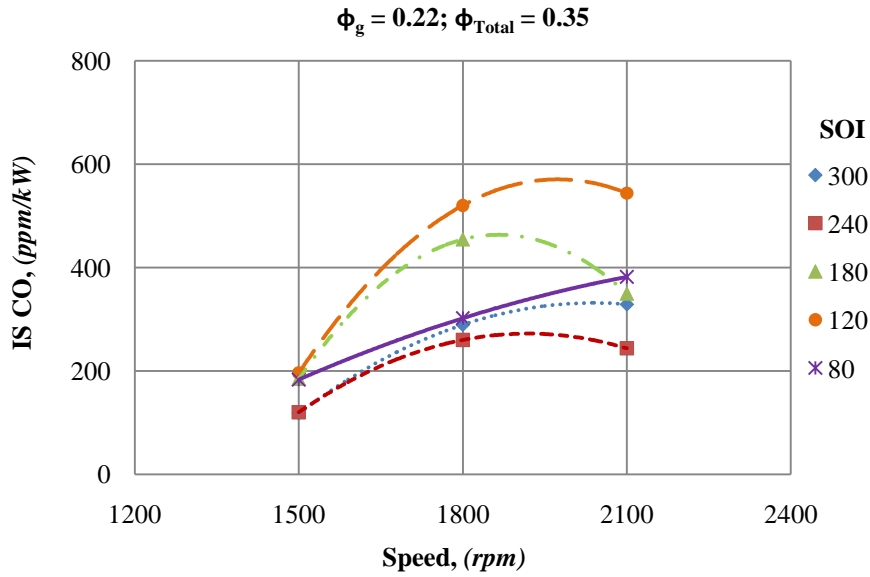
Figure 4.106 CO emissions at various degrees of stratification at higher CNG injection rate
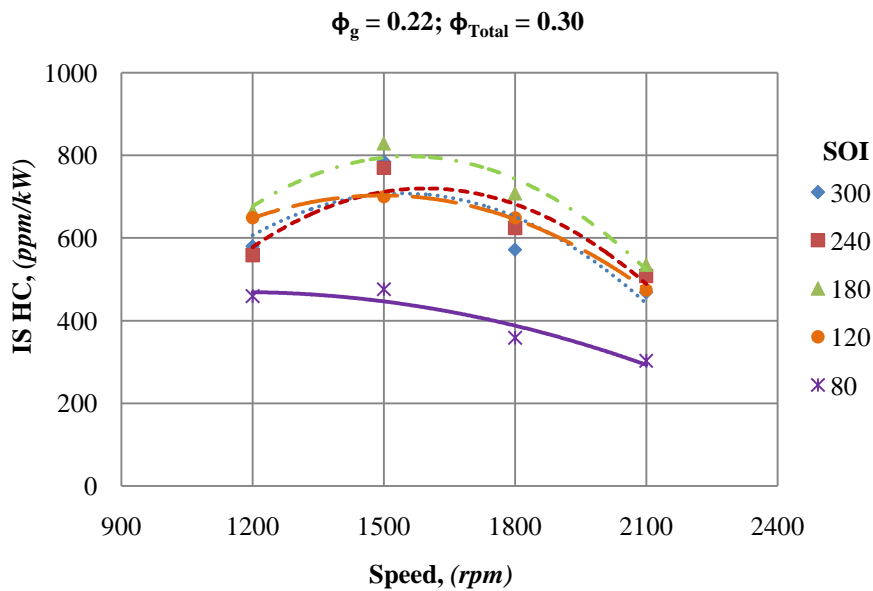
Figure 4.107 HC emissions at various degrees of stratification at a low CNG injection rate

As shown in Figure 4.107 and Figure 4.108, drastic reduction in HC emission were obtained with high degree of stratification of CNG at both ϕ_{Total} = 0.30 and 0.35. At ϕ_{Total} = 0.30, highest HC emissions resulted at 1500 rpm and CNG injection at 180° BTDC. At ϕ_{Total} = 0.35, HC emissions were the lowest at 80° BTDC, higher at 300° BTDC and 240° BTDC and the highest at 180 and 120° BTDC. HC emissions reduced with an increase in engine speed above 1500 rpm at ϕ_{Total} = 0.30 and 0.35.

116
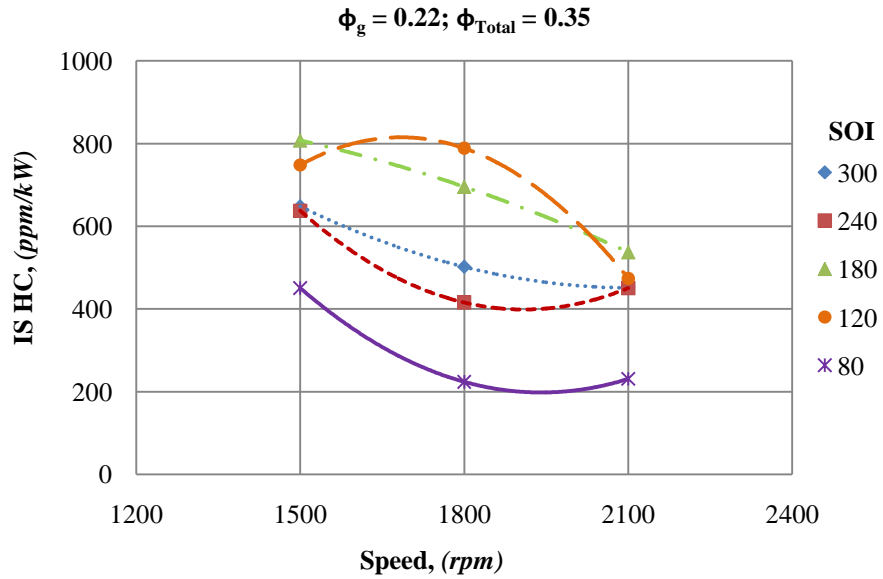
Figure 4.108 HC emissions at various degrees of stratification at a low CNG injection rate

As shown in Figure 4.109, CH_4 emissions were remarkably reduced with CNG injection at 80° BTDC due to high degree of stratification. There is a further reduction in CH_4 emissions at $\phi_{Total} = 0.35$ due to higher amounts of stratified CNG in the mixture as shown in Figure 4.110. While CNG injection at 300° and 240° BTDC resulted in moderate levels of CH_4 emissions, high CH_4 emissions were observed with CNG injection at 180° BTDC.
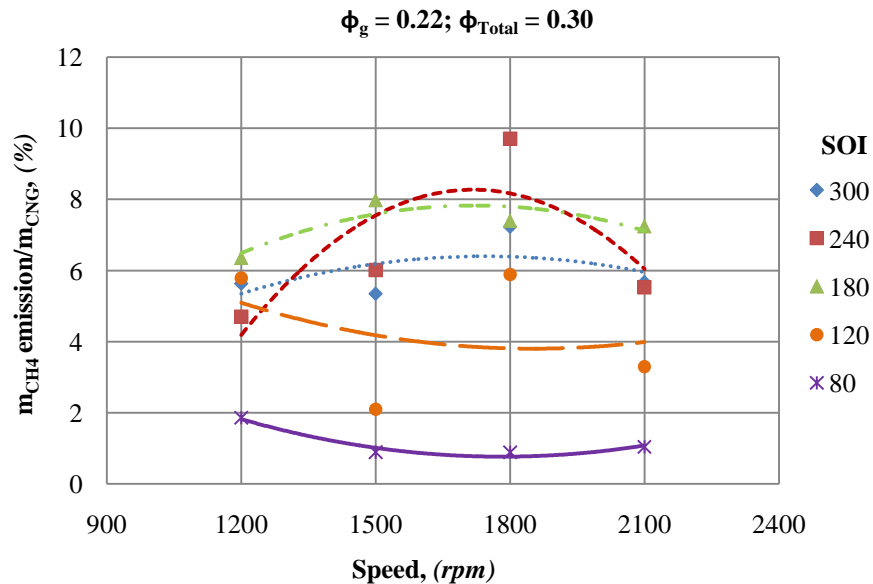
Figure 4.109 Effect of degree of stratification on CNG combustion at higher CNG injection rate

117
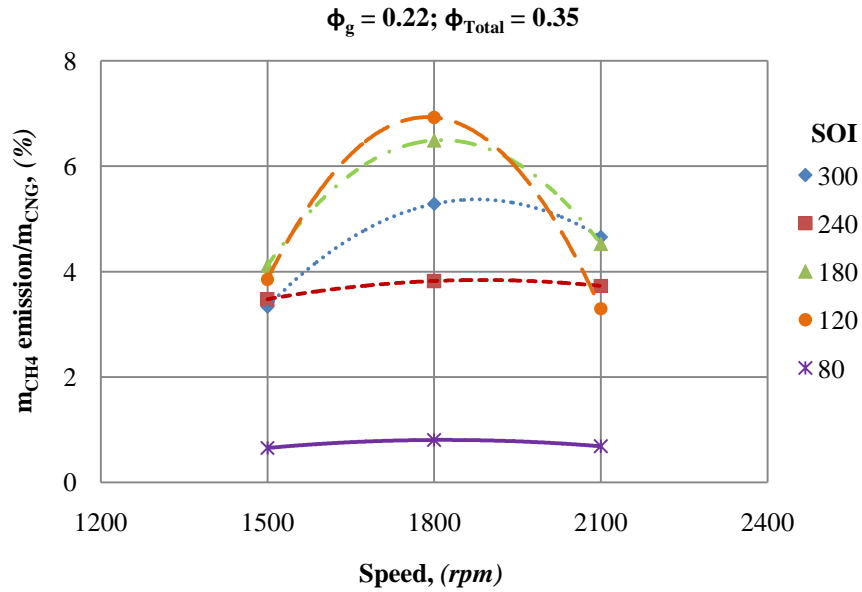
Figure 4.110 Effect of degree of stratification on CNG combustion at $\phi_{Total} = 0.35$.

At $\phi_{Total} = 0.35$, CH_4 emissions were high at 120° BTDC due to higher amounts of CNG that required higher degree of stratification than that created by injection at 120° BTDC. As CH_4 emission is an indicator of individual combustion efficiency of CNG in the mixture, it has significant effects on the overall combustion efficiency as discussed earlier in this section.

4.5 Effect of Gasoline Equivalence Ratio and Engine Speed with CNG and Temperature Stratification

The scope of this section is to analyse the effects of gasoline equivalence ratio when CNG was injected at 180° BTDC. As discussed earlier, CNG injection at 180° BTDC results in combined mixture and thermal stratification and has significantly different trends of effects of CNG direct injection. Therefore, it becomes important to analyse the results obtained at 180° BTDC. This section presents the discussion on the effects on combustion characteristics by CNG injection at 180° BTDC.

Two total equivalence ratios ($\phi_{Total} = 0.30$ and 0.40) that represented moderate and high engine loads were selected for the discussion. However, at 1200rpm, the engine could not be operated at $\phi_{Total} = 0.40$ due to knocking at $\phi_g = 0.22$; 0.24 and

0.26. Also, as CNG injection rate was high at $\phi_{Total} = 0.40$, energy required to initiate CNG combustion was higher than that released by the HCCI combustion of gasoline at $\phi_g = 0.20$. Therefore, combustion could not be achieved at $\phi_{Total} = 0.40$ with $\phi_g = 0.20$ at all speeds due to misfire.

$\phi_{Total} = 0.30$; SOI = 180°BTDC
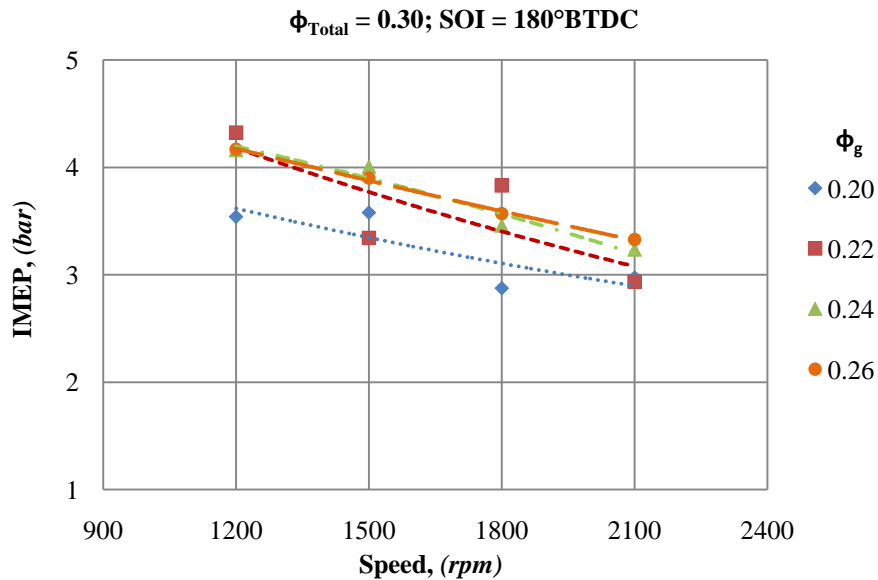
Figure 4.111 Effect of ϕ_g on IMEP generated at a low CNG injection rate

SOI = 180°BTDC; $\phi_{Total} = 0.40$
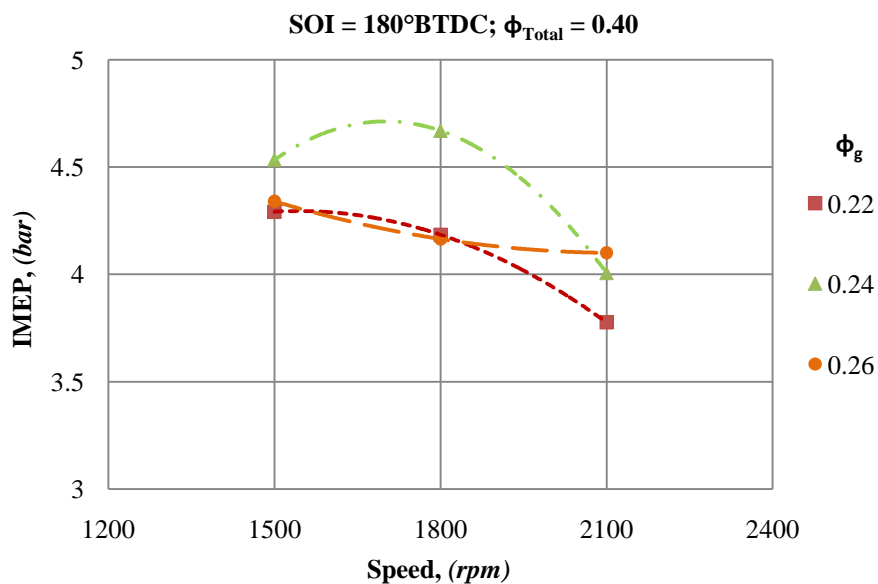
Figure 4.112 Effect of ϕ_g on IMEP generated at a higher CNG injection rate

As shown in Figure 4.111, at $\phi_{Total} = 0.30$, with an increase in engine speed, IMEP decreased for all values of ϕ_g. At $\phi_g = 0.20$, the IMEP obtained was significantly lower than that resulted with higher ϕ_g. This shows that the overall

combustion of the dual fuels was dependent on gasoline equivalence ratio. The significance of gasoline equivalence ratio was more pronounced in terms of indicated thermal efficiency as shown in Figure 4.113.

SOI = 180°BTDC; ϕ_{Total} = 0.30
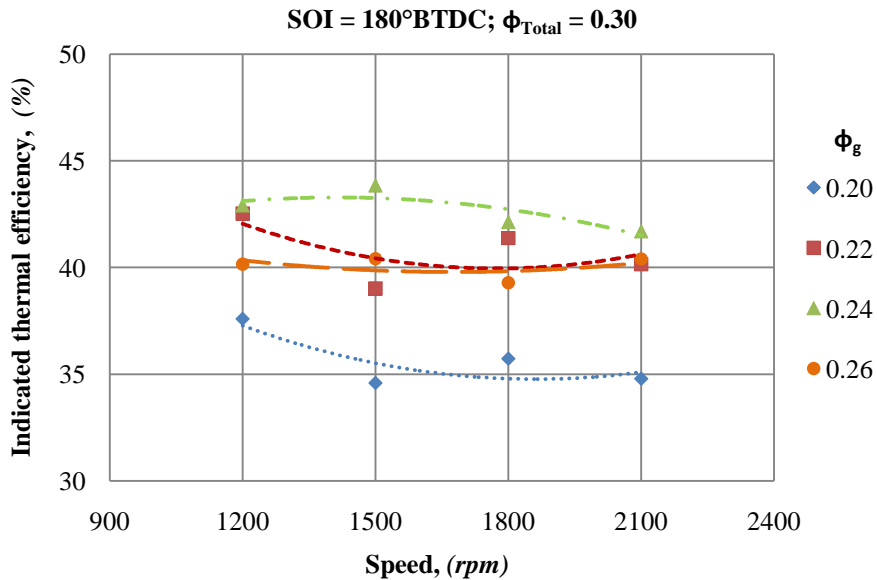
Figure 4.113 Effect of ϕ_g on indicated thermal efficiency at a low CNG injection rate

SOI = 180°BTDC; ϕ_{Total} = 0.40
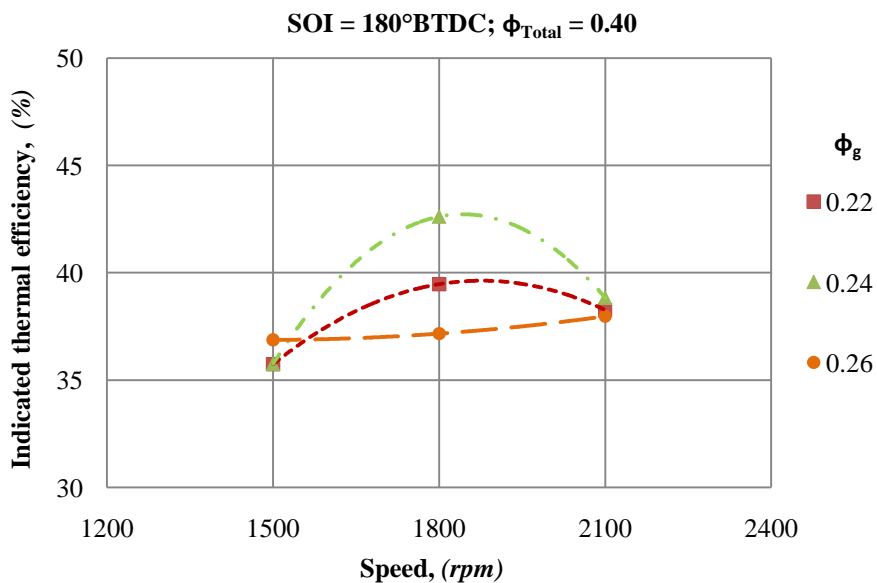
Figure 4.114 Effect of ϕ_g on indicated thermal efficiency at higher CNG injection rate

At ϕ_{Total} = 0.40, a drastic increase in IMEP was obtained with ϕ_g = 0.24. At 1800 rpm and ϕ_g = 0.24, the highest IMEP was obtained as shown in Figure 4.112. The corresponding values of indicated thermal efficiency are shown in Figure 4.114.

120

At $\phi_{Total} = 0.30$, ignition timing was a stronger function of ϕ_g than engine speed as shown in Figure 4.115. An increase in ϕ_g resulted in an advance in ignition timing at all speeds, however, the effect was less significant at 2100 rpm. At $\phi_g = 0.20$, as the engine speed was increased it resulted in a significant advance in ignition timing which may be partially due to low temperature heat release resulted at $\phi_g = 0.20$ and 2100rpm as shown in Figure 4.18. At $\phi_g = 0.22$, 0.24 and 0.26, ignition timing was marginally affected by engine speed.
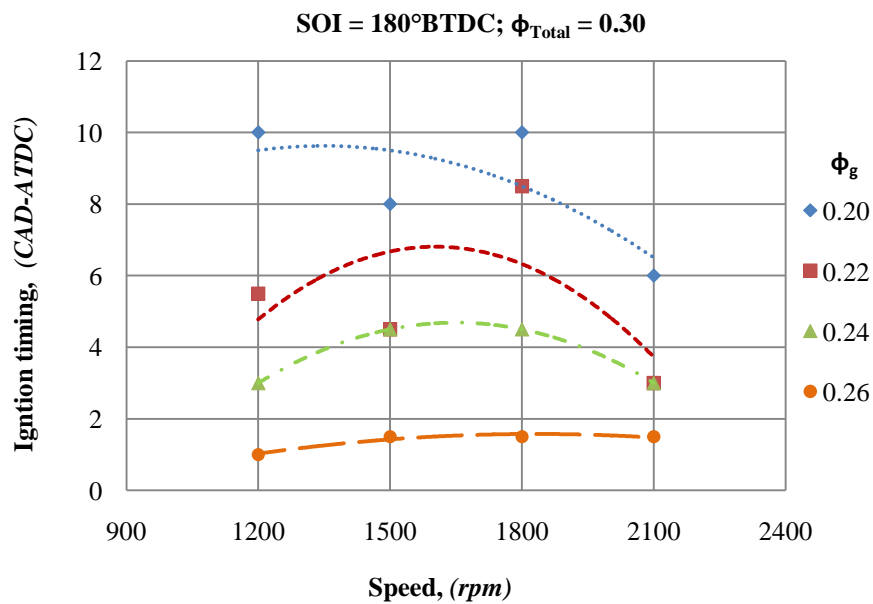
Figure 4.115 Effect of ϕ_g on ignition timing at a low CNG injection rate
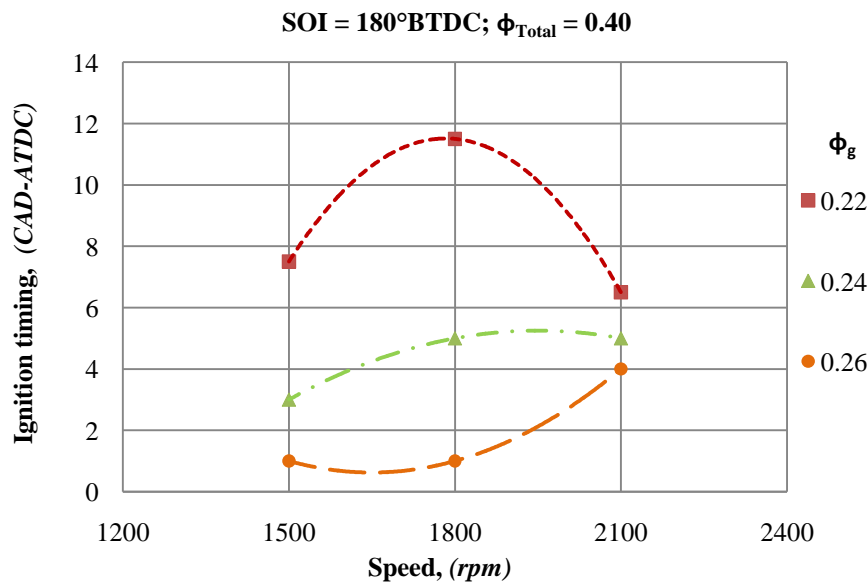
Figure 4.116 Effect of ϕ_g on ignition timing at higher CNG injection rate

121
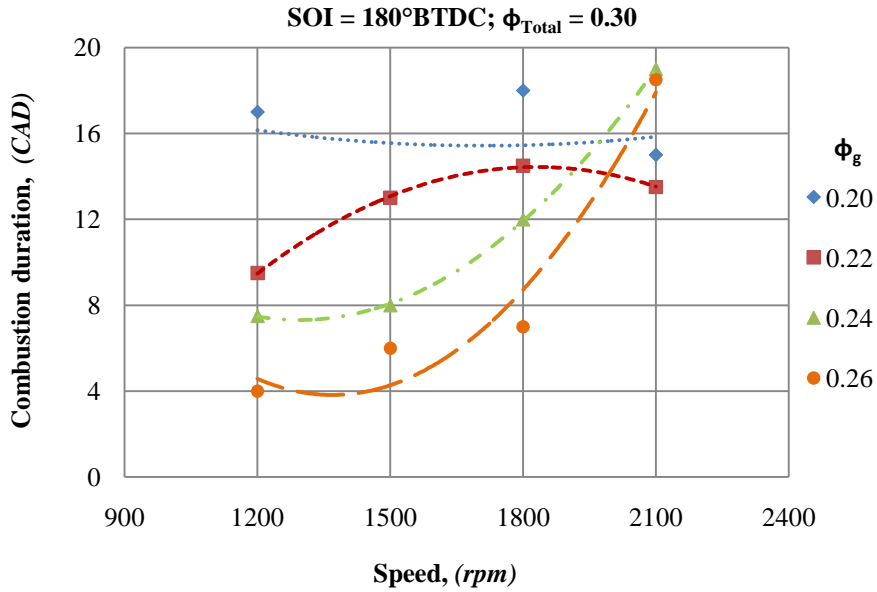
Figure 4.117 Effect of ϕ_g on combustion duration at a low CNG injection rate
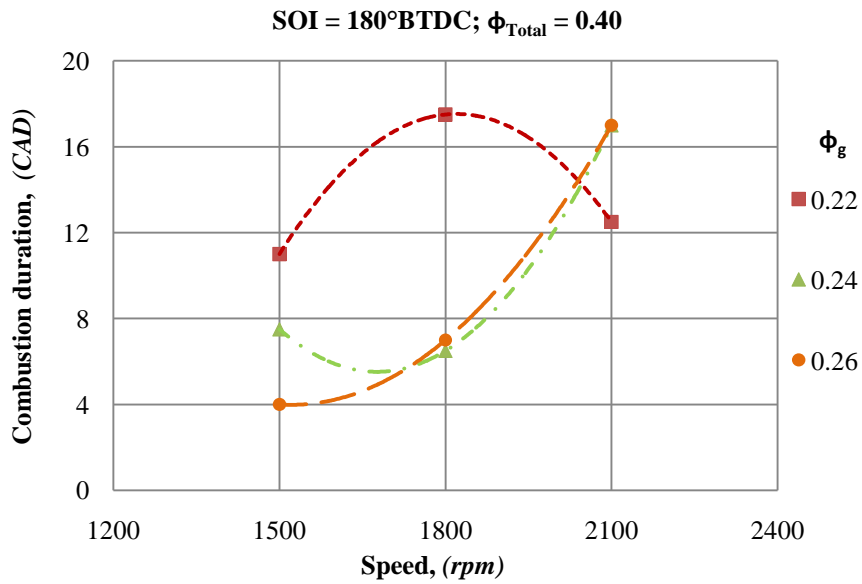
Figure 4.118 Effect of ϕ_g on combustion duration at higher CNG injection rate

At $\phi_g = 0.22$, when CNG injection rate was increased to $\phi_{Total} = 0.40$, there was a significant delay in ignition timing especially at 1800 rpm. As higher amount of CNG at $\phi_{Total} = 0.40$ required higher ϕ_g, it resulted in more delay in ignition as shown in Figure 4.116 and Figure 4.115. Similarly, at $\phi_g = 0.22$ and 2100 rpm, ignition was advanced again due to low temperature reactions as shown in Figure 4.18. At $\phi_g = 0.24$ and 0.26, there was marginal difference in ignition timing at $\phi_{Total} = 0.30$ and 0.40 at all speeds. However, at $\phi_{Total} = 0.40$, at $\phi_g = 0.24$ and 0.26, ignition

timing retarded as the engine speed was increased to 2100 rpm due to reduced time available for the fuels to react at higher speeds as shown in Figure 4.116.

At $\phi_{Total} = 0.30$ and $\phi_g = 0.20$, combustion duration was longest and was marginally affected by change in engine speed as shown in Figure 4.117. However, at higher gasoline equivalence ratios, combustion duration increased with an increase in engine speed due to reduction in reaction time at high engine speeds. At 1200, 1500 and 1800 rpms, combustion duration decreased with an increase in ϕ_g. But at 2100 rpm, when ϕ_g was increased from 0.22 to 0.24 and 0.26, combustion duration increased. Similarly, at $\phi_{Total} = 0.40$, combustion duration with an increase in engine speed at $\phi_g = 0.24$ and 0.26 as shown in Figure 4.118. However, at $\phi_{Total} = 0.40$ and $\phi_g = 0.22$, combustion duration was higher than that at 1500 and 2100 rpm.

As shown in Figure 4.119, at $\phi_{Total} = 0.30$ and $\phi_g = 0.20$, the peak pressures were lower than that observed with $\phi_g = 0.22$, 0.24 and 0.26 as the heat released due to gasoline combustion was insufficient to promote complete combustion. At $\phi_g = 0.20$, this reduction in peak pressure and incomplete combustion resulted in a decrease in thermal efficiency as shown in Figure 4.113. However, at 1200 rpm, low peak pressures were partially due to retarded ignition timing as at this point the thermal efficiency and combustion efficiency were slightly higher than those at other speeds as suggested from Figure 4.130. At 1500 and 2100 rpm, the peak pressure was higher than that at 1200 and 1800 rpm. However, this did not result in an increase in thermal efficiency as the combustion duration was longer at these speeds leading to higher wall heat losses.

At $\phi_{Total} = 0.30$ and $\phi_g = 0.22$, peak pressure and heat release rate were higher at 1200 rpm as shown in Figure 4.121. However, as the engine speed was increased to 1500 rpm, peak pressure and heat release rates reduced. However, more significant reduction was obtained at 1800 rpm. When the engine speed was increased from 1800rpm to 2100 rpm, peak pressure increased again.

At $\phi_{Toal} = 0.30$, when gasoline equivalence ratio was increased to $\phi_g = 0.24$, higher peak pressure and heat release rates resulted at all speeds as shown in Figure 4.120. A more significant increase in peak pressure and more advances in ignition

timing were observed at 1800 rpm. Therefore, at $\phi_g = 0.24$, it became that higher the engine speed was lower the peak pressure and heat release rate. However, the highest reduction was obtained with an increase in speed from 1200 rpm to 1500 rpm. Similar trends were observed with $\phi_g = 0.26$, however, peak pressure and heat release rates were higher than those obtained with $\phi_g = 0.24$ at all speeds as shown in Figure 4.122.
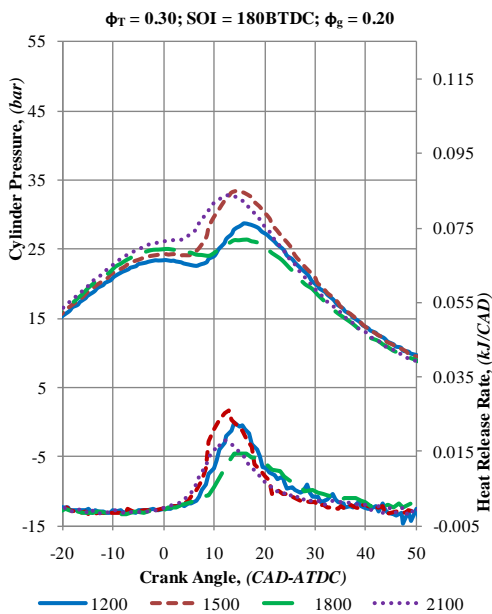
Figure 4.119 Pressure and heat release rates at $\phi_g = 0.20$ and $\phi_T = 0.30$.
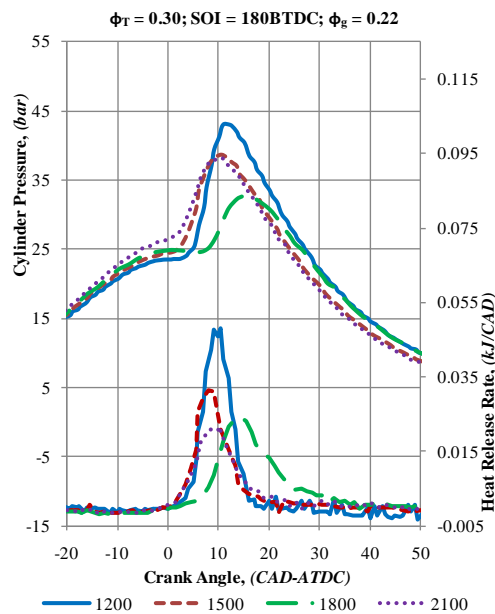
Figure 4.121 Pressure and heat release rates at $\phi_g = 0.22$ and $\phi_T = 0.30$.
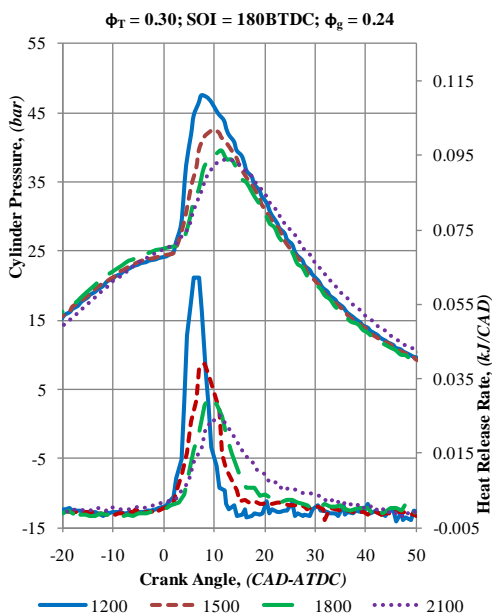
Figure 4.120 Pressure and heat release rates at $\phi_g = 0.24$ and $\phi_T = 0.30$.
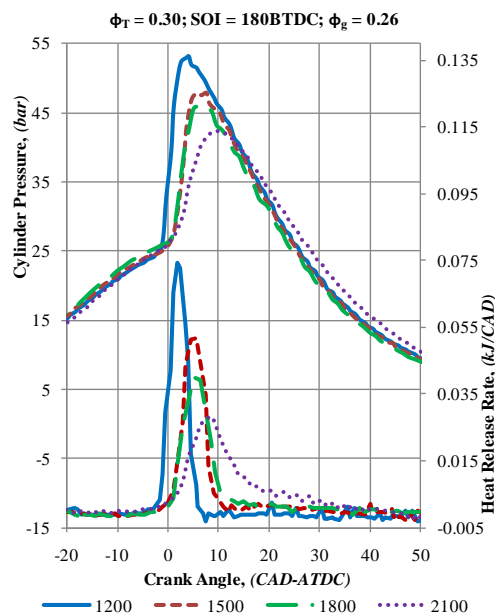
Figure 4.122 Pressure and heat release rates at $\phi_g = 0.26$ and $\phi_T = 0.30$.
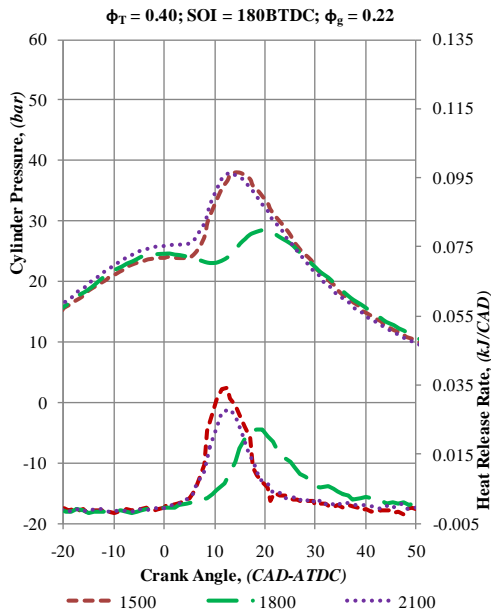
Figure 4.123 Pressure and heat release rates at ϕ_g = 0.22 and ϕ_T = 0.40.
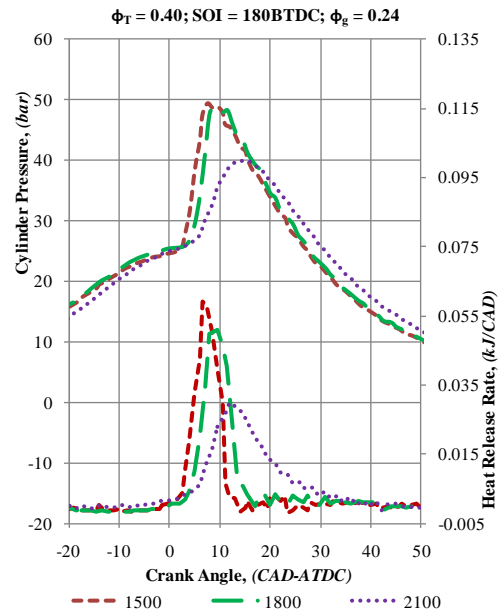
Figure 4.124 Pressure and heat release rates at ϕ_g = 0.24 and ϕ_T = 0.40.
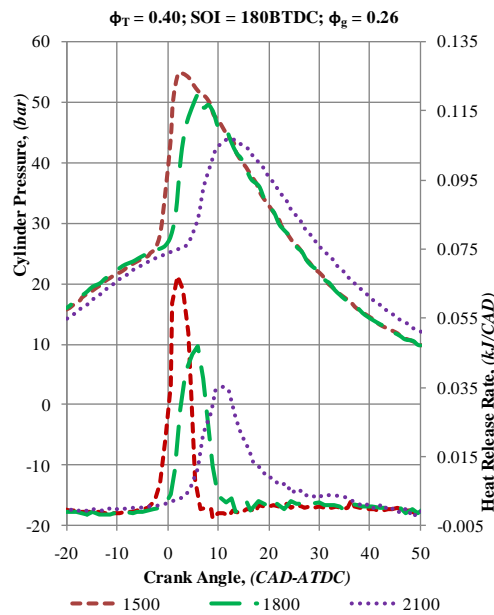
Figure 4.125 Pressure and heat release rates at ϕ_g = 0.26 and ϕ_T = 0.40.

At ϕ_{Total} = 0.40 and ϕ_g = 0.22, higher peak pressure and heat release rate at 1500 and 2100 rpm than 1800 rpm. The pressure rise and heat release rate were marginally different at 1500 and 2100 rpm. At 1800 rpm, there was remarkable reduction in peak pressure and heat release rates due to significantly delayed ignition timing and lower combustion efficiency as shown in Figure 4.123 and Figure 4.131. However, as ϕ_g was increased to 0.24, peak pressure and heat release rate significantly

increased at 1800 rpm due to higher combustion efficiency as shown in Figure 4.124 and Figure 4.131. However, at 2100 rpm, increase in ϕ_g from 0.22 to 0.24 had less significant effect on pressure and heat release rates. Similar trends were obtained at $\phi_g = 0.26$ as shown in Figure 4.125. However, there was a further increment in peak pressure and heat release rates as ϕ_g was increased from 0.24 to 0.26 at all speeds.
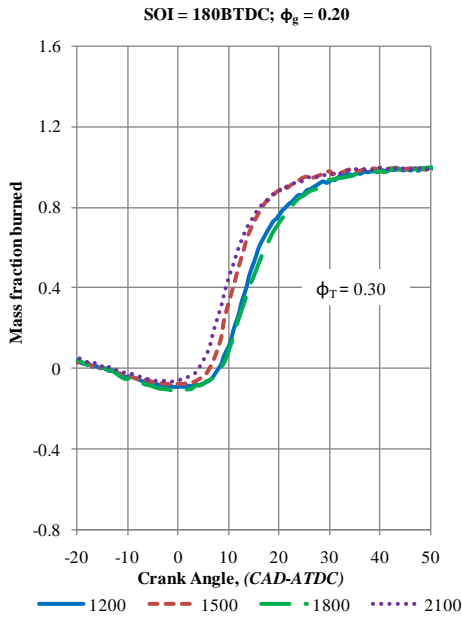
Figure 4.126 Mass fraction burned at $\phi_g = 0.20$ and $\phi_T = 0.30$.
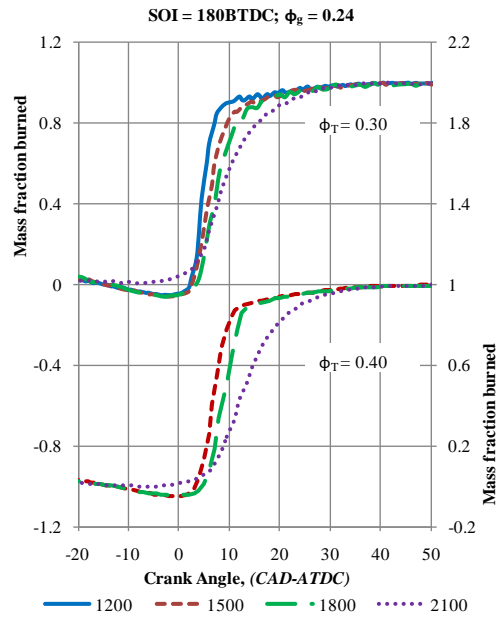
Figure 4.128 Mass fraction burned at $\phi_g = 0.24$ and $\phi_T = 0.30$ and 0.40.
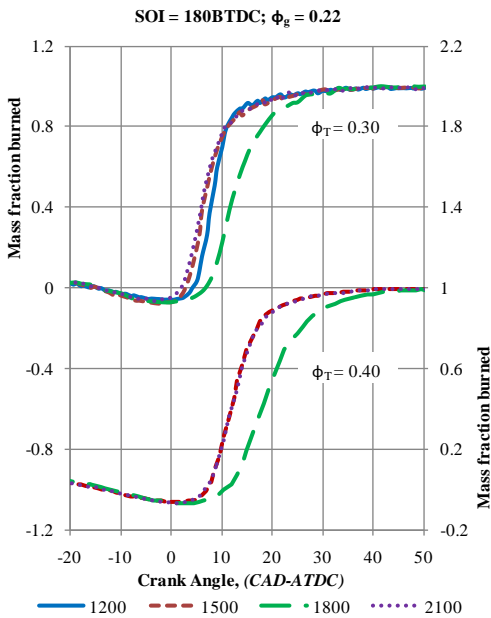
Figure 4.127 Mass fraction burned at $\phi_g = 0.22$ and $\phi_T = 0.30$ and o.40.
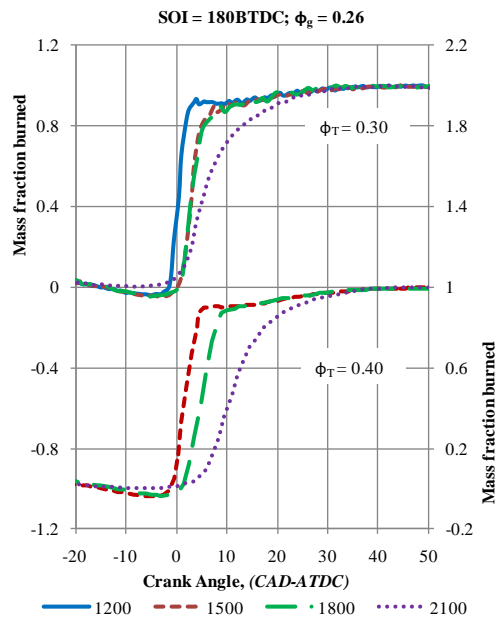
Figure 4.129 Mass fraction burned at $\phi_g = 0.26$ and $\phi_T = 0.30$ and o.40.

As shown in Figure 4.126, at $\phi_{Total} = 0.30$ and $\phi_g = 0.20$, burning rate of the fuels were low at all the speeds. At 1500 rpm, the burning rate was marginally lower than 2100 rpm at the initial stage of combustion; however, at the last stage of combustion there was no difference observed.

At $\phi_{Total} = 0.30$, with an increase in gasoline equivalence ratio from $\phi_g = 0.20$ to 0.22, burning rate significantly increased at 1200, 1500 and 2100 rpm and major portion of the fuels burned within 10 CAD after TDC. However, at 1800 rpm, effect of ϕ_g was least significant as shown in Figure 4.127. At $\phi_{Total} = 0.40$, with higher CNG injection rate, burning rate decreased at the last stages of combustion at all speeds. This suggested that gasoline burned at the initial stages and major portion of CNG burned at the last stages of combustion. That is, increase in ϕ_g resulted in higher burning rate in the initial stages and increase in CNG resulted in retarded ignition and slower burning at the last stages of combustion.

Similar trends were observed when ϕ_g was increased to 0.24 and 0.26 as shown in Figure 4.128 and Figure 4.129. However, at 2100 rpm, when ϕ_g was increased from 0.22 to 0.24 and 0.26, there was no significant increase in burning rate at the initial stages of combustion due to reduced reaction time at high speeds.
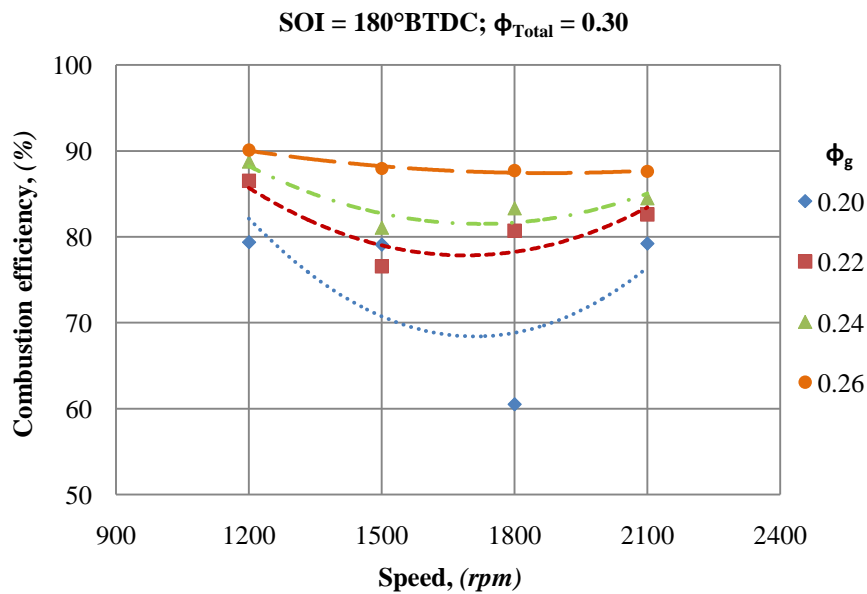
Figure 4.130 Effect of ϕ_g on combustion efficiency at a low CNG injection rate

SOI = 180°BTDC; ϕ_{Total} = 0.40
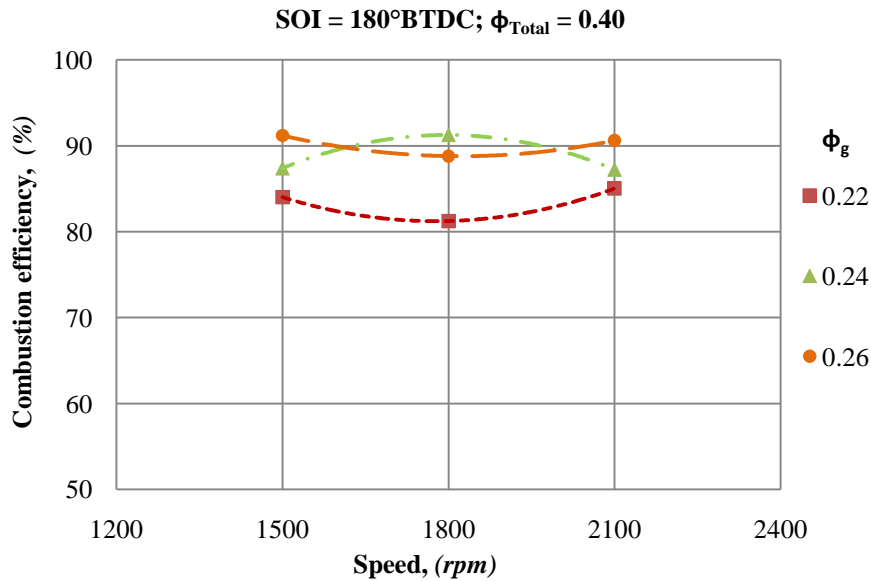
Figure 4.131 Effect of ϕ_g on combustion efficiency at higher CNG injection rate

As shown in Figure 4.130, at ϕ_{Total} = 0.30 combustion efficiency increases with an increase in ϕ_g at all speeds. At ϕ_{Total} = 0.30, combustion efficiency was the highest at ϕ_g = 0.26 and it decreased marginally with an increase in engine speed. At ϕ_g = 0.22 and 0.24, combustion efficiency was higher at 1200 rpm due to longer time available for mixing and 2100 rpm due to higher in-cylinder turbulence that would have resulted in better mixing thereby reducing the level of thermal stratification created by CNG injection at 180° BTDC.

Similarly, at ϕ_{Total} = 0.40, combustion efficiency was a stronger function of ϕ_g than engine speed as shown in Figure 4.131. At ϕ_{Total} = 0.40 and at ϕ_g = 0.24 and 0.26, combustion efficiency was significantly higher than that obtained at ϕ_{Total} = 0.30.

At ϕ_{Total} = 0.30, NO$_x$ emissions were observed to be lower than 500 ppm/kW for all cases except at 1200rpm and ϕ_g = 0.26 as shown in Figure 4.132. At ϕ_{Total} = 0.40, the lowest NO$_x$ emissions were observed at ϕ_g = 0.22 as shown in Figure 4.133. At 1200 rpm higher gasoline equivalence ratios resulted in higher NO$_x$ emissions. However, as the engine speed increased NO$_x$ emissions reduced to a level below 200ppm/kW at 2100 rpm for all cases of ϕ_g.

SOI = 180°BTDC; $\phi_{Total} = 0.30$
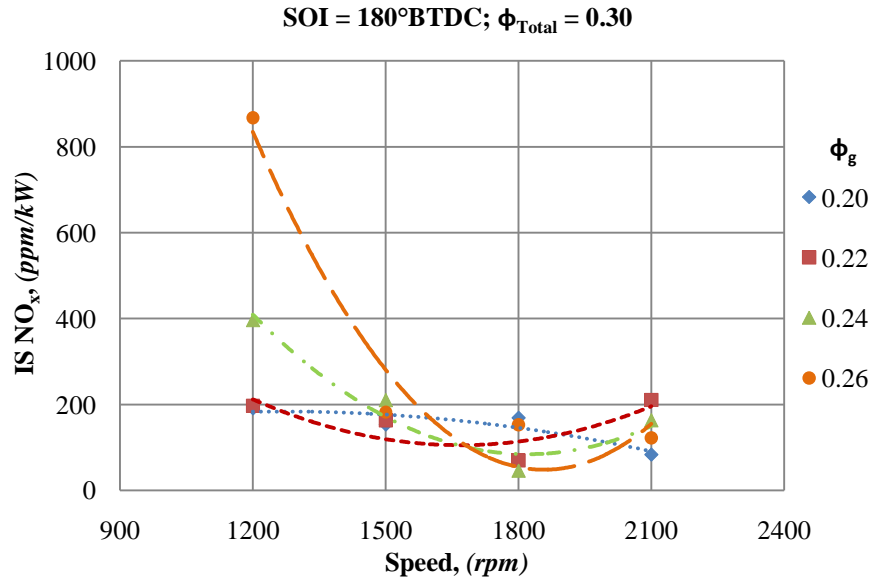
Figure 4.132 Effect of ϕ_g on NOx emissions at a low CNG injection rate

SOI = 180BTDC; $\phi_{Total} = 0.40$
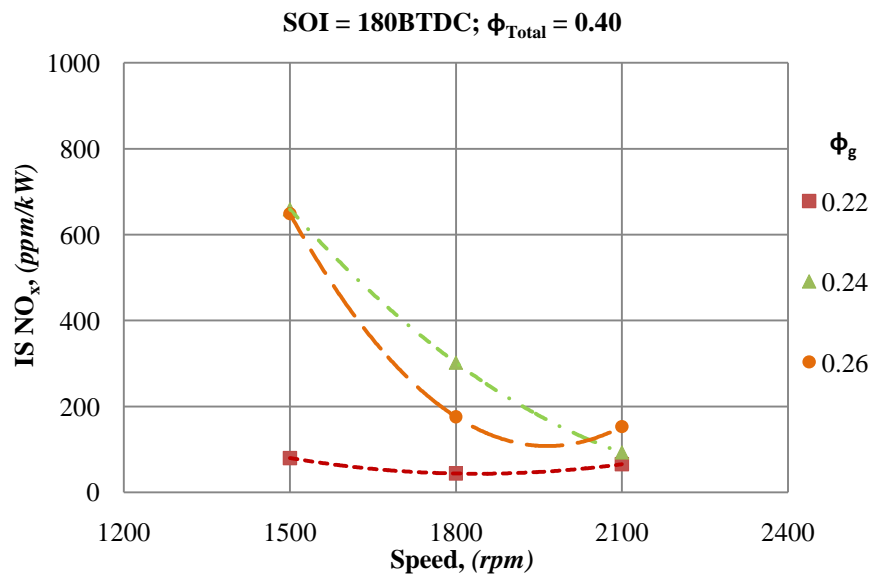
Figure 4.133 Effect of ϕ_g on NOx emissions at higher CNG injection rate

As shown in Figure 4.134, at $\phi_{Total} = 0.30$ and $\phi_g = 0.20$, NO_2/NO_x ratio increased with an increase in engine speed. As at 1200 rpm, due to longer time available for the mixture, the degree of mixture and thermal stratification was reduced and resulted in higher combustion temperatures. This led to high NO_x at 1200 rpm at both loads as shown in Figure 4.132 and Figure 4.133. As at 2100 rpm, lower combustion temperature and shorter resident time available for the NO_2 formation from NO, it resulted in high NO_2 emissions, and low NO_x emissions. NO_2 formation also increased with an increase in ϕ_g, as higher gasoline equivalence ratio

129

resulted in decreased combustion duration, which resulted in more NO_2 formation at both loads as shown Figure 4.134 and Figure 4.135.
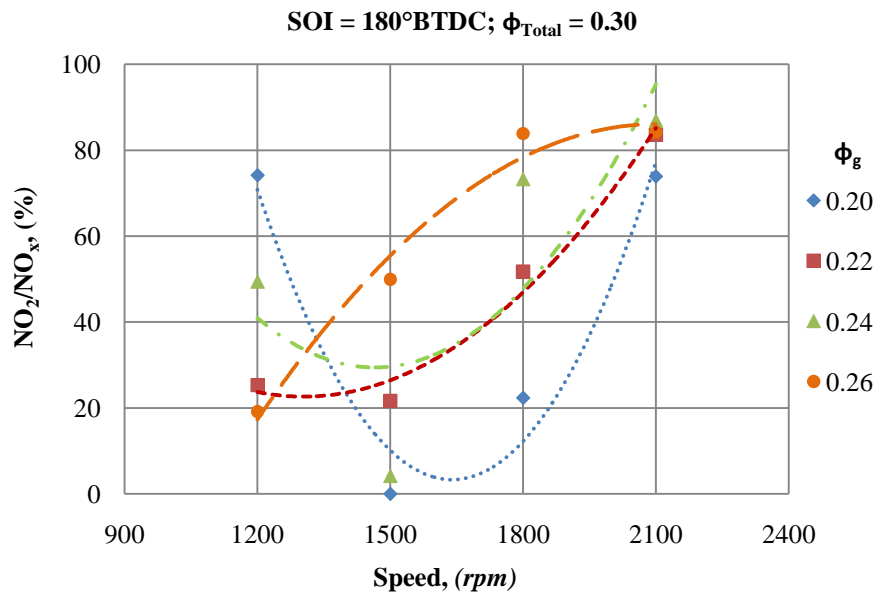
Figure 4.134 Effect of ϕ_g on NO_2 formation at a low CNG injection rate
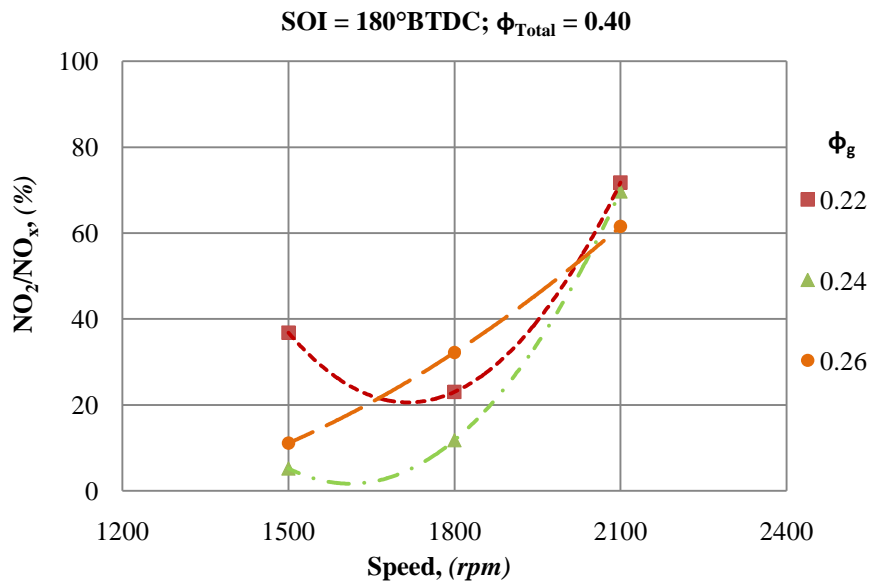
Figure 4.135 Effect of ϕ_g on NO_2 formation at higher CNG injection rate

At $\phi_{Total} = 0.30$, CO emissions were high at $\phi_g = 0.20$ at all speeds due to incomplete combustion as shown in Figure 4.136. However, at higher gasoline equivalence ratios CO emissions significantly reduced. CO emissions increased marginally at 2100rpm and it was a stronger function of ϕ_g than engine speed. As

shown in Figure 4.137, similar trends were observed at $\phi_{Total} = 0.40$ and CO emissions were less than 450 ppm/kW at all engine speeds and ϕ_g.

SOI = 180°BTDC; $\phi_{Total} = 0.30$
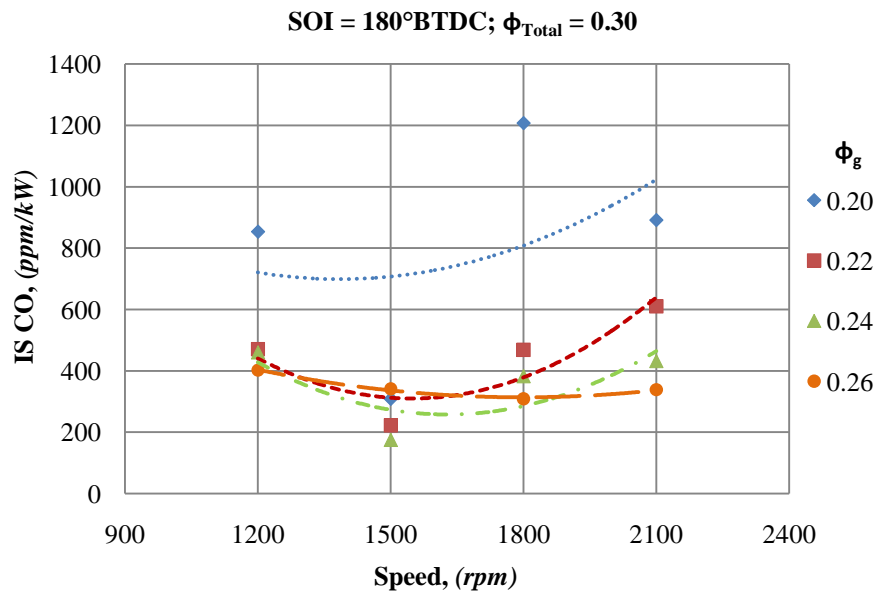
Figure 4.136 Effect of ϕ_g on CO emissions at a low CNG injection rate

SOI = 180°BTDC; $\phi_{Total} = 0.40$
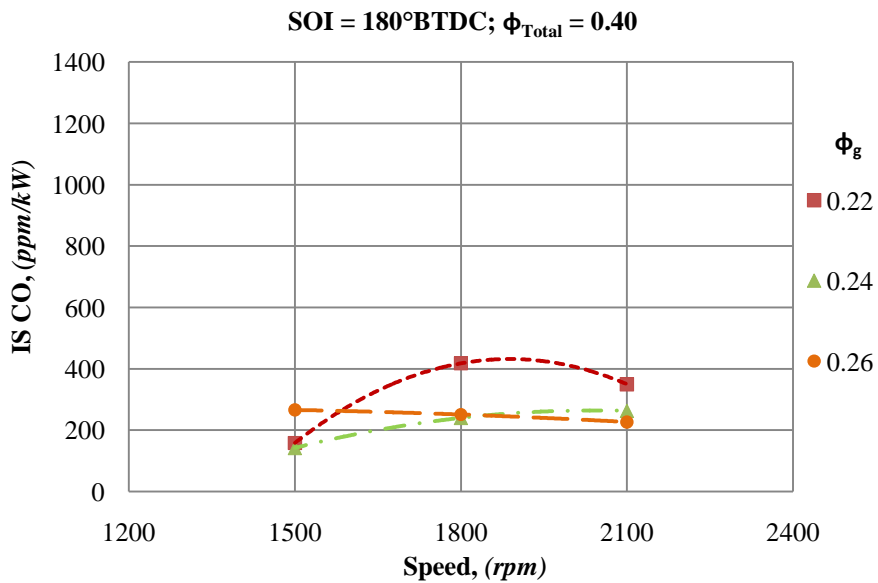
Figure 4.137 Effect of ϕ_g on CO emissions at higher CNG injection rate

With an increase in ϕ_g, HC emission significantly reduced as shown in Figure 4.138 and Figure 4.139. At $\phi_g = 0.20$, HC emissions were very high due to incomplete combustion coupled with thermal and mixture stratification resulted with CNG injection at 180° BTDC. There was a marginal impact on HC emissions due to

131

change in engine speed at both ϕ_{Total} = 0.30 and 0.40. Except at ϕ_g = 0.20, HC emissions were lower than 800 ppm/kW for all ϕ_g and engine speed.

SOI = 180°BTDC; ϕ_{Total} = 0.30
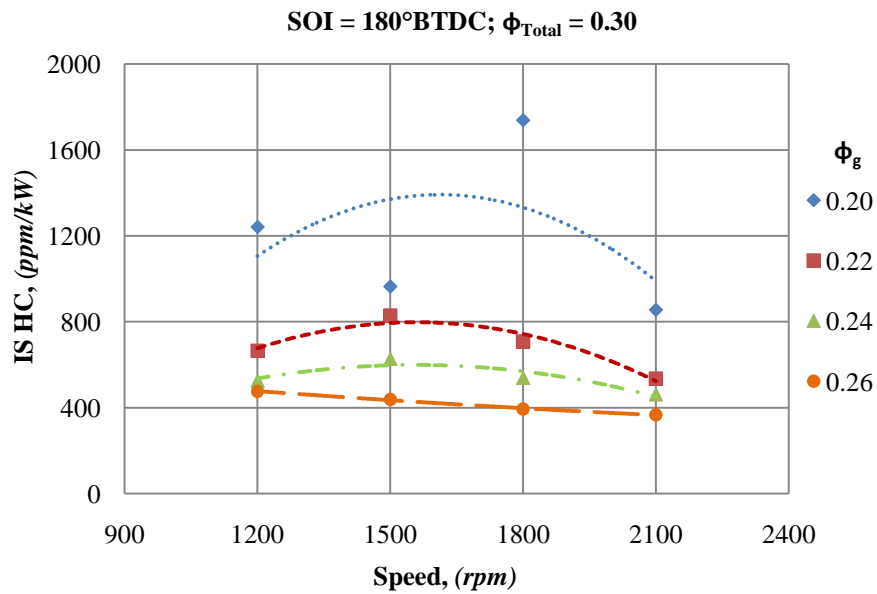
Figure 4.138 Effect of ϕ_g on HC emissions at a low CNG injection rate

SOI = 180°BTDC; ϕ_{Total} = 0.40
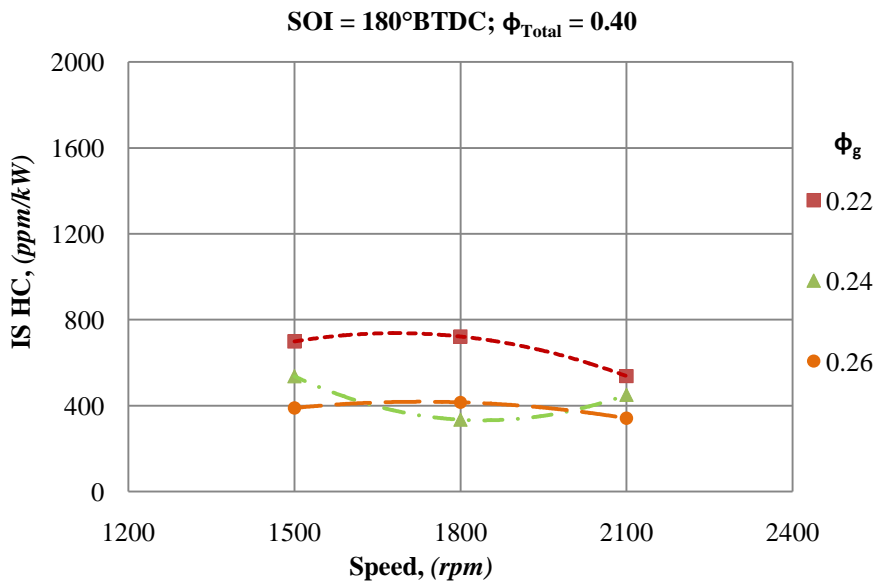
Figure 4.139 Effect of ϕ_g on HC emissions at higher CNG injection rate

As shown in Figure 4.140, at ϕ_{Total} = 0.30, CH_4 emissions reduced with an increase in ϕ_g, and there was a marginal impact by engine speed. However, as CNG injection rate was increased to ϕ_{Total} = 0.40, there was a significant reduction CH_4 emissions at all speeds and ϕ_g as shown in Figure 4.141.

SOI = 180°BTDC; ϕ_{Total} = 0.30
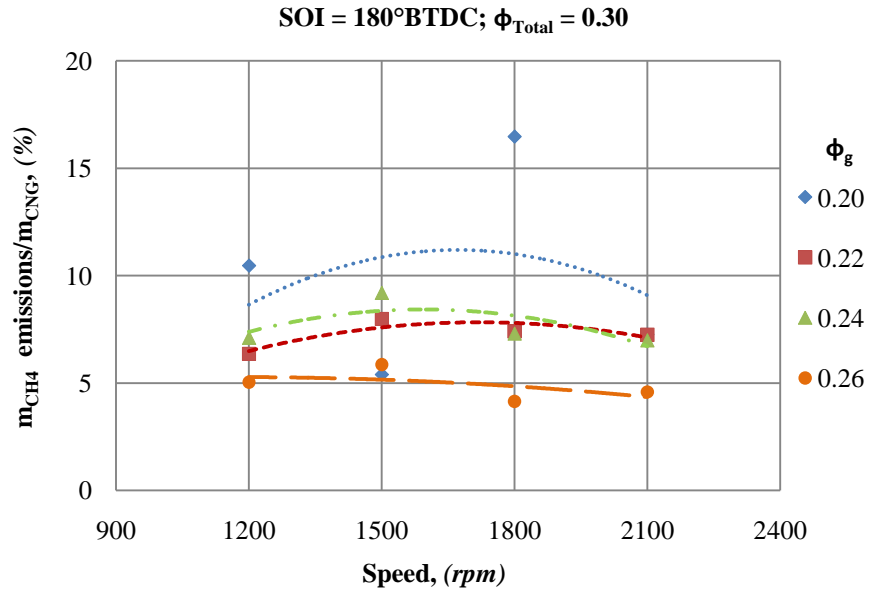
Figure 4.140 Effect of ϕ_g on the combustion of CNG at a low CNG injection rate

SOI = 180°BTDC; ϕ_{Total} = 0.40
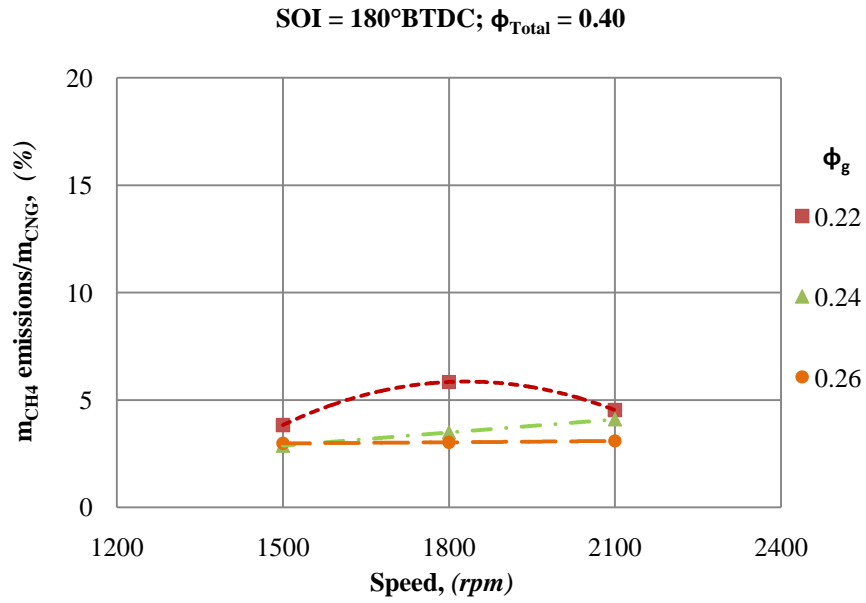
Figure 4.141 Effect of ϕ_g on the combustion of CNG higher CNG injection rate

Therefore, it can be concluded that gasoline equivalence ratio plays a significant role in the combustion of CNG along with thermal stratification of the mixture.

4.6 Comparison of Effect of Gasoline Equivalence Ratio with Homogeneous Mixing of CNG and with High Degree of CNG Stratification

The scope of this section is to compare the effect of equivalence ratio of gasoline on the characteristics of combustion with homogeneously mixed CNG and that with high degree of CNG stratification. The injection timing was kept at 300° BTDC to create homogeneous mixing of CNG with gasoline charge and to create a high degree of CNG stratification injection timing was kept at 80° BTDC. The effects of ϕ_g is discussed at $\phi_g = 0.30$ as it could be operated at both 300° BTDC and 80° BTDC at all gasoline equivalence ratios and over wide range of engine speeds.

The gasoline equivalence ratio and engine speed play a significant role on IMEP generated. Figure 4.142 shows the IMEP produced with $\phi_{Total} = 0.3$. It was observed that higher was the gasoline equivalence ratio higher the IMEP generated at all speeds except 1200 rpm. The lowest IMEP was achieved at 2100 rpm for all values of ϕ_g. At $\phi_g = 0.20$ and 0.22, the highest IMEP was achieved at 1200 rpm.
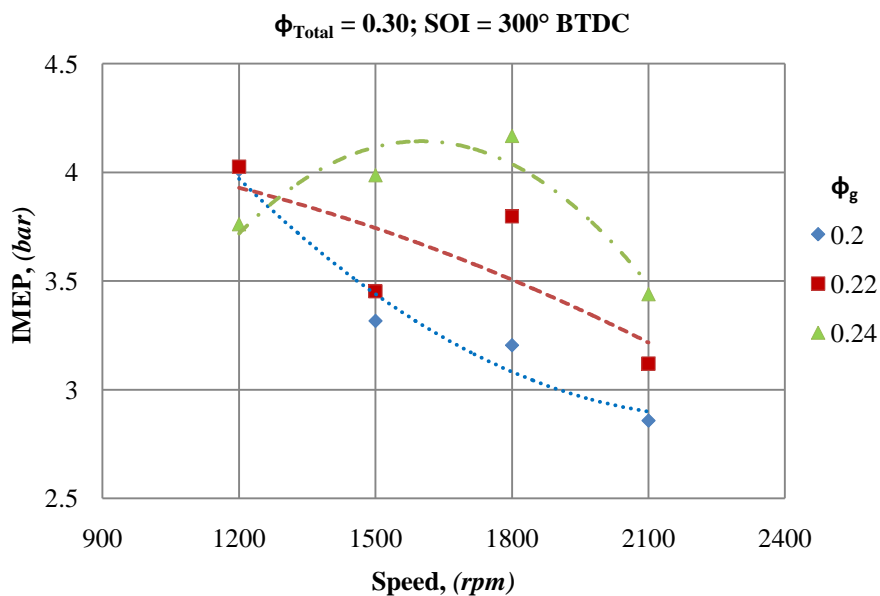
Figure 4.142 Effect of ϕ_g on the IMEP with homogenous mixing of CNG.

134

$\phi_{Total} = 0.30$; SOI = 80° BTDC
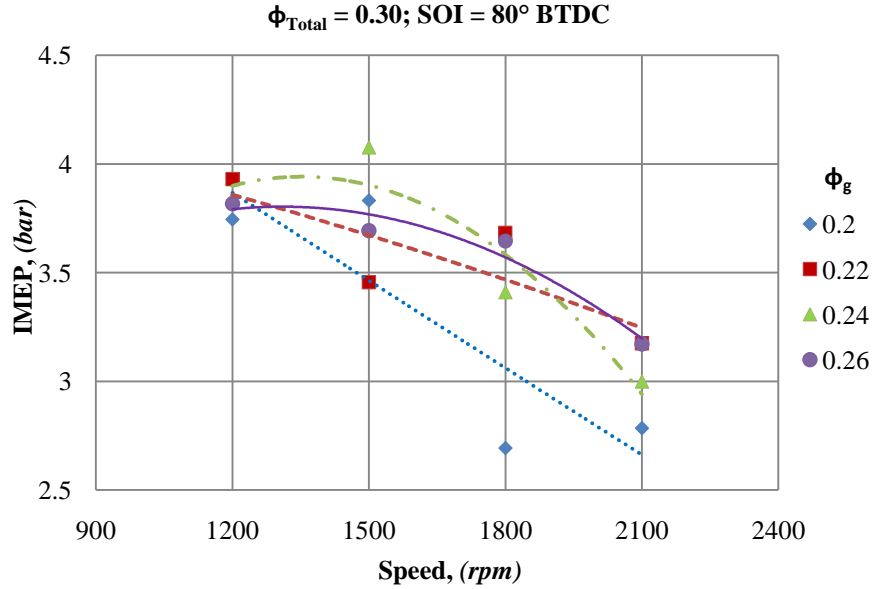
Figure 4.143 Effect of ϕ_g on the IMEP with high degree of CNG stratification.

The IMEP reduced with increase in engine speed and the maximum IMEP and thermal efficiency were obtained at 1800 rpm and $\phi_g = 0.24$ as shown in Figure 4.142 and Figure 4.144. At $\phi_g = 0.24$ and 1200 rpm, the IMEP reduced due to knocking as the ignition occurred before TDC as shown Figure 4.146. As an exception, this data point was included to the analysis for reference to compare the characteristics of acceptable and knocking HCCI combustion.

With high degree of CNG stratification, the engine could be operated with $\phi_g = 0.26$ at all speeds as the stratified CNG suppressed effects of ϕ_g on heat release rates which increased with an increase in gasoline equivalence ratio. As shown in Figure 4.143, at $\phi_g = 0.20$, lowest IMEP was obtained. However, at higher gasoline equivalence ratios, IMEP was a stronger function of engine speed and as IMEP reduced with increasing engine speed at all cases of ϕ_g. At $\phi_g = 0.26$, IMEP reduced at 1200rpm due to high heat release rates as shown in Figure 4.156, however, at 2100rpm, highest IMEP was obtained at $\phi_g = 0.26$ due to shorter time duration consumed per crank angle rotation at a higher engine speed.

$\phi_{Total} = 0.30$; SOI = 300° BTDC
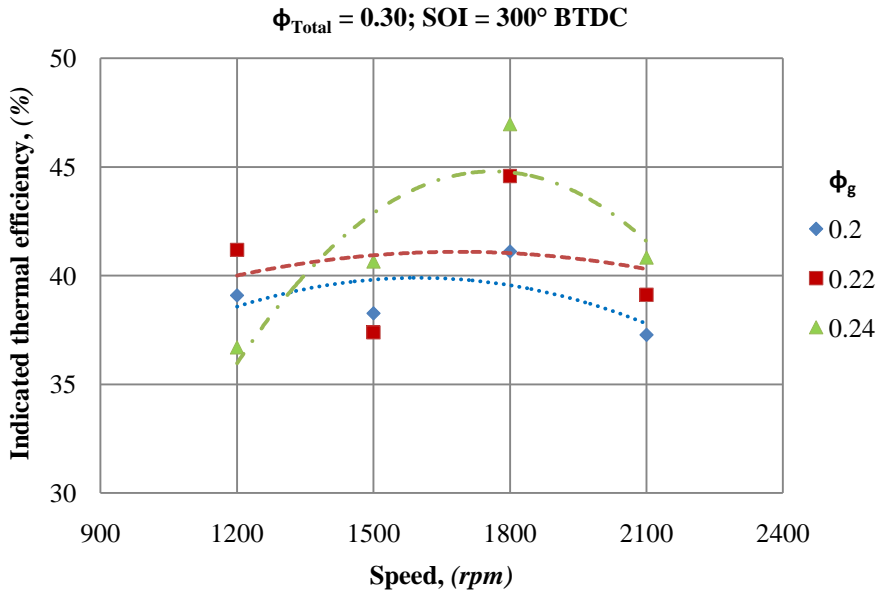
Figure 4.144 Indicated thermal efficiency with homogeneous mixing of CNG.

$\phi_{Total} = 0.30$; SOI = 80° BTDC
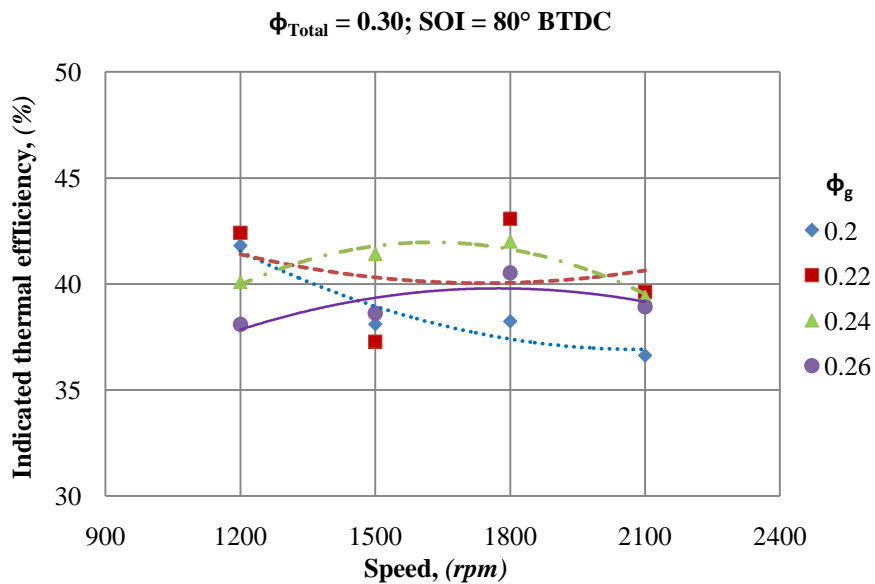
Figure 4.145 Indicated thermal efficiency with high degree of CNG stratification.

With CNG injection at 300° BTDC or homogeneous CNG mixing, thermal efficiency increased with an increase in ϕ_g and the highest efficiency was obtained at 1800 rpm as shown in Figure 4.144. Similarly, with CNG injection at 80° BTDC, high thermal efficiencies were obtained at $\phi_g = 0.22$ and 0.24 at 1200 and 1800rpm as shown in Figure 4.145. At $\phi_g = 0.26$, thermal efficiency was the lowest at 1200rpm and it increased as the engine speed was increased.

136
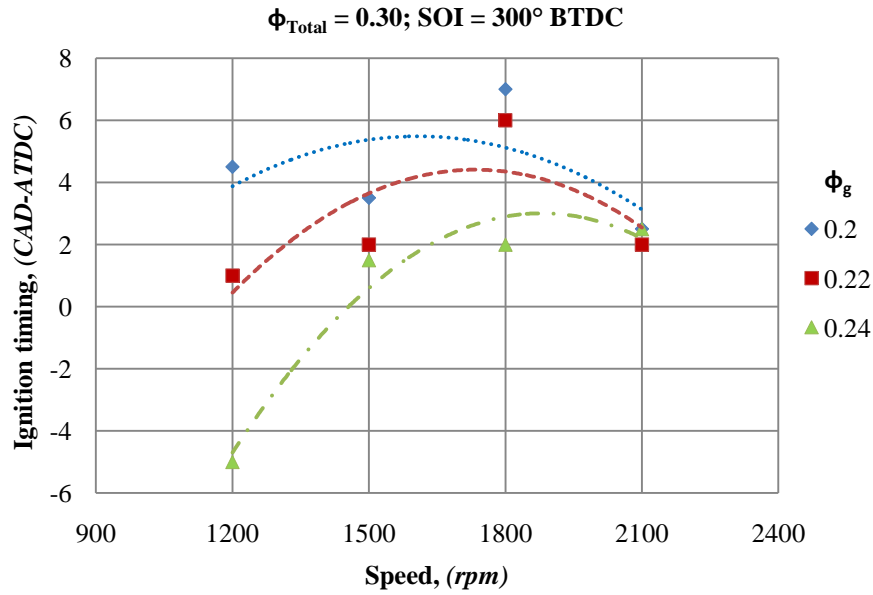
Figure 4.146 *Effect of ϕ_g on ignition timing with homogenous mixing of CNG.*
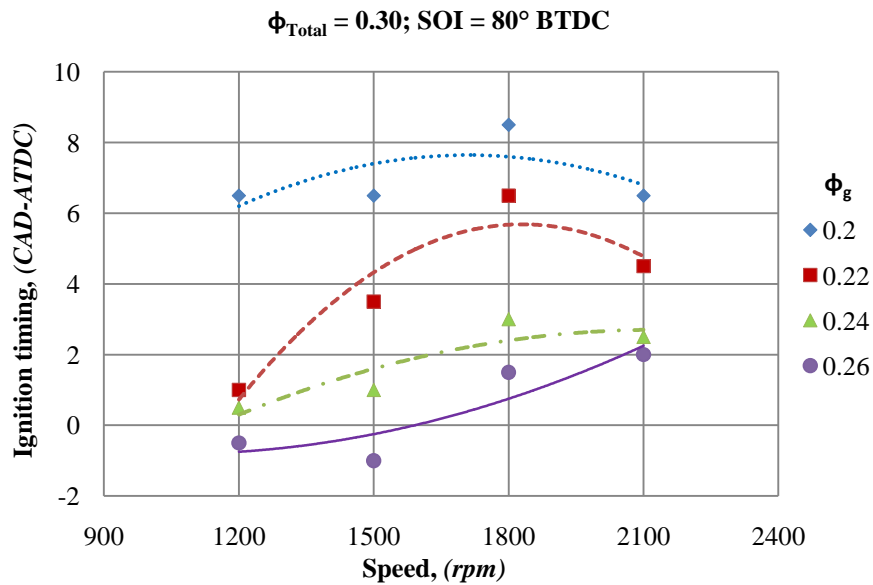
Figure 4.147 *Effect of ϕ_g on ignition timing with high degree of CNG stratification.*

The gasoline equivalence ratio significantly affected the ignition timing and combustion duration with both homogeneous and stratified distribution of CNG in the mixture. When ϕ_g was increased the ignition timing was advanced at all the speeds with CNG injection at 300° and 80° BTDC. At 300° BTDC and 2100 rpm, the effect of ϕ_g was less noticeable and the highest advance in ignition timing was observed at1200 rpm as shown in Figure 4.146. As the time duration available for the fuels to mix and react increased when the engine speed was reduced, the effect of ϕ_g was more significant at low speeds.

137

However, with stratification (80° BTDC), the effect of ϕ_g became significant at 2100rpm as shown in Figure 4.147. Or in other words, at 2100 rpm, by changing ϕ_g with high degree of CNG stratification ignition timing could be more significantly altered which otherwise was not controllable with CNG injection at 300° BTDC. With CNG injection at 80° BTDC, except at $\phi_g = 0.20$, the ignition timing advanced with decreasing engine speed.

At 1200 rpm and 80° BTDC, the effect of ϕ_g was less noticeable at $\phi_g = 0.22$; 0.24 and 0.26. At 1200rpm, drastic ignition advance resulted at $\phi_g = 0.24$ with CNG injection at 300° BTDC; but with high degree of CNG stratification, ignition timing was around TDC at $\phi_g = 0.24$ and did not significantly advance with an increase in ϕ_g, thereby making it possible to run the engine without knocking at $\phi_g = 0.26$.

With CNG injection at 300° BTDC, combustion duration increased as the engine speed was increased at all values of ϕ_g as shown in Figure 4.148. However, at a given speed, the combustion duration increased with a decrease in ϕ_g below 2100 rpm. It may be remembered here that the combustion duration is presented in terms of crank angle degrees and as the engine speed is increased the time taken for rotation of one crank angle is reduced.
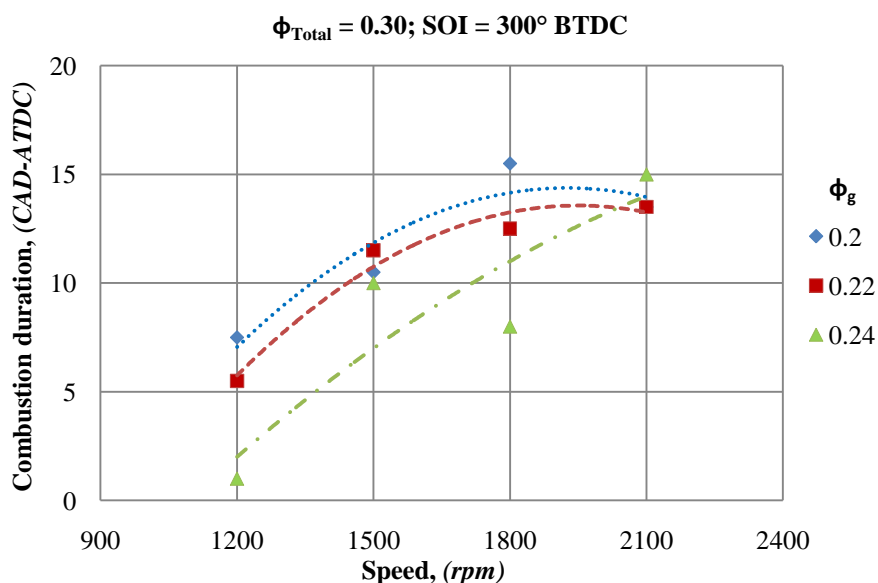
Figure 4.148 Effect of ϕ_g on the combustion duration with homogeneous mixing of CNG.

$\phi_{Total} = 0.30$; SOI = 80° BTDC
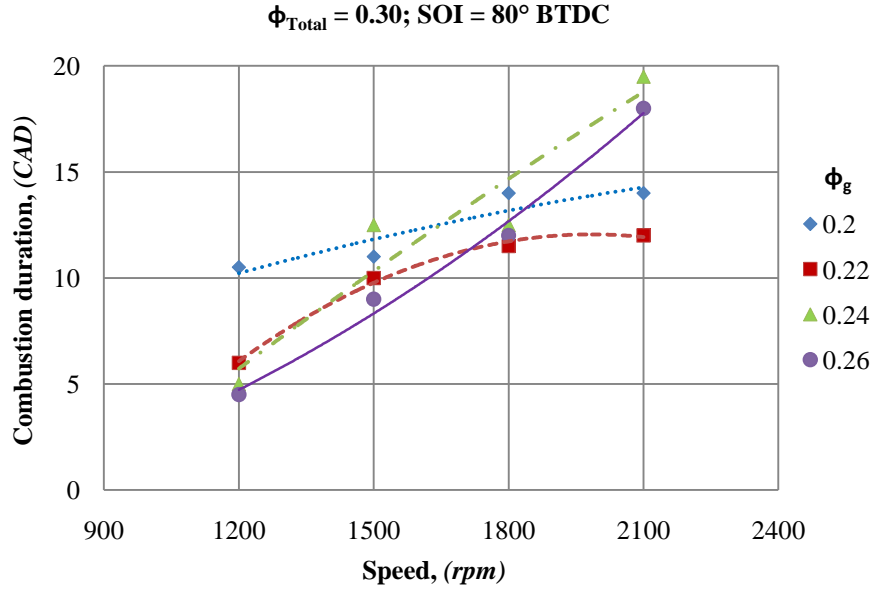
Figure 4.149 Effect of ϕ_g on the combustion duration with high degree of CNG stratification.

As shown in Figure 4.149, CNG injection at 80° BTDC, combustion duration increased with an increase in engine speed. However, the increase was more significant at $\phi_g = 0.24$ and 0.26 than that at $\phi_g = 0.20$ and 0.22. At $\phi_g = 0.22$ the combustion duration was longer than that at $\phi_g = 0.20$; similarly, at $\phi_g = 0.24$, combustion duration was longer than that resulted at $\phi_g = 0.26$ at all engine speeds. This was due to more complete combustion obtained at $\phi_g = 0.24$ and 0.26, which resulted in lower CO and HC emissions as shown in Figure 4.168 and Figure 4.170 respectively.

Figure 4.150 to Figure 4.152 show the pressure traces at different ϕ_g and engine speeds and with CNG injection at 300° BTDC. As shown in Figure 4.150 and Figure 4.151, at $\phi_g = 0.20$ and 0.22, the peak pressure and heat release rates were reduced as the engine speed was increased from 1200 to 1800rpm and they again increased at 2100 rpm. At $\phi_g = 0.20$ and 0.22, the higher turbulence in the cylinder at 2100 rpm might have resulted in increased peak pressures and advanced ignition timing. Similar trends were observed at $\phi_g = 0.20$ and 0.22 with CNG injection at 80° BTDC as shown in Figure 4.153 and Figure 4.155.

139
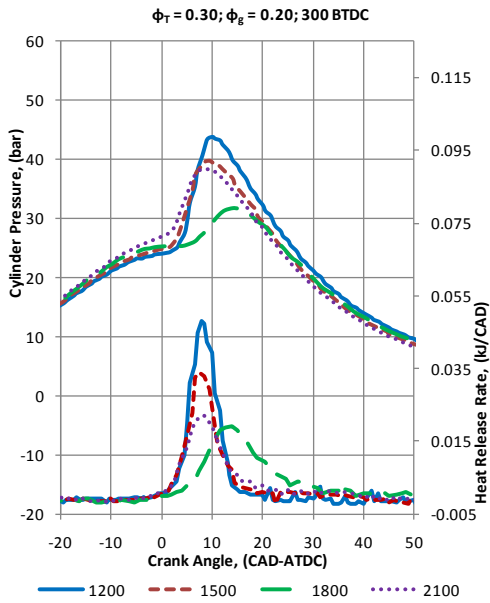
Figure 4.150 Pressure history and heat release rates with homogeneous mixing CNG at ϕ_g =0.20.
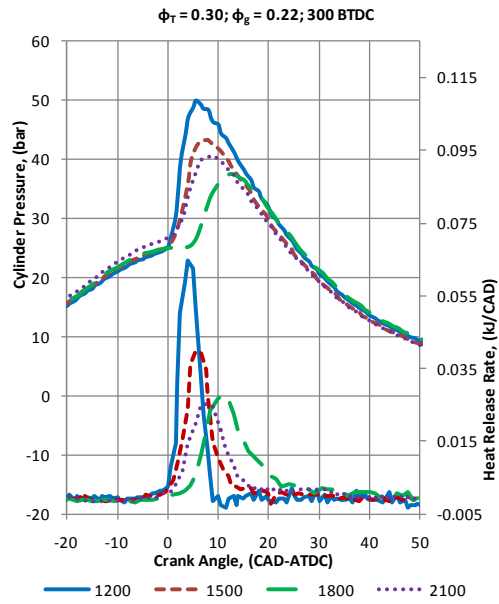
Figure 4.151 Pressure history and heat release rates with homogeneous mixing of CNG at ϕ_g =0.22.
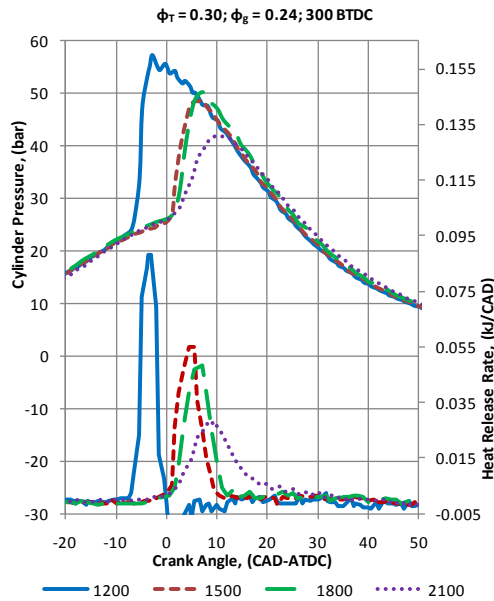
Figure 4.152 Pressure history and heat release rates with homogeneous mixing of CNG at ϕ_g =0.24.

At ϕ_g = 0.20 and 0.22, peak pressures decreased with an increase in engine speed from 1200rpm and 1800 rpm and then increased at 2100 rpm. However, at ϕ_g = 0.20 and 0.22, as shown in Figure 4.150 and Figure 4.151, peak pressures resulted in with CNG injection at 300° BTDC were higher than those resulted in with CNG injection at 80° BTDC as shown in Figure 4.153 and Figure 4.155.

However, at $\phi_g = 0.24$, unlike the trends observed at $\phi_g = 0.20$ and 0.22, the peak pressures continued to reduce as the engine speed was increased from 1800 to 2100 rpm, due to the low energy released by the low temperature reactions as shown in Figure 4.22.
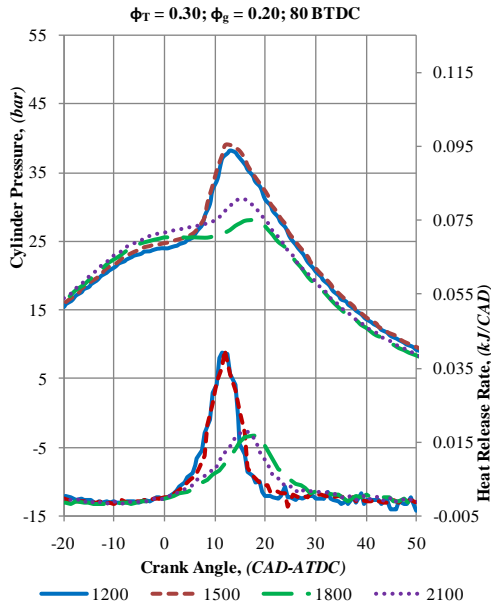
Figure 4.153 Pressure history and heat release rates with high degree of CNG stratification at $\phi_g = 0.20$.
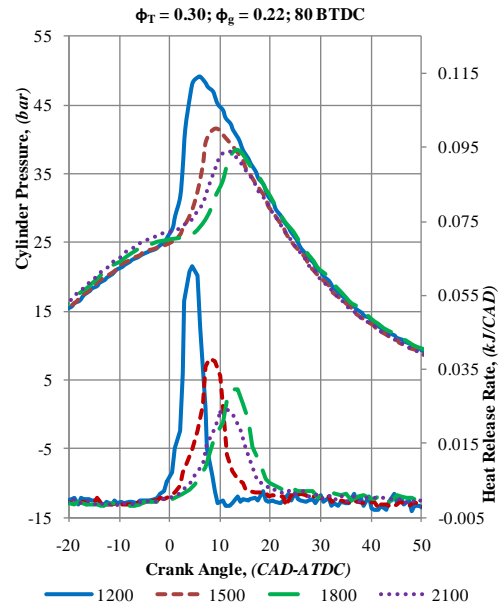
Figure 4.155 Pressure history and heat release rates with high degree of CNG stratification at $\phi_g = 0.22$.
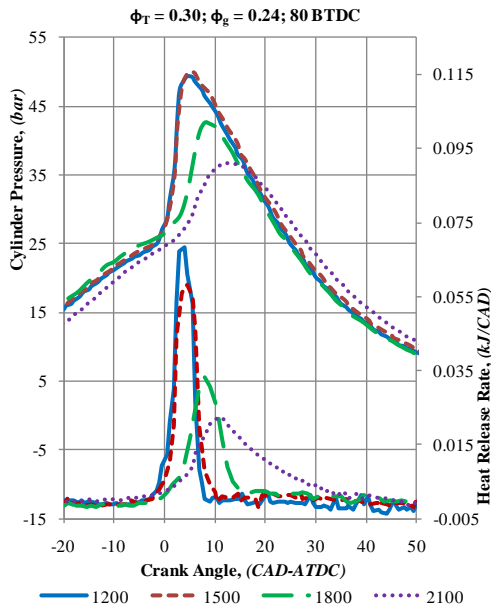
Figure 4.154 Pressure history and heat release rates with high degree of CNG stratification at $\phi_g = 0.24$.
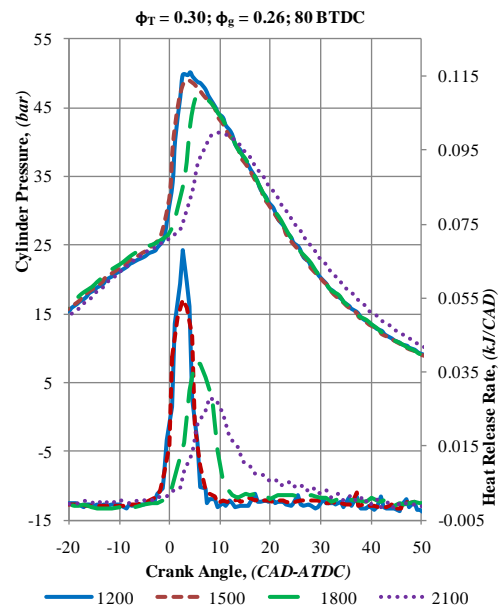
Figure 4.156 Pressure history and heat release rates with high degree of CNG stratification at $\phi_g = 0.26$.

Similar trend was observed with CNG injection at 80°BTDC, at $\phi_g = 0.24$ and 0.26 as shown in Figure 4.154 and Figure 4.156. However, peak pressures resulted at 80°BTDC was lower than those obtained at 300° BTDC at $\phi_g = 0.24$ and the engine could be operated at $\phi_g = 0.26$. That is, at $\phi_{Total} = 0.30$, CNG stratification reduced peak pressures resulted at all ϕ_g and all engine speeds.

At 1200 rpm, high heat release rates and peak pressures were observed at all ϕ_g. As shown in Figure 4.152, at $\phi_g = 0.24$ and 1200 rpm, the engine was knocking due to ignition before TDC and excessive pressure rise and heat release rates.

At 1500 rpm, high heat release rates and peak pressure rates resulted and were marginally less than those observed at 1200 rpm. However, at $\phi_g = 0.22$, the difference between the heat release rates and peak pressure observed at 1200 and 1500 rpm more significant than at other values of ϕ_g.

At 1800 rpm, peak pressure and heat release rate were the lowest due to delayed ignition timing at $\phi_g = 0.20$ and 0.22 with CNG injection at both 300° BTDC and 80° BTDC. However, at $\phi_g = 0.24$ and 0.26, higher peak pressures than that resulted at 2100 rpm as shown in Figure 4.152, Figure 4.154 and Figure 4.156. At $\phi_g = 0.24$ and 0.26, the highest thermal efficiencies were obtained at 1800 rpm due to optimum ignition timing and combustion phasing, thus making 1800 rpm as optimum speed for a range of conditions.

At 2100 rpm, with CNG injection at 300° BTDC and at all ϕ_g, the pressure traces and heat release rates resulted were slightly different from those obtained at 1500 rpm as shown in Figure 4.150 and Figure 4.151. Due to higher engine speed, peak pressures and heat release rates were moderate and led to high limits of maximum operable ϕ_{Total} with homogeneous mixing of CNG as shown in 4.3. With CNG injection at 80° BTDC and at $\phi_g = 0.20$ and 0.22, significantly lower peak pressures and heat release rates were observed at 2100 rpm than at 1500 rpm as shown in Figure 4.153 and Figure 4.155. Significant reduction in peak pressure and heat release rates were observed at $\phi_g = 0.24$ and 0.26 and 80° BTDC as shown in Figure

4.154 and Figure 4.156 due to high degree of CNG stratification coupled with shorter duration consumed for rotation of one degree crank angle.
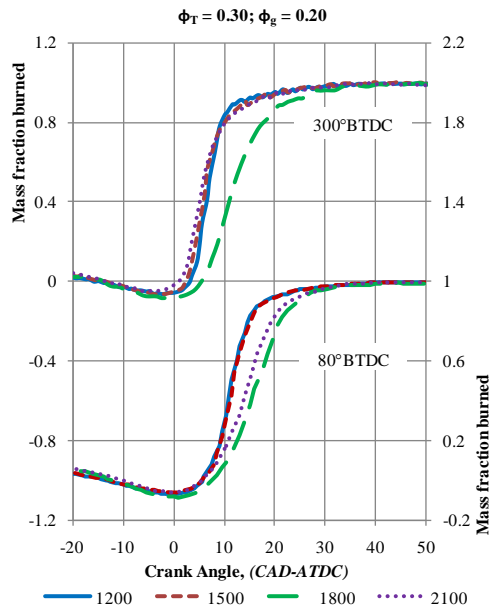
Figure 4.157 Mass fraction burned with homogenous and highly stratified CNG at ϕ_g =0.20.
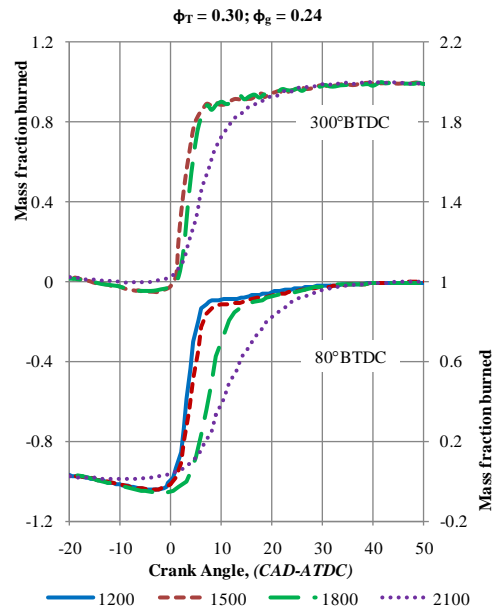
Figure 4.159 Mass fraction burned with homogenous and highly stratified CNG at ϕ_g =0.24.
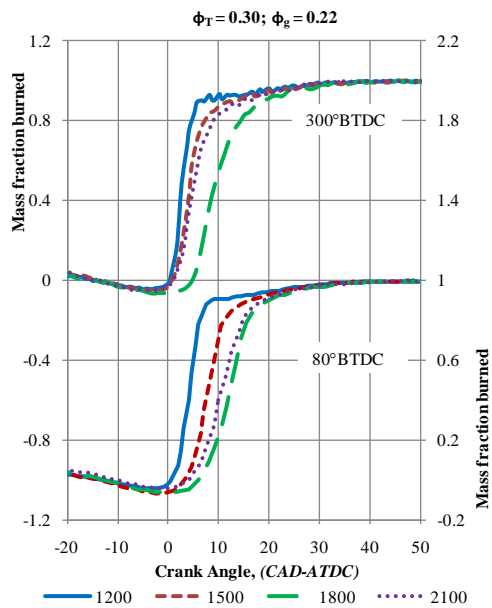
Figure 4.158 Mass fraction burned with homogenous and highly stratified CNG at ϕ_g =0.22.
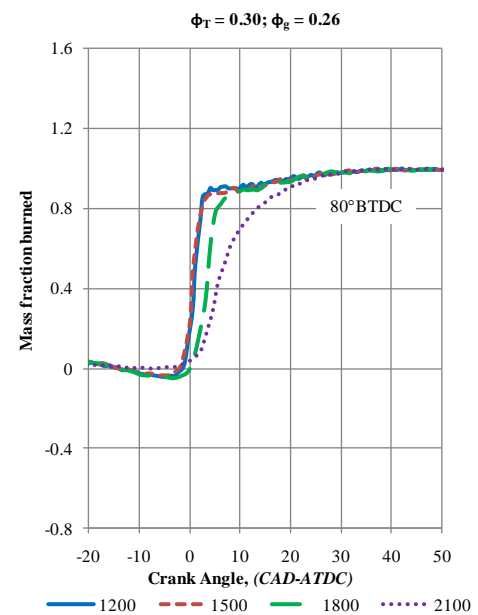
Figure 4.160 Mass fraction burned with homogenous and highly stratified CNG at ϕ_g =0.2

Figure 4.157 to Figure 4.160 show the effect of CNG stratification on the mass fraction and rate of burning of the dual fuels at various ϕ_g and engine speeds. At 300 BTDC, there was no significant difference in burning rate among 1200, 1500 and

2100 rpm.   As shown in Figure 4.157, at 300° BTDC and $\phi_g = 0.20$, mass fraction of about 80% of the fuels burned within 10 CAD at all speeds except at 1800rpm.

At 1800 rpm, due to later ignition, the fuels burned gradually. At $\phi_g = 0.20$ and with CNG injection at 80° BTDC, due to higher energy required to ignite stratified CNG and reduced time available for CNG to get heated up, ignition timing was delayed as shown in Figure 4.147 and major part of burning was placed between 10 to 20 CAD-ATDC. However, at 2100 rpm, burning occurred earlier and was faster than at 1800 rpm.

At $\phi_g = 0.22$ and 300° BTDC, the rate of burning was higher at 1200 rpm and reduced as the engine speed was increased to 1800 rpm as shown in Figure 4.158. However, at 2100 rpm, there was a significant advance in ignition timing and rate of burning was almost same as that at 1500 rpm. At $\phi_g = 0.22$ and 80° BTDC, the rate of burning was reduced at all speeds as compared to that with CNG injection at 300° BTDC. At 1800 rpm the slowest rate of burning was observed. However, significant reduction in burning rate due to CNG stratification was observed at 1500 and 2100 rpm.

At 300° BTDC and $\phi_g = 0.24$, at 1500 and 1800 rpm, the fuels burnt rapidly but at 2100 rpm the rate of burning was significantly less than that at other speeds as shown in Figure 4.159. With CNG injection at 80° BTDC, the rate of burning at 1500 rpm was slightly reduced compared to the case of 300° BTDC and the engine could be operated at 1200 rpm at $\phi_g = 0.24$. At 80° BTDC, there was a significant reduction in burning rate was observed at 1800 rpm and 2100 rpm.

At 300° BTDC and $\phi_g = 0.26$, the engine could not be operated due to knock. At 80° BTDC and $\phi_g = 0.26$, except at 2100 rpm, the fuels burned very rapidly as shown in Figure 4.160. At 1200 and 1500 rpm, major portion of the fuels burnt around TDC. At 1800 rpm, there was a delay in ignition timing but rate of burning was almost same as that at 1200 and 1500 rpm.

As shown in Figure 4.161, at 1200 rpm, with CNG injection at 300° BTDC, combustion efficiency was high and ϕ_g had less significant effect. As at 1200 rpm, as

144

there was ample time available for CNG to mix, the gasoline concentration was more uniform in the mixture even with low ϕ_g.

$\phi_{Total} = 0.30$; SOI = 300° BTDC
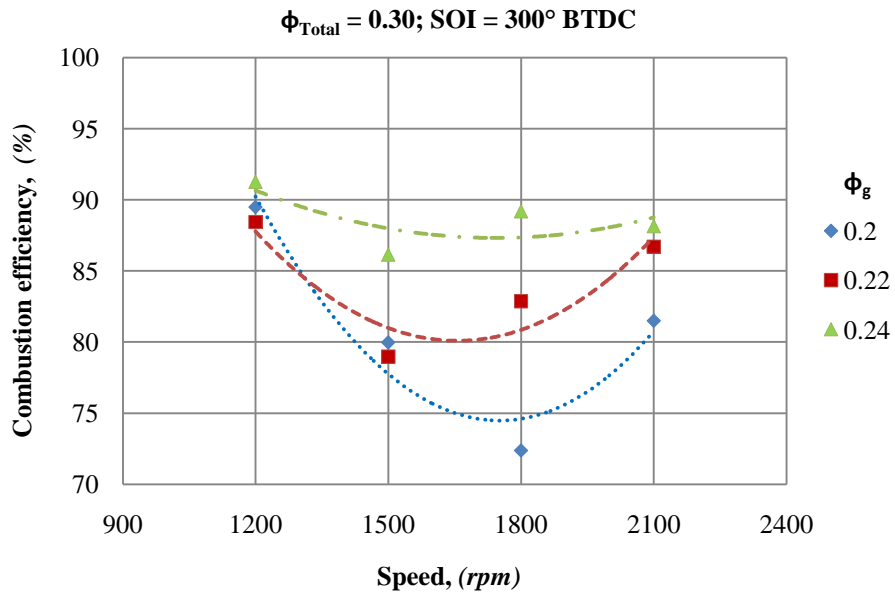
Figure 4.161 Combustion efficiency of homogeneous mixture of gasoline and CNG

$\phi_{Total} = 0.30$; SOI = 80° BTDC
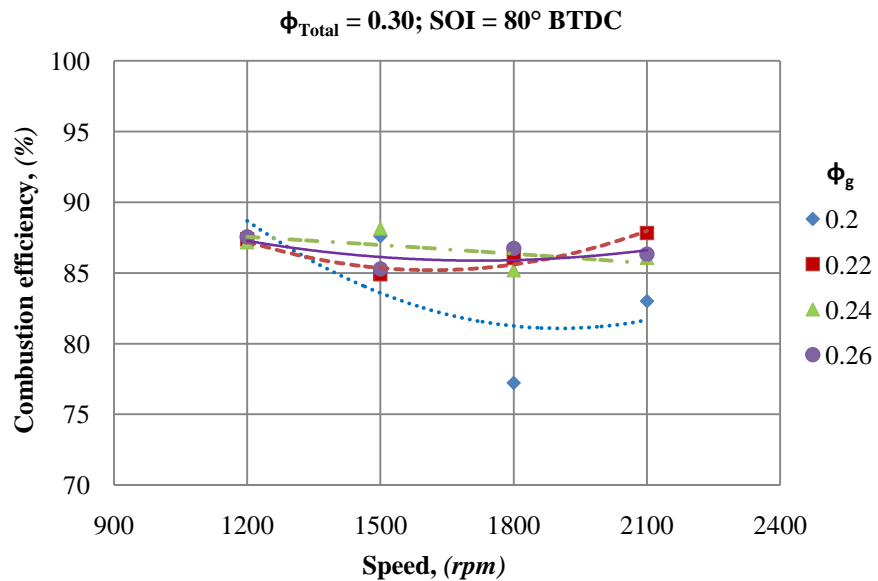
Figure 4.162 Combustion efficiency with high degree of CNG stratification

At 2100 rpm, combustion efficiency again increased for $\phi_g = 0.22$ and 0.24, because of some degree of stratification due to reduced time available for CNG. However, at $\phi_g = 0.20$, combustion efficiency was lower due to low gasoline concentration combined with shorter reaction time available at 2100 rpm.

145

At 1500 and 1800 rpm, ϕ_g had significant effect and higher the ϕ_g, higher was the combustion efficiency. With CNG injection at 80 BTDC, the influence of engine speed and ϕ_g was reduced by degree of stratification of CNG as shown in Figure 4.162. However, at $\phi_g = 0.20$, there was decrease in combustion efficiency at 1800 and 2100 rpm.

As shown in Figure 4.163 and Figure 4.164, with CNG injection at 300° BTDC, NO_x emissions were lower than 500 ppm/kW for all the cases except at $\phi_g = 0.24$ and 1200 rpm due to rapid burning and unacceptable levels of heat and pressure rise rates resulted in as the entire combustion process occurred at the end of the compression stroke. At this point, NO_2/NO_x was less than 10% due to prevalence of high combustion temperatures that led to more NO formation than NO_2 as shown in Figure 4.165.

With CNG injection at 80° BTDC, NO_x were slightly higher at 1200 rpm at $\phi_g > 0.20$, and at other speeds NO_x emissions were lower at all ϕ_g. With high degree of CNG stratification, higher NO_x emissions resulted at $\phi_g = 0.24$ as shown in Figure 4.164. As the ϕ_g increased from 0.24 to 0.26, NO_x emission reduced as high gasoline equivalence ratio led to higher combustion temperatures.
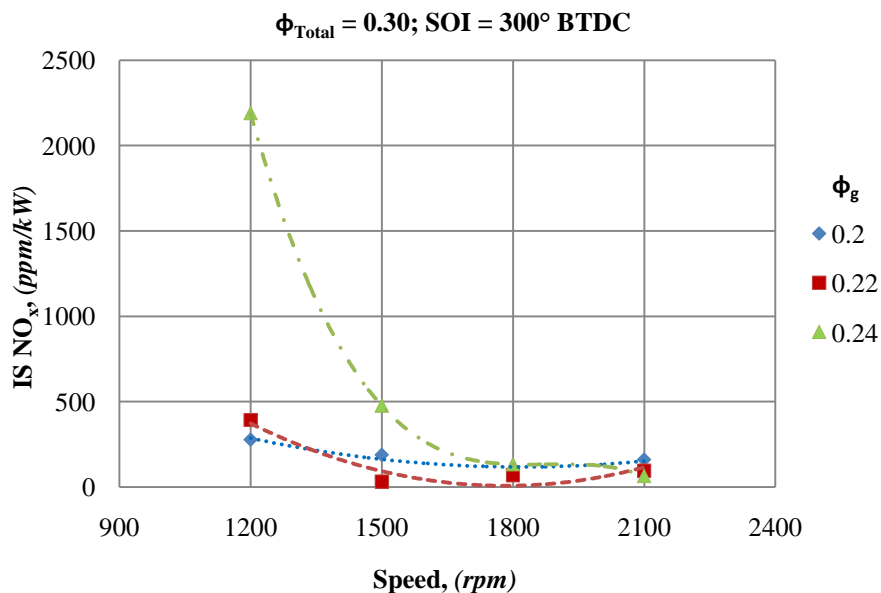
Figure 4.163 Effect of ϕ_g on NO_x emission with homogeneous mixing of CNG

$\phi_{Total} = 0.30$; SOI = 80° BTDC
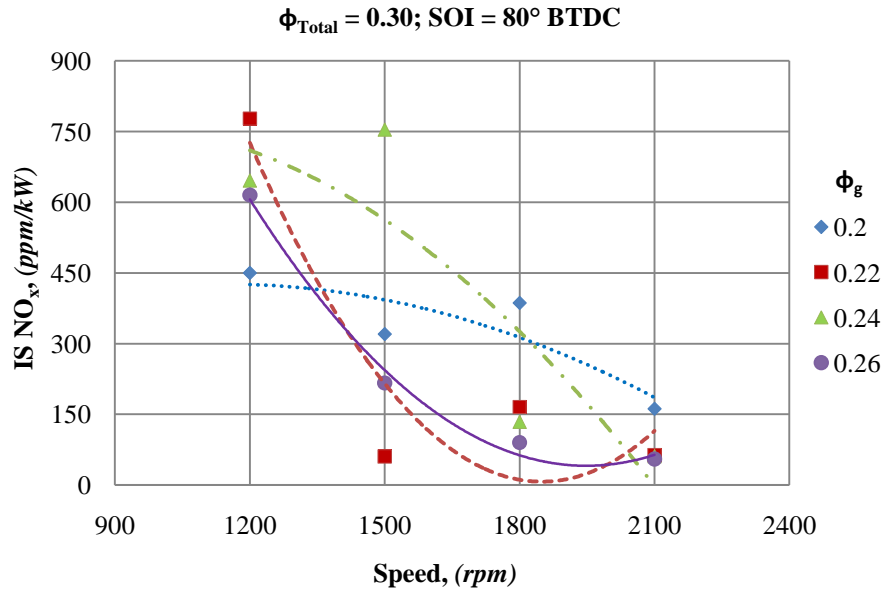
Figure 4.164 Effect of ϕ_g on NO_x emission with high degree of CNG stratification

With CNG injection at 80° BTDC, NO_x were slightly higher at 1200 rpm at $\phi_g >$ 0.20, and at other speeds NO_x emissions were lower at all ϕ_g. With high degree of CNG stratification, higher NO_x emissions resulted at $\phi_g = 0.24$ as shown in Figure 4.164. As the ϕ_g increased from 0.24 to 0.26, NO_x emission reduced as high gasoline equivalence ratio led to higher combustion temperatures.

$\phi_{Total} = 0.30$; SOI = 300° BTDC
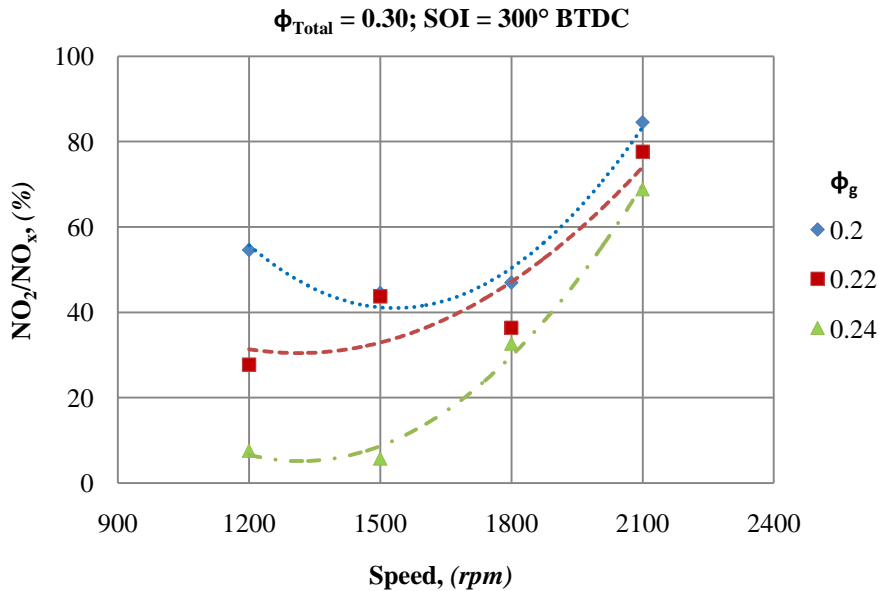
Figure 4.165 Effect of φ_g on NO_2 formation with homogeneous mixing of CNG

147
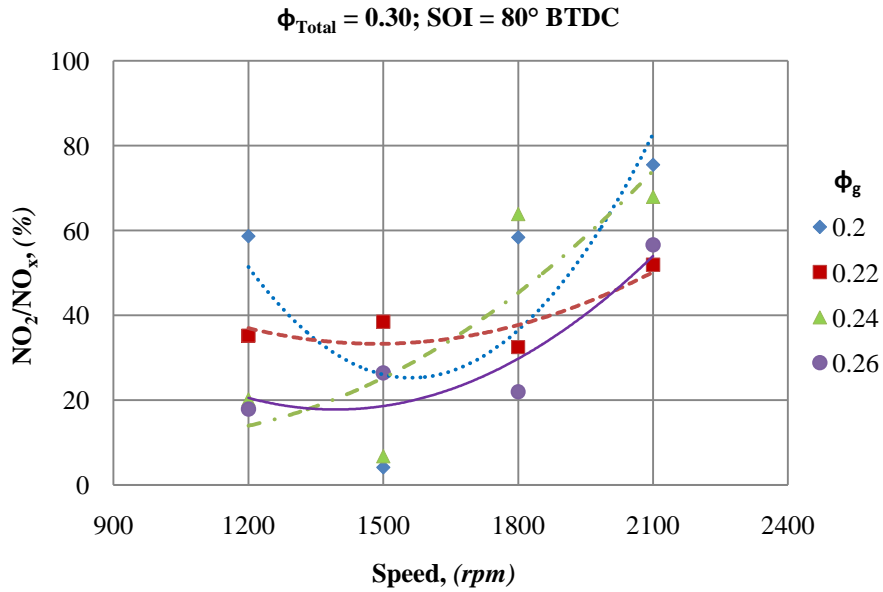
Figure 4.166 Effect of φ_g on NO_2 formation with high degree of CNG stratification

The ratio of NO_2 to NO_x was a function of ϕ_g and engine speed at both $300°$ BTDC and $80°$ BTDC as shown in Figure 4.165 and Figure 4.166. At a constant $\phi_{Total} = 0.3$, decrease in ϕ_g means higher CNG injection rates, and as an increase in the amount of CNG reduced the combustion temperature resulting in higher NO_2 emission. However, NO_2/NO_x ratio increased as the engine speed increased for all values of ϕ_g at both injection timings of CNG at $300°$ BTDC and $80°$ BTDC.

This was due to that increasing engine speeds reduces the resident time available for further reactions involving the formation of NO from NO_2. However, at 2100 rpm and $80°$ BTDC, NO_2/NO_x was less than that resulted with CNG injection at $300°$ BTDC as high degree of stratification coupled with higher ϕ_g increased the combustion temperatures and reduced NO_2 formation.

148

ϕ_{Total} = 0.30; SOI = 300° BTDC
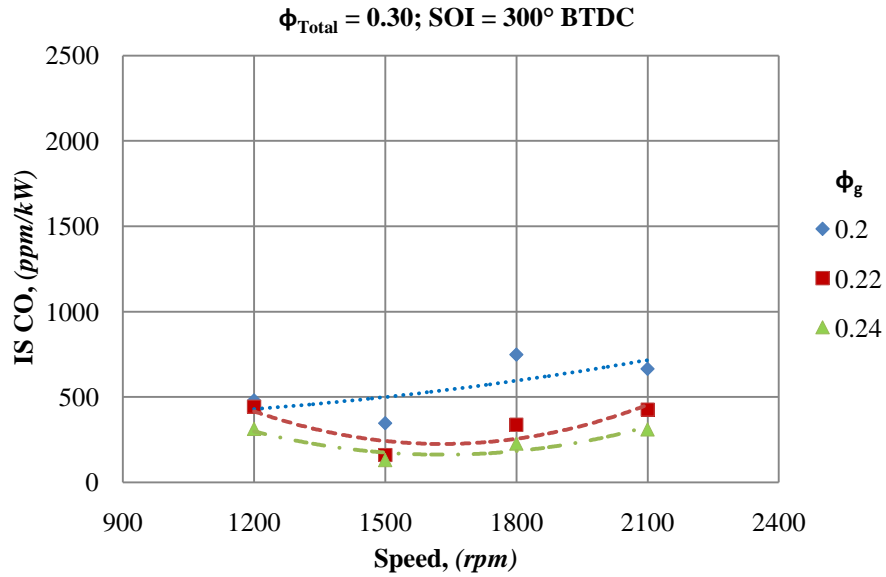
Figure 4.167 CO emissions at different ϕ_g with homogeneous mixing of CNG.

ϕ_{Total} = 0.30; SOI = 80° BTDC
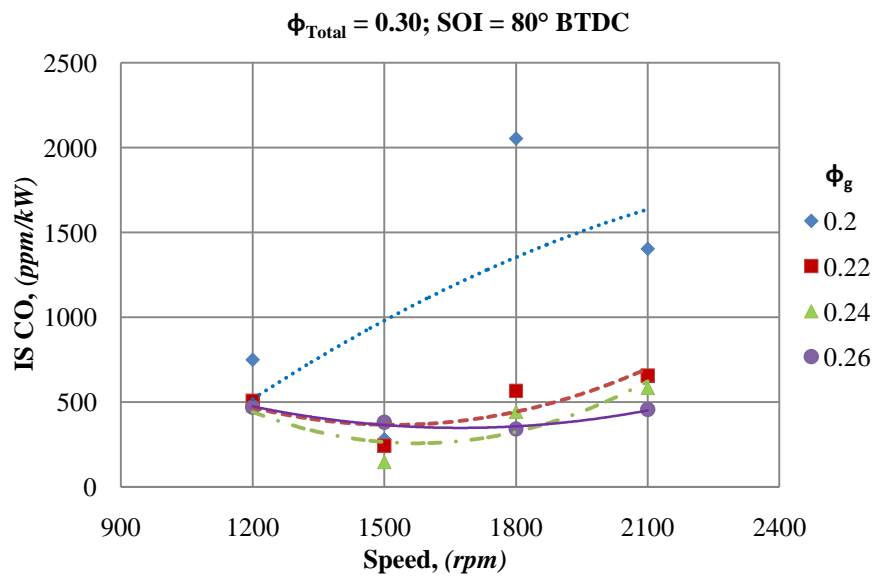
Figure 4.168 CO emissions at different ϕ_g with high degree of CNG stratification.

With CNG injection at 300° BTDC and 80° BTDC, CO emissions decreased with an increase in ϕ_g at all engine speeds, as higher values of ϕ_g resulted in more complete combustion as shown in Figure 4.167 and Figure 4.168. The highest CO emission was recorded at the lowest value of ϕ_g = 0.20. The engine speed had marginal effect on the CO emissions at both 300° BTDC and 80° BTDC and CO emissions were significantly less than typical CO emissions by HCCI combustion.

149
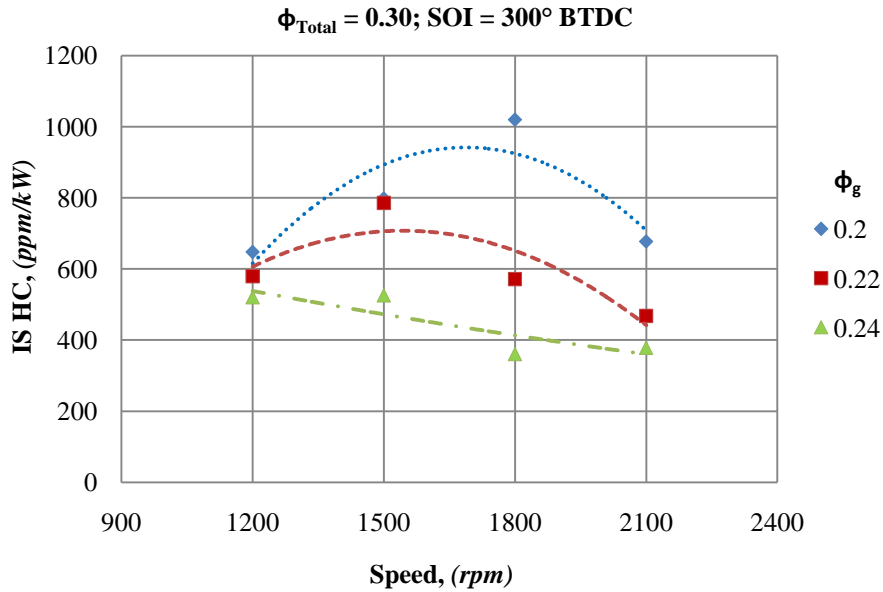
Figure 4.169 Effect of ϕ_g on HC emissions with homogeneous mixing of CNG
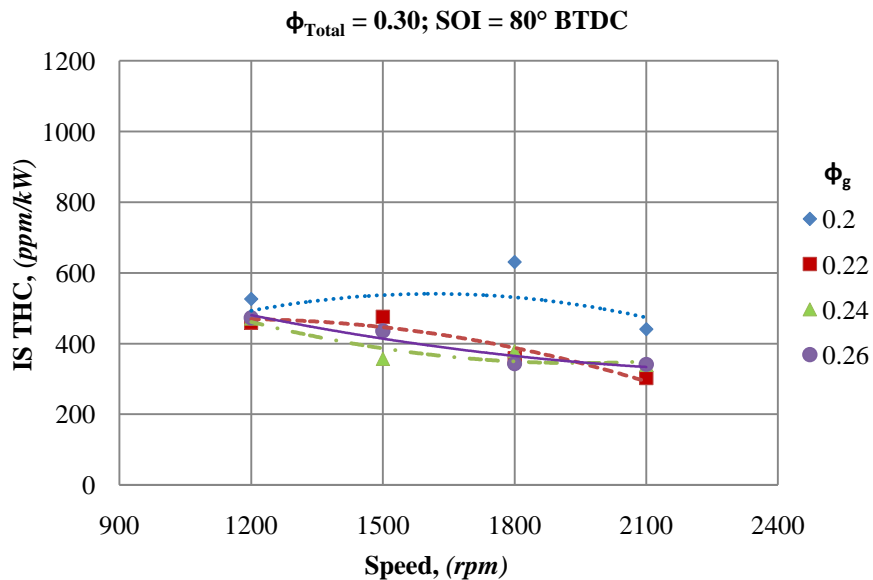
Figure 4.170 Effect of ϕ_g on HC emissions with high degree of CNG stratification

Both with CNG injection at 300° BTDC and 80° BTDC, HC emissions reduced with an increase in gasoline equivalence ratio at all engine speeds as shown in Figure 4.169 and Figure 4.170. With CNG injection at 300° BTDC, the effect of ϕ_g on HC emissions was more significant at 2100 rpm than at 1200 rpm. This was because of better mixing of the CNG and the gasoline-air mixture due to longer time available at 1200rpm leading to a better distribution of gasoline in the mixture than at 2100rpm, which reduces the influence of ϕ_g on HC emissions. With CNG injection at 80°

BTDC, HC emissions were lower than 600 ppm/kW for all cases due to high degree of CNG stratification that resulted in more complete combustion of CNG.
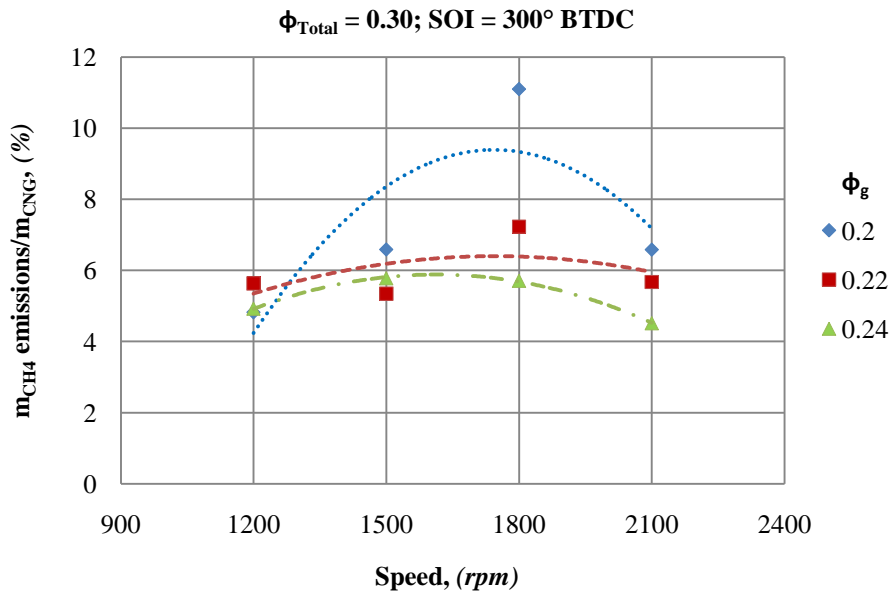
Figure 4.171 Effect of ϕ_g on the combustion of homogeneously mixed CNG
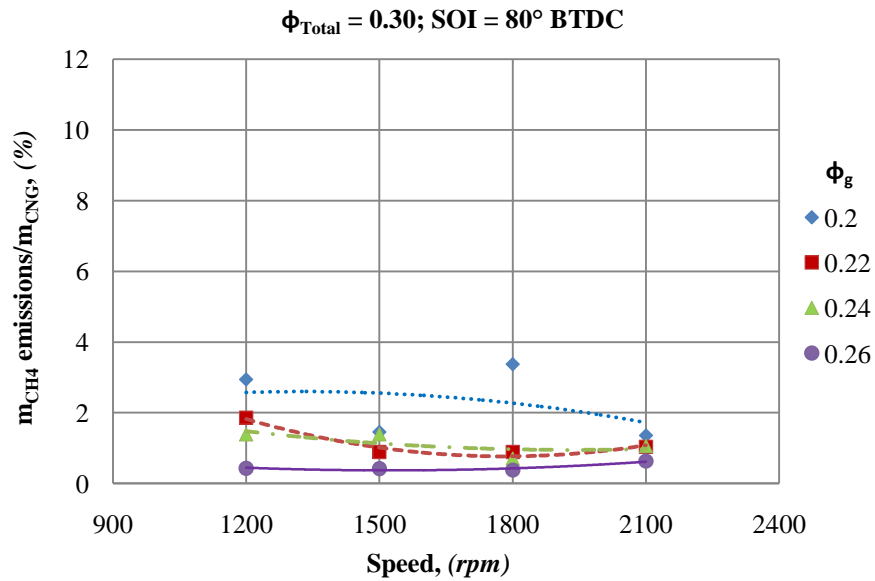
Figure 4.172 Effect of ϕ_g on the combustion of highly stratified CNG

As shown in Figure 4.171, the CH_4 emissions was highest at $\phi_g = 0.20$ and at 1800rpm. However, CH_4 emissions were a stronger function of ϕ_g than engine speed. With an increase in ϕ_g, CH_4 emissions reduced suggesting that higher amounts of gasoline resulted in more complete combustion of CNG. However, as shown in Figure 4.172, CNG injection at 80° BTDC resulted in less than 4% of CH_4 emissions

at all ϕ_g and speeds. At 80° BTDC, CH_4 emissions reduced with an increase in ϕ_g, and was least affected by engine speed. At $\phi_g = 0.20$, the maximum CH_4 emissions were observed and it may be noted that at this condition overall combustion efficiency was also the lowest as shown in Figure 4.162.

4.7 Summary of Results

In this chapter, the characteristics of dual fuel HCCI combustion with homogeneous mixtures of gasoline and CNG were discussed. The effect of varying the degree of stratification of CNG and the influence of gasoline equivalence ratio on combustion were also discussed. An extended analysis on the combustion characteristics at different engine speeds was also included. Finally, a comparison of role of gasoline equivalence ratio on combustion between homogeneously mixed and highly stratified CNG was presented. The effects of proportions of fuels, the degree of CNG stratification and the influence of engine speed on these effects are summarized in the following sections.

4.7.1 Effect of Proportion of Fuels

The proportion of gasoline and CNG injection rates had significant effects on the performance, combustion and emission characteristics.

1. The equivalence ratio of gasoline was observed to be an essential parameter for the subsequent ignition and combustion of CNG. This resulted in increased thermal efficiencies as ϕ_g was increased. However, when ϕ_g was increased above 0.24, it resulted in a deterioration in performance and a reduction in the maximum load limits due to excessive increase in heat release and pressure rise rates.

2. Ignition timing could be altered by varying the gasoline equivalence ratio (ϕ_g) in the overall mixture. Increasing the proportion of ϕ_g resulted in advanced ignition timing and shorter combustion durations and increasing the CNG injection rate resulted in a delayed ignition. However, above a certain limit of total equivalence ratio, the ignition significantly advanced

regardless of the proportion of gasoline and CNG defining the controllable limit of combustion by fuel proportions.

3. Total hydrocarbon (HC) and methane (CH_4) emissions could be reduced by increasing the gasoline equivalence ratio due to better combustion of the overall mixture and CNG. However, the decrease in HC emissions obtained reduced when ϕ_g was increased from 0.24 to 0.26. CO emissions also followed the same trend. For loads above $\phi_{Total} = 0.35$, ϕ_g became less significant both HC and CO emissions were significantly reduced at all ϕ_g. NO_x emissions were found to be dominated by the formation of NO_2. Increasing ϕ_g resulted in a decreased NO_2/NO_x for all values of ϕ_g. Increasing CNG injection rate increased the NO_2/NO_x ratio for $\phi_{T} \leq 0.33$ but above this value it reduced again.

4.7.2 Effect of CNG Stratification

1. Increased gasoline equivalence ratios were required to achieve combustion when degree of stratification of CNG was increased.

2. At $\phi_g = 0.20$ and 0.22 and low CNG injection rates, as the degree of stratification was increased by retarding injection to 180° and 120° BTDC, both the IMEP generated and thermal efficiency decreased. However, IMEP again increased when injection was retarded further to 80° BTDC or when the CNG injection rate was increased. Increasing ϕ_g resulted in higher IMEP at all degrees of CNG stratification and $\phi_{Total,}$ however, it was limited due to increased knock tendency.

3. HC and CH_4 emissions reduced with increasing degree of stratification at all values of ϕ_g, loads and speeds. Similarly, increasing ϕ_g also resulted in a reduction in THC emissions at a given degree of stratification. However, CO emissions increased when the degree of stratification was increased. This formed a trade-off between HC and CO emissions when the mixture was stratified. NOx emissions increased when the degree of stratification and engine load were increased. Formation of NO_2 was a stronger function of ϕ_{CNG}/ϕ_{Total} than degree of stratification as there were marginal effects on

153

NO_2/NO_x when the injection was retarded. When CNG injection rate was increased it initially increased NO_2/NO_x and then decreased.

4.7.3 Influence of Engine Speed

1. The effects of CNG injection and the degree of stratification were found to be significantly influenced by engine speed.

2. At 1200 rpm, operable load range was narrow as heat release and pressure rise rates were higher than those resulted at higher speeds. With homogeneous mixing of CNG, heat release rates were sensitive to gasoline equivalence ratio and CNG injection rate was limited due to knocking for $\phi_g > 0.24$. However, high ϕ_g values could be operated by retarding CNG injection to 180° BTDC to 120° BTDC. However, retarding CNG injection to 80° BTDC again resulted in high heat release rates led to knocking. At 1500 rpm, similar trends were observed with heat release rates marginally different from those obtained at 1200 rpm. High thermal efficiency was obtained for a wide range of ϕ_g and ϕ_{Total} at 1800 rpm. At 1800 rpm, ignition timing was least changed with an increase in ϕ_g, degree of CNG stratification and ϕ_{Total} and increase in heat release rates and pressure rise rates were moderate. This led to high range of IMEP operable over a wide range of gasoline equivalence ratio and CNG injection timings. At 2100 rpm, high engine loads in terms of ϕ_{Total} were operable over a wide range of injection timings and ϕ_g as the effects of high release rates were reduced at high engine speeds.

3. HC and CH_4 emissions were marginally affected by engine speed and were stronger functions of ϕ_{Total}, ϕ_g and degree of CNG stratification. While CNG injection at 80° BTDC drastically reduced HC emissions, there was a marginal increase in CO emissions at all speeds. With high rates of CNG injection, CO emissions increased with an increase in engine speed. However, engine speed had less effect on CO emissions at low loads and low degree of CNG stratification. NO_x emissions significantly reduced as engine speed was increased. NO_2/NO_x ratio increased with an increase in engine

154

speed and at 2100 rpm, highest NO_2/NO_x ratios were observed over a wide range of ϕ_{Total} at various ϕ_g and injection timings.

CHAPTER 5

CONCLUSIONS AND RECOMMENDATIONS

The HCCI combustion could be controlled by CNG injection by varying its degree of stratification and injection rate. The heat released by combustion of gasoline caused the autoignition of CNG at all speeds and at a range of degrees of stratification.

The experimental results showed that increasing proportion of CNG in the fuel resulted in delayed ignition timing and reduced peak pressures. However, there was an increase in HC and CO emissions at low engine loads. Increasing the proportion of gasoline resulted in improved performance and higher combustion efficiencies with reduced HC emissions. However, increasing gasoline equivalence ratio beyond a certain value led to lack of combustion control with CNG direct injection. NO_x emissions increased slightly at certain conditions and at high engine loads, however, were much lower than conventional combustion methods. Engine speed had significant influence on the effects of proportion of fuels. At lower engine speeds, combustion was more difficult to control and maximum load attainable was limited.

It was found that more amount of gasoline was needed to ignite stratified CNG. Increasing the degree of CNG stratification resulted in delayed ignition and reduced peak pressures. The combustion efficiency of overall mixture and that of CNG were higher at high degree of CNG stratification. When the degree of CNG stratification was increased, significant reduction in HC emissions could be achieved even at low gasoline equivalence ratios. However, NO_x and CO emissions increased especially at low engine loads and high speeds. Maximum load attainable at low engine speeds could be extended by increasing the degree of CNG stratification.

It was found that both the proportion of fuels and stratification of CNG were effective parameters for controlling HCCI combustion and defining the maximum

limit of load. By employing the strategy proposed in this project, load limits could be extended and HC emissions could be significantly reduced.

5.1 Recommendations

1. The study carried out in this project lacks discussion on the combustion phenomena such as mixture preparation, ignition spots, and temperature and pressure histories in the cylinder etcetera. Having these in mind, a combustion visualisation study would be more meaningful. A proposed strategy for continuous operation of the engine at optimal condition of engine speed and load when employing CNG stratification would be useful.

2. The effect of intake temperature on the combustion characteristics and emissions with CNG stratification may lead to a better understanding of formation of NO_2 and other temperature sensitive pollutants.

3. Similarly, studies on the combustion using fuels having lower octane number than gasoline and lower intake temperatures may provide better understanding of the combustion.

4. The studies on combustion combined with EGR and CNG stratification may extend the load limits achieved in this project.

REFERENCES

[1]   Alex M.K.P. Taylor, "Science review of Internal Combustion Engines," *J. of Energy Policy,* vol. 36, pp. 4657-4667, 2008.

[2]   L. E. Doman, "International Energy Outlook 2010," U.S. Energy Information Administration, Washington DC DOE/EIA -0484 (2010), July, 2010.

[3]   "World Energy Outlook," International Energy Agency, Parice OECD/IEA (2009), 2009.

[4]   O. Erlandsson, "Early Swedish Hot-Bulb Engines-Efficiency and Performance Compared to Contemporary Gasoline and Diesel Engines," *SAE Paper 2002-01-0115,* 2002.

[5]   S. Onishi, Hong Jo, S., Shoda, K., Do Jo, P., and Kato, S., "Active thermo-atmosphere combustion (ATAC) - A new combustion process for internal combustion engines," SAE Paper 790507, 1979.

[6]   M. Noguchi, Tanaka, Y., Tanaka, T., and Takeuchi, Y., "A study on gasoline engine combustion by observation of intermediate reactive products during combustion," SAE Paper 790840, 1979.

[7]   P. M. Najt and D. E. Foster, "Compression-ignited homogeneous charge combustion." vol. SAE Paper 830264, 1983.

[8]   R. H. Thring, "Homogeneous-charge compression-ignition (HCCI) engines," *SAE Paper 892068,* 1989.

[9]   M. Stockinger, Schapertons, H., and Huhlmann, P., "Investigation on a Gasoline Engine Working with Self-Ignition by Compression," *MTZ Vole. 53,* vol. 2, pp. 80-85, 1992.

[10] H. Zhao, Jian Li., and N. Ladommatos, "Performance and Analysis of a 4-Stroke Multi-Cylinder Gasoline Engine With Cai Combustion," *SAE Paper 2002-01-0420,* 2002.

[11] J. Lavy, J. C. Dabadie, C. Angelberger, P. Duret, A. Juretzka, J. Schäflein, T. H. Ma, Y. Lendresse, A. Satre, and C. Schulz, "Innovative ultra-low NOx controlled auto-ignition combustion process for gasoline engines: the 4-space project," *SAE Paper 2001-01-1837,* 2001.

[12] L. Koopmans and I. Denbratt, "A Four-Stroke Camless Engine, Operated in Homogeneous Charge Compression Ignition Mode With Commercial Gasoline," *SAE Paper 2001-01-3610,* 2001.

[13]   R. H. Stanglmaier and C. E. Roberts, "Homogeneous charge compression ignition (HCCI): benefits, compromises, and future engine applications," *SAE Paper 1999-01-3682,* 1999.

[14]   H. Zhao, *HCCI and CAI engines for the automotive industry.* Cambridge: Woodhead Publications, 2007.

[15]   M. Lida, M. Hayashi, D. E. Foster, and J. K. Martin, "Characteristics of homogeneous charge compression ignition (HCCI) engine operation for variations in compression ratio, speed, and intake temperature while using n-butane as a fuel," *Journal of engineering for gas turbines and power,* vol. 125, pp. 472 - 478, 2003.

[16]   K. Epping, S. M. Aceves, R. L. Bechtold, and J. E. Dec, "The potential of HCCI combustion for high efficiency and low emissions," *SAE Paper 2002-01-1923,* 2002.

[17]   J. B. Heywood, *Internal combustion engine: Fundamentals, .* New York: Mc Graw Hill, 1988.

[18]   S. Grice, J. Stedman, A. Kent, M. Hobson, J. Norris, J. Abbott, and S. Cooke, "Recent trends and projections of primary NO2 emissions in Europe," *Atmospheric Environment,* vol. 43, pp. 2154-2167, 2009.

[19]   J. E. Dec, "A Computational Study of the Effects of Low Fuel Loading and EGR on Heat Release Rates and Combustion Limits in HCCI Engines," *SAE Paper 2002-01-1309,* 2002.

[20]   A. Bhave, M. Kraft, L. Montorsi, and F. Mauss, "Sources of CO emissions in an HCCI engine: A numerical analysis," *Combustion and Flame,* vol. 144, pp. 634-637, 2006.

[21]   M. Christensen, A. Hultqvist, and B. Johansson, "Demonstrating the multi-fuel capability of a homogeneous charge compression ignition engine with variable compression ratio," *SAE Paper 1999-01-3679,* 1999.

[22]   M. Sjöberg and J. E. Dec, "Comparing late-cycle autoignition stability for single-and two-stage ignition fuels in HCCI engines," *Proceedings of the Combustion Institute,* vol. 31, pp. 2895-2902, 2007.

[23]   Z. Zheng and M. Yao, "Numerical study on the chemical reaction kinetics of n-heptane for HCCI combustion process," *Fuel,* vol. 85, pp. 2605-2615, 2006.

[24]   C. K. Westbrook, "Chemical kinetics of hydrocarbon ignition in practical combustion systems," *Proceedings of the Combustion Institute,* vol. 28, pp. 1563-1577, 2000.

[25]   M. Jia and M. Xie, "A chemical kinetics model of iso-octane oxidation for HCCI engines," *Fuel,* vol. 85, pp. 2593-2604, 2006.

[26]   H. Liu, M. Yao, Bo Zhang, and Z. Zheng, "Influence of Fuel and Operating Conditions on Combustion Characteristics of a Homogeneous Charge Compression Ignition Engine," *Energy & Fuels,* vol. 23, pp. 1422-1430, 2009.

[27]   L. Xing-Cai, W. Chen, and Z. Huang, "A fundamental study on the control of the HCCI combustion and emissions by fuel design concept combined with controllable EGR. Part1. The basic characteristics of HCCI combustion," *Fuel,* vol. 84, pp. 1074-1083, 2005.

[28]   H. Zhao, Z. Peng, J. Williams, and N. Ladommatos, "Understanding the effects of recycled burnt gases on the controlled autoignition (CAI) combustion in four-stroke gasoline engines," *SAE Technical Paper, 2001-01-3607,* 2001.

[29]   A. Oakley, H. Zhao, Tom Ma, and N. Ladommatos, "Dilution effects on the controlled auto-ignition (CAI) combustion of hydrocarbon and alcohol fuels," *SAE Paper 2001-01-3606,* 2001.

[30]   L. Xing-Cai, W. Chen, and Z. Huang, "A fundamental study on the control of the HCCI combustion and emissions by fuel design concept combined with controllable EGR. Part 2. Effect of operating conditions and EGR on HCCI combustion," *Fuel,* vol. 84, pp. 1084-1092, 2005.

[31]   C. Yang, "Investigation of combustion and performance characteristics of CAI combustion engine with positive and negative valve overlap," in *Scholl of Engineering and Design.* vol. Doctor of Philosophy: Brunel University, UK, 2008.

[32]   A. Babajimopoulos, D. N. Assanis, and S. B. Fiveland, "An Approach for Modeling the Effects of Gas Exchange Processes on HCCI Combustion and Its Application in Evaluating Variable Valve Timing Control Strategies," *SAE Paper 2002-01-2829,* 2002.

[33]   J. O. Olsson, P. Tunestal, B. Johansson, S. Fiveland, R. Agama, M. Willi, and D. Assanis, "Compression ratio influence on maximum load of a natural gas fuelled HCCI engine," *SAE Paper 2002-02-0111,* 2002.

[34]   D. Flowers, S. M. Aceves, J. M. Frias, J. R. Smith, M. Au, J. Girard, and R. Dibble, "Operation of a Four-Cylinder 1.9 L Propane Fueled HCCI Engine," Lawrence Livermore National Laboratory (LLNL), Livermore, CA 2001.

[35]   M. Sjöberg and J. E. Dec, "An investigation into lowest acceptable combustion temperatures for hydrocarbon fuels in HCCI engines," *Proceedings of the Combustion Institute,* vol. 30, pp. 2719-2726, 2005.

[36]   S. C. Kong and R. D. Reitz, "Use of detailed chemical kinetics to study HCCI engine combustion with consideration of turbulent mixing effects," *Journal of engineering for gas turbines and power,* vol. 124, pp. 702-707, 2002.

[37]   Y. Z. Zhang, E. H. Kung, and D. C. Haworth, "A PDF method for multidimensional modeling of HCCI engine combustion: effects of turbulence/chemistry interactions on ignition timing and emissions," *Proceedings of the Combustion Institute,* vol. 30, pp. 2763-2771, 2005.

[38]   S. M. Aceves, D. L. Flowers, J. Martinez-Frias, F. Espinosa-Loza, M. Christensen, B. Johansson, and R. P. Hessel, "Analysis of the Effect of Geometry Generated Turbulence on HCCI Combustion by Multi-Zone Modeling," Lawrence Livermore National Lab., Livermore, CA (US) 2004.

[39]   M. Richter, J. Engstrom, A. Franke, M. Alden, A. Hultqvist, and B. Johansson, "The influence of charge inhomogeneity on the HCCI combustion process," *SAE Paper, 2000-01-2868,* 2000.

[40]   T. Noda and D. E. Foster, "A numerical study to control combustion duration of hydrogen-fueled HCCI by using multi-zone chemical kinetics simulation," *SAE Paper 2001-01-0250,* 2001.

[41]   M. Christensen and B. Johansson, "Influence of mixture quality on homogeneous charge compression ignition," *SAE Paper, 982454,* 1998.

[42]   Z. Zheng and M. Yao, "Numerical simulation of the effects of charge stratification on combustion and emissions," *Energy Fuels,* vol. 21, pp. 2018-2026, 2007.

[43]   G. S. Jung, Y. H. Sung, B. C. Choi, and M. T. Lim, "Effects of mixture stratification on HCCI combustion of DME in a rapid compression and expansion machine," *International Journal of Automotive Technology,* vol. 10, pp. 1-7, 2009.

[44]   R. Schießl and U. Maas, "Analysis of endgas temperature fluctuations in an SI engine by laser-induced fluorescence," *Combustion and Flame,* vol. 133, pp. 19-27, 2003.

[45]   Z. Wang, W. Jian-Xin, S. Shi-Jin, and F. Zhang, "Numerical simulation of HCCI engine with multi-stage gasoline direct injection using 3D-CFD with detailed chemistry," *SAE Transactions,* vol. 113, pp. 367-380, 2004.

[46]   M. Sjoberg, L. O. Edling, T. Eliassen, L. Magnusson, and H. E. Angstrom, "GDI HCCI: Effect of Injection Timing and Air Swirl on Fuel Stratification, Combustion and Emissions Formation," *SAE Paper 2002-01-0106,* 2002.

[47]   C. D. Marriott and R. D. Reitz, "Experimental investigation of direct injection gasoline for premixed compression-ignited combustion-phasing control," *SAE Paper 2002-01-0418,* 2002.

[48]   B. Kim, M. Kaneko, Y. Ikeda, and T. Nakajima, "Detailed spectral analysis of the process of HCCI combustion," *Proceedings of the Combustion Institute,* vol. 29, pp. 671-677, 2002.
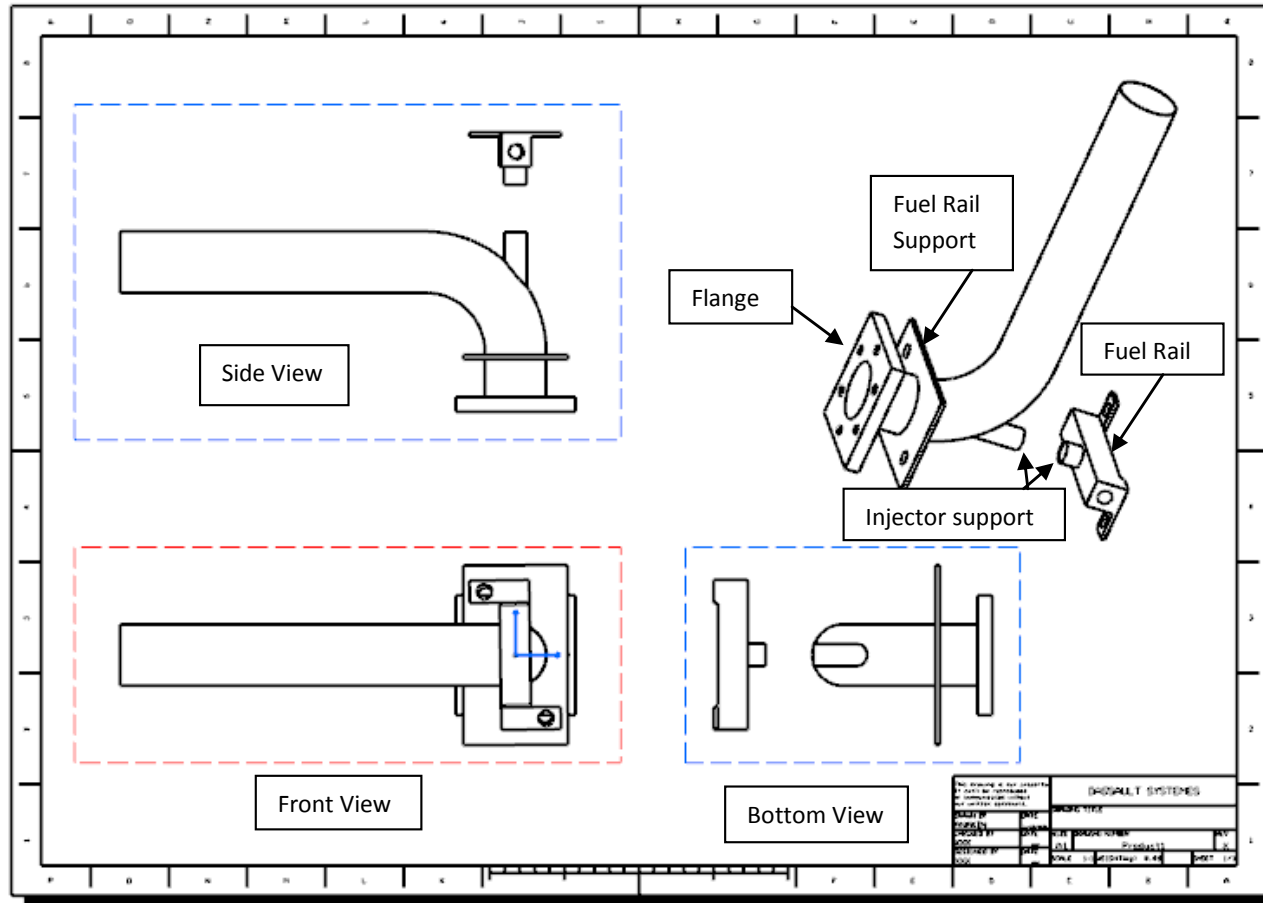
[49] J. Kashdan and G. Bruneaux, "Mixture Preparation and Combustion in an Optically-Accessible HCCI, Diesel Engine," *Oil & Gas Science and Technology,* vol. 61, pp. 25-42, 2006.

[50] H. Kim, J. Ryu, and K. Lee, "A study on the characteristics of spray and combustion in a HCCI engine according to various injection angles and timings," *Journal of mechanical science and technology,* vol. 21, pp. 133-140, 2007.

[51] Z. Huang, S. Shiga, T.Ueda, H. Nakamura, T. Ishima, T. Obekata, M.Tsue, and M.Kono, "Effect of Fuel Injection Timing Relative to Ignition Timing on the Natural-Gas Direct-Injection Combustion," *Journal of engineering for gas turbines and power,* vol. 125, pp. 783-790, 2003.

[52] J. Ma, X. Lu, L. Ji, and Z. Huang, "Evaluation of SCCI potentials in comparison to HCCI and conventional DICI combustion using n-heptane," *Energy & Fuels,* vol. 22, pp. 954-960, 2008.

[53] T. Ishiyama, H. Kawanabe, K. Ohashi, M. Shioji, and S. Nakai, "A study on premixed charge compression ignition combustion of natural gas with direct injection," *International Journal of Engine Research,* vol. 6, pp. 443-451, 2005.

[54] M. Canakci and R. D. Reitz, "Effect of optimization criteria on direct-injection homogeneous charge compression ignition gasoline engine performance and emissions using fully automated experiments and microgenetic algorithms," *Journal of engineering for gas turbines and power,* vol. 126, pp. 167 - 178, 2004.

[55] Z. Wang, S. J. Shuai, J. X. Wang, and G. H. Tian, "A computational study of direct injection gasoline HCCI engine with secondary injection," *Fuel,* vol. 85, pp. 1831-1841, 2006.

[56] Z. Wang, J. X. Wang, S. J. Shuai, G. H. Tian, and X. L. An, "Experimental and computational studies on gasoline HCCI combustion control using injection strategies," *Journal of engineering for gas turbines and power,* vol. 129, pp. 870-876, 2007.

[57] K. Yoshizawa, A. Teraji, H. Miyakubo, K. Yamaguchi, and T. Urushihara, "Study of high load operation limit expansion for gasoline compression ignition engines," *Journal of engineering for gas turbines and power,* vol. 128, pp. 377-388, 2006.

[58] K. Lee and C. Lee, "An Experimental Study on the Combustion Characteristics Using the Stratified Charge Compression Ignition in a Direct Injection Gasoline Engine," *JSME International Journal,* vol. 49, pp. 864-868, 2006.

[59] C.H. Lee and K. H. Lee, "An experimental study on the combustion and emission characteristics of a stratified charge compression ignition (SCCI) engine," *Energy Fuels,* vol. 21, pp. 1901-1907, 2007.

[60] J. Chang, Z. S. Filipi, T. W. Kuo, D. N. Assanis, P. M. Najt, and R. B. Rask, "Investigation of Mixture Preparation Effects on Gasoline HCCI Combustion Aided by Measurements of Wall Heat Flux," *Journal of engineering for gas turbines and power,* vol. 130, pp. 61- 69, 2008.

[61] M. Canakci, "An experimental study for the effects of boost pressure on the performance and exhaust emissions of a DI-HCCI gasoline engine," *Fuel,* vol. 87, pp. 1503-1514, 2008.

[62] M. Yao, Z. Zheng, B. Zhang, and Z. Chen, "The effect of PRF fuel octane number on HCCI operation," *SAE Paper 2004-01-2992,* 2004.

[63] B. Thanapiyawanit and L. J. Huai, "A Dual-Fuel System to Achieve High Equivalence Ratio and High Engine Performance in Homogeneous Charge Compression Ignition (HCCI) Mode," *SAE Paper 2009-32-0035,* 2009.

[64] Y. C. Hou, X. C. Lu, L. L. Zu, L. Ji, and Z. Huang, "Effect of high-octane oxygenated fuels on n-heptane-fueled HCCI combustion," *Energy Fuels,* vol. 20, pp. 1425-1433, 2006.

[65] X. Lü, Y. Hou, L. Zu, and Z. Huang, "Experimental study on the auto-ignition and combustion characteristics in the homogeneous charge compression ignition (HCCI) combustion operation with ethanol/n-heptane blend fuels by port injection," *Fuel,* vol. 85, pp. 2622-2631, 2006.

[66] C. Arcoumanis, C. Bae, R. Crookes, and E. Kinoshita, "The potential of di-methyl ether (DME) as an alternative fuel for compression-ignition engines: A review," *Fuel,* vol. 87, pp. 1014-1030, 2008.

[67] M. Yao, Z. Zheng, and J. Qin, "Experimental study on homogeneous charge compression ignition combustion with fuel of dimethyl ether and natural gas," *Journal of engineering for gas turbines and power,* vol. 128, pp. 414-423, 2006.

[68] S. C. Kong, "A study of natural gas/DME combustion in HCCI engines using CFD with detailed chemical kinetics," *Fuel,* vol. 86, pp. 1483-1489, 2007.

[69] S. V. Gusakov, P. R. Valjeho Maldonado, I. V. Epifanov, and Louis Lastra Espinosa, "Use of natural gas-dimethyl ether mixture as fuel for HCCI process in internal combustion engines," *Chemical and Petroleum Engineering,* vol. 44, pp. 510-513, 2008.

[70] Y. Tsutsumi, A. Iijima, K. Yoshida, H. Shoji, and J. T. Lee, "HCCI combustion characteristics during operation on DME and methane fuels," *International Journal of Automotive Technology,* vol. 10, pp. 645-652, 2009.

[71] M. Yao, Z. Chen, Z. Zheng, B. Zhang, and Y. Xing, "Study on the controlling strategies of homogeneous charge compression ignition combustion with fuel of dimethyl ether and methanol," *Fuel,* vol. 85, pp. 2046-2056, 2006.

[72]   N. K. Miller Jothi, G. Nagarajan, and S. Renganarayanan, "LPG fueled diesel engine using diethyl ether with exhaust gas recirculation," *International Journal of Thermal Sciences,* vol. 47, pp. 450-457, 2008.

[73]   K. Yeom, J. Jang, and C. Bae, "Homogeneous charge compression ignition of LPG and gasoline using variable valve timing in an engine," *Fuel,* vol. 86, pp. 494-503, 2007.

[74]   K. Yeom and C. Bae, "Gasoline- Di-methyl Ether Homogeneous Charge Compression Ignition Engine," *Energy Fuels,* vol. 21, pp. 1942-1949, 2007.

[75]   A. P. Carlucci, A. De Risi, D. Laforgia, and F. Naccarato, "Experimental investigation and combustion analysis of a direct injection dual-fuel diesel-natural gas engine," *Energy,* vol. 33, pp. 256-263, 2008.

[76]   C. Cinar, O. Can, F. Sahin, and H. S. Yucesu, "Effects of premixed diethyl ether (DEE) on combustion and exhaust emissions in a HCCI-DI diesel engine," *Applied Thermal Engineering,* vol. 30, pp. 360-365, 2010.

[77]   M. Ghazikhani, M. R. Kalateh, Y. K. Toroghi, and M. Dehnavi, "An experimental study on the effect of EGR and engine speed on CO and HC emissions of dual fuel HCCI engine," *Journal of engineering and technology,* vol. 52, pp. 137-141, 2009.

[78]   D. S. Kim, M. Y. Kim, and C. S. Lee, "Effect of premixed gasoline fuel on the combustion characteristics of compression ignition engine," *Energy Fuels,* vol. 18, pp. 1213-1219, 2004.

[79]   J. Ma, X. Lü, L. Ji, and Z. Huang, "An experimental study of HCCI-DI combustion and emissions in a diesel engine with dual fuel," *International Journal of Thermal Sciences,* vol. 47, pp. 1235-1242, 2008.

[80]   D. S. Kim and C. S. Lee, "Effect of n-heptane premixing on combustion characteristics of diesel engine," *Energy Fuels,* vol. 19, pp. 2240-2246, 2005.

[81]   Z. Chen, M. Yao, Z. Zheng, and Q. Zhang, "Experimental and numerical study of methanol/dimethyl ether dual-fuel compound combustion," *Energy & Fuels,* vol. 23, pp. 2719-2730, 2009.

[82]   L. Ji, X. Lu, J. Ma, C. Huang, D. Han, and Z. Huang, "Experimental study on influencing factors of iso-octane thermo-atmosphere combustion in a dual-fuel stratified charge compression ignition (SCCI) engine," *Energy & Fuels,* vol. 23, pp. 2405-2412, 2009.

[83]   "Basic Operation Manual of Single Cylinder Research Engine (SCRE)," Orbotol Corporation Ltd., Australia, 2004.

[84]   Firmansya, "Optimization of injection parameters on the performance of CNG DI engine," in *Mechanical Engineering, MSc Thesis,* Bandar Seri Iskandar: Universiti Teknologi PETRONAS, 2007.

[85]   Raja Shahzad Hassan, "Combustion characteristics CNG DI engine under lean stratified conditions " in *Mechanical Engineering, MSc Thesis,* Bandar Seri Iskandar: Universiti Teknologi PETRONAS, 2008.

[86]   D. Law, D. Kemp, J. Allen, G. Kirkpatrick, and T. Copland, "Controlled combustion in an IC-engine with a fully variable valve train," *SAE Paper 2001-01-0251,* 2001.

[87]   G. Kontarakis, N. Collings, and T. Ma, "Demonstration of HCCI using a single-cylinder, four-stroke SI engine with modified valve timing," *SAE Paper 2000-01-2870,* 2000.

[88]   G. M. Rassweilor and L. Withrow, "Motion pictures of engine flames correlated with pressure cards," *SAE Transactions,* vol. 47, pp. 185-204, 1938.

[89]   J. H. Mack, R. W. Dibble, and D. L. F. B. A. Buchhholz, "The effect of the Di-Tertiary Butyl Peroxide (DTBP) additive on HCCI combustion of fuel blends of ethanol and diethyl ether," *SAE Paper 2005-01-2135,* 2005.

[90]   M. A. Kalam, H. H. Masjuki, M. A. Maleque, M. A. Amalina, H. Abdesselam, and T. M. I. Mahlia, "Air-Fuel Ratio Calculation for a Natural Gas-Fuelled Spark Ignition Engine," *SAE Paper 2004-01-0640,* 2004.

[91]   M. U. Aslam, H. H. Masjuki, M. A. Kalam, H. Abdesselam, T. M. I. Mahlia, and M. A. Amalina, "An experimental investigation of CNG as an alternative fuel for a retrofitted gasoline vehicle," *Fuel,* vol. 85, pp. 717-724, 2006.

[92]   L. Xingcai, H. Yuchun, Z. Linlin, and H. Zhen, "Experimental study on the auto-ignition and combustion characteristics in the homogeneous charge compression ignition (HCCI) combustion operation with ethanol/n-heptane blend fuels by port injection," *Fuel,* vol. 85, pp. 2622-2631, 2006.

[93]   P. Maigaard, F. Mauss, and M. Kraft, "Homogeneous charge compression ignition engine: A simulation study on the effects of inhomogeneities," *Journal of engineering for gas turbines and power,* vol. 125, pp. 466-471, 2003.

APPENDIX A

MODIFIED INTAKE MANIFOLD

Side View

Front View

Bottom View

Flange

Fuel Rail
Support

Fuel Rail

Injector support

APPENDIX B

EXPERIMENTAL SETUP